Department of Spatial Sciences

Quasigeoid Modelling in New Zealand to Unify Multiple Local Vertical Datums

Matthew James Amos

This thesis is presented for the Degree of
Doctor of Philosophy
of
Curtin University of Technology

October 2007

Declaration

To the best of my knowledge and belief this thesis contains no material previously published by any other person except where due acknowledgement has been made.

This thesis contains no material which has been accepted for the award of any other degree or diploma in any university.

Signature: ……..

Date: …….

ABSTRACT

One goal of modern geodesy is the global unification of vertical datums so that height data from them can be properly integrated. This thesis studies the unification of the 13 disparate levelling- and tide-gauge-based vertical datums in New Zealand (NZ). It proposes a new NZ-wide single vertical datum based on a gravimetric quasigeoid model to unify the existing local vertical datums. This will also include methods to transform height data in terms of the existing datums to the new datum and *vice versa*.

After defining and comparing the main types of height system and vertical datum used around to world, the system of heights used in NZ was shown to be normal-orthometric. Consequently, datum unification was achieved using a quasigeoid model, as opposed to a geoid model. The quasigeoid was computed by combining the GRACE-based GGM02 and EGM96 global geopotential models with land gravity data (40,737 observations) and a 56-m resolution digital elevation model (DEM). Marine gravity data came from a least-squares collocation combination of 1,300,266 crossover-adjusted ship track observations and gravity anomalies derived from multi-mission satellite altimetry.

To ensure that the best quasigeoid was computed for the NZ datasets, a number of computation processes were compared and contrasted. The Hammer chart, fast Fourier transform (FFT) and prism integration methods of computing terrain corrections (TCs) were compared. This showed that the prism integration TC is the most realistic in NZ. The mean Helmert gravity anomalies, required for numerical integration of Stokes's formula, were computed via refined Bouguer anomalies with the prism TCs, and reconstruction with heights from the DEM used to 'reconstruct' more representative mean anomalies. In addition, five deterministic modifications to Stokes's formula were compared. There was little difference between three of them, so the Featherstone *et al*. (1998) modification ($\psi_0 = 1.5°$, $M = 40$) was chosen because it is theoretically better than its predecessors.

The global geopotential, gravimetric geoid, sea surface topography and geodetic boundary-value problem approaches to vertical datum unification were then contrasted. As none was likely to be effective in NZ, a new iterative quasigeoid

approach was adopted. This procedure computes an initial quasigeoid from existing data on the various local vertical datums to estimate the vertical datum offsets from co-located GPS-levelling data. These offsets were then subsequently applied to the gravity observations by way of additional reductions to the initially computed quasigeoid to reduce gravity anomaly biases caused by the vertically offset datums. These adjusted gravity anomalies were then used to compute a new quasigeoid model, and the process repeated until the computed offsets between the local vertical datums (or equivalently two quasigeoid solutions) converged, which took only two iterations.

The computed offsets were then compared with spirit-levelled height differences among adjoining datums, where these were available, giving an average agreement of 7 cm. Since the local vertical datums are effectively unified, the new national vertical datum for NZ will comprise the iteratively computed gravimetric quasigeoid model, accompanied by local vertical datums. This approach is implemented to give a new national vertical datum for NZ. When used with the appropriate offset, this enables the transformation of heights in terms of the national vertical datum to the 13 precise-levelling datums and the ellipsoidal national geodetic datum, NZ Geodetic Datum 2000.

ACKNOWLEDGEMENTS

I am sincerely indebted to my supervisor, Will Featherstone. He has provided excellent motivation, guidance and constructive input throughout this project. Without his assistance and encouragement it is unlikely that this study would have been so successful.

I greatly appreciate the support of my employer, Land Information New Zealand, who provided me with the opportunity to undertake this research. Specific credit needs to be given to Graeme Blick who initially persuaded me to start this project and gave me excellent suggestions and support throughout its progression. The previous and current Surveyors-General, Tony Bevin and Don Grant, are also thanked for ensuring that the necessary time and resources were available to me and also for engaging in perceptive discussions throughout this study. I would also like to acknowledge the Office of the Surveyor-General and the wider LINZ staff for their assistance over the past few years.

Finally I would like to thank my wife Trudi who has been unwavering in her support for me during this endeavour, even with the longer work hours and the extended time spent apart during my regular trips to Perth.

TABLE OF CONTENTS

LIST OF FIGURES

LIST OF TABLES

LIST OF ABBREVIATIONS

AHD	Australian Height Datum
CGG2000	Canadian Gravimetric Geoid 2000
CGVD28	Canadian Geodetic Vertical Datum 1928
CHAMP	Challenging Mini-satellite Payload
CI	Confidence interval
DC	Downward continuation
DEM	Digital elevation model
DoSLI	Department of Survey and Land Information
DOT	Dynamic ocean topography
DTE	Direct topographical effect
EDS	Earth deformation study
EGM07/8	Earth Gravity Model 2007/8
EGM96	Earth Gravity Model 1996
ESA	European Space Agency
EUVN	European Vertical Reference Network
FEO	Featherstone, Evans and Olliver (1998) kernel modification
FFT	Fast Fourier transformation
GA	Geoscience Australia
GBVP	Geodetic boundary-value problem
GEODAS	Geophysical data system
GGM	Global geopotential model
GIA	Glacial isostatic adjustment
GLONASS	Globalnaya Navigaysionnaya Sputnikovaya Sistema
GLOPOV	General law of propagation of variance
GMT	Generic Mapping Tools
GNS	GNS Science
GNSS	Global Navigation Satellite System
GOCE	Gravity field and steady state Ocean Circulation Explorer
GPS	Global Positioning System
GPU	Geopotential units
GRACE	Gravity Recovery and Climate Experiment
GRS67	Geodetic Reference System 1967

GRS80	Geodetic Reference System 1980
HG	Heck and Grüninger (1983) kernel modification
HRB	Hammer chart terrain correction refined Bouguer quasigeoid
IAG	International Association of Geodesy
IGSN71	International Gravity Standardisation Network 1971
ITRF96	International Terrestrial Reference Frame 1996
L&S	Department of Lands and Survey
LINZ	Land Information New Zealand
LSC	Least-squares collocation
LVD	Local vertical datum
ML	Meissl (1971) kernel modification
M-P	Moritz-Pellinen downward continuation
MRB	Moritz FFT terrain correction refined Bouguer quasigeoid
MSB	Moritz FFT terrain correction simple Bouguer quasigeoid
MSL	Mean sea level
NAP	Normaal Amsterdams Peil
NAVD88	North American Vertical Datum 1988
NGVD29	National Geodetic Vertical Datum 1929
NOAA	National Oceanic and Atmospheric Administration
NOC	Normal-orthometric correction
NRCan	Natural Resources Canada
NZ	New Zealand
NZGD49	New Zealand Geodetic Datum 1949
NZGD2000	New Zealand Geodetic Datum 2000
NZMS	New Zealand Map Service
PITE	Primary indirect topographical effect
PRB	Prism integration terrain correction refined Bouguer quasigeoid
PSB	Prism integration terrain correction simple Bouguer quasigeoid
RB	Refined Bouguer gravity anomaly
RCR	Remove-compute-restore
RMS	Root mean square
RTK	Real-time kinematic
SB	Simple Bouguer gravity anomaly
SI	Système International

SITE	Secondary indirect topographical effect
SS	Spherical Stokes kernel
SSTop	Sea surface topography
STD	Standard deviation
TC	Terrain correction
UELN	United European Levelling Network
UNB	University of New Brunswick
UNCLOS	United Nations Convention on the Law of the Sea
VK	Vaníček & Kleusberg (1987) kernel modification
V-M	Vaníček-Martinec downward continuation
WG	Wong and Gore (1969) kernel modification
WGS72	World Geodetic System 1972
WGS84	World Geodetic System 1984

LIST OF SYMBOLS

a	Semi-major axis of the reference ellipsoid
dn	Height difference
$d\psi$, $d\alpha$	Surface spherical coordinates
$d\sigma$	Surface area element on the sphere
$d\gamma / dh$	Vertical free-air gradient
e^2	Squared eccentricity of reference ellipsoid
e_{nk}	Vaníček & Kleusberg (1987) kernel modification coefficients
f	Flattening of the reference ellipsoid
f^*	Gravity flattening constant
g	Gravity vector along the plumbline
g_0	Constant gravity
g_m	Gravity observation in the mean Earth-tide model
g_z	Gravity observation in the zero Earth-tide model
g_n	Gravity observation in the tide-free Earth-tide model
g_{mean}	Average surface gravity
g_S	Surface gravity observation
$\overline{g}$	Integral mean gravity along the plumbline
$\overline{g}^{\text{Helmert}}$	Helmert approximation of integral mean gravity along plumbline
$\overline{g}^{\text{Neithammer}}$	Neithammer approximation of integral mean gravity along plumbline
$\overline{g}^{\text{Mader}}$	Mader approximation of integral mean gravity along plumbline
h	Ellipsoidal height
(r, ϕ, λ)	Geocentric polar coordinates
k	Normal gravity constant
l	Planar distance between two points
m	Order of spherical harmonics
m	Geodetic parameter
n	Degree of spherical harmonics

r	Geocentric radius of the Earth
t_k	Vaníček & Kleusberg (1987) kernel modification coefficients
C	Geopotential number
C'	Normal geopotential/spheropotential number
G	Universal gravitational constant
GM	Product of Newtonian gravitational constant and mass of Earth
H_{av}	Average height
H_0	Null hypothesis
H^{dyn}	Dynamic height
H^{ortho}	Orthometric height
H^{N}	Normal height
$H^{\text{N-O}}$	Normal-orthometric height
K	Stokes error kernel function
L	Degree of Molodensky-type kernel modification
M	Degree of GGM expansion
$M_{\max}$	Maximum complete degree of harmonic expansion
N	Geoid height
N_{ind}	Primary indirect effect
N_M	Geoid undulation from GGM
P	Degree of spheroidal kernel modification
P	Observation point
P_0	Position of P projected onto the geoid
P_n	Legendre polynomial
$\overline{P}_{nm}$	Associated Legendre function
Q_n	Truncation error coefficients
R	Mean radius of the Earth
S	Spherical Stokes's kernel function
S^M	Spheroidal Stokes function
U	Normal potential
U_Q	Normal potential on telluroid at point Q

W_0	Global geopotential
W_P	Geopotential at point P
α	Azimuth
δ	Earth-tide constant
δs	Horizontal distance
δg_A	Atmospheric correction
δg_B	Planar Bouguer correction
δg_F	Free-air correction
δg^T	Terrain effect at topographic surface
δg_0^T	Terrain effect at geoid
$\delta \overline{C}_{nm}$, $\overline{S}_{nm}$	Fully normalised spherical harmonic coefficients
$\delta \zeta$	Truncation error in quasigeoid
$\delta \phi$	Difference in latitude
$\delta \Delta g$	Effect of datum offset on gravity observation
$\overline{\delta} g^T$	Integral mean terrain effect of gravity along plumbline
η	East-west vertical deflection
γ	Normal gravity of reference ellipsoid
γ_0	Normal gravity at 45ºN/S
$\overline{\gamma}$	Normal gravity along the ellipsoidal normal
γ_a	Normal gravity at equator
λ	Geodetic longitude
λ'	Longitude of variable surface element $d\sigma$
μ	True value
o	Vertical datum offset
ϕ	Geodetic latitude
ϕ'	Latitude of variable surface element $d\sigma$
ϕ_{av}	Average latitude
ψ	Angular distance between two points
ψ_0	Angular integration cap radius

ρ	Topographic mass density
σ	Sphere of integration
σ_{average}	Weighted average standard deviation
υ, β	NZ normal-orthometric correction coefficients
ξ	North-south vertical deflection
ζ	Quasigeoid height/height anomaly
ΔC	Geopotential difference
Δg	Gravity anomalies reduced to the quasigeoid
Δg_B	Simple Bouguer anomaly
Δg_F	Free air gravity anomaly
Δg_M	Residual gravity anomaly
ΔH_m	Height difference in mean Earth-tide model
ΔH_n	Height difference in tide-free Earth-tide model
ΔH_z	Height difference in zero Earth-tide model
$\mathcal{O}$	Landau symbol

1 INTRODUCTION

1.1 Background

New Zealand (NZ) does not currently have a single national vertical datum. Instead, 13 separate datums based on local mean sea level (MSL) observed at tide-gauges around the country are used. These tide gauges have been used as the datum for the precise-levelling observations made from them. Despite some early evidence to the contrary (e.g., Humphries, 1908), the datums were assumed to be stable and thus capable of being linked by precise-levelling, so that they could eventually be linked to form a single national datum (e.g. Hannah, 2001).

It is well-known that NZ is tectonically active (e.g., Walcott, 1984). In recent years the phenomenon of sea surface topography has become more widely recognised by geodesists (e.g. Hipkin, 2000). This, combined with sea level rise (e.g. Hannah, 1990), has meant that the MSL at the tide-gauge datum origins does not lie on a single equipotential surface. Thus, the prospect of forming a national height network based solely on the adjustment of the regional precise-levelling networks based on MSL at a number of tide-gauges is becoming more remote with time (e.g. Hannah, 2001).

An alternative technique is to obtain vertical datum unification is via a geoid model (cf. Kumar and Burke, 1998). When a GNSS (Global Navigation Satellite System) receiver is used at a benchmark such a model enables each of the vertical datums to have an offset calculated for it (i.e., $o = h - H - N$), and so the datums can be related to each other. This technique also has the benefit of allowing geocentric observations (e.g., Global Positioning System; GPS) to be converted into heights in terms of an orthometric height system in relation to each of the vertical datums.

Recent improvements in technology have meant that systems such as GPS are now able to readily observe three-dimensional positions with respect to an ellipsoid. Because GPS is referenced to a geocentric ellipsoid, heights that are obtained from it are not in relation to a geopotential surface of the Earth's gravity field. In most cases, users need heights that are referenced to the gravity field, primarily to determine fluid flows and to be consistent with the existing spatial infrastructure. To convert GPS-derived ellipsoidal heights (h) to orthometric heights (H), it is necessary

to use a geoid (N) model (i.e., $H = h - N$). Because normal-orthometric heights (H^{N-O}) are used in NZ (cf. Section 2.4.2), the conversion to ellipsoidal heights is achieved using a quasigeoid (ζ) model (i.e., $H^{N-O} = h - \zeta$).

Unlike many countries (e.g., Australia, Featherstone *et al*., 2001; the United States, Smith and Roman, 2001; the United Kingdom, Featherstone and Olliver, 1994; and Europe, Ihde *et al*., 2002), NZ does not currently have a high-resolution regional quasigeoid model (cf. Section 1.2.2). An evaluation of user groups by Pearse (2001) determined that an initial gravimetric quasigeoid with an accuracy of 10-15 cm would meet a majority of their requirements.

1.2 New Zealand setting

1.2.1 Basic geological setting

NZ is an isolated country located in the South Pacific Ocean, approximately 2,200 km south-east of Australia. It consists of three main islands (North, South and Stewart/Rakiura) and a number of smaller offshore islands (Figure 1.1). It has a long narrow shape with a heavily indented coastline that has been estimated as between 11,000 km and 15,000 km in length. Mountain ranges and hill country dominate the NZ landscape, with one of the most striking features being the Southern Alps/Kā Tiritiri o te Moana. These, along with fiords, glaciers, lakes and the coastal plains of Canterbury characterise the South Island geography. The North Island volcanic interior contains NZ's largest lake, Lake Taupo (~600 km^2) and several active volcanoes. Hot pools, geysers and mud pools also form part of the volcanic system centred around Rotorua.

Geologically, NZ straddles the boundary between the Australian and Pacific tectonic plates (Figure 1.1). The North Island is at the southern end of the Tonga-Kermadec-Hikurangi oblique subduction zone where the Pacific plate is subducting westward beneath the Australian plate to the west of the Hikurangi Trench. In the south of NZ, the opposite occurs where the Australian plate is subducting eastward under the Pacific plate to the east of the Puysegur Trench. Between the subduction zones, two (submerged) continental fragments, the Challenger Plateau and the Chatham Rise, collide obliquely (e.g. Pearse, 1998; Walcott, 1984).

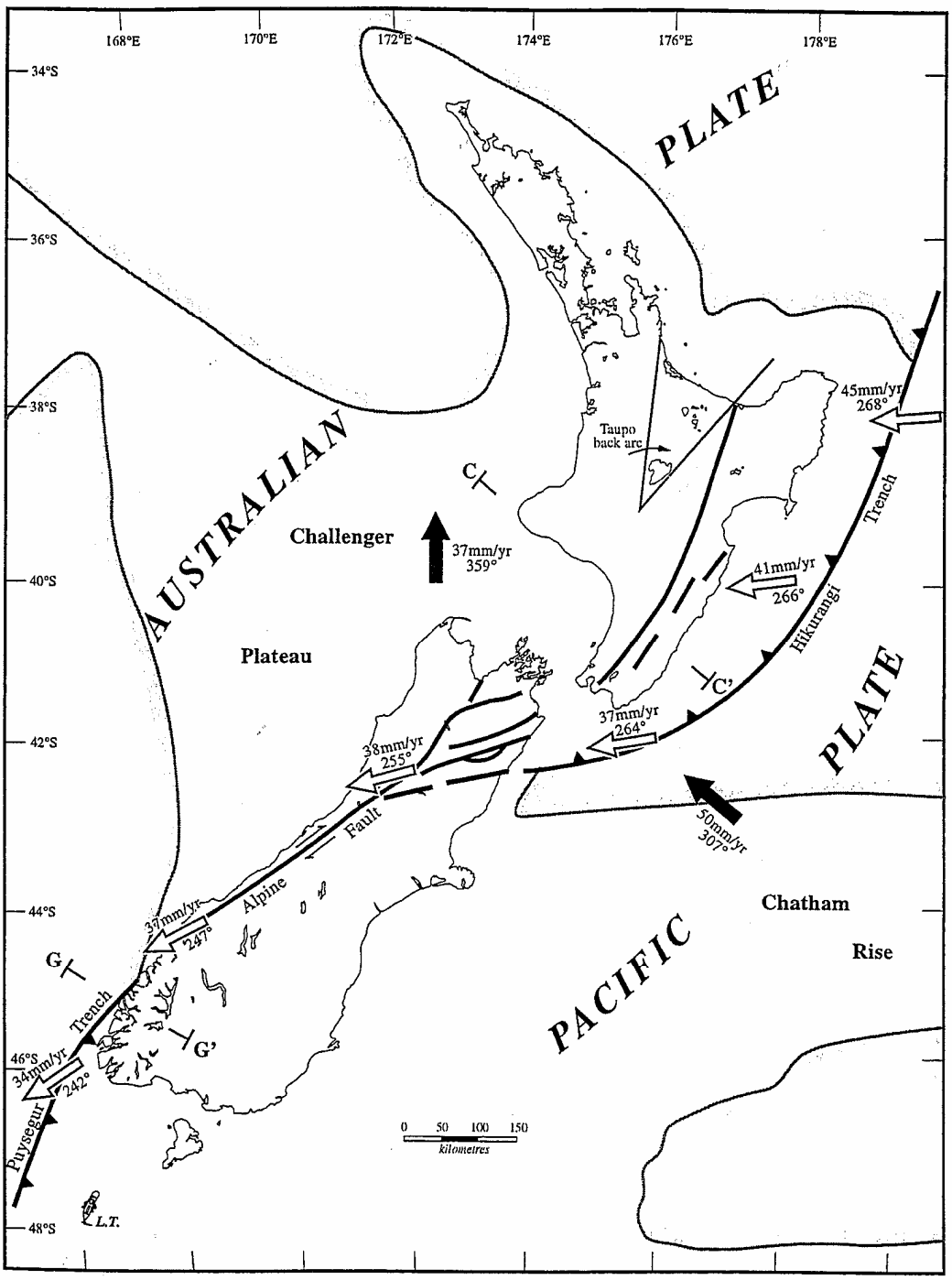

Figure 1.1 Location of the Pacific and Australian plate boundary in the NZ region (adapted from Pearse, 1998; Cole, 1990; Anderson and Webb, 1994). The solid arrows represent the absolute plate motion in terms of the Nuvel-1A (De Mets *et al.*, 1994) tectonic plate model. The hollow arrows represent the relative plate motion between the Australian (fixed) and Pacific plates.

This location in the active tectonic zone has shaped the physical terrain of NZ. The mountainous topography is a result of the ongoing plate collision and subsequent uplift (notably along the Alpine fault in the South Island, e.g., Berryman, 1984).

There is also significant volcanic activity in the Taupo back-arc (Figure 1.1) that is typically associated with a major tectonic boundary zone (e.g., Walcott, 1984). This results in regular seismic activity that is considered a "normal" part of life in NZ (Hannah, 2001).

1.2.2 Previous quasigeoid computations in New Zealand

There have been two previous attempts to compute quasigeoid models for the NZ region. Gilliland (1990) produced a gravimetric quasi-co-geoid for NZ on a 0.25° grid by combining gravity data and the OSU81 (Rapp, 1981) global geopotential model (GGM) to degree and order 180. However, without ellipsoidal heights no comparison with the precisely-levelled normal-orthometric heights could be made.

Mackie (1982) determined quasigeoid heights at 18 stations, distributed across NZ, by comparing Doppler-derived WGS72 ellipsoidal heights with spirit levelled normal-orthometric heights. Mackie's work did not use local gravity data, though when Gilliland compared his results with those of Mackie, root-mean-square (RMS) quasigeoid height differences of less than 1.3 metres were obtained (Pearse, 2001). At the time this was a reasonable result given the accuracy of Doppler heights, but with current techniques quasigeoid heights of better than 10 cm should be achievable.

1.3 Thesis aim

The primary objective of the research is to unify the multitude of vertical datums that currently exist in NZ. This will produce a single national vertical datum that has a relationship to ellipsoidal (e.g., Global Navigation Satellite System, GNSS) reference frames.

As part of this objective, a secondary task will the computation of a gravimetric quasigeoid for the NZ region to enable users of its geodetic system to convert heights between the precise-levelling-based vertical datums and GNSS-derived ellipsoidal heights. Such a model does not currently exist for such use in NZ. This quasigeoid will be initially evaluated using existing data sets and "standard" computation techniques, (e.g., the techniques used to determine AUSGeoid98; Featherstone *et al.*, 2001), and then iterating the calculations with information from the previous

solutions to remove the distortions in the downward-continued gravity anomalies. To the best of the author's knowledge, this is the first time an "iterative" computation scheme and quasigeoid have actually been used to unify vertical datums.

1.4 Significance of research

This study is significant for the three reasons. Firstly, it will for the first time create a unified national vertical datum for NZ that is linked to global geocentric coordinate systems such as the International Terrestrial Reference Frame (ITRF) via a gravimetric quasigeoid (Chapter 7). The current vertical datums are defined in relation to local MSL at separate tide-gauges. From this unified datum, it will be possible to use new technologies (e.g. GNSS) to determine normal-orthometric heights throughout NZ. This will be highly significant as the new technologies are significantly cheaper than traditional techniques (e.g., precise-levelling) over longer distances (i.e., hundreds of kilometres). The use of a gravimetric quasigeoid to unify vertical datums is different to the conventional approach that uses a least-squares adjustment of precisely levelled height differences. It is shown that while it is technically possible to complete a precise-levelling adjustment in NZ, such an approach is subject to a number of limitations (e.g., vertical deformation, limited spatial coverage, incompatibility with GNSS heights) that make its implementation unfavourable.

Second, it will provide an opportunity to develop and test quasigeoid determination techniques in the NZ context (Chapters 4 and 5). NZ has not been an area of major quasigeoid investigation in the past due to its isolation and difficult topography – particularly with respect to the acquisition of gravity observations. It is this topography however that makes it a suitable "field laboratory" for testing terrain correction computation techniques (Chapter 4). It is in areas of high topographical change that the traditional terrain correction (TC) computations start to fail. For example, when terrain slopes are greater than 45°, the fast Fourier transform (FFT) technique becomes unstable (e.g., Martinec *et* al., 1996; Tsoulis, 2001).

The third and most significant feature of this research is the use of an iterative technique for determining a gravimetric quasigeoid based on the fit with the existing vertical datum data (Chapter 6). Most other countries have a national vertical datum

that a quasigeoid can be compared against so iterating is of little additional benefit (e.g., the Australian Height Datum and the North American Vertical Datum). However in NZ, the lack of a single vertical datum means that to obtain a quasigeoid that agrees with the existing offset vertical datums, it is necessary to input this (offset) information into the quasigeoid through a series of iterations until convergence occurs. This novel technique has not been attempted before in practice, although a useful preliminary mathematical framework is given by Rummel and Teunissen (1988).

1.5 Outline and structure of thesis

This thesis is divided into seven chapters. Chapter one is an introductory section that explains the context for vertical datum (and height system) definition and the need for different vertical datums in NZ to be unified. It also describes the physical geographic characteristics of NZ to provide the necessary context for the remainder of the thesis.

Chapter two describes height systems and vertical datums. It starts with the comparison of ten different types of height that can be used to define a height system. Several different approaches to the definition and practical realisation of vertical datums are then addressed along with a number of phenomena that can affect their accuracy. This leads into a description of the current NZ vertical datums and the problems that exist with them. The advantages and disadvantages of defining a unified NZ vertical datum by the least-squares adjustment of the existing precise levelling observations are discussed. To ascertain the feasibility of this approach in NZ, an adjustment of the levelling observations is then undertaken. To provide an international context to the NZ situation, the height systems and approaches to vertical datum definition of five different jurisdictions are also compared and contrasted. The chapter is concluded with a proposal for a new modernised height system for NZ.

Chapter three describes each of the datasets and the preparation that was undertaken on them before they were used in the computation of a gravimetric quasigeoid and the unified vertical datum in NZ. This required the selection of the "best" GGM for the NZ region and the application of reductions to the terrestrial gravity observations

(cf. Amos and Featherstone, 2003a, 2003b). The marine gravity observations were crossover adjusted under contract by *Intrepid Geophysics* (Brett, 2004) before their combination with a grid of satellite altimetry derived gravity anomalies (Amos *et al*., 2005). The digital elevation model (DEM) used for gravity interpolation and TC computation is also presented with the GPS-levelling data set that is necessary to verify the computed quasigeoids and the vertical deflections used to assess the GGMs (Amos and Featherstone, 2004).

When quasigeoids are computed using Stokes's formula, a pre-requisite is that all of the topographic masses have been condensed on or below the quasigeoid. Chapter four describes the different topographic reductions (TC, downward continuation, co-geoid, and the primary and secondary indirect effects) that need to be applied to gravity anomalies before they can be used to compute a quasigeoid. Three approaches to the computation of TCs are compared in NZ to determine the best method for the subsequent quasigeoid computations. It was found that the prism integration derived corrections were superior to those computed by FFT or Hammer charts.

Stokes's function also requires a regular grid of gravity observations. Chapter four also shows that the interpolated grids of gravity observations can be adversely affected if the source observations are not regularly spaced. The Featherstone and Kirby (2000) gravity reconstruction method is implemented with the Goos *et al*. (2003) tests to determine the best way to interpolate gravity observations and their associated TCs. The refined Bouguer anomaly solution was selected because it produced a smoother surface in areas of sparse gravity observations. This study concluded that the solutions using prism integration computed TCs were the best.

The computation of gravimetric quasigeoids using Stokes's kernel function is covered in Chapter five, specific emphasis being placed on the deterministic modification of the kernel as a method of reducing the truncation error associated with the use of spatially limited gravity data. Stochastic modifications were not tested because reliable estimates of the error variances of the Earth's gravity data are not currently known in NZ. Five deterministic modifications are compared in the NZ environment with the purpose of identifying the optimum modification and cap size for the NZ dataset. The Featherstone *et al*. (1998) deterministic modification (with

an integration cap of 1.5° and modification degree 40 was chosen for use in the NZ quasigeoid computations.

Chapter six addresses the unification of the 13 NZ vertical datums. Three existing techniques (geopotential number, gravimetric geoid and the geodetic boundary value problem) are contrasted. The weakness of these approaches is that their solutions do not properly incorporate the effect of using data in terms of multiple offset vertical datums. Consequently, a new "iterative quasigeoid unification" methodology is described that accounts for the effects of local vertical datum offsets in the datasets used to compute a gravimetric quasigeoid. The "iterative" approach is implemented over NZ to demonstrate its validity and to generate a quasigeoid that can be used to unify the vertical datums.

The thesis is concluded in Chapter seven with a recommendation for a new vertical datum for NZ that unifies the 13 existing disparate vertical datums using a gravimetric quasigeoid. Several recommendations for future work to improve the proposed datum based on prospective new data sets are also suggested, especially given the forthcoming Gravity Recovery and Climate Experiment (GRACE), Gravity field and steady state Ocean Circulation Explorer (GOCE) and Earth Gravity Model 2007/8 (EGM07/8) global geopotential models (e.g., Kenyon *et al*., 2006).

an integration cap of 1.5° and modification degree 40 was chosen for use in the NZ quasigeoid computations.

Chapter six addresses the unification of the 13 NZ vertical datums. Three existing techniques (geopotential number, gravimetric geoid and the geodetic boundary value problem) are contrasted. The weakness of these approaches is that their solutions do not properly incorporate the effect of using data in terms of multiple offset vertical datums. Consequently, a new "iterative quasigeoid unification" methodology is described that accounts for the effects of local vertical datum offsets in the datasets used to compute a gravimetric quasigeoid. The "iterative" approach is implemented over NZ to demonstrate its validity and to generate a quasigeoid that can be used to unify the vertical datums.

The thesis is concluded in Chapter seven with a recommendation for a new vertical datum for NZ that unifies the 13 existing disparate vertical datums using a gravimetric quasigeoid. Several recommendations for future work to improve the proposed datum based on prospective new data sets are also suggested, especially given the forthcoming Gravity Recovery and Climate Experiment (GRACE), Gravity field and steady state Ocean Circulation Explorer (GOCE) and Earth Gravity Model 2007/8 (EGM07/8) global geopotential models (e.g., Kenyon *et al*., 2006).

2 HEIGHT SYSTEMS AND VERTICAL DATUMS IN NEW ZEALAND

2.1 Introduction

Contrary to the perception of most laypeople, the concept of "height" is not straightforward. For example, there are a number of different height systems that can be defined; most (but not all) are related to the Earth's gravity field or an approximation of it (e.g., Featherstone and Kuhn, 2006; Hannah, 2001; Heiskanen and Moritz, 1967, Chapter 4). This Chapter presents the major types of height systems that are available and describes how they are used in the definition of a vertical datum. The height systems and vertical datums currently used in NZ are then presented and discussed in the context of the merits of each system. This is used as the context for the proposal for a modernised unified height system for NZ.

2.2 Height Systems

There are many different types of height system that can be broadly classified according to the way that the Earth's gravity field is modelled (i.e., gravity can be observed, modelled or not used). This Section defines and compares the major height systems proposed over the years. It also points out their respective advantages and disadvantages using information that has been adapted from Heiskanen and Moritz (1967, Chapter 4); Vaníček *et al*. (1980); Vaníček and Krakiwsky (1986); Jekeli (2000); Dennis and Featherstone (2003); and Featherstone and Kuhn (2006). Also new height systems are covered (e.g. Tenzer *et al*., 2005; Santos *et al*., 2006).

2.2.1 Geopotential numbers

Strictly, all natural or physical height systems must be based on geopotential numbers, C (Featherstone and Kuhn, 2006; Vaníček and Krakiwsky, 1986; Heiskanen and Moritz, 1967, Chapter 4). A geopotential number is the difference in potential from a reference equipotential surface, W_0, (usually the geoid) to the potential at the point of interest, W_P (cf. Figure 2.1). This definition is shown algebraically in Equation (2.1) (Heiskanen and Moritz, 1967, Eq. 2-25) where: P is the point of interest; P_0 is the corresponding intersection of P with the geoid along the plumbline; and g is the gravity vector along the plumbline, dz.

$$C = W_0 - W_P = \int_{P_0}^{P} g\, dz \tag{2.1}$$

Geopotential numbers are measured in geopotential units (GPU), where 1 GPU = 10 m^2s^{-2}. Because they do not have units of length, they are less intuitive to non-technical users. They accurately predict the flow of water (water will flow from a higher geopotential number to a lower one based on laws of physics and potential theory) and provide a theoretical zero misclosure regardless of the levelling route taken, i.e. holonomity (e.g., Heiskanen and Moritz, 1967, Chapter 4; Sansò and Vaníček, 2006).

Geopotential numbers can not be directly observed because there is no instrument that can actually measure gravity potential. Instead, they are practically determined using geopotential differences (ΔC) that are derived from precise levelling and gravity observations (e.g. Torge, 2001, p.208):

$$\Delta C = g_{mean}\ dn \tag{2.2}$$

where g_{mean} is the average surface gravity value and dn is the difference in height (both along the precise levelling route). The requirement for surface gravity observations is common to most types of height (cf. Sections 2.2.2 to 2.2.8).

2.2.2 Dynamic heights

To overcome the intuitive problem with geopotential numbers not being expressed in units of length, the dynamic height, H^{dyn}, was proposed by Helmert (1884). These heights are obtained by dividing the geopotential number by a constant gravity value, g_0, often chosen to be the value of normal gravity, γ, at 45°. The dynamic height is defined by:

$$H^{\text{dyn}} = \frac{C}{g_0} \tag{2.3}$$

Dynamic heights are very simple to compute (if the geopotential number is known) and because they retain the same characteristics as the geopotential number they predict the flow of fluids correctly and give a holonomic zero levelling loop closure. Its unit of length changes depending on the gravity constant used and so it is

therefore generally not the same as a Système International (SI) metre. The dynamic height does not have a geometrical meaning because it is a purely physical quantity (e.g., Heiskanen and Moritz, 1967, Chapter 4; Jekeli, 2000).

These heights are typically obtained by applying a dynamic correction to spirit levelled height differences. These corrections can be very large if g_0 is not representative of the region concerned. For example a levelling line with a height difference of 1000 metres at the equator, $g \approx 978{,}000$ mGal, $g_0 = 980{,}600$ mGal, then the dynamic correction is -2.7 metres (Torge, 2001). No evidence has been found to suggest that dynamic heights have actually been used in practice.

2.2.3 Orthometric heights

The orthometric height, H^{ortho}, is defined as the length of the curved plumbline from a point, P, to its intersection with the geoid, P_0, as shown in Figure 2.1 and is given by:

$$H^{\text{ortho}} = \frac{C}{\overline{g}} \tag{2.4}$$

where $\overline{g}$ is the integral mean value of gravity along the plumbline and is given by:

$$\overline{g} = \frac{1}{H^{\text{ortho}}} \int_0^H g(z)\, dz \tag{2.5}$$

To determine $\overline{g}$, the exact path of the plumbline through the Earth and also the gravitational acceleration at all points along that plumbline need to be known. This requires knowledge of gravity variations (cf. Strange, 1982) or the mass-density distribution (cf. Sünkel, 1986; Allister and Featherstone, 2001) through the topography (Dennis and Featherstone, 2003; Featherstone and Kuhn, 2006). Because this information is not available, it is not possible to observe or compute a *true* orthometric height, despite what many people seem to believe.

To overcome this limitation, several approaches have been developed to approximate $\overline{g}$. Each approximation results in a different kind of orthometric height, which is normally named after its proponent.

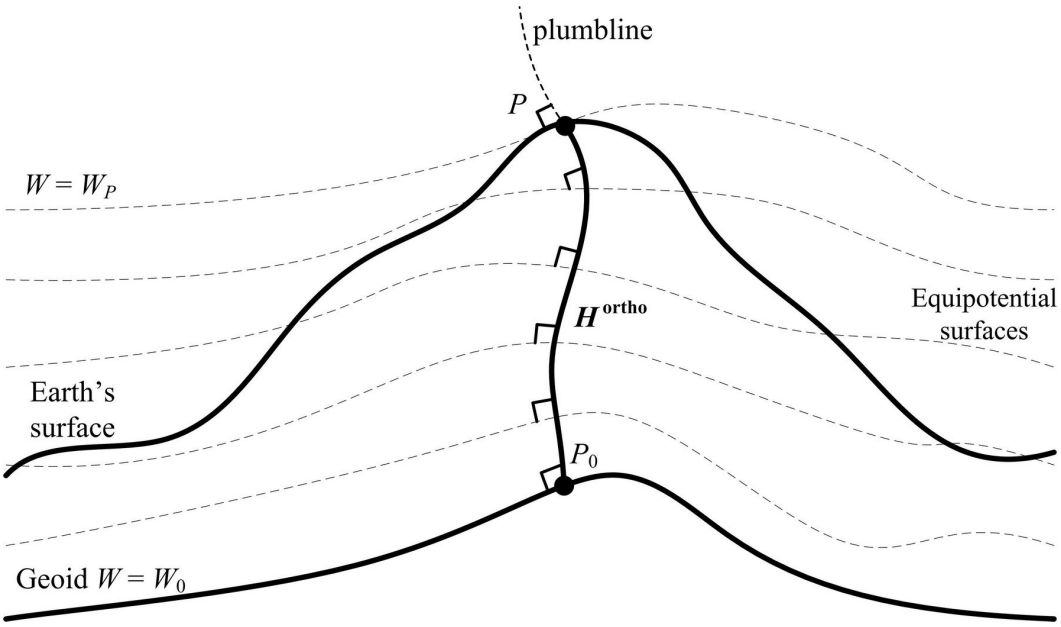

Figure 2.1 The orthometric height (H^{ortho}) of P (adapted from Featherstone and Kuhn, 2006)

2.2.4 Helmert orthometric heights

The approximation of Helmert (1890) is based on the Poincaré-Prey relationship for integral mean gravity (Heiskanen and Moritz, 1967, p. 167):

$$\overline{g}^{\,\text{Helmert}} = g^{s} + \frac{1}{2}\frac{d\gamma}{dh} H^{\,\text{ortho}} - 2\pi G\rho H^{\,\text{ortho}} \tag{2.6}$$

where $g^{\,\text{s}}$ is the observed gravity at the topographic surface, $d\gamma/dh$ is the vertical free-air gradient of gravity (Equation 3.7), G is the universal gravitational constant, and ρ is the (assumed constant) topographic mass density. The right-most term in Equation (2.6) is the Bouguer shell gravity expression (divided by two) that accounts for the topographic mass above the geoid but neglects the terrain effects.

Helmert-orthometric heights are simple to compute as they do not require assumptions to be made about the mass-density or terrain corrections. This simplification means that the Helmert-orthometric height is not a very good approximation. Their computation requires either a geopotential number (computed from precise levelling and gravity observations, Section 2.2.1) or the application of an orthometric correction (OC) to precisely levelled height differences. The OC of a

height difference between points *A* and *B* is given by Heiskanen and Moritz (1967, p. 168) as:

$$OC_{AB} = \sum_{A}^{B} \frac{g^s - \gamma_0}{\gamma_0} dn + \frac{\overline{g}_A - \gamma_0}{\gamma_0} H_A - \frac{\overline{g}_B - \gamma_0}{\gamma_0} H_B \tag{2.7}$$

where *dn* is the spirit levelled height increment; $\overline{g}_A$ and $\overline{g}_B$ are Poincaré-Prey estimates of the integral mean values of gravity along the plumblines by Equation (2.6); and γ_0 is normal gravity at 45°N/S.

Helmert-orthometric heights can be quite different from their *true* orthometric counterparts due to the large corrections to precise levelling observations that are necessary. Nevertheless they are probably the most common type of "orthometric" height in actual use (Featherstone and Kuhn, 2006).

The integral mean gravity formula in Equation (2.6) uses an (assumed) constant value for the topographic mass-density. Allister and Featherstone (2001) demonstrated that in the Darling Ranges of Western Australia, the use of a variable density in this equation can affect the computed OC by up to ~0.08 mm. Because no digital density information is available it is not possible to corroborate these findings for NZ (cf. Section 4.10).

2.2.5 Neithammer orthometric heights

Neithammer (1932) orthometric heights are based on a mean gravity approximation such that (Rapp, 1961; Krakiwsky, 1965):

$$\overline{g}^{\,\text{Neithammer}} = g^s + \frac{1}{2}\frac{d\gamma}{dh} H^{\,\text{ortho}} - 2\pi G\rho H^{\,\text{ortho}} + \delta g^T - \overline{\delta} g^T \tag{2.8}$$

where δg^T is the terrain effect at the topographic surface and $\overline{\delta} g^T$ is the integral mean terrain effect on gravity along the plumbline between the topographic surface and the geoid. The latter is given by:

$$\overline{\delta} g^T = \frac{1}{H^{\,\text{ortho}}} \int_0^{H^{\,\text{ortho}}} \delta g^T \, dH \tag{2.9}$$

These heights are a closer approximation of the true orthometric height than the Helmert height (although the Tenzer *et al*. (2005) methodology is better) and also apply the smallest corrections to precise levelling observations (Dennis and Featherstone, 2003). They are, however, more computationally demanding than Helmert and so are used in practise less frequently.

2.2.6 Mader orthometric heights

Mader (1954) orthometric heights use the mean gravity approximation such that (Krakiwsky, 1965):

$$\overline{g}^{\,\text{Mader}} = g^{s} + \frac{1}{2}\frac{d\gamma}{dh}H^{\,\text{ortho}} - 2\pi G\rho H^{\,\text{ortho}} + \frac{\delta g^{T} - \delta g_{0}^{T}}{2} \tag{2.10}$$

where δg^{T} and δg_{0}^{T} are the terrain corrections (TCs; cf. Chapter 4) applied at the topographic surface and the geoid, respectively. This assumes that the value of the TC changes linearly along the plumbline to the geoid so an average value is used in the height computation. The requirement to determine two TC terms makes them more complex than Helmert to compute, however they are simpler to evaluate than Neithammer heights.

2.2.7 Rigorous orthometric heights

Tenzer *et al*. (2005) and Santos *et al*. (2006) show that in order to obtain a more rigorous orthometric height, it is necessary to take into account (in addition to the effect of terrain roughness and normal gravity) the additional effects coming from the masses contained in the geoid that is not accounted for by the Helmert approach and from mass-density variations within the topography. This approach takes into account (in addition to Helmert's approximation) the effects coming from the second-order correction for normal gravity, second-order correction for the Bouguer shell, the geoid-generated gravity disturbance, the terrain-roughness-generated gravity and the lateral variation of topographical mass-density.

Rigorous heights have not been implemented in any national height systems. Numerical computations have been performed in the Canadian Rocky Mountains which are similar to NZ (e.g., Kingdon *et al*., 2005; Santos *et al*., 2006). They

showed that the corrections for the geoid-generated gravity disturbance, terrain-roughness gravity and lateral variation of topographic density are the most important contributors. In these tests the total rigorous correction was approximately 13 cm (elevation ~2,800 m) in comparison to Mader (1954) and Niethammer (1936) corrections of approximately 3 cm. The consequence of the heights being rigorous is that they are relatively complex to compute, but they rely on terms already computed for a geoid model (e.g., terrain corrections).

2.2.8 Normal heights

The *normal gravity field* is defined as the gravity field defined by an Earth-fitting ellipsoid that contains the total mass of the Earth (including its atmosphere) and rotates with at a constant angular velocity more or less equivalent to that of the Earth (Moritz, 1980a). The normal gravity field can be used to define a height that avoids the density hypothesis for the crust. The normal height (H^N) was proposed in 1954 by Molodensky (cited in Molodensky *et al*., 1962). It replaces $\overline{g}$ in Equation (2.4) with normal gravity measured along the curved ellipsoidal normal (of the reference ellipsoid), $\overline{\gamma}$, hence (Jekeli, 2000):

$$H^N = \frac{C}{\overline{\gamma}} \tag{2.11}$$

where

$$\overline{\gamma} = \frac{1}{H^N} \int_0^{H^N} \gamma(h)\, dh \tag{2.12}$$

It is defined geometrically as the distance along the ellipsoidal surface normal from the reference ellipsoid to the telluroid (Figure 2.2). The telluroid was defined by Molodensky as the surface whose normal potential, U, at every point, Q, is equal to the actual potential, W, at the corresponding surface point, P, or $U_Q = W_P$. The distance between P and the telluroid, Q, is called the height anomaly, ζ. This is related to the ellipsoidal height, h, (see Section 2.2.10) by:

$$\zeta = h - H^N \tag{2.13}$$

Normal heights are simple to compute because they do not require knowledge of the internal mass-density structure of the Earth; this is a virtue of Molodensky's theory. Figure 2.2 also shows that the height anomaly is also defined as the distance between the ellipsoid and the quasigeoid (see Section 2.2.9), hence the normal heights can be compatible with GPS heights when they are derived from the quasigeoid. Because normal heights do not have any physical meaning (being defined by a gravity model), they are not as applicable to the real Earth as the orthometric height, additionally they can not universally predict fluid flows (Featherstone and Kuhn, 2006).

The difference between normal and orthometric-type heights increases with elevation. Marti (2003) showed that the differences (between normal and Helmert orthometric heights) in the Swiss Alps are typically less than 2 cm but they can exceed 10 cm on the mountain tops (< 3000 m). The Swiss assessment is comparable in NZ where the highest peak (Aoraki/Mount Cook) is 3754 m. Like the other heights described above, normal heights can be computed by applying a correction to spirit levelled height differences if there are suitably dense gravity measurements along the levelling route.

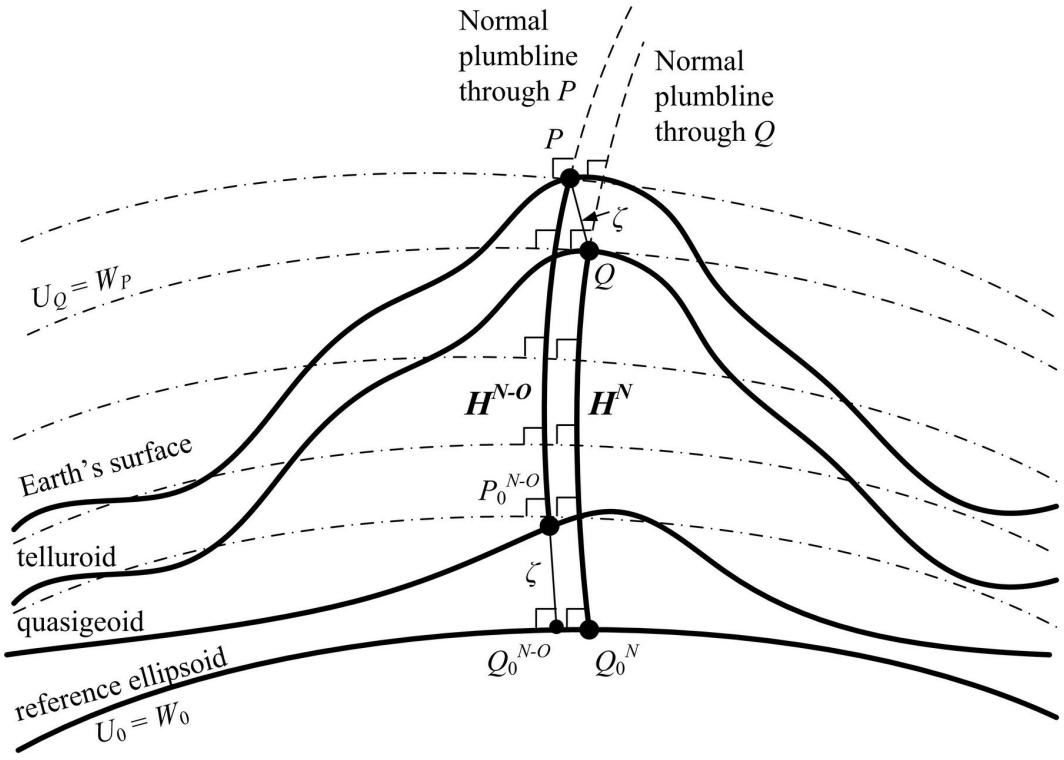

Figure 2.2 The normal and normal-orthometric heights (from Featherstone and Kuhn, 2006)

2.2.9 Normal-orthometric heights

Because many countries do not have gravity observations along all the precise levelling routes, the computation of [approximate] orthometric or normal heights is not strictly possible (cf. Sections 2.2.3 and 2.2.8). To overcome this limitation, the normal-orthometric height system was developed (e.g., Rapp, 1961; Heck, 2003a). The normal-orthometric height is given by:

$$H^{N-O} = \frac{C'}{\bar{\gamma}} \tag{2.14}$$

where C' is the normal-geopotential or spheropotential number given by (cf. Equation 2.1):

$$C' = \int_{P_0}^{P} \gamma \, dn \tag{2.15}$$

This height uses only the normal gravity field to approximate all of the gravity field-related values in the height computation so gravity observations along precise levelling routes are not required. The consequence of this is that normal-orthometric heights are less likely to predict fluid flows correctly than normal and orthometric heights. The normal-orthometric height is defined as the distance from the quasigeoid to the surface of the Earth along the curved ellipsoidal normal (Figure 2.2).

The quasigeoid is identical to the geoid over the oceans and coincides within a few decimetres of it over most land areas, however in areas of large Bouguer anomalies and high topography significant differences can occur (e.g., Featherstone and Kirby, 1998; Tenzer *et al*., 2006). For example, differences of up to about 3.4 m occur in the Himalayas (Rapp, 1997a; Sjöberg, 1995); in Australia the maximum reaches around 0.15 m (Featherstone and Kirby, 1998); the NZ maximum is approximately 0.5 m at Aoraki/Mt Cook (Amos and Featherstone, 2003a). Because the quasigeoid is not a level (i.e. equipotential) surface, it does not have a physical interpretation (Heiskanen and Moritz, 1979, Section 8-3).

In practise, normal-orthometric heights are obtained by applying a normal-orthometric correction (NOC) to precisely levelled height differences (e.g. Heck,

2003a; Torge, 2001). The NOC is a function of latitude and ellipsoidal height. Heck (2003a, p. 295) gives this correction as:

$$\mathrm{NOC} = -\frac{f^*}{R}\sum_{P_1}^{P_2}\left(H_k^S \sin 2\phi_{av} \cos\alpha_k \ \delta s_k\right) \tag{2.16}$$

Where f^* is a GRS80 normal gravity flattening constant (0.0053024; Moritz, 1980a); R is the radius of the Earth (6,371 km); Σ indicates the sum of the individual levelled height difference components between points P_1 and P_2 (i.e., each precise levelling change point between P_1 and P_2); H_k^S is the height at the start point of each levelled height difference; ϕ_{av} is the average latitude between the change points, α_k is the azimuth between the change points; and δs_k is the horizontal distance between the change points; the k subscript indicates a single height difference in the precise levelling line.

Equation (2.16) is quite hard to implement in practise, primarily due to the requirement for the latitude and azimuth to be known for each levelling setup. As such, although normal-orthometric heights have been widely implemented around the world, this has been done using different approximations of Equation (2.16). These approximations typically evaluate the NOC between benchmarks (as opposed to each setup point), only consider the latitudinal change and use simplified coefficients, e.g. NZ (DoSLI, 1989), Australia (Roelse *et al*., 1975). The use of normal-orthometric heights in NZ is discussed further in Section 2.4.2.

2.2.10 Ellipsoidal heights

The ellipsoidal height (h) is the distance from the reference ellipsoid to the Earth's surface along the ellipsoidal surface normal as shown in Figure 2.3. Unlike the heights discussed in the Sections above, it is defined independently of the Earth's gravity field, i.e., it is a purely geometric quantity. Consequently, ellipsoidal heights cannot reliably predict the flow of fluids. They are however relatively easy to define mathematically and as such are the type of height obtained from GNSS receivers (such as GPS).

Ellipsoidal heights are related to orthometric heights by $H = h - N$ and the normal and normal-orthometric heights by $H^N = h - \zeta$ and $H^{N-O} = h - \zeta$ (cf. Figure 2.2 and Figure 2.3). Therefore, the difference between the geoid and quasigeoid is given by $N - \zeta$ (cf. Section 2.2.9).

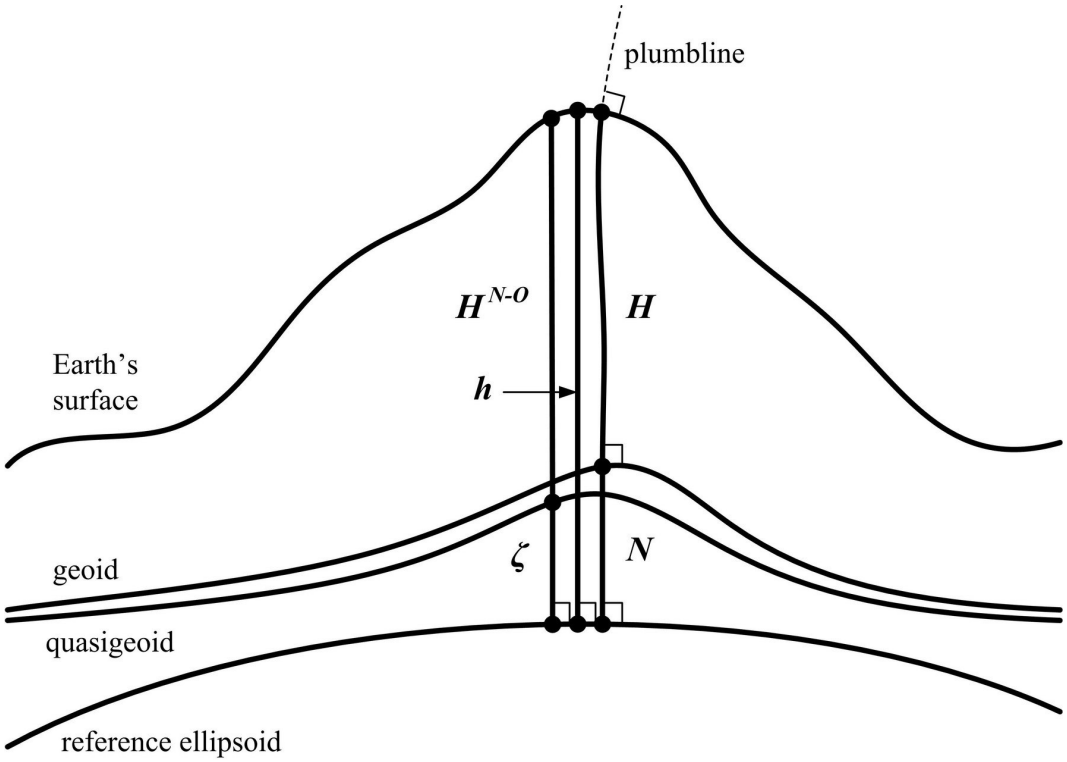

Figure 2.3 The normal-orthometric (H^{N-O}), quasigeoid (ζ), ellipsoid (h), orthometric (H), and geoid (N) heights

2.2.11 Height system summary

This section has defined and compared the major height systems that have been proposed over the years. The dynamic height is the most physically rigorous because it can accurately predict fluid flows and give a holonomic zero levelling loop closure. All of the other systems make successive approximations of the Earth's gravity field. The orthometric, Helmert, Neithammer, Mader, rigorous orthometric and normal heights are all based on geopotential numbers (and therefore require surface gravity observations), the difference between them being the way that they model the integral mean gravity through the Earth. The normal-orthometric height system differs in that it only uses a normal gravity field to approximate the integral mean gravity. The ellipsoidal height is a purely geometric system, so while being easy to

define mathematically, it is not a physical height. Ellipsoidal heights can be related to orthometric heights by defining a geoid, and to normal-orthometric heights by defining a quasigeoid.

2.3 Vertical Datums

2.3.1 Vertical datum definition

To realise a vertical datum, it is necessary to select a type of height system and a compatible reference surface. Once these choices are made, and the observed height differences have been corrected for systematic errors affecting their observation (e.g. Vaníček *et al*., 1980), a vertical datum can be realised point-wise by performing a least-squares adjustment of the corrected height differences to minimise the impact of random errors and to account for the non-holonomity of the levelling loops (e.g. Sansò and Vaníček, 2006).

Ideally this adjustment should be performed on either geopotential numbers or on height differences in a height system that exhibits holonomity (e.g., Feathersone and Kuhn, 2006; Sansò and Vaníček, 2006). However, this is not always possible (e.g., due to the unavailability of gravity observations or the corrections being imperfect). Furthermore, if the heights of multiple points are constrained in the adjustment, then they should all be on the same equipotential surface. If they are not (e.g., where local MSL is fixed at multiple locations around an island or continent), then the vertical datum will be distorted and not represent an equipotential surface over its extents (cf. Featherstone, 2004).

The type of height system chosen normally depends on the data that was available to the agency responsible at the time of datum definition (or the system can be chosen and the necessary data then acquired). For example, if gravity observations are unavailable, then only the normal-orthometric or ellipsoidal height systems can be used (the NOC only requires ϕ and α for computation). The choice of reference surface is guided by the choice of height system, i.e. orthometric heights use the geoid; normal heights the telluroid; normal-orthometric heights the quasigeoid and ellipsoidal heights the ellipsoid.

While it is possible to obtain ellipsoidal heights from GNSS technology, it is not currently possible to directly observe the vertical datum surface in natural/physical height systems (e.g. Featherstone and Kuhn, 2006). Using the assumption that the geoid/quasigeoid and mean sea-level (MSL) in the open oceans are coincident it is possible to relate a vertical datum to the geoid/quasigeoid using local MSL observations. This approach to practical vertical datum definition introduces several issues that are discussed in the following Sections.

A vertical datum can also be defined by computing the geopotential number of the origin point using its ellipsoidal height (from GNSS observations) and absolute gravity value. This approach is well-suited to for the connection of continental height datums (i.e. across large water bodies) and is analogous to the geopotential number method of datum unification (Section 6.3.1). Because it is defined using a discrete number of points it also suffers from the adjustment weaknesses described above.

2.3.2 Determination of mean sea-level (MSL)

In the ideal situation, the datum surface (i.e. zero height) of a height system will coincide with the geoid (true orthometric height system) or quasigeoid (normal-orthometric height system). Because there is no instrument that can directly measure the absolute value of the Earth's geopotential, it is not possible to physically observe the geoid. Recall that over the oceans the geoid and quasigeoid are coincident and that they represent an equipotential surface that generally approximates MSL in the open oceans. Thus, the acquisition of sea-level observations at tide-gauges is the most common method of MSL determination and thence vertical datum definition. MSL observations are affected by three major problems: 1) sea-level is affected by the presence of tides and other temporal phenomena; 2) the presence of sea surface topography (SSTop), storm surges, non-linear tides etc. in the coastal zone (e.g., Merry and Vaníček, 1983; Pugh, 1987; Hipkin, 2000; Featherstone and Kuhn, 2006); and 3) secular changes in sea level due to climate-related effects (e.g., Pugh, 2004).

To determine MSL at a coastal tide-gauge, it is necessary to make sea-level observations over a sufficiently long period to take into account the full tidal signature. The major tidal effects (caused by the precession and nutation of the

Moon and Sun over an 18.6 year metonic cycle) result in the diurnal (daily) and semi-diurnal (twice-daily) tides that are most noticeable at the coast (e.g., Melchior, 1981). Other celestial objects (e.g., planets) also have effects on the observed tides, but these are much smaller in magnitude than those of the sun and moon (e.g., Pugh, 2004). Therefore, to determine MSL independent of these tidal effects, it is necessary to make regular (e.g., hourly) sea-level observations over at least an 18.6 year period. For many of the NZ datums, this duration requirement has not been achieved (cf. Section 2.4.1).

2.3.3 Sea surface topography and sea-level changes

In addition to accounting for the 18.6 year tidal cycle, the observed MSL will depart from the geoid due the phenomenon called sea surface topography (SSTop). Also called dynamic ocean topography (DOT), it includes the effects of changes in sea water temperature, salinity, atmospheric pressure, prevailing winds, water currents, etc. (Pugh, 1987). SSTop is dynamic in that it is constantly changing (e.g., due to seasonal weather variations). The magnitude of SSTop in the open oceans can be estimated by differencing a global geopotential model (cf. Section 3.2) with satellite-altimetry derived sea-surface heights (e.g., Hipkin, 2000; Hwang *et al.*, 2002; Rio and Hernandez, 2004; Pugh, 2004).

The magnitude of SSTop in the open oceans can cause MSL to depart from the geoid by up to two metres (e.g. Rapp, 1983; 1994; 1991a, 1995). In coastal areas (where most tide-gauges are located), the determination of SSTop becomes more even more difficult (e.g. Merry and Vaníček, 1983; Hipkin, 2000). This is because satellite altimetry does not work well close to the coast (e.g., Deng and Featherstone, 2006) and also many tide-gauges are located in estuaries or river mouths where they are also used for monitoring shipping-lanes. These areas are influenced by the freshwater outflows that can significantly alter the observed MSL at different times. Other non-SSTop effects, such as storm surges, also cause irregular short-term rises in sea-level (Pugh, 1987; Featherstone and Kuhn, 2006). The presence of SSTop causes the MSL measured at tide-gauges to depart from a single equipotential surface, thus offsets can occur between adjacent or overlapping vertical datums (e.g., Hipkin, 2000; Hipkin *et al.*, 2004).

2.3.4 Land uplift, subsidence and glacial isostatic adjustment

Precise levelling-based vertical datums are established on the assumption that the benchmarks and tide-gauges used in their definition will remain stable. Given that sea-level observations spanning at least 18.6 years are required to obtain a tide-free MSL determination (Section 2.3.2), it is essential that the tide-gauge remain stable for that period (or its motion be monitored). Because tide-gauges are frequently sited on reclaimed land or wharves, they can be subject to subsidence over their operating period. Localised subsidence (e.g. within a few hundred metres) can be determined from precise levelling, however, more widespread movements are more difficult to isolate. The best way to determine the absolute movement of tide-gauges (and therefore identify changes in MSL) is by the co-location of continuous GNSS receivers and/or absolute gravimeters (e.g., Bevis *et al*., 2002; Teferle, 2000; Teferle *et al*., 2007; Woodworth *et al*., 1999).

As well as the physical tide-gauge the benchmarks that physically form a vertical datum are also affected by uplift and subsidence. The gradual (and/or sudden, e.g., earthquakes) movement of the benchmarks progressively degrades the quality of the vertical datum because the documented heights will progressively become out of date. The two major causes of these movements (at a regional scale) are tectonics and glacial isostatic adjustment (GIA). Additional sources of movements include groundwater changes (causing swelling/contraction), water/mineral/oil extraction, etc.

Tectonic uplift or subsidence can be either long-term gradual changes or sudden irregular movements. The longer term velocities are small (i.e. mm/year, e.g., Walcott, 1984; Otway *et al*., 2002; Beavan *et al*., 2004) but the cumulative effect can be significant over time (e.g. metres/100 years). Because of the long time-frames involved, they can often be predicted. The sudden irregular movements are often unpredictable and frequently violent. The major cause is the rupture of tectonic faults during earthquakes. Vertical movements of > 2 m along tectonic fault ruptures are not unusual in NZ (e.g. Beanland *et al*., 1990; Begg and McSaveney, 2005).

During the last ice age (~10,000 years ago), parts of the Earth's crust (notably northern Canada and Scandinavia) were depressed by the weight of several kilometres of ice. When the ice melted, this weight was removed and the Earth's

surface started rebounding to an equilibrium level (which is still ongoing today). This phenomenon is called GIA. The observed rates of uplift vary depending on location but they can reach rates of 7 mm/yr in northern Canada (Mainville and Craymer, 2005) and 8 mm/yr in Scandinavia (e.g., Lambeck *et al*., 1998; Fjeldskaar *et al*., 2000; Lidberg *et al*., 2007). The observed GIA uplift in Scandinavia may also be affected by tectonic uplift of ~1 mm/yr (e.g., Wu *et al*., 1999; Fjeldskaar *et al*., 2000).

An attribute of GIA is that when elastic rebound occurs as a result of land-based ice melt, the resulting redistribution of mass from the melt-water into the oceans can cause elastic compression in other areas. For example, in northern Europe where uplift of 8 mm/yr is observed in Sweden, this decreases (in a regular radial pattern around Scandinavia) to an uplift of 3 mm/yr in the North Sea (Lambeck *et al*., 1998).

2.3.5 Earth tides

The definition of the vertical datum zero level is also affected by the permanent deformation of the Earth caused by the Sun and the Moon (and other planets to a lesser extent). There are three models for dealing with these permanent tidal effects: 1) the *mean-tide* includes both the permanent and elastic effects and so retains masses external to the Earth; 2) the *tide-free* or *non-tidal* eliminates both the permanent and elastic effects; and 3) the *zero-tide* eliminates only the permanent effect but retains elastic effect (e.g., Ekman, 1989, 1995; Poutanen *et al*., 1996; Rapp, 1989; Rapp *et al*., 1991b; Burša 1995).

The choice of tidal model used in geoid computation, height system definition and the reduction of gravity observations has been the subject of much conjecture. Arguments have been made both for and against each of the options (e.g. Ekman, 1989; Poutanen *et al*., 1996). The mean-tide model approximates the shape of sea-level in its long term equilibrium state and so is physically meaningful. Because it includes the external masses caused by the tidal deformation, it is not consistent with the requirements of Stokes's formula (e.g., Poutanen *et al*., 1996). Also it uses an integral mean gravity for height determination and so will introduce a bias due to the inclusion of the external masses.

The tide-free model is compliant with Stokes formula because the permanent and time-independent external masses are removed. However, its use requires different Love numbers to be assigned to the permanent and time-dependent deformations. Since Love numbers are not well known for the real Earth, this introduces an error. The zero-tide model is also compliant with Stokes formula (because all of the external masses are removed). Its advantage over the tide-free model is that it does not require the use of an assumption regarding elasticity (in the removal of the indirect effect) and so the reduction can be done completely by potential theory (Poutanen *et al*., 1996).

Resolution 16 of the International Association of Geodesy (IAG) in 1983 (IAG, 1984) endorsed the use of the zero-tide as the preferred tidal model. However, this endorsement has not been universally adopted. For example, the definition of the International Gravity Standardisation Net 1971 (IGSN71, Morelli *et al*., 1974) gravity system is in terms of the mean-tide model (Poutanen *et al*., 1996), while EGM96 (Lemoine *et al*., 1998) and the United States G96SSS and GEOID96 geoid models (Smith and Milbert, 1999) have been produced in terms of the tide-free model because the majority of the source data for these appeared to be in terms of that model (Lemoine *et al*., 1998).

For the purpose of this study, the IAG-recommended option of the zero-tidal system will be used to ensure that any new NZ height system is in agreement with international standards. Although the difference between the zero-tide and tide-free models only ranges from 0.12 cm to 1.78 cm over NZ (for latitudes of 34.5°S and 47.0°S respectively), it is still important for consistency purposes that all quantities (i.e. heights, gravity observations, geoid models) are in terms of the same tidal system.

Equations to transform height differences, gravity observations and geoid heights between tidal systems were presented in Ekman (1989). Using the subscripts m, n, and z to denote the mean-tide, tide-free and zero-tide models respectively the relations for height differences between two stations are given by:

$$\begin{aligned}
\Delta H_m - \Delta H_z &= 29.6 \left(\sin^2 \phi_N - \sin^2 \phi_S\right) \text{ cm} \\
\Delta H_z - \Delta H_n &= 29.6 \left(\gamma - 1\right)\left(\sin^2 \phi_N - \sin^2 \phi_S\right) \text{ cm} \\
\Delta H_m - \Delta H_n &= 29.6 \ \gamma\left(\sin^2 \phi_N - \sin^2 \phi_S\right) \text{ cm}
\end{aligned} \tag{2.17}$$

where ϕ_N and ϕ_S are the latitudes of the northern and southern stations respectively. The corresponding transformations for gravity observations at latitude ϕ are given by (where δ is an unobservable arbitrary constant ≈ 1.53, Ekman, 1989):

$$\begin{aligned}
g_m - g_z &= -30.4 + 91.2 \sin^2 \phi \ \ \mu\text{Gal} \\
g_z - g_n &= \left(\delta - 1\right)\left(-30.4 + 91.2 \sin^2 \phi\right) \ \ \mu\text{Gal} \\
g_m - g_n &= \delta\left(-30.4 + 91.2 \sin^2 \phi\right) \mu\text{Gal}
\end{aligned} \tag{2.18}$$

2.4 New Zealand's vertical datums

2.4.1 Tide-gauges

Historically, the tide-gauges used in NZ have been established in harbours and rivers by local port authorities for use in the prediction and verification of tide tables (Blick *et al*., 1997). Data from these gauges was also analysed by Land Information NZ (LINZ) and its predecessor agencies (Department of Survey and Land Information – DoSLI; Department of Lands and Survey – L&S) to determine MSL at each site. This MSL value was then used as the zero height (of the local vertical datum) to which a local levelling network was referenced.

The NZ tide-gauges are generally in locations that are less-than-optimal for vertical datum definition purposes. They are frequently situated in harbours or rivers (within a few kilometres of the coast), whereas the ideal locations are either offshore or on the open coast to minimise the non-linear tidal effects that occur near the coast (e.g., Pugh, 2004). This means that the observed MSL will not necessarily be representative of the region in which the datum is to cover (e.g., Hipkin, 2000; Cross *et al*., 1987; Merry and Vaníček, 1983; etc.).

2.4.2 Precise levelling networks

First-order precise levelling in NZ ($\pm 2\,\text{mm}\sqrt{k}$, where k is the distance in km; Blick, 2006, pers. comm.) has historically been the method for precise height transfer in NZ. Trigonometric and barometric levelling (±0.5 – 15 metres; Blick, 2006, pers. comm.) has also been used to densify the precise levelling networks. However, due to the lesser accuracy, this is not generally considered part of the NZ precise height network.

There currently exist >16,000 km of two-way first-order precise levelling that has been observed since the 1960s to give the coverage current shown in Figures 2.4 and 2.5 (e.g., Gilliland, 1987). These networks were observed in a piece-meal fashion and the large loop around the South Island (Figure 2.5) was only completed in the late 1980s. Each local vertical datum (LVD) has been defined using a least-squares adjustment to give heights for its constituent marks.

It can be seen from Figures 2.4 and 2.5 that the levelling coverage is not uniform over NZ. Some areas, such as the central North Island (Figure 2.4) in the vicinity of the Moturiki tide-gauge (37º 38'S, 176º 10'E), have a very strong network configuration, but other areas, notably the south-west of the South Island (Figure 2.5), are particularly sparse.

The irregular coverage has a great deal to do with the topography over which the levelling runs traverse and the lack of roads in the sparser areas along which precise levelling lines are placed for stability and access reasons. The South Island levelling lines that transect the Southern Alps/Kā Tiritiri o te Moana (Figure 2.5) are limited to the three mountain passes over them. It is not practicable (or in some cases possible) to obtain a denser spirit levelling network in these remote areas due to the steep and rugged topography (gradients are frequently over 45º in the mountainous areas, cf. Section 4.9).

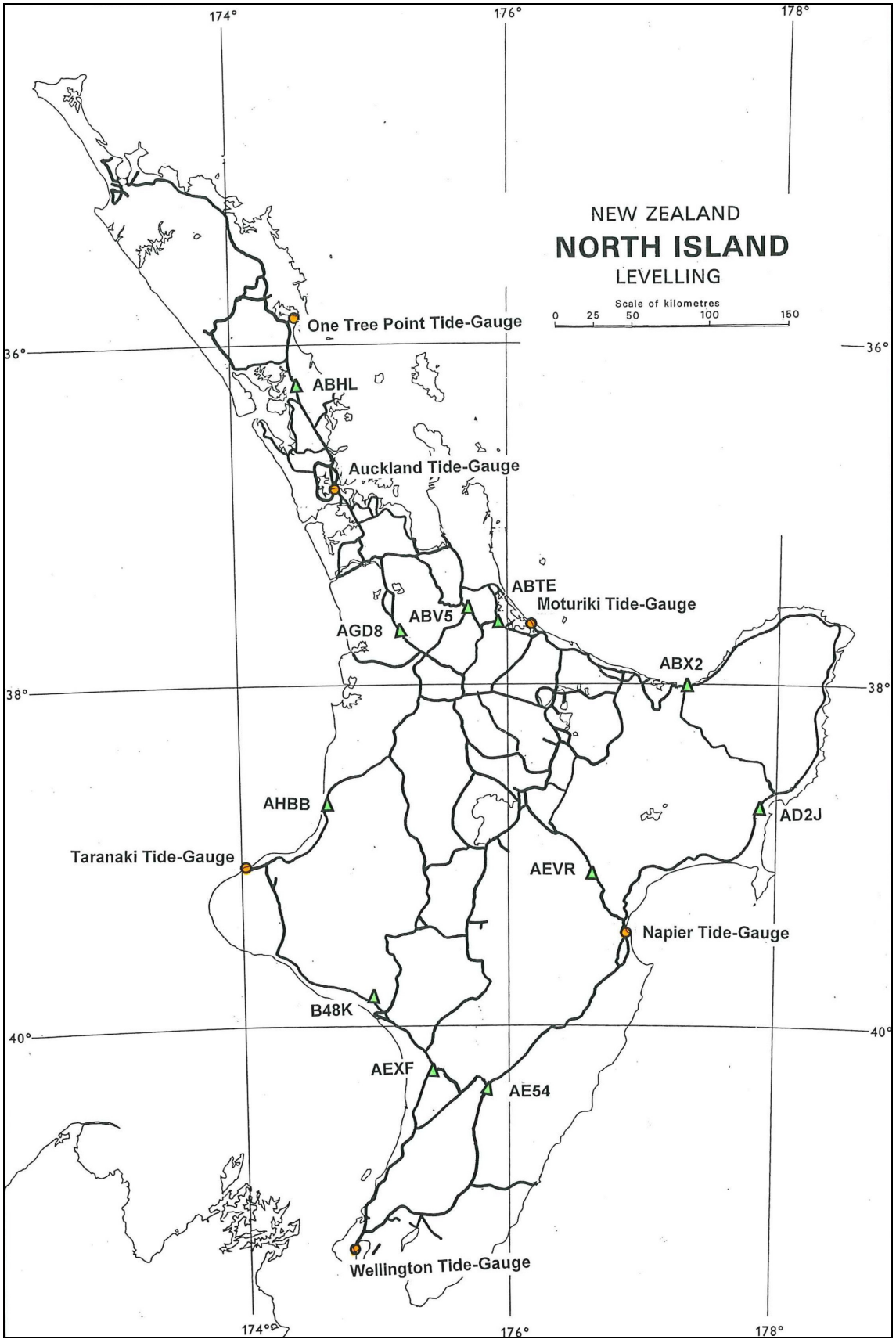

Figure 2.4 NZ North Island precise levelling networks, tide-gauges and vertical datum junction points (adapted from NZNCGG, 1991; Mercator projection)

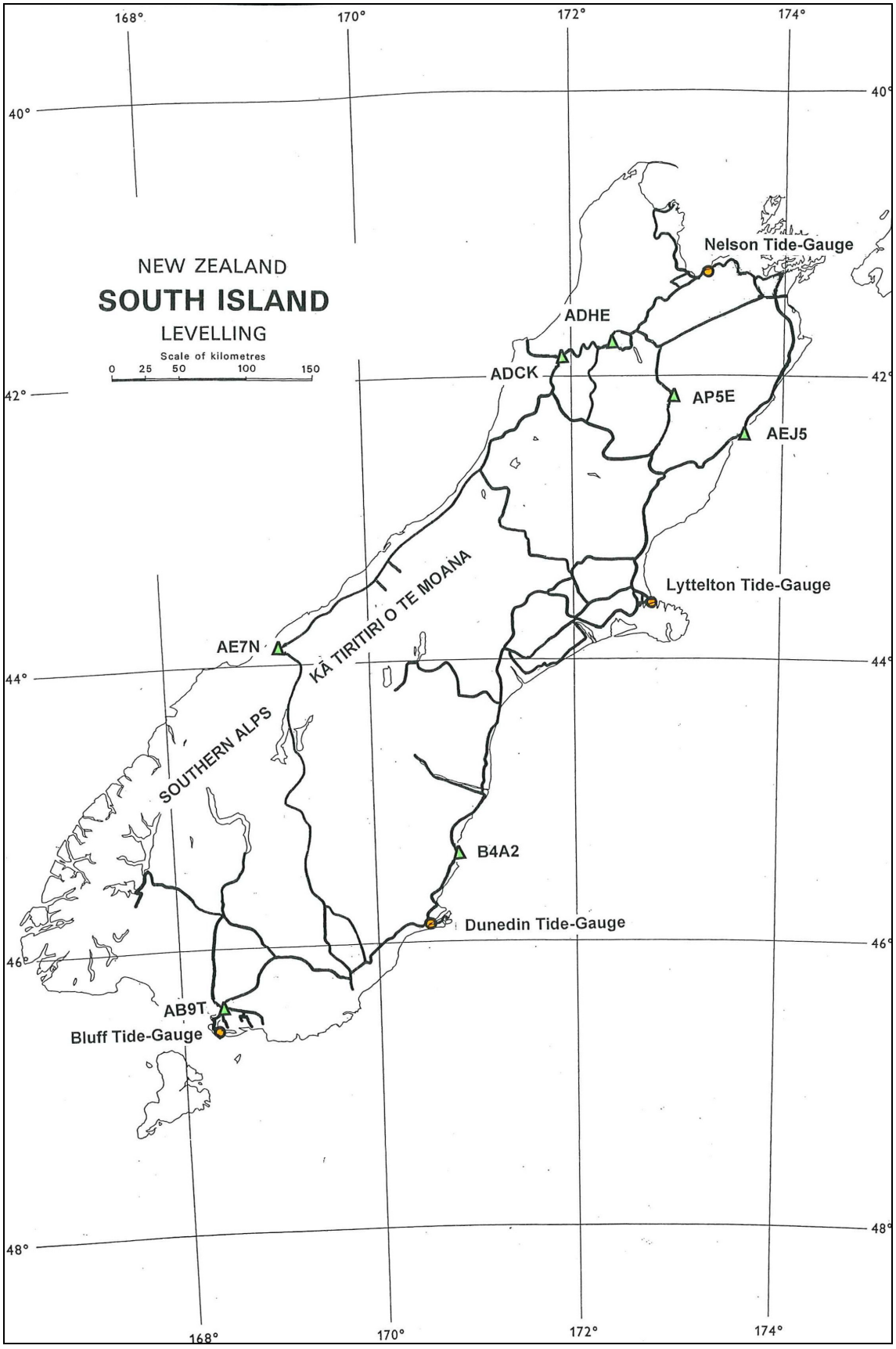

Figure 2.5 NZ South Island precise levelling networks, tide-gauges and vertical datum junction points (adapted from NZNCGG, 1991; Mercator projection)

LINZ currently uses the normal-orthometric height system for the publication of its official heights in NZ (DoSLI, 1989). These heights are incorrectly referred to as *orthometric* heights by the LINZ geodetic database (www.linz.govt.nz/gdb) and in many publications (e.g. Gilliland, 1987; DoSLI, 1989; Reilly, 1990). True orthometric heights can never be realised because of the (impossible) requirement to know integral mean gravity through the topography at each point (cf. Section 2.2.3).

The NZ normal-orthometric heights are derived by the application of a cumulative normal-orthometric correction, $\mathrm{NOC_{NZ}}$, to the precisely levelled height differences. This correction uses a static potential value and is given by:

$$\mathrm{NOC_{NZ}} = -\left[2\upsilon \sin 2\phi_{\mathrm{mid}} \left[1 + \left(\upsilon - 2\beta / \upsilon \right) \cos 2\phi \right] z \right] H_{\mathrm{av}}\, \delta\phi \qquad (2.19)$$

The coefficients υ and β are respectively 0.002 506 and 0.000 007; ϕ_{mid} is the mid-latitude between the levelling benchmarks; z is one arc-minute (in radians); H_{av} is the average height of the instrument at all setups between the benchmarks (in metres); and $\delta\phi$ is the latitude difference (in arc-minutes, positive southwards) between the benchmarks. This formula was printed incorrectly in Gilliland (1987), but Equation (2.19) is correct (DoSLI, 1989).

The NOC used in NZ is a generalised version of the more rigorous NOC given by Equation (2.16). Australian heights are reduced by a generalised form of Rapp's (1961) formula (Roelse *et al.*, 1975), however this version is more rigorous than Equation (2.19). When the NOC is evaluated using Equations (2.16) and (2.19) (45º 00' S, 1000 m altitude, 1 km north-south levelling line with 20 change points 50 m apart) corrections of 0.83 mm and 0.73 mm respectively are obtained. If the comparison is repeated with a more typical average height of 200 m the resulting NOC's are 0.17 mm and 0.15 mm respectively. At the summit of Aoraki/Mt Cook (3754 m, 43º 36' S, 1 km north-south levelling line), the respective NOCs are 3.12 mm and 2.73 mm. The cumulative effect of the differences between the equations at typical heights is insignificant (e.g. a 100 km levelling line at a height of 1000 m would have a cumulative difference of 1 cm).

2.4.3 Local vertical datums

Each of the NZ LVDs is based on a determination of MSL at different tide-gauges over a varying range of time intervals (normally three years) and epochs (primarily 1920 – 1970). Heights for each LVD are in terms of the normal-orthometric height system (Section 2.4.2). Table 2.1 lists each of the 13 major LVDs with the approximate location of the origin and the time period over which MSL was observed for its definition. The locations of these gauges are also shown in Figures 2.4 and 2.5.

The Dunedin-Bluff 1960 datum is a notable anomaly in Table 2.1. Unlike the other datums, it was defined by fixing a Dunedin 1958 height in Balclutha and a Bluff 1955 height in Invercargill. Also the Stewart Island 1977 datum is not defined by a "long"-term-tide-gauge derived estimate of MSL. Instead its "zero" is based on the MSL value determined from three temporary tide-gauges established around Stewart Island/Rakiura using observations over three to five successive (but not simultaneous) tides. The Stewart Island approach was based on trigonometric heights that could be in error by 0.2-0.3 metres, consequently the resulting MSL could be in error by 0.5 metres from the long-term trend.

Datum	**Approximate Location**		**Observation Period**
	Latitude (S)	**Longitude (E)**	
One Tree Point 1964	35° 52'	174° 30'	1960 - 1963
Auckland 1946	36° 52'	174° 47'	1909 - 1923
Moturiki 1953	37° 38'	176° 10'	1949 - 1952
Gisborne 1926	38° 39'	178° 02'	1926
Napier 1962	39° 28'	176° 55'	*Unknown*
Taranaki 1970	39° 03'	174° 02'	1918 - 1921
Wellington 1953	41° 17'	174° 47'	1909 - 1946
Nelson 1955	41° 15'	173° 16'	1939 - 1942
Lyttelton 1937	43° 38'	172° 42'	1918 - 1933
Dunedin 1958	45° 54'	170° 28'	1918 - 1937
Dunedin – Bluff 1960	*Datum defined by adjustment only, no physical origin*		
Bluff 1955	46° 34'	168° 24'	1918 - 1934
Stewart Island 1977	46° 55'	168° 04'	1976 - 1977 (*5 tides only*)

Table 2.1 Levelling datum origins and periods of MSL observation, compiled from Gilliland (1987); Pearse (1998); and LINZ internal records

Over the years, many smaller or special-purpose datums have also been defined. A significant number of these (e.g. Tekapo, Karapiro and Maraetai; Table 2.2) were defined with respect to other existing datums for specific hydro-electric power projects. Others (e.g. Deep Cove, Tikinui, and Chatham Island) were defined from short periods (e.g. several months) of tidal data and are only used for local purposes (Hannah, 2001).

In 2001, as part of the LINZ survey and title automation project, Landonline, (www.landonline.govt.nz), the large number of disparate datums was amalgamated into a smaller subset of major ones. Table 2.2 lists the 13 current major datums and the "historical" datums that they now comprise. Also, shown in brackets in Table 2.2 are any vertical offsets that have been applied (by LINZ) to ensure that the datums are consistent with each other. These offsets were determined from observed precise levelling differences. The "EDS" datums are not truly separate datums. They were "defined" in terms of the same tide-gauges (and levels) as their parent datums; the different name was only used to identify the more recent precise levelling that was used to generate heights in terms of them (cf. Figures 2.4 and 2.5), consequently no offset has been applied.

Where two or more vertical datums abut or overlap, it is possible to estimate the offset that exists between the datums at that point. This offset will be affected by the length and route of the precise levelling to get to the junction point; any deformation that has occurred while the levelling was being carried out (although this deformation will be "spread-out" by the least-squares adjustment); as well as observational and reduction errors; etc. The consequence of this is that when vertical datums join at multiple places, the observed offsets will also differ.

The observed (post-adjustment) NZ vertical datum offsets have been obtained from the LINZ geodetic database by comparing the heights of marks that are located at the junction points of the adjacent datums. The offsets are shown in Table 2.3; the junction points are shown on Figures 2.4 and 2.5. The Taranaki-Moturiki offset observed at AHBB (-0.455 m) is abnormally large compared to the other offsets. This is probably due to mark movement between the observation of the respective levelling lines, however it was not possible to confirm or disprove this hypothesis from analysis of the precise levelling records.

Major Datum	Constituent datums
One Tree Point 1964	One Tree Point 1964
	Unahi (-0.1859 m)
	Pouto Point (+0.0396 m)
	Island Point (+0.0701 m)
	Tikinui (+0.0244 m)
	Tinopai (+0.0853 m)
Auckland 1946	Auckland 1946
Moturiki 1953	Moturiki 1953
	Maraetai (-2.3304 m)
	Moturiki EDS (0.0000 m)
	Wanganui 1953 (-0.0604 m)
Gisborne 1926	Gisborne 1926
Napier 1962	Napier 1962
Taranaki 1970	Taranaki 1970
	Port Taranaki (0.0000 m)
	Taranaki EDS (0.0000 m)
Wellington 1953	Wellington 1953
	Kaitoke (-0.0148 m)
Nelson 1955	Nelson 1955
Lyttelton 1937	Lyttelton 1937
	Lyttelton EDS (0.0000 m)
	Pahau (+2.2265 m)
	Waitaki (+1.3015 m)
Dunedin 1958	Dunedin 1958
	Alexandra (+0.9235 m)
	Dunedin EDS (0.0000 m)
Dunedin – Bluff 1960	Dunedin – Bluff 1960
Bluff 1955	Bluff 1955
Stewart Island 1977	Stewart Island 1977

Table 2.2 Major New Zealand height datums and their constituent datums, offsets to major datums are shown in brackets

Mark	Vertical Datum 1	Vertical Datum 2	Offset
ABHL	One Tree Point 1964	Auckland 1946	+0.206
AGD8	Auckland 1946	Moturiki 1953	-0.069
ABTE	Auckland 1946	Moturiki 1953	-0.075
ABV5	Auckland 1946	Moturiki 1953	-0.067
ABX2	Gisborne 1926	Moturiki 1953	-0.075
AD2J	Napier 1962	Gisborne 1926	+0.166
AEVR	Napier 1962	Moturiki 1953	+0.099
AE54	Napier 1962	Taranaki 1970	+0.046
AE54	Taranaki 1970	Wellington 1953	+0.191
AE54	Napier 1962	Wellington 1953	+0.237
AHBB	Taranaki 1970	Moturiki 1953	-0.455
B48K	Taranaki 1970	Moturiki 1953	-0.014
AEXF	Taranaki 1970	Moturiki 1953	-0.019
AEXF	Taranaki 1970	Wellington 1953	+0.102
AEXF	Moturiki 1953	Wellington 1953	+0.121
AEJ5	Nelson 1955	Lyttelton 1937	+0.014
AP5E	Nelson 1955	Lyttelton 1937	+0.039
ADHE	Nelson 1955	Lyttelton 1937	-0.086
ADCK	Nelson 1955	Lyttelton 1937	-0.076
B4A2	Lyttelton 1937	Dunedin 1958	-0.054
AE7N	Lyttelton 1937	Dunedin 1958	-0.087
ADP2	Dunedin-Bluff 1960	Dunedin 1958	-0.019
AB9T	Dunedin-Bluff 1960	Bluff	-0.001

Table 2.3 Datum offsets determined from height differences and junction points of vertical datums (metres)

2.4.4 Sea-level variability and vertical datum definition

Sea-level observed at tide-gauges can vary on annual, inter-annual and inter-decadal cycles, hence the particular epoch of data used will affect the determined level of MSL (Bell *et al*., 2000). Analysis of sea-level observations by LINZ (Rowe, 2006, pers. comm.) has shown that variations in the observed MSL can differ from the long-term average by 10 cm over a three-year period. Figure 2.6 shows the monthly sea-level trends for the Wellington tide-gauge (Rowe, 2006, pers. comm.). Given that a number of the vertical datums were defined by only three years of sea-level observations (cf. Table 2.1) it is very likely that they are based on a MSL that is not representative of the long-term average. For example if MSL was defined from data

indicated by either of the horizontal lines in Figure 2.6 rather than the full set, the resulting MSL could be offset from the long term average by over 50 mm.

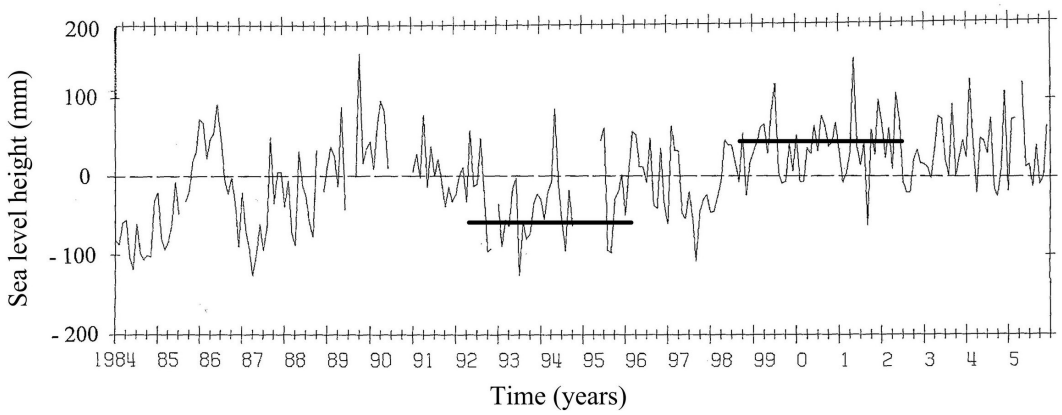

Figure 2.6 Monthly sea-level observations for Wellington tide-gauge from LINZ records, 1984 – 2006 (mm)

The sea-level observations for the periods when the vertical datums were defined have not yet been processed by LINZ so it was not possible to quantify if they were affected by such anomalies. Based on the very limited data available (e.g., Figure 2.6) an offset of 5-10 cm could readily be attributed to the choice of epoch for the shorter duration definitions (e.g., One Tree Point 1946, Moturiki 1953, Gisborne 1926, Napier 1962, Taranaki 1970, Nelson 1955, Stewart Island 1977; cf. Table 2.1).

2.4.5 Relative sea-level from tide-gauges

Because the LVD zero levels have not been updated since their definition, it is likely that they would be affected by any changes in MSL since then (e.g. Douglas, 1991). Hannah (1988; 2004) analysed the historic sea-level observations made at the Auckland, Wellington, Lyttelton and Dunedin tide-gauges. This analysis showed positive MSL trends over the period of the observations at all four gauges; these trends are summarised in Table 2.1. Hannah (2004) concluded an average sea level rise rate of 1.6 mm/yr (±0.2 mm/yr) that when corrected for present-day GIA effects (using Peltier, 2000) gives an average absolute sea level rise of 2.1 mm/yr. The later rate is comparable with global estimates of sea level rise thereby inferring that, on average, there is little differential uplift occurring in NZ.

To verify the sea level observation derived uplift rates, the University of Otago and GNS Science have operated continuous GPS receivers at the four tide-gauges for the

last 6.5 years (on average). The daily height solutions for these records (www.geonet.org.nz) show uplift at three ports and subsidence in Wellington (Table 2.4; cf. Section 2.4.6). The MSL sea level trend determinations will be better long-term estimates than the GPS determinations because they use a longer time-series and so will be less affected by shorter-term variations in sea level (cf. Section 2.4.4). The MSL change since the definition of the vertical datums has been calculated by adding the tide-gauge and GPS trends and multiplying by the number of years since the establishment of the vertical datum.

The large changes at Auckland and Lyttelton (15 and 28 cm respectively) show that it is likely that the vertical datum zero levels do not coincide with the current MSL. This comparison assumes that the change in sea-level is linear. Recent studies (e.g., Church and White, 2006; Holgate and Woodworth, 2004) show that sea-level rise may have accelerated in the 20th century and hence the tide-gauge estimated trends may be conservative. Although this analysis has not been undertaken at the other tide-gauges, it is reasonable to expect that the MSL changes would be of a similar magnitude.

Tide-gauge / vertical datum	**Sea-level observation data period**	**Tide-gauge observed MSL trend (mm/yr)**	**Tide-gauge height trend from GPS (mm/yr)**	**MSL change since datum definition to 2007 (m)**
Auckland 1946	1899 – 1999	+1.30	+1.2 (5.4 yrs)	+0.153
Wellington 1953	1891 – 1893 1903 – 2001	+1.78	-1.4 (6.9 yrs)	+0.021
Lyttelton 1937	1901 – 2001	+2.08	+1.9 (6.7 yrs)	+0.279
Dunedin 1958	1899 – 1986 1989, 1990, 1996, 1998	+0.94	+0.9 (6.9 yrs)	+0.090

Table 2.4 MSL trends observed by Hannah (1988; 2004) and GPS observed height changes at tide-gauges

2.4.6 Vertical deformation in New Zealand

The Earth's surface in the NZ region experiences relative movements that deform its shape (e.g., earthquakes). The horizontal movements are reasonably well known (e.g. Beavan and Haines, 1997; Beavan, 1998; Walcott, 1984), but in comparison the vertical movements are not. There are regional studies that show areas within the

Taupo Volcanic Zone (see Figure 2.7) are subsiding by up to 10 mm/yr (Otway *et al*., 2002). At the local level, subsidence of as much as 8.5 m has been reported as occurring in the Wairakei area (38º 37' S, 176º 06' E) due to geothermal energy draw-off for electricity generation (Bevin *et al*., 1984).

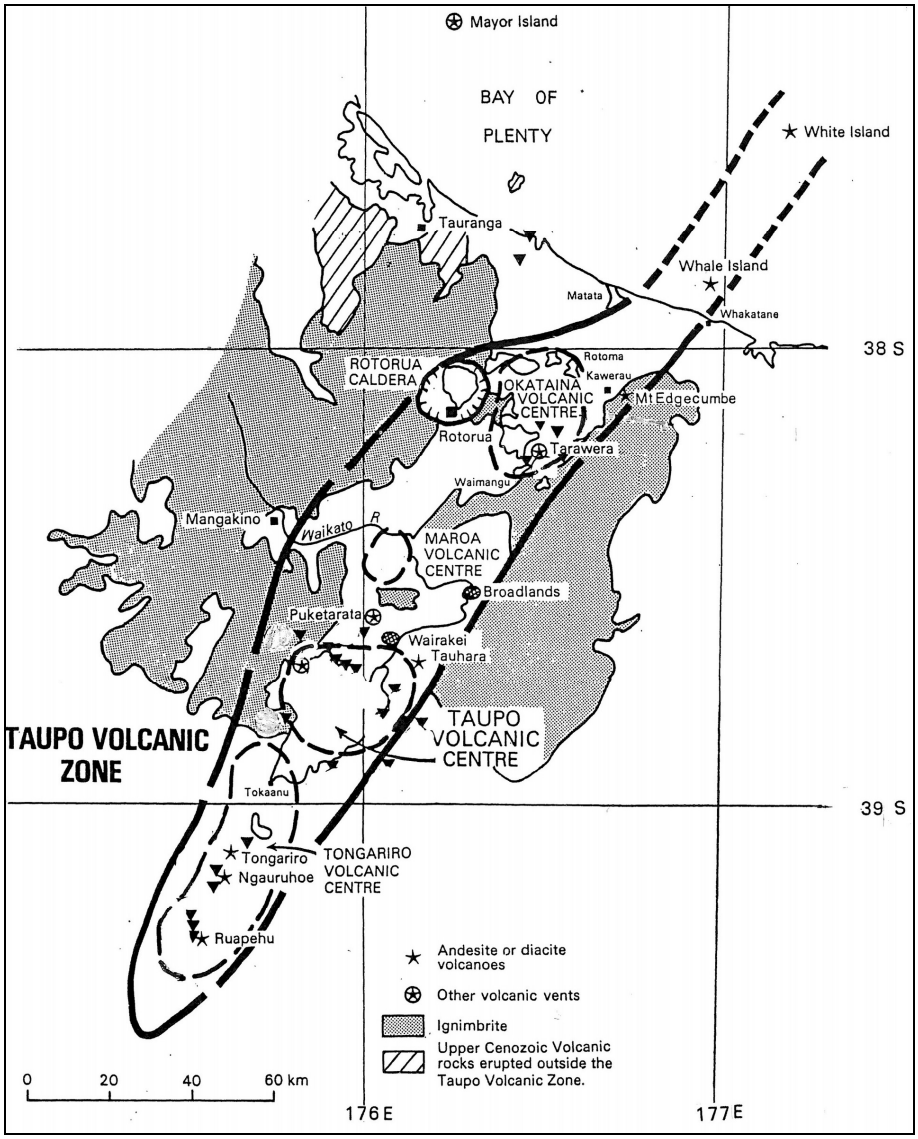

Figure 2.7 Taupo Volcanic Zone (adapted from Bevin *et al*., 1984)

The Southern Alps/Kā Tiritiri o te Moana (cf. Figure 2.5) are subjected to uplift rates in the order of 10 mm/yr due to the interaction of the Pacific and Australian tectonic plates along the Alpine Fault (e.g., Beavan *et al*., 2004; Walcott, 1984; Wellman, 1979). These subsidence and uplift rates have a slow but continuous effect on the height of stations and the gravity observations (cf. Section 3.3).

Earthquakes, however, often have the largest short-term effect on heights. Important NZ examples include, subsidence of up to 2 m from the Edgecumbe earthquake of 1987 (Beanland *et al*., 1990); uplift of 2.7 m from the Inangahua earthquake of 1968 (Lensen and Otway, 1971); uplift of 2.4 m and subsidence of 0.9 m from the Napier earthquake of 1931 (Henderson, 1933); and uplift of 1.3 – 2.1 m (6.4 m maximum) in Wellington Harbour from the 1855 Wairarapa earthquake (Begg and McSaveney, 2005).

Unfortunately, there is currently no national model of vertical deformation in NZ that can be used for transforming heights and gravity anomalies observed at one epoch to another (a horizontal deformation model is used in NZGD2000, e.g., Blick, 2003). Vertical deformation models are now available for other regions (e.g., Fennoscandia, Vestøl, 2006). To obtain a general impression of the uplift/subsidence that is currently occurring in NZ, the vertical components of the daily coordinate solutions from 28 PositioNZ (www.linz.govt.nz/positionz) and GeoNet (www.geonet.org.nz) continuous GPS stations with records of longer than two years were computed (Table 2.5). This revealed an average uplift/subsidence rate of 2 mm/yr for NZ (Table 2.6), although, the quality of this estimate is limited by the short (4.1 year) data span and potential presence of systematic errors in the data. Geological estimates of uplift rates of 1-5 mm/yr can be obtained from raised beaches etc. (e.g., Ota *et al*., 1992; Stirling, 1992; Cooper and Norris, 1995; Berryman *et al*., 2000). It is important to note that these geological rates have been deduced from movements occurring over geological time scales and therefore may not be representative of sea level movements in the last century.

Although the evidence for uplift is not conclusive it is still useful to evaluate its potential effect. Given that most of the NZ LVDs were defined about 50 years ago, this could mean that the heights of the benchmarks and that of the datum origins may have risen by 10 cm on average from then until 2006 (assuming linear uplift). As well as the effect on the vertical datum origins, uplift will also cause a gravity decrease at the gravity observation points in proportion to the height change. Ekman (1989) approximates gravity to decrease at a rate of 0.02 mgal/mm of uplift, therefore the NZ average uplift of 2 mm/yr will result in an annual gravity decrease of 0.04 mgal/yr (or 2.0 mgal over 50 years).

Site	Longitude	Latitude	Rate (mm/yr)	Duration (years)
WHNG	174º 19’ E	35º 48’ S	3.19	3.6
AUCK	174º 50’ E	36º 36’ S	1.18	6.9
CORM	175º 45’ E	36º 52’ S	2.97	3.5
HAMT	175º 07’ E	37º 48’ S	2.57	3.5
TRNG	176º 16’ E	37º 44’ S	5.34	3.8
HIKB	178º 18’ E	37º 34’ S	2.90	3.5
GISB	177º 53’ E	38º 38’ S	1.87	4.4
TAUP	176º 05’ E	38º 45’ S	7.27	4.7
MAHO	174º 51’ E	38º 31’ S	2.16	2.8
NPLY	174º 07’ E	39º 11’ S	3.06	3.7
WANG	174º 49’ E	39º 47’ S	1.87	3.6
HAST	176º 44’ E	39º 37’ S	0.98	4.2
DNVK	176º 10’ E	40º 18’ S	3.94	4.1
MAST	175º 35’ E	37º 44’ S	0.48	3.9
WGTN	176º 16’ E	41º 04’ S	1.47	6.9
NLSN	173º 26’ E	41º 11’ S	0.75	2.8
GLDB	172º 32’ E	40º 50’ S	0.15	2.8
WEST	171º 48’ E	41º 45’ S	-0.57	2.2
KAIK	173º 32’ E	42º 26’ S	0.48	2.8
LKTA	172º 16’ E	42º 47’ S	2.18	2.8
MQZG	172º 39’ E	43º 42’ S	3.09	6.9
HOKI	170º 59’ E	42º 43’ S	5.49	6.9
MTJO	170º 28’ E	43º 59’ S	1.95	6.3
HAAS	168º 47’ E	44º 04’ S	0.21	2.4
OUSD	170º 31’ E	45º 52’ S	2.00	6.9
LEXA	169º 18’ E	45º 14’ S	-0.01	2.7
MAVL	168º 07’ E	45º 22’ S	-1.22	2.5
BLUF	168º 17’ E	46º 35’ S	0.55	2.7

Table 2.5 GPS observed uplift rates at PositioNZ stations with more than two years observations

Max	Min	Average	STD
7.3	-1.2	2.0	1.9

Table 2.6 Statistics of NZ uplift/subsidence estimates from continuous GPS observations at 28 PositioNZ sites (mm/yr)

2.4.7 NZ national levelling adjustment

One proposal (Hannah, 2001) for the establishment of a new vertical datum for NZ is to undertake a least-squares adjustment of all the NZ precise levelling observations to give a single vertical datum for NZ (or more strictly one datum for each of the North and South Islands). This approach would "complete" the adjustment of precise levelling programme that was commenced in the 1960's (cf. Section 2.4.2). Establishing vertical datums by precise levelling is the traditional methodology that has been used by many countries (cf. Section 2.5) hence defining a NZ vertical datum in this way would follow international "best-practise".

A risk of using this methodology is that, during the ~40 year period that the precise levelling observations have been acquired, the levelled benchmarks may have been subjected to non-uniform localised vertical deformation due to earthquakes, geothermal draw-off, etc. (cf. Section 2.4.6). The deformation may have occurred (1) since the levelling was carried out and (2) between the individual levelling campaigns that were used to complete a particular levelling line (or loop).

This means that although an adjustment may provide a statistically strong solution, a proportion of the adjusted heights will not be representative of the current ground positions. Also, because not all of the precise levelling lines are connected into "adjustable" loops there is a risk that the adjustment would be ill-conditioned and therefore give a weak result. Such an adjustment is less likely to identify the systematic (non-random) errors caused by the vertical deformation during the acquisition of the precise levelling observations. An additional constraint is that only the reduced height differences between benchmarks are available (i.e., the individual setup information is not accessible). It would also be necessary to only constrain one tide-gauge for each (North and South Island) adjustment to prevent the distortions of the type that are present in the Australian Height Datum (Roelse *et al*., 1975).

Nevertheless an adjustment of the precise levelling observations was undertaken as part of this study to determine the effect on benchmark heights (cf. Figures 2.4 and 2.5). The first step was to capture the 23,892 height differences between 10,108 benchmarks from the original computation sheets into a *Microsoft Access* database so that they could be effectively manipulated. A least-squares adjustment was then performed on the observations for each datum using the LINZ in-house *SNAP*

software (www.linz.govt.nz/downloadsoftware) to determine any capture errors by identifying "large" height changes or residuals. The results of these adjustments (North Island - Table 2.7; South Island - Table 2.8) were used to identify and correct erroneous or conflicting observations (e.g., from levelling carried out before and after major earthquakes, regional deformations, etc.).

Datum	Pts	Obs	Standard error	$\sum(\text{resid})^2$	Average error	Outliers (> 99%)
One Tree Point 1964	566	1,230	0.803	428.8	0.020	9
Auckland 1946	694	1,462	0.300	69.1	0.027	0
Moturiki 1953	2,702	6,138	0.409	576.0	0.021	0
Gisborne 1926	705	1,772	0.429	196.9	0.029	0
Napier 1962	452	990	0.241	31.4	0.024	0
Taranaki 1970	274	752	0.308	45.5	0.025	0
Wellington 1953	632	1,502	0.397	137.9	0.023	8
North Island	5,967	13,846	0.461	1,672.1	0.031	21

Table 2.7 Summary of North Island precise levelling adjustments, average error of heights is 95% confidence level in metres, "outliers" are observations over 99% confidence level and are included in adjustment

Datum	Pts	Obs	Standard error	$\sum(\text{resid})^2$	Average error	Outliers (> 99%)
Nelson 1955	865	1,970	0.412	188.0	0.028	9
Lyttelton 1937	2,139	5,382	0.423	579.7	0.032	0
Dunedin 1958	613	1,550	0.447	187.7	0.025	0
Dunedin-Bluff 1960	409	838	0.237	24.1	0.024	0
Bluff 1955	134	306	0.292	14.7	0.014	0
South Island	4,141	10,046	0.412	1,000.2	0.046	7

Table 2.8 Summary of South Island precise levelling adjustments, average error of heights is 95% confidence level in metres, "outliers" are observations over 99% confidence level and are included in adjustment

Once the separate datum adjustments were working, they were incorporated into combined least-squares adjustments for the North and South Islands (bottom rows of Tables 2.7 and 2.8). Because the combined solutions adjust all of the observations within an island simultaneously the statistics in bottom rows of Tables 2.7 and 2.8 are not the sum individual datum statistics. Some of the connections between datums are tenuous, such as, only single one-way height differences between terminal

benchmarks. Overall the adjustment statistics were consistent between the individual datums and the combined networks with no major problems occurring during the combination. This demonstrates that it is technically feasible to undertake a combined adjustment of the observations.

The spatial extent of a vertical datum established by the adjustment of precise levelling observations is limited to the location of those observations. In NZ this restricts the vertical datum coverage to the major highways (cf. Figures 2.4 and 2.5) and urban areas. Consequently there are large areas of NZ (notably Fiordland and the Southern Alps/Kā Tiritiri o te Moana in the South Island, and Rakiura/Stewart Island) that can not be covered by such a datum. New levelling observations could be acquired to fill some of the gaps in the levelling networks and to identify/quantify the effect of vertical deformation, however the high cost of doing so makes this an impractical on a national scale.

There is also no clear demand from users of the LVDs for a nationally adjusted precise levelling network, most probably because such an adjustment would not provide any additional practical benefits (on a local scale) in addition to those of the LVDs. Also, GNSS users require a quasigeoid that is compatible with the LVD, so a quasigeoid would still need to be computed. Therefore this thesis develops and analyses an alternative approach to establishing a new vertical datum for NZ.

2.4.8 New Zealand Geodetic Datum 2000

The current official horizontal geodetic datum for NZ is New Zealand Geodetic Datum 2000 (NZGD2000; Blick, 2003). It is a three-dimensional geocentric datum that uses the GRS80 ellipsoid (Motitz, 1980) and is aligned to the ITRF96 (Boucher *et al.*, 1998) global reference frame. To incorporate the effects of deformation, NZGD2000 uses a horizontal deformation and velocity model to "correct" observations for the effects of deformation from the time of acquisition to the datum's reference epoch (01 January 2000). This approach enables the integration of observations into the LINZ Landonline database (www.landonline.govt.nz) that are acquired at different times. No vertical deformation or velocity model is used in NZGD2000.

NZGD2000 uses GRS80 ellipsoidal heights as its official height system (Blick, 2003). The use of ellipsoidal heights is becoming increasingly popular amongst users of the geodetic system, even with the limitations described in Section 2.2.10. The most significant of these limitations is the inability of ellipsoidal heights to predict the flow of fluids. Consequently there is a need for any new NZ vertical datum to support the use of ellipsoidal heights and to provide the ability to convert them to naturally based heights that can predict fluid flows (Blick *et al*., 2001).

2.5 International height systems and vertical datums

Before finally deciding on an approach for developing a modernised height system for NZ (and taking for granted the current unique situation of 13 LVDs), it is sensible to examine the height systems and vertical datums that are used in other countries to ascertain if there are any lessons that can be learnt from them. The following Sections compare and contrast the height systems and vertical datums of a selection of countries with the system of NZ (cf. Hannah, 2001).

2.5.1 Australia

Australia differs from New Zealand in that it has a single unified vertical datum (excluding Tasmania) called the Australian Height Datum (AHD; Roelse *et al*., 1975). It was defined in May 1971 by the adjustment of 97,230 km of two-way (mainly third order; ICSM, 2002) precise levelling that was constrained to MSL at 32 tide-gauges around the coast (Roelse *et al*., 1975). The AHD uses a modified version of the normal-orthometric height system (e.g. Holloway, 1988; Featherstone and Kuhn, 2006) where a truncated form of Rapp's (1961) normal-orthometric correction was applied to the spirit levelling observations (cf. Section 2.2.9). As in NZ, no gravity observations were used in the reductions so the AHD is not rigorously based on a physical/natural height system (Featherstone and Kuhn, 2006).

Several gravimetric quasigeoid models have been computed for Australia (e.g., Featherstone *et al*., 2001; Steed and Holtznagel, 1994; Kearsley and Govind, 1991; Gilliland, 1989) that provide a conversion between GNSS derived heights and the AHD. However, because the AHD is not an equipotential surface and the effect of SSTop has been neglected, a slope of approximately 70 cm exists between the north

and the south of the country (Featherstone, 2004, 2006) as well as 1.5 m local distortions (Roelse *et al*., 1975). At the present time, there are no plans to readjust the AHD.

2.5.2 United States of America

The current vertical datum in the United States of America (USA) is the North American Vertical Datum of 1988 (NAVD 88; Zilkoski *et al*., 1992). Its predecessor, the National Geodetic Vertical Datum of 1929 (NGVD 29) is still used in some areas. NAVD 88 incorporated approximately 730,000 km of two-way first- and second-order precise levelling in both the USA and Canada, including 81,500 km of re-levelling. The datum was realised by the adjustment of American, Mexican and Canadian levelling data constrained to a single benchmark (Rimouski, Quebec, Canada) located at the mouth of the St Lawrence River (Zilkoski *et al*., 1992). This differed from NGVD 29, which was constrained at 26 coastal tide-gauge sites. NAVD 88 heights are in terms of the Helmert orthometric height system (see Section 2.2.4); as such observed gravity was used for the height computations. The vertical datums and height systems of the USA are described in detail in Meyer *et al*. (2004; 2005; 2006a, 2006b).

There are currently two official geoid models for the USA that can be used to convert ellipsoidal heights to their [Helmert] orthometric counterparts (Roman *et al*., 2004). These models are the latest in a succession of models (Milbert, 1991; Smith and Milbert, 1999; Smith and Roman, 2001). USGG2003 is a gravimetric geoid that has been computed for the contiguous USA and GEOID03, which is based on USGG2003, but uses 14,185 GPS-levelling heights to fit it to the NAVD 88 height system using least-squares collocation (Roman *et al*., 2004).

2.5.3 Canada

Canada's official vertical datum is called the Canadian Geodetic Vertical Datum 1928 (CGVD28). It was established through the adjustment of approximately 124,000 km of precise levelling that was constrained to MSL observed at six tide-gauges (spread on both coasts of Canada) in 1928. This adjustment (like NAVD 88) used Helmert orthometric heights (Kingdon *et al*., 2005).

Until 1993, 4000 km to 5000 km of levelling was carried out by Natural Resources Canada (NRCan), with about 3000 km of this for maintenance purposes. This reduced to 1200 km from 1994 to 2000; from 2001 only minimal targeted levelling has been undertaken (Véronneau *et al*., 2006). Like NZ, the coverage of the precise levelling data is not uniform, primarily as a result of large areas terrain being unsuitable for this activity and the remoteness of northern Canada. In the case of Canada, the levelling is concentrated along the southern edge of the country.

The Canadian Gravimetric Geoid 2000 (CGG2000; Véronneau, 2002) has been computed to enable users to transform ellipsoidal heights to the CGVD. However this has been seen as an interim step towards a modernised datum (CGRSC, 2004). The current NRCan proposal is to adopt a gravimetric geoid as the new vertical datum and therefore provide a definition in terms of an ellipsoid. This will allow users to access heights in terms of a common reference surface over the entire country rather than just at precise levelling points along the precise levelling routes (Véronneau *et al*., 2006). While enabling the use of GNSS positioning technology, the new datum would be implemented over a long (10 year) period to enable users to properly migrate data from CGVD28. Given the similarities between the existing height systems and the physical environments of NZ and Canada, the Canadian approach to modernisation of its vertical datum can also be applied to NZ. This approach is also advantageous from a financial point of view because it does not require the 16,000 km of precise levelling to be repeated or for gravity observations to be acquired at each levelling point (cf. Section 2.4.2).

2.5.4 Europe

The height systems and vertical datums used in Europe are characterised by their diversity. The vertical datums of the different countries are generally related to MSL estimated at one or more tide-gauges. The tide-gauges are located at various oceans and inland seas (e.g. Baltic Sea, North Sea, Mediterranean Sea, Black Sea, Atlantic Ocean) between which sea-levels can differ by several decimetres (Ihde *et al*., 2002). The height datums are (in many cases) historical and so not all datums represent MSL, some relate to high and low tides instead. Three different height systems are used throughout Europe: [Helmert] orthometric (Belgium, Denmark, Finland, Italy and Switzerland); normal (France, Germany, Sweden, most countries of Eastern

Europe); and normal-orthometric (Norway, Austria, countries of former Yugoslavia) (EUREF, 2006).

The European Vertical Reference Network (EUVN) has been developed as a method of unifying the different national vertical datums to a proposed accuracy of a few centimetres (Ihde *et al*., 2002). The EUVN and the United European Levelling Network 1995/1998 (UELN95/98) adjustment (Ihde *et al*., 2000) define the European Vertical Reference Frame 2000 (EVRF2000). The vertical datum of the EVRF2000 is realised using the zero level through the Normaal Amsterdams Peil tide-gauge (NAP) with a geopotential number of zero; related parameters are defined according to the GRS80; and the zero-tide Earth-tide model (EUREF, 2006).

EVRF2000 has shown that the zero levels of the national vertical datums typically vary in the order of a decimetre, but can reach 50 cm in France and Spain (Ihde *et al*., 2002). This approach to the unification of vertical datums works well in Europe where it is possible to precisely level between datums. In jurisdictions where this is not possible (e.g., NZ which comprises three main islands), an alternative approach (e.g. hydrodynamic levelling, e.g., Cartwright and Crease, 1963) needs to be considered.

2.5.5 Fennoscandia

The height systems of the Fennoscandian countries (Denmark, Finland, Norway and Sweden) are very comprehensive (e.g., Ihde *et al*., 2002; Ádám *et al*., 2000). They are characterised by frequent first- and second-order re-levelling and vertical datum readjustments that are possibly as a result of their long history of settlement and significant uplift due to GIA of over 7 mm/yr (e.g., Lidberg *et al*., 2007; Fjeldskaar *et al*., 2000; Lambeck *et al*., 1998; Pan and Sjöberg, 1998; Ekman, 1996; 1989; Vestøl, 2006). A notable feature that is present in each of the four Nordic countries is that after each major re-levelling, a new vertical datum is released.

Cross *et al*. (1987) report that later versions of the Danish and Finnish height systems have not been well received by users of the systems because they introduced small changes to all benchmark heights for no perceived practical (as opposed to scientific) benefit. It also introduces the potential for confusion if the height datum is not

clearly stated. These are important considerations that need to be taken into account when defining a new vertical datum for NZ. For example, the national precise-levelling adjustment (Section 2.4.7) gives new heights that are typically less than 10 cm different to their existing values.

2.6 A modernised height system for New Zealand

The existing NZ vertical datums can be characterised as disparate, offset (Table 2.3) levelling networks that are (relatively) dense in the populated (flat, coastal) regions and very sparse in the uninhabited or mountainous areas (cf. Section 2.4.2, Figures 2.4 and 2.5). Levelling-based LVDs cannot be easily extended into areas where there are no roads. Trigonometric heighting is able to be used away from roads and can achieve accuracies of 1-2 mm/km if sight lines are 100 to 300 metres in length (Torge, 2001, p254). Such short sight lines can be difficult to achieve (especially in areas of rough topography where roads do not exist) and can therefore make trigonometric heighting as time consuming as precise levelling; hence a different approach is required. Even with the limited spatial extent of the levelling datums, users appear happy to continue using these local systems for many of their applications because their observation technology works well with them (e.g., spirit levels). There is also an increasing demand from users of NZ heights for the ability to convert ellipsoidal heights obtained from GPS receivers to the 13 local normal-orthometric datums (Blick *et al*., 2001).

The issues faced by NZ in regards to the selection of a new vertical datum and height system are very similar to those which are currently being addressed by Canada. Both NZ and Canada have national precise levelling networks that are relatively dense in populated areas and also very sparse (if not non-existent) in their more remote regions. As such, they do not provide uniform vertical datum coverage over the whole of their jurisdictions. A key difference between the two countries LVDs is that while Canada has a single vertical datum, NZ has 13. Also, precise levelling based vertical datums are not compatible with GNSS technology (i.e., ellipsoidal heights) unless they are combined with a precise quasigeoid undulation model (cf. Section 6.3.2). Given that Blick *et al*. (2001) identified "compatibility with ellipsoidal heights" as an essential criterion for any new NZ vertical datum, the

retention of precisely levelled heights on their own as the basis for a vertical datum will not be satisfactory.

Both NZ and Canada experience vertical deformation, although it is caused by different phenomena. In NZ it is a result of tectonics (cf. Section 2.4.6), whereas in Canada it is primarily as a result of GIA (e.g., Mainville and Craymer, 2005). Both GIA and tectonic deformations are broadly predictable on a regional scale, however if they are ignored, the rates are sufficiently high (7 mm/yr) that they will introduce errors into their respective vertical datums. It is therefore important that the effects are accounted for. This is most effectively achieved with a vertical deformation model like that being used horizontally in NZGD2000 (cf. Section 2.4.8; Vestøl, 2006).

There are therefore two main approaches that could be used to define a new vertical datum for NZ, undertake a combined adjustment of the precise levelling networks or define a gravimetric quasigeoid that can be used as the datum surface. The advantages and disadvantages of both options have been described in the previous sections. On balance, the quasigeoid approach was chosen for the development of the new vertical datum, even though its computation may be affected by errors in the gravity data (cf. Section 6.5.1).

A new vertical datum for NZ should be defined using a gravimetric quasigeoid (Figure 2.8). This approach will allow points to have official heights in terms of both a LVD and the ellipsoid (i.e., in terms of NZGD2000). To enable the transformation of heights from the LVDs an additional offset will also need to be used with the quasigeoid. This approach will allow the continued use of the LVDs by users and enable the use of GPS positions with the official height network (Amos, 2006). To ensure that the relationship between the NZ height system and any future world height system is known, absolute gravity observations should be made at one (or more) of the continuous GNSS points defining NZGD2000.

Figure 2.8 Proposed new vertical datum for NZ using a quasigeoid (ζ) and LVD offset (o) to relate heights in the 13 normal-orthometric LVDs and the ellipsoidal NZGD2000

The remainder of this thesis presents the preparations for and computations of the gravimetric quasigeoid that is essential to implement this vertical datum proposal. A unique issue that occurs in NZ is that the input datasets relate to different vertical datums, this aspect is treated in the iterative geoid computation approach discussed further in Section 6.4.

2.7 Summary

This Chapter has discussed several different types of heights as a precursor to the presentation of the existing height systems that are currently used in NZ. Similarly the methodology for the establishment of a vertical datum was described and this was also related to the NZ situation. The NZ height systems and vertical datums were discussed from a historical context and their strengths and weaknesses identified.

An analysis of the readjusted precise-levelling observations showed that, while it is technically possible to develop a new vertical datum in this way, the methodology is subject to several significant disadvantages in NZ (e.g., vertical deformation during and since the precise-levelling observations were made, high cost to obtain new levelling observations, and the poor spatial coverage of resulting datum). Therefore, this thesis develops and analyses an alternative approach to establishing a new vertical datum for NZ.

A number of international vertical datums were investigated to determine which aspects of these that would be useful in a modernised NZ system. This resulted in a conceptual model for the development of a new national vertical datum for NZ that is

very similar to the proposal also being considered in Canada. This proposal will retain the normal-orthometric height system that NZ currently uses. The 13 existing vertical datums will also be retained, but they will be related to a reference ellipsoid through an official quasigeoid model coupled with additional local offsets. This will ensure that the new national vertical datum is compliant with ellipsoidal heights as well as the existing 13 LVDs. Since a regional quasigeoid model does not currently exist for NZ, the remainder of this thesis deals with the computation of such a quasigeoid model that takes into account the fact that the input data is referenced to 13 existing datums that are offset from each other.

3 DATA PREPARATION

3.1 Introduction

This Chapter describes the different data sets that have been compiled for use in the quasigeoid computations described in the remainder of this thesis. The Chapter is divided into seven sections that discuss each of the datasets, with a number of sections having Appendices that describe the actual analysis in more detail. Global geopotential models are introduced first, and the results of the model comparisons in Appendix A are summarised. The terrestrial gravity data is then presented with an outline of the various gravity anomaly reductions that need to be performed. The actual database is described in Appendix B. The marine gravity and satellite altimetry datasets are then described with the crossover adjustment summarised in Appendix C. The combination of these two datasets by least-squares collocation (LSC) is then presented. The Chapter concludes with a description of the digital terrain model and the GPS-levelling points that are to be used to compute the LVD offsets and to determine the fit of the quasigeoid.

3.2 Global Geopotential Models

3.2.1 Background

A global geopotential model (GGM) comprises a set of fully normalised spherical harmonic coefficients that model the long-wavelength features of the Earth's external gravity field. The quasigeoid height ζ is computed from a GGM using Equation (3.1) and the gravity anomaly Δg from Equation (3.2), where GM is the product of the Newtonian gravitational constant and mass of the Earth (assumed equal to that of the geocentric reference ellipsoid); γ is normal gravity on the surface of the reference ellipsoid; (r,θ,λ) are the geocentric spherical polar coordinates of the computation point; a is the semi-major axis length of the geocentric reference ellipsoid; $\overline{P}_{nm}(\cos\theta)$ are the fully normalised associated Legendre functions for degree n and order m; $\delta\overline{C}_{nm}$ and $\overline{S}_{nm}$ are the fully normalised spherical harmonic coefficients of the GGM, reduced for the even zonal harmonics of the geocentric reference ellipsoid (e.g. Torge, 2001, pp. 271-272).

$$\zeta_M = \frac{GM}{r\gamma}\sum_{n=2}^{M}\left(\frac{a}{r}\right)^n \sum_{m=0}^{n}\left(\delta\bar{C}_{nm}\cos m\lambda + \bar{S}_{nm}\sin m\lambda\right)\bar{P}_{nm}\left(\cos\theta\right) \tag{3.1}$$

$$\Delta g_M = \frac{GM}{r^2}\sum_{n=2}^{M}\left(\frac{a}{r}\right)^n (n-1)\sum_{m=0}^{n}\left(\delta\bar{C}_{nm}\cos m\lambda + \bar{S}_{nm}\sin m\lambda\right)\bar{P}_{nm}\left(\cos\theta\right) \tag{3.2}$$

The highest resolution attainable from a GGM at the Earth's surface is determined by its maximum degree of complete harmonic expansion, $M_{\max}$. The maximum wavelength is given approximately by:

$$\lambda_{\max} \approx \frac{2\pi R}{M_{\max}}\cos\phi \tag{3.3}$$

where ϕ is the evaluation latitude. The maximum resolution is equal to half the maximum wavelength:

$$\rho_{Max} = \frac{\pi R}{M_{Max}}\cos\phi \tag{3.4}$$

Therefore, assuming an Earth radius of R, = 6,378.137 km, the maximum resolution attainable from a degree 360 GGM (e.g., EGM96, Lemoine *et al*., 1998) is ~55 km at the equator. Over NZ ($\phi \approx 45$º) the maximum resolution is approximately 39 km.

3.2.2 Merged GGMs

There are three main types of GGM that are available for use today (satellite-only, combined and tailored) that differ according to the types of gravity data used, their computation methodologies and their region of applicability. These models (and their source data) are discussed in detail in Appendix A. Several GGMs, termed "merged" models, have been created specifically for this study. These models take advantage of the fact that the different types of GGM are better in different parts of the gravity field spectrum (cf. Vergos *et al*., 2006).

A merged GGM is generated by replacing the lower order spherical harmonic coefficients of a combined model (cf. Appendix A.2.2) with those obtained from a satellite-only model (cf. Appendix A.2.1). The degree at which the satellite-only and combined GGMs are merged together is determined by plotting the degree and error-

degree variances of the two models that are being merged and then ascertaining where the degree-variance curves diverge (cf. Figure 3.1). The development of a new Earth Gravity Model (EGM07/8) to degree and order 2160 (~6.5 km resolution in NZ) is currently scheduled for release in 2008 (Kenyon *et al*., 2006). This model has been reported to be of much higher accuracy than its predecessors, so it should be evaluated when it becomes available.

For the combination of the UCPH2002_02 (Howe *et al*., 2002) and EGM96 (Lemoine *et al*., 1998) GGMs the degree- and error-degree variances of both models were plotted (Figure 3.1). It can be seen that the error-degree curves diverge at degree 41. Hence the UCPH2002_02 coefficients from degrees 2 to 41 (inclusive) were used to replace the corresponding EGM96 coefficients. This roughly agrees with the estimates of degree 20 and 30 made by Vaníček and Sjöberg (1991) and Rummel *et al*. (2002) respectively. It is also noted from Figure 3.1 that the degree variances (power) of UCPH2002_02 begins to decay quickly with respect to EGM96 beyond degree ~40. The other six merged GGMs listed in Table 3.1 are shown in Figures A.4 to A.10 have been computed using the same procedure.

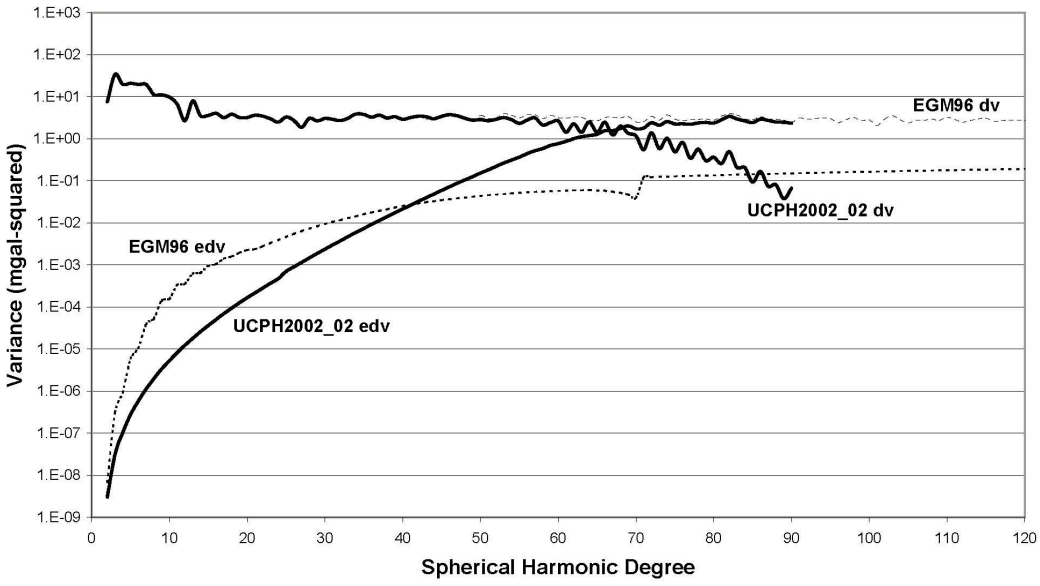

Figure 3.1 Error-degree (edv) and degree (dv) variance of UCPH2002_02 and EGM96 global geopotential models

3.2.3 GGM Evaluation

Amos and Featherstone (2003b) evaluated the fit of the then available GGMs to the NZ gravity field, which includes [Molodensky] free-air gravity anomalies (Section 3.3) on land, GPS-levelling data (Section 3.8) and vertical deflection data (Section 3.9).

If the gravity field implied by a GGM is a close fit to these local gravity field data, it is then reasonable to expect that it is suitable as the basis for a regional gravimetric quasigeoid model. These tests have been repeated with an increased number of GPS-levelling points over NZ (cf. Section 3.8) and the additional recent GGMs given in Table 3.1 (a total of 24 models are compared here). All of the models (except the merged models) have been obtained from the International Centre for Global Earth Models (http://icgem.gfz-potsdam.de/ICGEM/ICGEM.html), which is a service of the International Gravity Field Service under the auspices of the International Association of Geodesy (IAG).

Each GGM in Table 3.1 was evaluated to its maximum available degree and order using `harmonics.f`, which is a derivative of Rapp's (1982) software held at Curtin University of Technology, Perth, Australia. The computations were performed point-by-point, where the GGM-implied gravity field quantities were evaluated at the geocentric latitude and longitude of each terrestrial data point. The descriptive statistics of the differences were then computed. GRS80 (Moritz, 1980a) was used as the reference ellipsoid for all computations, but no zero- or first-degree terms were calculated (cf. Kirby and Featherstone, 1997). As such, the mean differences presented for all the datasets should be treated with some caution, and the standard deviations interpreted as the more informative statistic of the fit of each GGM to the terrestrial-gravity-field-related data.

Model	M_{max}	Class	Reference
UCPH2002_02	90	satellite-only	Howe *et al*. (2002)
UCPH2004	90	satellite-only	Howe & Tscherning (2005)
GRIM5-S1	99	satellite-only	Biancale *et al*. (2000)
EIGEN-1S	100	satellite-only	Reigber *et al*. (2002)
EIGEN-2	120	satellite-only	Reigber *et al*. (2003)
EIGEN-3P	120	satellite-only	Reigber *et al*. (2005a)
GGM01S	120	satellite-only	Tapley *et al*. (2004)
GGM02S	160	satellite-only	Tapley *et al*. (2005)
EIGEN-CHAMP03S	120	satellite-only	Reigber *et al*. (2005a)
EIGEN-GRACE02S	120	satellite-only	Reigber *et al*. (2005b)
JGM-3	70	combined	Tapley *et al*. (1996)
GRIM5-C1	120	combined	Gruber *et al*. (2000)
TEG-4	200	combined	Tapley *et al*. (2000)
GFZ97	359	combined	Gruber *et al*. (1997)
EGM96	360	combined	Lemoine *et al*. (1998)
PGM2000A	360	combined	Pavlis *et al*. (2000)
GGM01C	200	Combined	Tapley *et al*. (2004)
GGM02C	200	combined	Tapley *et al*. (2005)
EIGEN-CG03C	360	combined	Förste *et al*. (2005)
EIGEN-GL04C	360	combined	Förste *et al*. (2006)
GPM98C	1800	tailored	Wenzel (1998)
UCPH2002_02/EGM96	41/360	merged	see text
UCPH2004/EGM96	52/360	merged	see text
EIGEN2/EGM96	32/360	merged	see text
GGM01S/EGM96	90/360	merged	see text
GGM02S/EGM96	100/360	merged	see text
EIGEN-CHAMP03S/EGM96	60/360	merged	see text
EIGEN-GRACE02S/EGM96	120/360	merged	see text

Table 3.1 The GGMs tested over NZ

It is important to point out that terrestrial gravity anomalies do not form an unequivocal test of GGMs, especially the satellite-only GGMs derived from the new dedicated satellite gravity field missions. This is because terrestrial gravity data are highly susceptible to medium- and long-wavelength errors due to factors such as errors in vertical geodetic datums, which are used implicitly to compute gravity anomalies (particularly in NZ, cf. Section 2.4), and to gravimeter drift, which tends to accumulate over long distances (Pavlis, 1998). Heck (1990) gives a review of the systematic errors in terrestrial gravity anomalies.

When any GGM (or quasigeoid) is computed using Stokes's integral (the most common technique) it is deficient in the zero-degree term because the exact values of the product of the mass of the Earth and the Universal gravitational constant and the

potential of the GGM/quasigeoid are unknown (e.g. Kirby and Featherstone, 1997). This manifests itself as a bias in the position of the GGM/quasigeoid with respect to the Earth's geocentre. The zero-degree term can be controlled using geometrical geoid information (i.e. GPS-levelling points) to estimate its magnitude (Heiskanen and Moritz, 1967, Section 2-19); however, this approach is dependent on the GPS and levelling observations all being in terms of the same vertical datum (e.g. Featherstone, 2001). It is known that the NZ levelling observations are in terms of 13 offset vertical datums (cf. Section 2.4); therefore any zero-degree term computed from that data would be biased by the offsets between the datums. Consequently, the zero-degree term has not been computed for these GGM comparisons. Therefore the average difference between the GGM and GPS-levelling will be affected by this term.

3.2.4 Results of comparison

The results of the comparisons are summarised in Tables 3.2, 3.3 and 3.4 for the terrestrial gravity anomalies, GPS-levelling geometrical geoid heights and vertical deflections respectively. Due to the omission of the zero-degree term, the standard deviations (STD) will be used to infer the best fits of the various GGMs to the terrestrial gravity-field-related data.

In general (from Tables 3.2, 3.3 and 3.4), the lower the spherical harmonic degree of a GGM, the poorer the resulting fit (i.e. STD) of the GGMs to the data. This is because the terrestrially determined 'control' values contain all frequencies of the gravity field, whereas the GGMs do not because of the finite spherical harmonic expansion that renders them subject to the so-called omission error. As such, it is expected that the agreements will improve as the maximum degree of the GGM increases. This is simply due to a reduction in the omission error and should not necessarily be interpreted as an improvement in the low frequencies (i.e., a smaller commission error) modelled by these GGMs. The exception to this trend is GPM98C. This model is based on EGM96, which, because of a lack of NZ data in its computation, causes the coefficients to be poorly constrained in NZ, hence the STD becomes worse.

Model	M_{max}	Max	Min	Mean	STD
Raw Land Gravity Data	-	197.045	-162.258	16.462	42.586
UCPH2002_02	90	197.045	-162.258	16.462	42.586
UCPH2004	90	191.956	-151.965	4.904	38.941
GRIM5-S1	99	187.179	-157.982	2.438	40.016
EIGEN-1S	100	190.317	-161.487	6.036	40.444
EIGEN-2	120	187.276	-156.556	4.000	40.359
EIGEN-3P	120	175.400	-162.836	-14.429	39.726
GGM01S	120	188.014	-169.667	-0.483	40.811
GGM02S	160	205.001	-125.558	-13.506	40.877
EIGEN-CHAMP03S	120	211.870	-173.275	-15.418	48.469
EIGEN-GRACE02S	120	185.690	-154.676	-2.624	40.034
JGM3	70	199.517	-134.045	-15.314	41.324
GRIM5-C1	120	192.240	-147.336	1.436	38.625
TEG4	200	207.087	-135.803	-5.981	37.821
GFZ97	359	189.817	-102.627	-8.821	30.425
EGM96	360	171.161	-110.645	-5.891	26.787
PGM2000A	360	162.917	-113.320	-8.891	27.459
GGM01C	200	170.736	-121.633	-26.647	31.757
GGM02C	200	190.234	-142.846	-25.733	41.287
EIGEN-CG03C	360	162.803	-113.942	-9.204	27.462
EIGEN-GL04C	360	149.527	-128.650	-25.470	28.640
GPM98C	1800	239.009	-122.879	-11.340	29.909
UCPH2002_02/EGM96	41/360	163.413	-113.920	-9.441	27.506
UCPH2004/EGM96	52/360	161.798	-113.882	-10.259	27.902
EIGEN-2/EGM96	32/360	162.187	-113.227	-9.190	27.569
GGM01S/EGM96	90/360	155.477	-116.567	-14.533	29.232
GGM02S/EGM96	100/360	151.887	-119.234	-15.352	29.807
EIGEN-CHAMP03S/EGM96	60/360	163.481	-116.220	-11.154	28.031
EIGEN-GRACE02S/EGM96	120/360	150.126	-122.909	-16.594	30.242

Table 3.2 Fit of the geopotential models to land gravity observations (mGal)

The combined GGMs generally give better fits to the terrestrial gravity data than the satellite-only models (Tables 3.2, 3.3 and 3.4), which again is to be expected because most of the former include terrestrial gravity data from the NZ region. However, it is plausible that the satellite-only GGMs, notably those derived from recent mission data, are more precise than the combined GGMs because the latter will have been contaminated by long- and medium-wavelength errors in the terrestrial gravity data (described earlier). It is acknowledged that some filtering of the terrestrial biases is achieved in the GGM data combination process (Pavlis, 1998). Therefore, comparisons with terrestrial gravity data are not such a good means of unequivocally assessing the precision of satellite-only GGMs (cf. Reigber *et al*., 2002).

Model	M_{max}	Max	Min	Mean	STD
Raw GPS-Levelling Data	-	39.411	1.240	16.869	10.542
UCPH2002_02	90	4.443	-5.948	1.287	2.045
UCPH2004	90	4.034	-6.517	1.001	2.031
GRIM5-S1	99	4.558	-7.210	1.325	2.595
EIGEN-1S	100	4.479	-6.583	1.037	2.178
EIGEN-2	120	3.973	-7.596	0.742	2.150
EIGEN-3P	120	4.054	-5.725	0.373	1.396
GGM01S	120	3.965	-4.129	-0.388	1.084
GGM02S	160	3.913	-3.767	-0.515	1.511
EIGEN-CHAMP03S	120	4.055	-6.038	0.462	1.558
EIGEN-GRACE02S	120	3.644	-4.577	-0.523	1.190
JGM3	70	3.892	-5.350	0.799	1.622
GRIM5-C1	120	3.486	-4.708	0.138	1.202
TEG4	200	3.373	-2.398	0.128	0.777
GFZ97	359	4.636	-0.963	0.407	0.765
EGM96	360	3.712	-1.338	0.134	0.673
PGM2000A	360	3.660	-1.388	0.084	0.669
GGM01C	200	2.163	-2.469	-0.402	0.657
GGM02C	200	3.705	-4.408	-0.465	1.169
EIGEN-CG03C	360	1.210	-1.697	-0.458	0.495
EIGEN-GL04C	360	1.646	-1.441	-0.394	0.509
GPM98C	1800	3.325	-2.153	0.083	0.735
UCPH2002_02/EGM96	41/360	3.458	-1.284	0.076	0.679
UCPH2004/EGM96	52/360	2.989	-1.276	-0.008	0.609
EIGEN-2/EGM96	32/360	3.496	-1.377	0.064	0.653
GGM01S/EGM96	90/360	1.716	-1.414	-0.414	0.536
GGM02S/EGM96	100/360	1.421	-1.453	-0.411	0.474
EIGEN-CHAMP03S/EGM96	60/360	2.666	-1.372	-0.192	0.652
EIGEN-GRACE02S/EGM96	120/360	1.221	-1.526	-0.438	0.468

Table 3.3 Fit of the geopotential models to GPS-levelling data (metres)

3.2.5 Analysis of GGM Comparison

It is difficult to unequivocally ascertain the best degree-360 GGM from Tables 3.2, 3.3 and 3.4 simply from the statistical fit to the local gravity field data, principally due to the error budget of the latter. A crude upper estimate of the error of the GPS-levelling is ~14 cm (cf. Section 3.8), the terrestrial free-air gravity anomalies are ~0.1-0.5 mGal (cf. Reilly, 1972) and the vertical deflections ~0.3 seconds (Lee, 1978). Therefore, the 360-degree GGMs are, statistically, insignificantly different from one another in NZ. More importantly, long- and medium-wavelength errors in these terrestrial data may obscure the selection of the best GGM. Therefore, other considerations must be used in parallel.

Model	M_{max}	ξ				η			
		Max	Min	Mean	STD	Max	Min	Mean	STD
Raw Deflections	-	11.089	-27.797	-3.500	8.890	15.844	-16.798	0.154	8.163
UCPH2002_02	90	15.196	-19.465	1.752	7.900	14.401	-13.634	0.010	7.238
UCPH2004	90	15.283	-20.606	1.777	8.146	14.560	-14.005	-0.069	7.294
GRIM5-S1	99	14.790	-21.968	1.416	8.377	16.055	-14.561	0.658	7.747
EIGEN-1S	100	15.511	-21.056	1.786	8.268	14.010	-13.935	0.021	7.204
EIGEN-2	120	15.858	-20.595	2.037	8.260	15.960	-14.337	-0.180	7.752
EIGEN-3P	120	14.432	-17.583	1.746	7.405	14.093	-13.643	-0.355	7.101
GGM01S	120	13.324	-13.375	2.163	6.251	9.541	-11.383	-0.479	5.876
GGM02S	160	12.465	-13.276	2.855	5.777	11.824	-15.213	-2.082	6.152
EIGEN-CHAMP03S	120	14.697	-18.379	1.850	7.554	14.310	-13.206	-0.446	6.973
EIGEN-GRACE02S	120	13.209	-13.506	2.142	6.282	11.345	-11.063	-0.553	6.038
JGM3	70	14.072	-18.273	1.604	7.564	14.540	-12.869	0.015	7.145
GRIM5-C1	120	15.141	-14.838	2.123	7.148	10.185	-12.071	-0.444	6.355
TEG4	200	15.464	-7.119	2.762	5.636	10.076	-12.504	0.081	6.199
GFZ97	359	17.585	-7.210	3.180	5.543	10.198	-11.997	0.082	5.742
EGM96	360	13.671	-7.380	2.606	4.688	9.852	-12.596	-0.013	5.258
PGM2000A	360	13.670	-7.363	2.615	4.681	9.908	-12.610	-0.013	5.257
GGM01C	200	14.153	-6.647	2.670	4.939	11.606	-12.576	0.031	6.108
GGM02C	200	13.439	-13.856	2.139	6.379	10.161	-11.336	-0.607	5.935
EIGEN-CG03C	360	15.118	-6.071	2.882	4.342	11.395	-13.496	-0.039	5.425
EIGEN-GL04C	360	15.333	-6.178	2.865	4.608	11.642	-13.426	-0.016	5.627
GPM98C	1800	16.924	-5.926	0.154	8.163	9.549	-10.355	-0.450	5.369
UCPH2002_02/EGM96	41/360	13.570	-7.296	2.570	4.646	10.005	-12.535	-0.007	5.279
UCPH2004/EGM96	52/360	13.235	-7.560	2.549	4.568	10.203	-12.702	-0.012	5.267
EIGEN-2/EGM96	32/360	13.577	-7.499	2.559	4.681	9.840	-12.648	-0.040	5.254
GGM01S/EGM96	90/360	12.784	-7.480	2.491	4.199	10.557	-12.896	-0.194	5.124
GGM02S/EGM96	100/360	12.414	-7.404	2.503	4.032	10.363	-13.215	-0.193	5.068
EIGEN-CHAMP03S/EGM96	60/360	13.843	-7.152	2.590	4.583	10.191	-12.899	-0.169	5.279
EIGEN-GRACE02S/EGM96	120/360	11.995	-7.309	2.511	3.827	11.444	-13.182	-0.193	5.085

Table 3.4 Fit of the geopotential models to vertical deflections (seconds)

The argument in favour of the merged EIGEN-GRACE02S/EGM96 and GGM02S/EGM96 models is that they use high-quality dedicated GRACE satellite gravity data, whereas EGM96 uses probably the best coverage of terrestrial gravity data. Therefore, the merged models probably represent the best-available long-wavelength and medium-wavelength GGM data. The choice between the two merged GGMs described above is arbitrary. The GGM02S/EGM96 GGM was selected as the reference model for use in the gravimetric quasigeoid computations

because its combined standard deviation (between Table 3.2 and Table 3.3) was lower. Because the GGM02 model is in terms of the zero-Earth-tide model (EGM96 is in the tide-free system) and the Earth-tide only affects the C_{20} harmonic coefficient, the merged GGM02S/EGM96 GGM was therefore in terms of the zero-tide model so no conversion was required to comply with IAG (1984) (cf. Section 2.3.5).

3.3 Terrestrial Gravity

The terrestrial gravity data in NZ is held and maintained by GNS Science (www.gns.cri.nz). The database currently (2006) consists of 40,737 observations covering the NZ and Chatham Island groups (Figure 3.2). These data were primarily collected for the production of gravity anomaly maps in the 1960s and 1970s (Reilly, 1972). The database and its records are described more fully in Appendix B. Reilly (1972) estimates the accuracy of the gravity observations to be ~0.1-0.5 mGal.

The observation horizontal positions in the database are in terms of three different transverse Mercator projections that are based on non-geocentric datums. The heights of these positions are likely to be in terms of the 13 LVDs. The gravity observations are referenced to the Potsdam (NZ) gravity datum, which is known to give gravity values that are 14 mGal too large due to an error in the absolute gravity measurement (Torge, 1989; Grossman and Peschel, 1964). To ensure the consistency of the terrestrial data with other datasets used in gravimetric quasigeoid computation, it is necessary to convert the horizontal positions of the points onto the geocentric NZGD2000 and to change the gravity datum to IGSN71 (Morelli *et al*., 1974). These conversions are given in Appendix B.

The gravity anomalies that are supplied in the database have been computed for geophysical purposes (gravity mapping) and so do not use the rigorous formulae that are necessary for geodetic computations (cf. Featherstone and Dentith, 1997). It is therefore essential that the gravity anomalies used in the remainder of this thesis are recomputed. Sections 3.3.1 to 3.3.3 describe the reductions that are applied to the gravity observations to produce the [Molodensky] free-air and complete/refined Bouguer anomalies. [Geophysical] terrain corrections are also included in the database, which are discussed in Section 4.7.1.

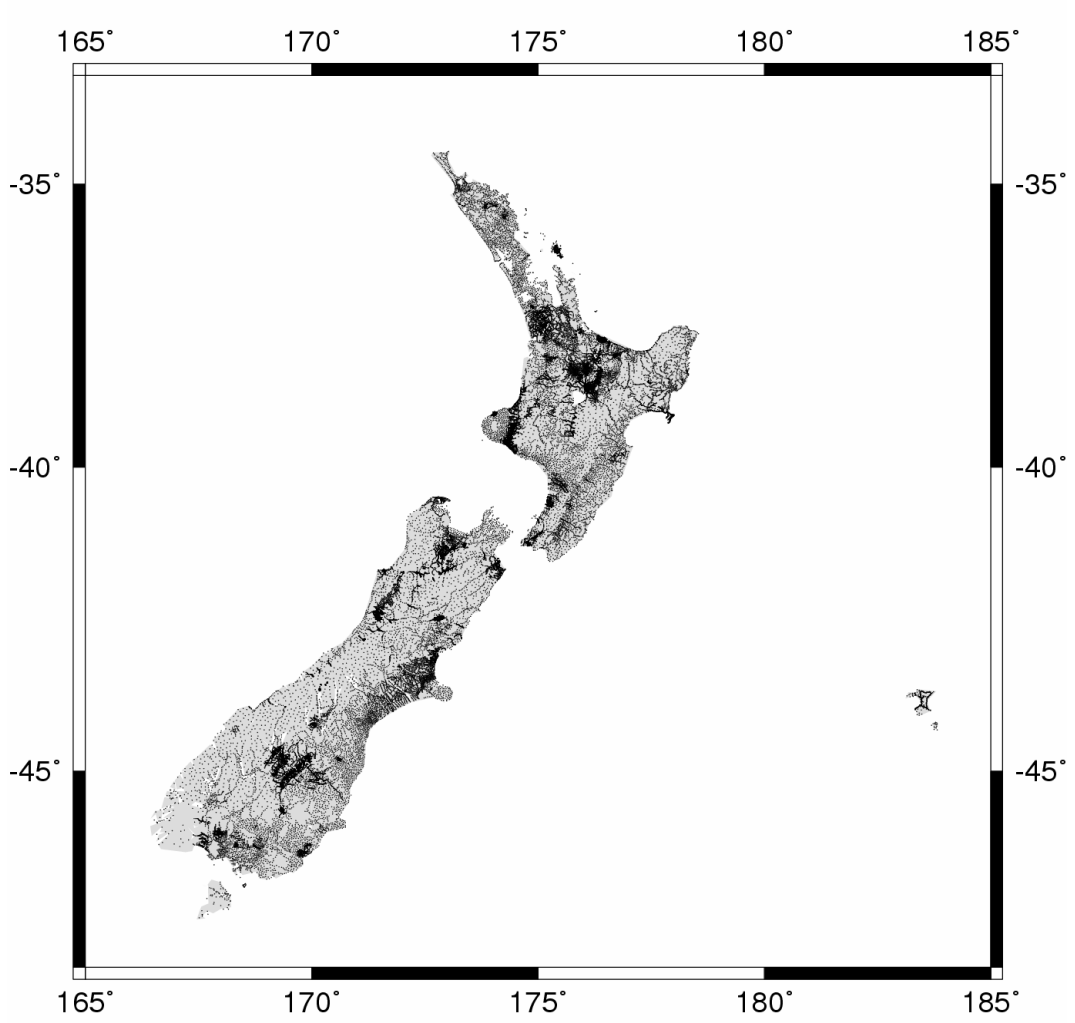

Figure 3.2 NZ (including the Chatham Islands) land gravity data (Mercator projection)

3.3.1 Normal gravity

The latitude correction (as it is called in geophysics; e.g., Hackney and Featherstone, 2003) attempts to eliminate the centrifugal acceleration that affects observed gravity and the oblate elliptical shape of the Earth, as a function of latitude, ϕ. The correction is calculated from an international gravity formula that has been adopted by the IAG. The current formula, which is used in this study, is the Geodetic Reference System 1980 (GRS80) as given in Moritz (1980a). The correction is applied through the use of Somigliana's closed formula (Moritz, 1980a). This is given in Equation (3.5) where k is the normal gravity constant, γ_a is normal gravity at the equator, e^2 is the square of the first eccentricity, and ϕ is the geodetic latitude on the mean Earth ellipsoid. The constants from Moritz (1980a) are given in Table 3.5.

$$\gamma = \gamma_a \frac{1 + k \sin^2 \phi}{\sqrt{1 - e^2 \sin^2 \phi}} \tag{3.5}$$

Constant	Value
γ_a	9.780 326 771 5 m s $^{-2}$
k	0.001 931 851 353
e^2	0.006 694 380 022 90
a	6 378 137 m
f	0.003 352 810 681 18
m	0.003 449 786 003 08

Table 3.5 Physical and geometrical constants of GRS80 used in gravity reductions

GRS80 was defined using satellite-derived data. This means that the GRS80 model includes the mass of the atmosphere, whereas observations made at the surface of the Earth do not. The atmospheric correction accounts for the mass-inconsistency between the GRS80 normal ellipsoid and gravity observed on the Earth's surface, as well as the atmosphere above the gravity observation point. The atmospheric correction (δg_A) is added to the gravity anomalies to account for this difference and to therefore make them consistent with those derived from a GGM. The atmospheric correction recommended by the IAG is given in Equation (3.6) where H is the terrain elevation of the observation point (in metres). The correction has units of mGal.

$$\delta g_A = 0.871 - 1.0298 \times 10^{-4} H \tag{3.6}$$

Sjöberg (2001) pointed out that the use of the above IAG atmospheric correction will incur a bias term if Stokes's integral is truncated to a limited region around the computation point during geoid computation. He presented an alternative correction strategy that is not subject to this bias. The limitations of Equation (3.6) identified in Sjöberg (2001) are acknowledged, however, to ensure consistency with its conventions the IAG approach given in Equation (3.6) have been used in this study.

The terrestrial gravity anomalies were provided in terms of the mean Earth-tide system (see Section 2.3.5). To comply with the IAG resolution on Earth-tide models (IAG, 1984) the gravity observations were converted to the zero-tide system using Equation 2.18. It was also necessary to assume that GNS Science properly removed instrumental drift and tidal effects during post-processing with frequent base-station ties (e.g., Torge, 1989).

3.3.2 Free-air correction

The free-air correction is used to partly downward- or upward-continue gravity observations to the quasigeoid using the vertical gradient of normal gravity as an approximation, i.e., the first derivative of Equation (3.5) with respect to the ellipsoidal height, *h* (Hackney and Featherstone, 2003). The free-air correction (δg_F) "carries up" the normal gravity from the ellipsoid to the Earth's surface by the height *H* giving the Molodensky free air anomaly Δg_F.

A second-order free-air correction is a more accurate representation of the vertical gradient of gravity for an ellipsoidal Earth because it takes into account the variation of normal gravity with latitude as well as higher order terms in height. Typically, this correction, which assumes an oblate ellipsoid shaped Earth, based on a Taylor expansion of normal gravity on the Earth that was derived in Heiskanen and Moritz (1967; p79), is given in Equation (3.7), where *f* is the geometrical flattening of the mean Earth ellipsoid (e.g. GRS80, Moritz, 1980a), *m* is the ratio of gravitational and centrifugal forces at the equator as given in Table 3.5. Because this equation is derived from Equation (3.5), the ellipsoidal height is strictly the height that should be used, but the normal orthometric height is used in practice.

$$\delta g_F = \frac{\delta \gamma}{\delta h} = \frac{2\gamma}{a}\left(1 + f + m - 2f\sin^2\phi\right)h - \frac{3\gamma}{a^2}h^2 \tag{3.7}$$

$$\Delta g_F = g_S - \gamma + \delta g_A + \delta g_F H \tag{3.8}$$

3.3.3 Bouguer correction

The free-air reduction neglects the gravitational attraction of the topography between the Earth's surface and the vertical datum surface. The simple (planar) Bouguer correction removes the mass of the topographic masses using the assumption that the topography can be represented by an infinitely lateral plate (Bouguer plate) of thickness to the observation elevation as given by Equation (3.9), where *G* is the Newtonian gravitational constant ($6.6742 \times 10^{-11} \pm 0.00015$ $m^3kg^{-1}s^{-2}$, Mohr and Taylor, 2007) and ρ is the topographic mass density that is often approximated by 2,670 kg m^{-3} (Heiskanen and Moritz, 1967, p130).

$$\delta g_B = 2\pi G \rho H \tag{3.9}$$

The assumption in the simple (planar) Bouguer reduction that the Earth's topography attracts as an infinitely lateral plate neglects the fact that the surface of the Earth is not a flat plane. At any point where a gravity observation is made the presence of topography (i.e. mountains and valleys) surrounding it will have an influence on the magnitude of the measurement. An additional "terrain" correction is therefore needed to account for the effect of the surface topography relative to the observation point. When the terrain correction (TC) is applied in conjunction with the Bouguer correction given in Equation (3.9) it results in a refined or complete Bouguer anomaly Δg_B. The computation of TCs is a rather involved process that is discussed further in Sections 4.4 and 4.7.

$$\Delta g_B = \Delta g_F + \delta g_B H \ (+\mathrm{TC}) \tag{3.10}$$

An alternative approach to the planar model (described above) is based on the assumption that the topography can be represented by a shell of thickness equal to the observation elevation (Bouguer shell). This "spherical" model also has an associated spherical terrain correction. Although the NZ gravity observations were reduced using the planar model, both approaches are discussed in Section 4.4.

3.4 Marine ship-track gravity

Marine gravity observations in the vicinity of NZ have been collected over the past 45 years by various agencies at different times for different purposes (Figure 3.3). The available databases comprise 1,300,266 gravity anomalies bound by 160°E ≤ λ ≤ 190°E and 25°S ≤ ϕ ≤ 60°S and auxiliary information including horizontal coordinates, gravity values and Eötvös corrections. Woodward (2001, pers. comm.) estimates the accuracy of the marine data to be approximately 1 mGal.

Until recently, these observations were stored in different formats, in terms of different (horizontal and gravity) datums, and no attempt had been made to ensure consistency among individual cruises, let alone the datasets. The problems with offsets and tilts in marine gravimetry are well known (e.g., Wessel and Watts, 1988). To remedy this problem a crossover adjustment of ~900,000 line-kilometres of

observations surrounding NZ was carried out by *Intrepid Geophysics* (www.intrepid-geophysics.com) under contract to LINZ (Brett, 2004). This has brought all the observations into a single, coherent, internally consistent dataset. The crossover adjustment process and its results are described in Appendix C.

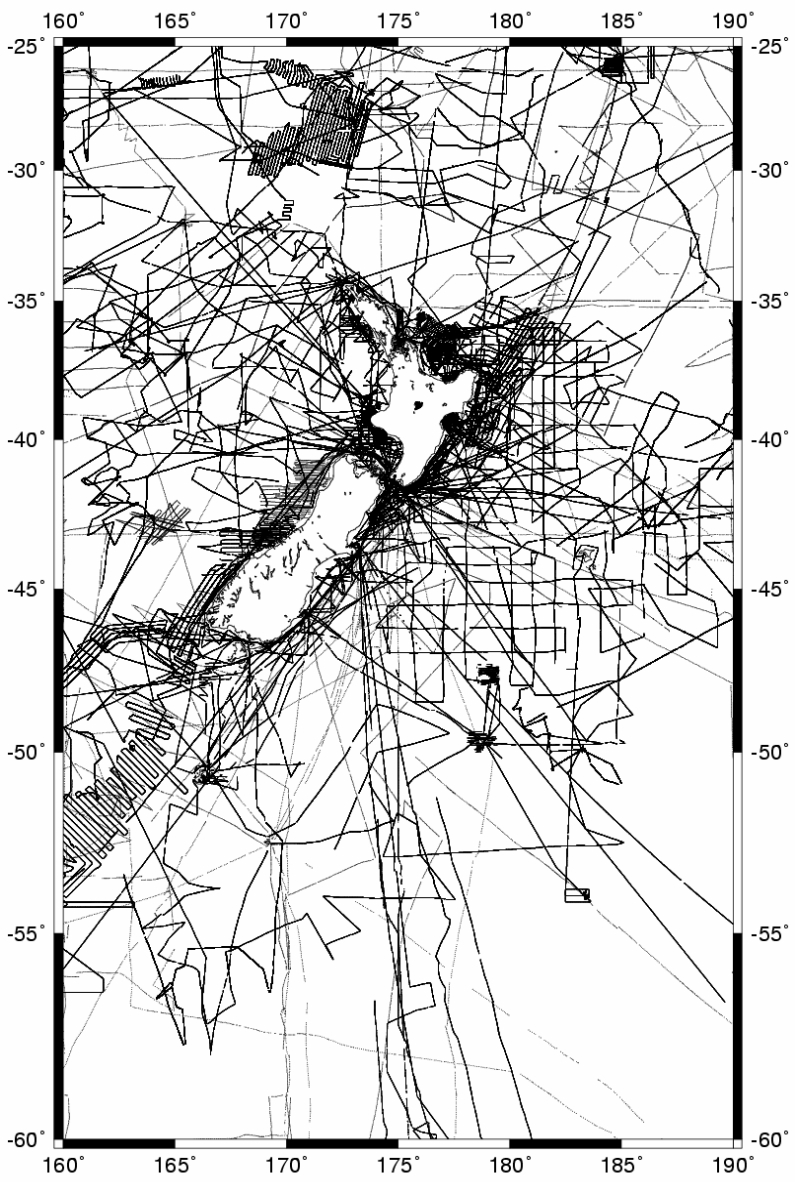

Figure 3.3 Coverage of ship-track gravity observations around NZ used for crossover adjustment (Mercator projection)

3.5 Satellite altimetry-derived gravity anomalies

The coverage of the crossover-adjusted marine gravity data is good near the coast, but it becomes relatively sparse further from land (cf. Figure 3.3). To achieve the necessary homogeneous coverage of gravity data over the computation area, it is

necessary to combine the ship-track observations with gravity anomalies derived from multi-mission satellite altimetry (e.g., Li and Sideris, 1997). This Section describes the comparisons that were performed in Amos *et al*. (2005) on four different altimetry-derived gravity grids so that the best grid could be selected for use in the NZ quasigeoid computations.

Satellite altimetry is based on a satellite-borne radar altimeter that transmits pulses in the nadir direction to the Earth's surface. The ocean's surface reflects these signals back to the satellite and the total travel time is used to determine the height of the satellite above the ocean after the application of various corrections (e.g. Torge, 2001, p. 154). The relative changes in height and the rate of these changes can then be used to determine the gravity anomalies.

There are several approaches for the actual gravity field recovery that are used in practise. These include: conversion of marine geoid heights (sea surface heights corrected for SSTop) using the inverse Stokes formula (e.g. Olgiati *et al*., 1995); conversion of vertical deflections (along-track first derivatives of sea surface heights) using the inverse Vening-Meinesz formula (e.g., Hwang *et al*., 1998, 2002); and conversion of vertical deflections through the integration of Laplace's equation (e.g., Haxby *et al*., 1983; Sandwell and Smith, 2005; 1997; Olgiati *et al*., 1995). Since this study only uses the final grids (see below) a detailed comparison of the different gravity field recovery methods will not be provided here (although a summary is provided in Featherstone, 2003a).

3.5.1 Altimetry-derived gravity anomaly grids

There are currently (2006) four recent global grids of marine gravity anomalies derived from a combination of multi-mission satellite altimetry (Table 3.6). Each grid is provided on a 2 arc-minute resolution and has used a different computation method, but all are based on EGM96-implied gravity anomalies (Lemoine *et al*., 1998; Equation 3.2) in a remove-compute-restore (RCR) procedure (cf. Section 5.2.4). The KMS02 and GSFC00 grids were computed using the inverse Stokes integral (Andersen *et al*., 2005 and Wang, 2001 respectively); SSv11.2 used Laplace's equation (cf. Sandwell and Smith, 1997); and GMGA02 the inverse Vening Meinesz formula (Hwang *et al*., 2002). Also, the altimetry grids were

provided in terms of the mean Earth-tide system (see Section 2.3.5). To comply with the IAG resolution on Earth-tide models (IAG, 1984) the grid values were converted to the zero-tide system using Equation (2.18).

Grid	Reference / URL
KMS02	Andersen *et al*. (2005) http://spacecenter.dk/data/gravity/download.html
SSv11.2	Sandwell and Smith (1997) http://topex.ucsd.edu/marine_grav/mar_grav.html
GMGA02	Hwang *et al*. (2002) ftp://gps.cv.nctu.edu.tw/pub/data/marine_gravity/
GSFC00	Wang (2001) http://magus.stx.com/mssh/mssh.html

Table 3.6 Public domain satellite-altimeter-derived marine gravity anomalies

3.5.2 Differences between altimetry grids

It is well known that satellite-altimeter-derived gravity anomalies are less accurate close to the coast (e.g., Hipkin, 2000; Andersen and Knudsen, 2000). This is due to factors such as poorly tracked altimetry close to the coast (Deng *et al*., 2002; Deng and Featherstone, 2006), poor shallow-water tidal models, and poor wet delay corrections (e.g. Andersen and Knudsen, 2000). In addition, there are significant differences close to the Australian coast among altimeter-derived anomalies derived by different groups (Featherstone, 2003b). This is also the case in NZ (Amos *et al*., 2005), albeit to a lesser extent than near Australia (Figure 3.4 and Table 3.7). Note that the maximum and minimum differences in Table 3.7 range from -366.2 mGal to 380.8 mGal, however, the differences shown in Figure 3.4 have been truncated for display purposes. All three grids have been derived from principally the same satellite data, so the differences between them are due to the way that they have been computed.

The largest differences among the altimeter grids occur along the western coast of NZ's South Island (centred at: ~45°S, ~167°E); see the example in Figure 3.4 and Amos *et al*. (2005). This is due to a combination of the problems with coastal satellite altimetry, coupled with the very steep gravity gradients at the boundary of the Australian and Pacific plates. The latter will give a large Gibbs phenomenon

when transforming the sea surface heights/gradients to gravity anomalies because there is no gravity data on land. From Table 3.7, the comparisons that involve the GMGA02 grid give the largest maximum and minimum differences. These differences are concentrated as several 'spikes' located close to the NZ and Chatham Islands (183°E, 44°S) coasts. This shows that it is the least consistent with the other grids, which are reasonably self-consistent (Table 3.7).

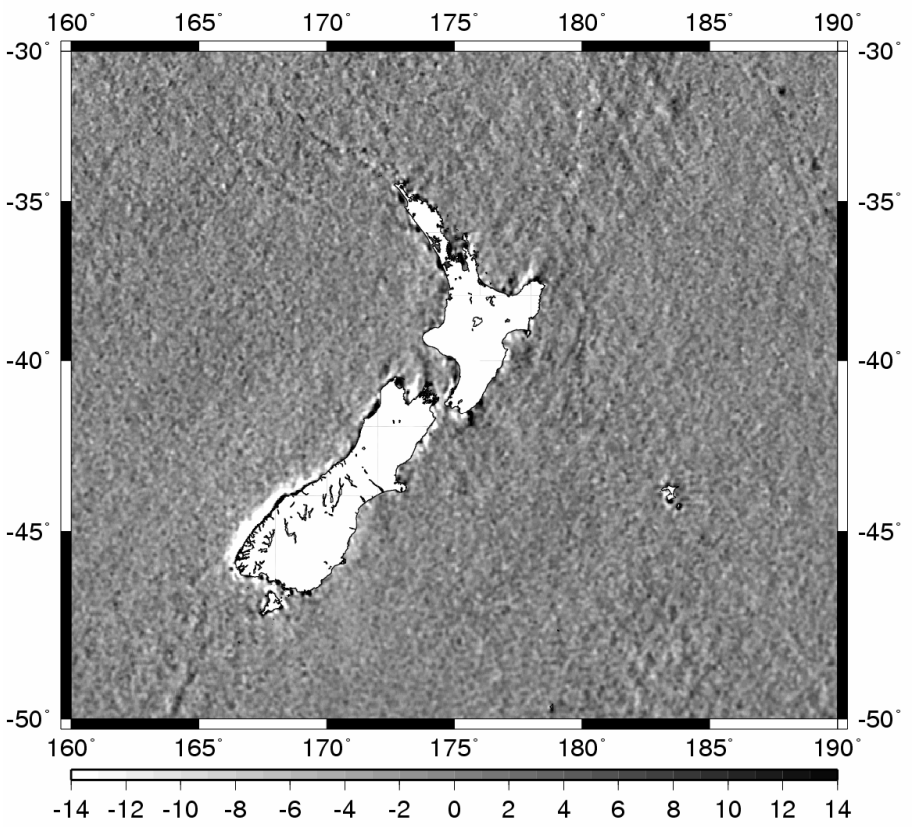

Figure 3.4 Example difference between KMS02 and SSv11.2 gravity anomalies (mGal; Mercator projection)

Data	Max	Min	Mean	Std
KMS02 – SSv11.2	139.4	-79.4	-0.1	3.0
KMS02 – GMGA02	371.8	-337.3	-0.0	4.2
KMS02 – GSFC00	117.2	-103.2	0.1	2.9
SSv11.2 – GMGA02	380.8	-334.7	0.0	4.0
SSv11.2 – GSFC00	123.9	-129.3	0.2	3.2
GMGA02 – GSFC00	334.7	-366.2	0.1	4.2

Table 3.7 Statistics of the differences between the different altimetry grids (mGal)

3.5.3 Comparisons of altimetry grids with ship-track data

Next, the various altimeter-derived anomalies (Table 3.6) were compared with the crossover-adjusted ship-track anomalies (Appendix C) in order to select the best grid for NZ quasigeoid computations. The altimeter-derived gravity anomalies (assumed to also be on a geocentric horizontal datum) were bi-cubically interpolated to the locations of the ship-track data. The statistics in Table 3.8 only compare the altimetry grids at the locations of the dense ship-track observations in a 50-400 km band around NZ and the Chatham Islands. The *Generic Mapping Tools* (GMT) *grdmask* function (Wessel and Smith, 1998) was used to create a "mask" for the 50-400 km band. This was then used to remove the ship-track observations which were outside the "mask". The observations were limited in this way because the altimeter data are less reliable within ~50 km from the coast (Figure 3.4). Conversely, the altimeter data are probably more reliable than the ship-track data in the open oceans, especially in areas with sparse data coverage where the crossover adjustment is less well constrained (e.g., south of 55°S; see Figure 3.3). The differences between the cross-over adjusted ship-track observations and the KMS02 altimetry grid within 400 km of the NZ and Chatham Island coasts are shown in Figure 3.5.

Data	Max	Min	Mean	Std
KMS02	194.5	-108.7	1.7	8.2
SSv11.2	196.0	-109.1	1.6	8.2
GMGA02	197.3	-107.7	1.7	8.2
GSFC00	193.9	-107.4	2.2	8.0

Table 3.8 Statistics of the differences between the altimetry grids and the crossover-adjusted ship-track observations within 50–400 km of the coast (mGal)

From the results in Table 3.8, no single altimeter grid is significantly better than another in the 50-400-km region around NZ. An analysis of the comparison between the altimetry grids and all 2,401,932 adjusted ship-track data (Table 3.9) also showed that no altimetry grid was significantly better than another. The selection of the KMS02 altimetry grid was thus arbitrary based on the justification that the standard deviation of the difference between it and the cross-over adjusted marine data was slightly lower (although it was equal to GSFGC00). The KMS02 model was chosen

over the GSFC00 model because it was more recent and the KMS group have produced altimetry models for many years.

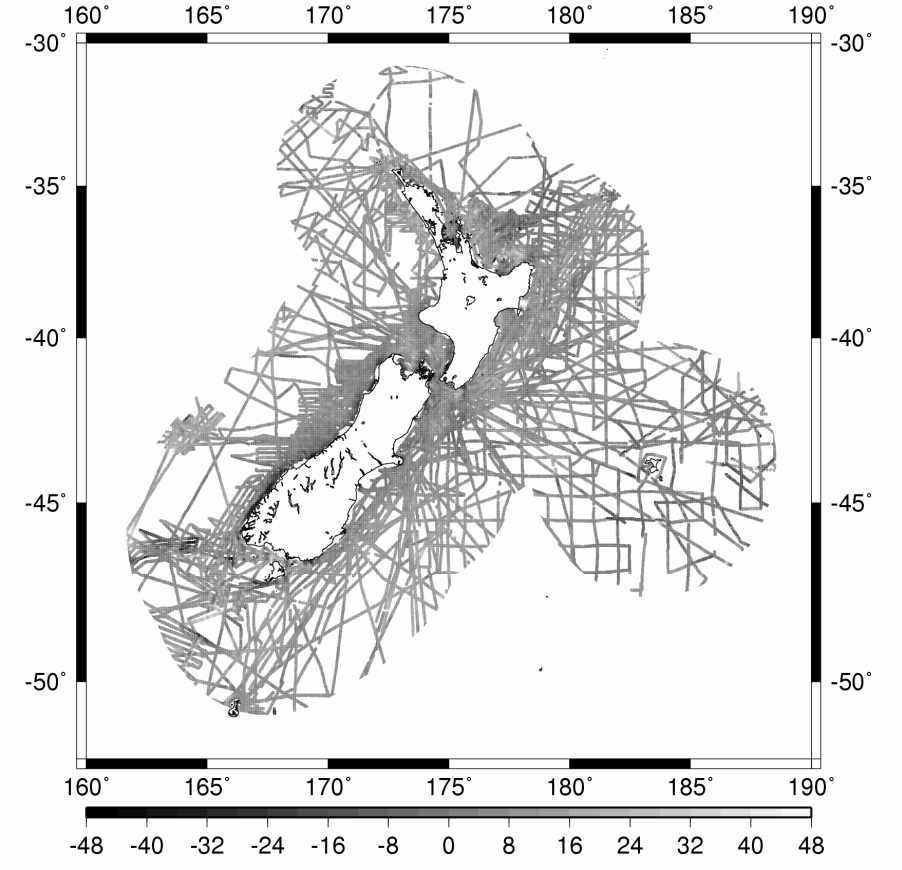

Figure 3.5 Difference between the adjusted ship-track observations and KMS02 altimetry anomalies up to 400 km from coast (mGal; Mercator projection)

Data	Max	Min	Mean	Std
KMS02	486.3	-789.5	1.4	11.2
SSv11.2	484.9	-789.1	1.0	12.0
GMGA02	486.4	-790.0	1.1	12.1
GSFC00	485.6	-789.6	1.8	11.2

Table 3.9 Statistics of the differences between the altimetry grids and all crossover-adjusted ship-track observations (mGal)

3.6 Combination of altimetry-derived and ship-track gravity anomalies

3.6.1 Overview

It is expected that the altimeter derived gravity anomalies are probably of better quality than the poorly constrained ship-track data far from shore (cf. Kirby and Forsberg, 1998); conversely the ship-track data is likely to be better than the altimetry near the coast (cf. Deng *et al*., 2002). To reduce the error in the altimetry data near the coast, the crossover-adjusted ship-tracks were used to "correct" it (cf. Strykowski and Forsberg, 1998). This was achieved using the least-squares collocation (LSC) interpolation routines in the GRAVSOFT suite (Tscherning *et al*., 1992) to "drape" the altimetry anomalies onto the crossover-adjusted ship track data.

3.6.2 Description of procedure

The LSC "draping" procedure was described in Amos *et al*. (2005) and broadly followed the procedures of Strykowski and Forsberg (1998). Firstly, the crossover-adjusted ship-track data was supplemented with land gravity information (Section 3.3) by the addition of free-air anomalies over the land areas. This was essential to ensure that the LSC algorithm performed correctly across the land/sea boundary. Next, the differences between the ship-track/land data and the KMS02 altimeter data within the study area were determined. These differences were then gridded (predicted with LSC) onto a 2 arc-minute correction grid over the computation area. A 2 arc-minute correction grid was used because this matched the resolution of the altimetry grids that were being draped.

A second-order Markov covariance model was used with a correlation length of 20 km and 3 mGal RMS noise of the gravity data. These parameters were optimised by testing them over a range of 5-100 km and 1-5 mGal, respectively (see Section 3.6.3). The correction grid was then added to the pre-gridded altimetry data. This yields an altimetry data set that is consistent with the ship-track data, thus correcting the well-known coastal errors in the altimetry data (e.g. Andersen and Knudsen, 1998; 2000; Hipkin 2000; Deng and Featherstone, 2006).

3.6.3 Results and discussion

The LSC data combination was (partly) independently tested by extracting 2,328 randomly scattered observations (~0.2%) from the adjusted ship-track data within 400 km of the coast. These observations were selected by removing every 2,328th record from the ship-track data file. These data were not used in the LSC combination, but used later to test the results; it also allowed empirical optimisation of the choice of RMS noise and correlation length. This is analogous to, but easier to implement than, cross-validation (Featherstone and Sproule, 2006). The "optimisation" resulted in the same values for the noise and correlation length as adopted by Strykowski and Forsberg (1998). The comparison between the 2,328 extracted marine observations and the KMS02 altimetry anomalies before and after draping revealed a significant improvement in the fit (Table 3.10). An additional comparison was made between all of the ship-track anomalies (Table 3.11). This also demonstrates an improved fit between the datasets after the LSC draping has been performed.

Grid	Max	Min	Mean	STD
Cross-over adjusted	61.2	-89.7	0.7	9.9
Draped	32.0	-32.1	0.0	3.2

Table 3.10 Statistics of the differences between 2328 ship-track observations (within 400 km of the coast) and the KMS02 anomalies before and after draping (mGal)

Grid	Max	Min	Mean	STD
Cross-over adjusted	486.3	-789.5	1.4	11.2
Draped	486.2	-789.5	0.9	9.1

Table 3.11 Statistics of the differences between 2,401,932 ship-track observations and the KMS02 anomalies before and after draping (mGal)

From this comparison, the precision/accuracy of the LSC combined gravity anomalies is cautiously estimated to be ~3.5 mGal, which is a GLOPOV (General Law of Propagation of Variance) combination of the standard deviation of crossover adjusted ship-track misclosures (0.3 mGal; Table C.2) and the standard deviation of the differences with the independent points (3.2 mGal; Table 3.10). The final marine gravity grid (LSC combined using all the ship-track data) is shown in Figure 3.6.

3.7 Digital elevation models

Auxiliary elevation data are necessary in gravimetric geoid determination because the gravitational effect of topographic masses outside the geoid has to be mathematically condensed onto, or below, the geoid in order to satisfy the boundary-value problem of physical geodesy (e.g., Heiskanen and Moritz, 1967). This so-called topographic effect is described more fully in Chapter 4 where different methods of computation are compared.

In addition to this theoretical demand, high-resolution terrain data can provide additional short-wavelength quasigeoid information and to help smooth the gravity field prior to gridding (Forsberg and Tscherning, 1981). Removing high-frequency signals from the gravity anomalies makes the gridding process less sensitive to aliasing (e.g., Goos *et al.*, 2003), where under-sampled high frequencies are incorrectly propagated into the low frequencies.

A digital elevation model (DEM) can also be used to 'reconstruct' mean free-air gravity anomalies (Featherstone and Kirby, 2000; Lemoine *et al.*, 1998). This is necessary in areas of rugged and high terrain, where the practicalities of collecting gravity data in the field mean that gravity is generally observed in the more accessible lowland regions. It will be shown in Section 4.11 that this reconstruction technique has a significantly positive effect in the Southern Alps/Kā Tiritiri o te Moana.

LINZ is the NZ government agency responsible for the topographic mapping of NZ at a scale of 1:50,000. It makes available its official topographic source data (that is used for the production of topographic maps) in a vector-based format. Spot heights in this data have heights with an accuracy of ±5 metres and contour lines ±10 metres (NTHA, 2006). All heights in this dataset are related to the "zero" contour line which approximates the level of mean high water springs. The heights are not explicitly referenced to one of the 13 LVDs.

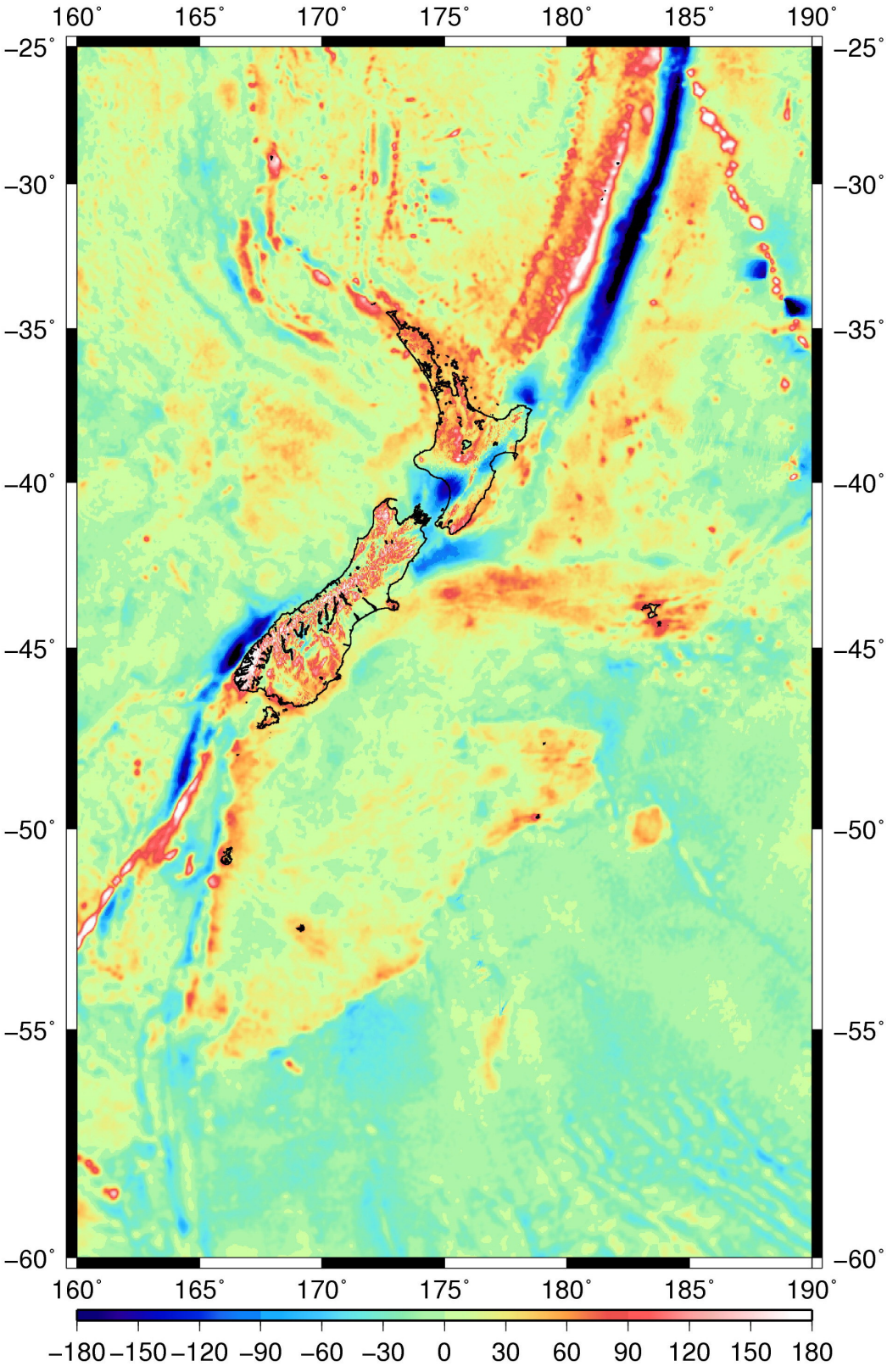

Figure 3.6 The 2' x 2' NZ gravity anomaly grid: comprising crossover adjusted and draped marine anomalies (ship-track and KMS02 altimetry) and reconstructed terrestrial Faye anomalies (mGal; Mercator projection)

Although no official DEM is published in NZ, a number of companies sell commercial DEM data that is derived from the official LINZ vector data. For this study a 1.8 arc-second (0.0005 degree) resolution DEM was purchased from *GeographX* (www.geographx.co.nz). At the NZ latitudes this has an effective resolution of approximately 56 metres. The DEM has an estimated precision of ±22 m horizontally and ±10 m vertically (Smith, 2001, pers. comm.).

3.8 GPS and spirit levelling data

Relative carrier-phase GPS observations co-located with precise geodetic levelling can provide external "control" with which to test a gravimetric quasigeoid on land, especially if the quasigeoid model is to be used subsequently for the recovery of heights above MSL from GPS (e.g., Featherstone, 1998).

Ellipsoidal heights in NZ (in terms of NZGD2000) have been established at geodetic marks by GPS observations using a combination of static and real-time kinematic (RTK) techniques (Blick, 2003). Although NZGD2000 is promoted as a three-dimensional datum, the emphasis of its development has been placed on establishing and maintaining the horizontal coordinates of marks. This is particularly evident with the urban cadastral control surveys where positions are typically established by double-occupation RTK surveys.

The absolute accuracy of the NZGD2000 ellipsoidal heights is estimated to be on average 10 centimetres (OSG, 2003; Blick, 2005, pers. comm.). The first- and second-order spirit levelling (and its derived normal-orthometric heights) is described in Section 2.4. A conservative estimate of the absolute accuracy of these heights is also 10 centimetres (*ibid.*). The absolute height accuracy is distinct to the relative height difference accuracy that is obtained from precise levelling. Precise levelling for the first- and second-order heights was undertaken to misclosure tolerances $\pm 2\,\mathrm{mm}\sqrt{k}$ and $\pm 7\,\mathrm{mm}\sqrt{k}$ respectively, where k is the distance in kilometres (cf. Section 2.4.2). It is therefore possible to derive a combined accuracy for the GPS-levelling points of 14 centimetres ($\sqrt{(0.1)^2 + (0.1)^2}$). This accuracy estimate does not take into account the effect of the offsets between the vertical datums.

GPS-levelling data do not give an unequivocal verification of a quasigeoid, predominantly because of the distortions in and offsets among the different vertical geodetic datums (Sections 2.4.3 – 2.4.5). However, simple blunders such as the neglect of the GPS antenna height can add ~1.5 m errors in single points, which can be difficult to discriminate between vertical datum and geoid errors if the surrounding control is sparse. In addition, the GPS data have been collected over a long period of time, while processing algorithms and data availability (notably precise orbits, from the International GNSS Service; Beutler *et al.*, 1999) have matured.

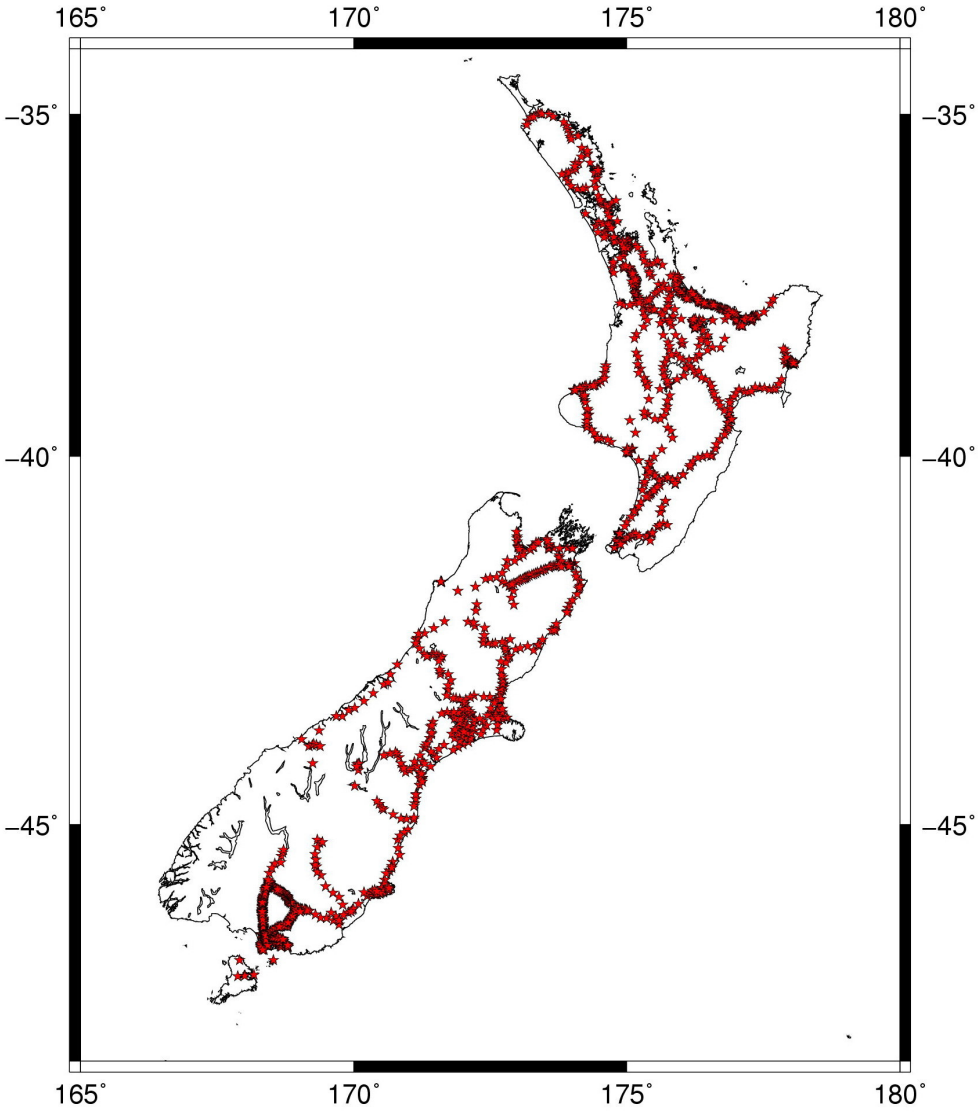

Figure 3.7 1422 NZ GPS-levelling points (Mercator projection)

A total of 1,422 points within NZ have both ellipsoidal and normal-orthometric heights (first- and second-order). The spatial distribution of the GPS-levelling points is not uniform and there are significant gaps in large parts of the South Island (Figure 3.7). These large gaps are in areas where the topography is particularly rugged and so the precise levelling coverage is restricted to the limited roads in the area. The GPS-levelling points are also split between thirteen vertical datums so they are also affected by the offsets between the datums. It is important to note that there are no GPS-levelling points on the Chatham Islands and the five points on Stewart Island only have less accurate normal-orthometric heights because no precise levelling network exists there.

3.9 Vertical deflections

The defection of the vertical is the angle that describes the deviation of the true vertical, as defined by the direction of the Earth's gravity vector, with respect to some (geometric or physical) reference direction. The classic definition of a reference direction identifies it as the perpendicular to an ellipsoid, often defining a geodetic datum (Jekeli, 1999). Vertical deflections are defined in terms of a north-south (ξ) and east-west (η) components.

Vertical deflections offer the most independent validation of GGMs (in comparison to GPS-levelling and gravity observations) because they have not been used in the construction of the models. There is a distinction between Helmert deflections of the vertical at the Earth's surface and Pizzetti deflections of the vertical at the geoid (e.g., Jekeli, 1999). To relate these two quantities requires the curvature of the plumbline through the topography, which is notoriously difficult to estimate (e.g. Bomford, 1980; Papp and Benedeck, 2000). The corrections required to convert between Helmert and Pizzetti deflections are typically so small as to be overwhelmed by the errors made when observing astro-geodetic deflections. Therefore Pizzetti deflections implied by GGMs will be compared with the astrogeodetically determined Helmert deflections.

In NZ, 33 Helmert vertical deflections (Figure 3.8) were observed at Laplace stations as part of the establishment of the NZGD49 (Lee, 1978) and the Earth Deformation Study (EDS) programme (Rowe, 1989). NZGD2000 coordinates were used to

compute the absolute Helmert deflections (cf. Featherstone and Rüeger, 2000; Jekeli, 1999) from the GGMs.

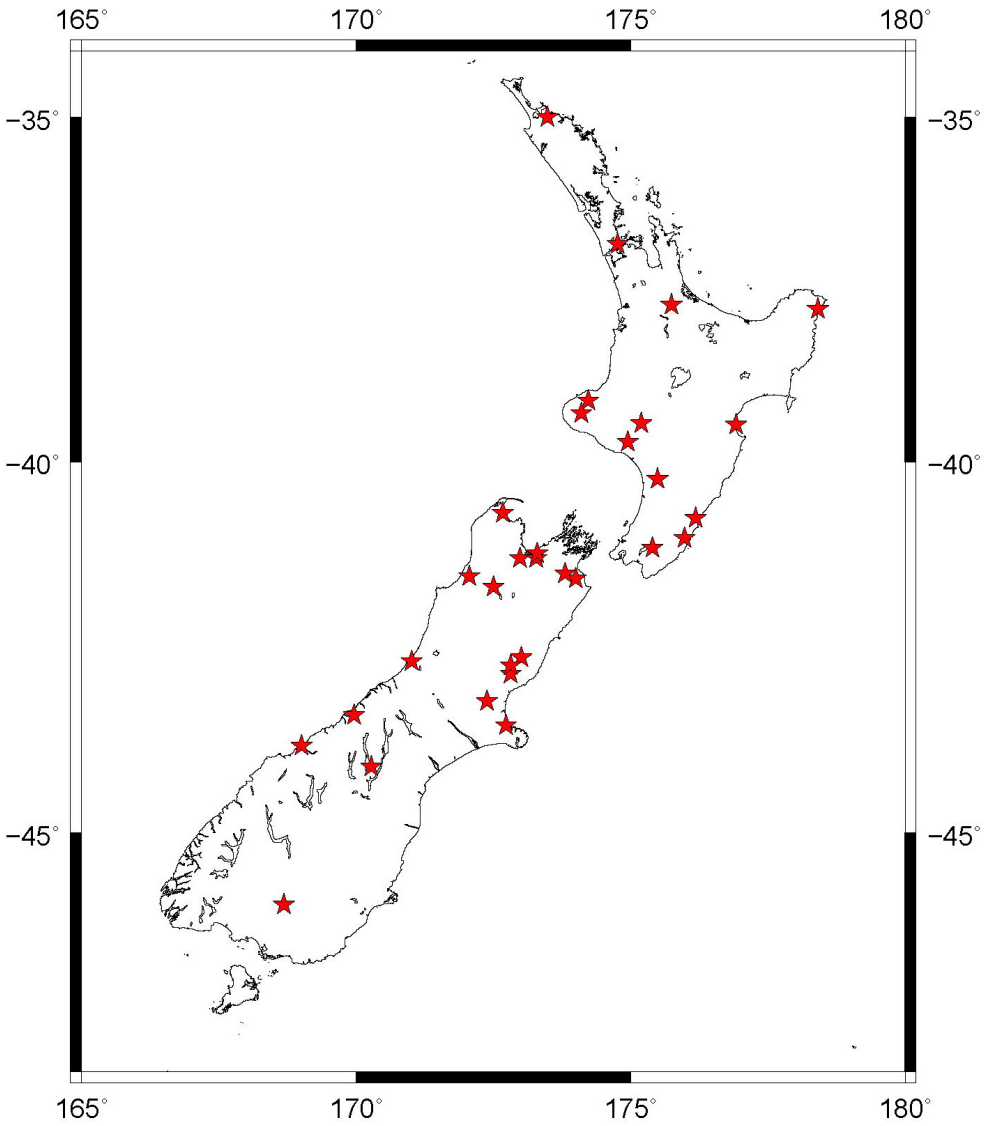

Figure 3.8 33 NZ vertical deflections (Mercator projection)

3.10 Summary

This Chapter has presented the datasets that will be used for computations and analysis in the remainder of this thesis. The merged GGM02S/EGM96 GGM was shown to have the best fit to the NZ gravity and GPS-levelling data. As such it has been selected for use as the reference GGM for quasigeoid computations (Chapters 4, 5 and 6). The terrestrial gravity anomalies from GNS Science have been re-reduced to convert them to the ISGN71 gravity datum, the GRS80 reference system, and to ensure that the other corrections were applied correctly (in the geodetic sense). The

marine data has been crossover adjusted and the KMS02 satellite altimetry grid was chosen. These were then combined using LSC to give a two arc-minute grid of free-air anomalies over the marine parts of the computation area. A description was given of the 1.8 arc-second DEM that will be used for the terrain correction tests and gravity reconstruction in Chapter 4. This Chapter was concluded with the GPS-levelling points that will be used to compute the LVD offsets and to verify the fit of the computed quasigeoid models to NZ in Chapters 5 and 6.

4 TOPOGRAPHICAL CORRECTIONS FOR GRAVIMETRIC GEOID COMPUTATION

4.1 Introduction

Terrain corrections (TCs) are one of the most important components in the solution of the Stokes-Helmert geodetic boundary-value problem (GBVP). The solution of the GBVP using Stokes's formula assumes harmonicity, i.e., that there should be no masses outside the geoid. To fulfil this assumption, it is necessary to regularise the effect Earth's topography on the input gravity anomalies so that they refer to the geoid. This is achieved by the application of the topographical correction (Bouguer plate/shell plus TC) and the downward continuation (DC) of the gravity anomalies (e.g., Martinec and Vaníček, 1994a; Vaníček *et al*., 1996). The mathematical and physical treatments of the TC play an important role in the computation of precise gravimetric quasigeoid models. This is particularly significant in rugged terrain, where the major part of the short-wavelength gravity field variation is caused directly by the topography (e.g. Forsberg, 1985; Sideris, 1990). When applied to gravity observations, TCs help to produce a gravity field that is smoother and thus more suited to gridding (Section 4.11).

Surface gravity observations need to be gridded prior to quasigeoid computation. To ensure that the grid is representative of the actual gravity field, the surface gravity observations would ideally be acquired such that there is a higher spatial density of observations where the gravity field is rapidly changing and a lower density where it changes more predictably. In general, the opposite occurs, i.e., where the gravity field is more variable (e.g., the mountains) the gravity observations are more sparsely located due to access difficulties, terrain roughness and problems with gravimeter drift (e.g., Janak and Vaníček, 2005). To overcome this, Section 4.11 applies the Featherstone and Kirby (2000) process of gravity reconstruction to account for the irregular spatial density in the NZ terrestrial gravity observations. It then repeats the Goos *et al*. (2003) experiments to determine the type of gravity anomaly and TC best suited to gridding in the NZ environment.

4.2 Helmert's second method of condensation

When attempting the gravimetric determination of the geoid using Stokes's formula, a prerequisite requirement is that there are no masses outside the geoid and that the gravity anomalies (observed at or above the surface of the Earth) are referred to the geoid (e.g. Heiskanen and Moritz 1967, p. 145). One method of achieving these requirements is to use Helmert's second method of condensation (e.g., Heiskanen and Moritz 1967, Sections 3-7, 4-3; Vaníček and Kleusberg 1987; Martinec and Vaníček, 1994a; Vaníček *et al*., 1996; Heck 2003b). Martinec *et al*. (1993) describe the five steps of this process to convert observed gravity anomalies to geoid undulations in the Stokes-Helmert scheme as:

1. **Direct topographical effect (DTE) on gravity:** replace the effect of the topographical masses on gravity at a point on the Earth's surface by the effect of the mass layer condensed on the geoid, also called the topographic correction (Section 4.3);

2. **Downward continuation (DC)**: reduce the gravity anomalies from the observed level/height (either on or above the Earth's surface) to the geoid (Section 4.5); because this is carried out after the masses are removed, the DC applies to a harmonic quantity (i.e., the Abel-Poisson integral is satisfied);

3. **Co-geoid**: use Stokes's formula to transform the reduced gravity anomalies to the co-geoid (Section 5.2.4);

4. **Primary Indirect topographical effect (PITE) on potential**: apply a (reverse) correction to account for the change in the potential of the Earth that occurs due to the condensation of its masses in steps 1 and 2 (Section 4.6);

5. **Secondary indirect topographical effect (SITE) on potential**: apply a (reverse) correction to account for the difference in height between the geoid and the Stokes-Helmert co-geoid. Vaníček *et al*. (1999) showed that the effect of this correction on the geoid is less than 1 mm so it can normally be disregarded.

4.3 Direct topographical effect on gravity

The effect of the topography on the computation of geoid undulations has been extensively researched (e.g., Helmert, 1884; Heiskanen and Moritz, 1967; Wichiencharoen, 1982; Forsberg, 1985; Vaníček and Kleusberg, 1987; Tziavos *et al*., 1988; Wang and Rapp, 1990; Sideris, 1990; Martinec and Vaníček, 1994a; Martinec *et al*., 1993; Heck, 1993, 2003b, 2005; Tscherning, 2005; Tsoulis, 1998, 2001, 2003; Bajracharya, 2003; Jekeli and Serpas, 2003; Huang and Véronneau, 2005). Because Stokes's method of geoid computation requires that all of the Earth's masses are contained within the geoid, it is necessary to "dispose" of the topography before the approach can be used. This disposal is achieved (under Helmert's second method of condensation) by condensing the topography onto an infinitesimally thin surface layer on the geoid with density equal to the cumulative vertical density of the topography at that point. This reduction is commonly termed the direct topographical effect (DTE) on gravity (Martinec and Vaníček, 1994a).

The computation of the DTE can be divided into two parts, the effect caused by a Bouguer plate or shell and the effect due to the departure of the topography from it (the terrain correction, TC). The Bouguer component is a first approximation of the topography above the geoid and is typically represented by either an infinitely lateral planar plate (Figure 4.1) or a spherical shell (Figure 4.2) of "height" equal to the height of the gravity observation point above the geoid (cf. Section 3.3.3). The TC is a measure of the effect on gravity of the actual topographic variation from the Bouguer component (cf. Figures 4.1 and 4.2). The sum of these two components is the DTE on gravity under the planar (DTE_P) and spherical (DTE_S) models (Equations (4.1) and (4.2) respectively).

$$DTE_P = 2\pi G\rho H + TC_P \tag{4.1}$$

$$DTE_S = 4\pi G\rho H + TC_S \tag{4.2}$$

Both the Bouguer plate/shell and the TC are evaluated at the Earth's (topographic) surface, after their application the gravity anomalies are reduced to the geoid. The addition of the TC to the free-air gravity anomaly gives an approximation of the Helmert gravity anomaly called the Faye gravity anomaly (Moritz, 1980b, p. 419). When the Bouguer component of the DTE is added to the free-air anomaly the

simple Bouguer anomaly is obtained. Similarly, the addition of the complete DTE (Bouguer plus TC) gives the refined or complete Bouguer anomaly (Heiskanen and Moritz, 1967, Section 3-3).

4.4 Moritz's terrain correction (TC)

The TC formula that approximates Helmert's condensation together with Moritz-Pellinen DC (Section 4.5) under a linear and planar approximation (Schwarz *et al*., 1990) is given by Moritz (1968, p.12) as:

$$\mathrm{TC} = \frac{G\rho R^2}{2} \iint_{\sigma} \frac{\left(H_P - H_{P'}\right)^2}{l^3} d\sigma \tag{4.3}$$

where G is Newton's gravitational constant, ρ is the topographic mass-density (normally assumed constant so is outside the integral), R is the mean Earth radius, H_P is the nominally orthometric height of the computation point, $H_{P'}$ the height of the roving point in the integral, $d\sigma$ is the surface area element, and l is the planar distance between the points P and P'.

The planar TC approximation (Figure 4.1) uses a Bouguer plate to approximate the effect of the topography above the geoid surface. Despite its popularity (e.g., Featherstone *et al*., 2001; Omang and Forsberg, 2000; Li and Sideris, 1994) it is not a realistic approximation of the real Earth (Vaníček *et al*., 2004). The use of a Bouguer plate causes the TC to diminish rapidly with distance from the computation point. These computations are typically limited to a relatively small calculation radius (e.g., 50 kilometres) because the magnitude of the TC reduces rapidly with distance (e.g., Moritz, 1980b, Section 49). The truncated computation area is often referred to as a Bouguer cap. In areas of rough topography, it has been shown to be necessary to compute over a larger (1° cap) radius (e.g., Huang *et al*., 2001). The planar approximation has been widely implemented for the computation of TCs for use in regional gravimetric geoid computations (e.g., Blais and Ferland, 1984; Schwarz *et al*., 1990; Ma and Watts, 1994; Li and Sideris, 1994; Tsoulis, 2001; Kirby and Featherstone, 1999, 2002).

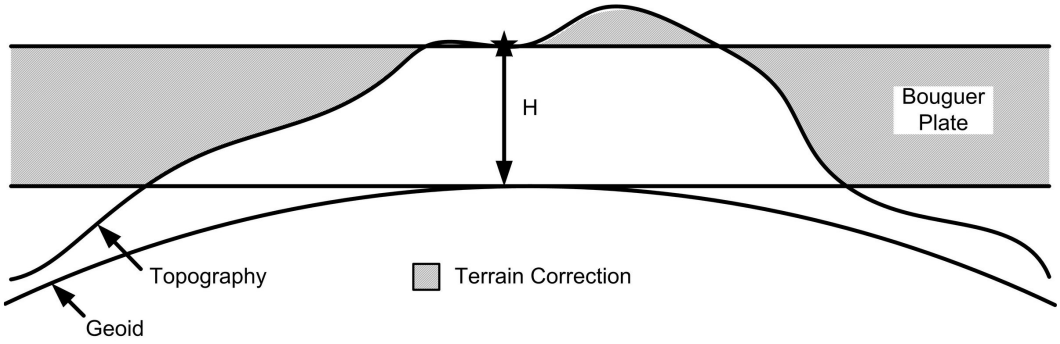

Figure 4.1 Planar approximation of the TC

In contrast to the planar approximation, the spherical approximation (Figure 4.2) uses a spherical Bouguer shell instead of a plate. It was proposed for use in geoid computation by Martinec and Vaníček (1994a) and is intuitively more representative of the real Earth. Because the Bouguer shell does not diminish with distance, the total global terrain effect can be very large (this is especially the case in areas of high altitude where a very "thick" Bouguer shell will be used). This means that it is imperative that the TC has to be computed globally, not just over a limited spherical cap, as is done under the planar approximation (e.g., Vaníček *et al.*, 2001, 2004).

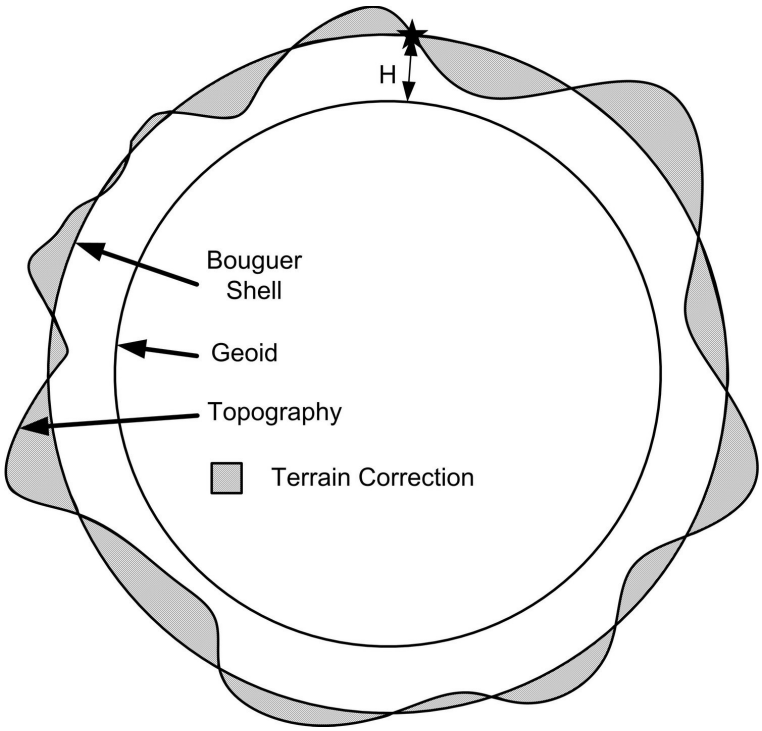

Figure 4.2 Spherical approximation of the TC

It has been argued by several authors (e.g., Sjöberg and Nahavandchi, 1999; Nahavandchi, 2000; Vaníček *et al.*, 2001; Novák *et al.*, 2001a) that the spherical approximation and the subsequent global computation of TCs is the conceptually superior method of determining the DTE on the gravity. Vaníček *et al.* (2004) take this argument further by pointing out that the DC of Bouguer anomalies can only be done meaningfully under the spherical approximation. The computation of spherical TCs is very time consuming (because the magnitude does not diminish with increasing distance from the computation point) and as such it is not normally implemented for regional geoid computations. Examples where spherical TCs have been computed include Nahavandchi and Sjöberg (2001), Huang and Véronneau, (2005) and Kuhn (2006).

The spherical model is a closer representation of physical reality than the planar model and is the theoretically better option for the delivery of high accuracy geoid results. Vaníček *et al.* (2001) note that the numerical evaluation of the spherical TC could be affected by systematic errors embedded in the global elevation data. The planar model is advantageous in this respect (it does not use a global DEM) and also produces a smoother field that is more suitable for the prediction of gravity data (Section 4.11).

While the theoretical arguments for implementing a spherical Bouguer model for the DTE computation are very compelling, from a practical perspective the alternative Bouguer plate approach is still widely used for geoid computation. Novák *et al.* (2001a) note that the differences in the computed TC between the spherical and planar models can be significant (up to 100 mGal in the Coastal Mountains in western Canada); however these differences are generally limited to the long wavelength part of the gravity spectrum. The difference between the planar and spherical TC models in NZ is likely to be similar to the 5.5 cm difference observed by Nahavandchi (2000) in a comparable region of Sweden (topography range of 354 m to 1147 m). Given the significant computational burden that is associated with implementing the spherical TC model, the TCs computed for NZ were restricted to the planar model (see Sections 4.7.2 and 4.7.3).

4.5 Downward continuation

The solution to the GBVP for geoid evaluation deals with the determination of the gravity potential on the geoid from gravity observations made on (or above) the Earth's surface. The Earth's surface for continental regions differs significantly from the geoid and so it is necessary to "downward continue" (DC) the observations from their point of observation to the geoid surface (Martinec, 1996).

The DC of gravity observations from both the surface of the Earth and from satellite or aerial altitudes above the Earth's surface is an ill-posed problem and therefore not easily achieved (e.g. Sun and Vaníček, 1998; Heck, 2003b; Jekeli and Serpas, 2003). It is ill-posed because the results (on the gravitational potential) do not continuously depend on the observations (Martinec, 1996). An additional constraint is that the more high-frequency content there is in the gravity field, the more difficult is the accurate DC with either method (Jekeli and Serpas, 2003). This problem has been described extensively in the literature (e.g. Heiskanen and Moritz, 1967; Schwarz, 1978; Moritz, 1980b; Jekeli, 1981a; Bjerhammar, 1987; Sideris, 1987; Wang, 1988; Engels *et al*., 1993; Sjöberg, 1996; Vaníček *et al*., 1996; Martinec, 1996; Grafarend and Krumm, 1998; Sun and Vaníček, 1998; Sjöberg, 1998; Nahavandchi, 2000; Wong, 2002; Novák and Heck, 2002; Sjöberg, 2003a; Jekeli and Serpas, 2003; Huang *et al*., 2003; Tsoulis, 2003; Ågren, 2004; Huang and Véronneau, 2005).

Steps 1 and 2 of the gravity to geoid conversion (Section 4.2) can be applied in slightly different ways that are theoretically equivalent. The two procedures (as described by Huang and Véronneau, 2005) are (i) Helmert gravity anomalies are evaluated above the irregular Earth before DC (i.e., the topographic masses are condensed onto the geoid prior to DC); and (ii) refined Bouguer anomalies on or above the surface of the Earth are DC to the geoid then Helmert anomalies evaluated on the geoid (i.e. mass-condensation is completed after DC). These alternatives are respectively equivalent to the Moritz-Pellinen, (Moritz 1968; Pellinen 1962) and the Vaníček-Martinec, (Vaníček and Kleusberg, 1987; Vaníček and Martinec, 1994) approaches (Jekeli and Serpas, 2003). In the Moritz-Pellinen (M-P) approach the DC is implicit in the TC, whereas in the Vaníček-Martinec (V-M) approach, DC is explicitly applied in the two separate stages described below.

The DC of gravity is typically split into two components: the normal gravity, γ; and the Molodensky free-air gravity anomaly, Δg. The normal gravity DC can be done easily since it only depends on the (known) normal field and the topographic height. The Δg component can be determined by the inverse solution of the Abel-Poisson integral (e.g. Heiskanen and Moritz, 1967, p. 318; Schwarz, 1978; Bjerhammar, 1987; Wang, 1988; Vaníček *et al*., 1996; Martinec, 1996; Sun and Vaníček, 1998) or Moritz's (1980b) analytical approach based on the Taylor series expansion (e.g. Moritz, 1980b; Sideris, 1987; Wang, 1988).

Huang and Véronneau (2005) compared the M-P and V-K approaches using both the Abel-Poisson integral and Moritz's DC. They found that the V-K approach was less sensitive to the DC because of the smooth Bouguer anomaly field. The DC of the refined Bouguer anomalies over Western Canada contributed to the geoid at the decimetre level, which was at the accuracy level of the height data used to evaluate it. This implies that the importance of DC in geoid computation (in this study area) may be more for theoretical rigor than a practical necessity. They also found little difference between the two DC methods.

Jekeli and Serpas (2003) undertook a similar study (also in the Canadian Rocky Mountains but in a different area) and also concluded that the difference between the two approaches is practically insignificant in areas of smooth topography. However, they also found that the M-P approach was superior in mountainous areas. The numerical differences between the two approaches noted in their findings agreed with the conclusions of both Wang and Rapp (1990) and Nahavandchi (2000). Huang and Véronneau (2005) countered these conclusions by suggesting that the significant differences noted by Jekeli and Serpas (2003) in the mountainous areas were most likely due to insufficient resolution of the DC rather than the condensed topographic effect. It is clear that some conjecture remains around the optimum treatment of DC and TC.

The process of DC is relatively easy when dealing with a harmonic function; conversely it is very difficult to perform with a non-harmonic function such as the topography of the Earth because it is affected by the density irregularities in the close proximity to the surface (Vaníček *et al*., 1996). This problem is usually overcome by smoothing (or regularisation) the disturbing potential by using a relatively coarse

DEM to introduce harmonocity into the topography (e.g. the Residual Terrain Model, RTM, method of Forsberg, 1984, 1985). Vaníček *et al*. (1996) showed that the use of averaged Helmert anomalies over a 5' by 5' grid was able to give a unique DC solution.

Given the small difference between DC approaches (Huang and Véronneau, 2005) and the fact that the implicit approach is simpler to implement (it is already accounted for in the TC software used), the M-P approach was selected for use in the NZ geoid computations.

4.6 Primary indirect topographic effect on potential

When the Earth's masses are condensed onto the geoid (as is done under Helmert's second method of condensation), the original gravitational potential of the Earth is also changed. The difference between the gravitational potential of the actual *in situ* topographical masses and the gravitational potential of the condensed topographical masses referred to a point on the geoid is typically referred to as the PITE (e.g. Heiskanen and Moritz, 1967, sec 3-6; Martinec and Vaníček, 1994b; Sjöberg and Nahavandchi, 1999).

Like the DTE discussed above, the magnitude of the indirect effect on the Earth's potential can be evaluated under either a planar or spherical approximation (e.g., Martinec and Vaníček, 1994b; Wichiencharoen, 1982). The planar formula for determining the PITE on the geoid at a point P for Helmert's second method of condensation is given by Wichiencharoen (1982) as:

$$N_{ind}\left(P\right)=\frac{-\pi G\rho H_P^2}{\gamma}-\frac{G\rho R^2}{6\gamma}\iint_{\sigma}\frac{H^3-H_P^3}{l^3}d\sigma \tag{4.4}$$

The spherical approximation (with constant mass-density) is given by Martinec and Vaníček (1994b) as:

$$N_{ind}(P) = \frac{2\pi G\rho H_P^2}{\gamma} + \frac{G\rho R^2}{\gamma}\iint_\sigma \left[2\frac{\sqrt{l^2+H^2}-\sqrt{l^2+H_P^2}}{R} + \ln\frac{\frac{l}{2R}+H+\sqrt{l^2+H^2}}{\frac{l}{2R}+H_P+\sqrt{l^2+H_P^2}} - \frac{H-H_P}{l}\right] d\sigma \tag{4.5}$$

Equation (4.4) has been developed further in terms surface spherical harmonics to the power H^2 (Sjöberg, 1995) and to the power H^3 (Nahavandchi and Sjöberg, 1998a). Martinec *et al*. (1996) showed that when Equation (4.4) is written as a Taylor series, it becomes divergent after the quadratic term when evaluated with a dense (1 km grid) topographic DEM in the Canadian Rocky Mountains. Consequently, for practical geoid applications, it is common to only evaluate the PITE using the first (quadratic) term of Equation (4.4) (e.g. Featherstone *et al*., 2001). Because of the rough topography in NZ, a 56-metre DEM was used for the NZ quasigeoid computations. Consequently, the planar PITE was computed using only the first term of Equation (4.4). The use of the planar PITE is then also consistent with the planar DTE described in Section 4.4.

4.7 Terrain correction computation techniques

4.7.1 Terrain corrections by Hammer charts

The method that Hammer (1939) devised to make TCs involved dividing the area surrounding the station into concentric circular zones and compartments (Table 4.1, Figure 4.3). These are then overlaid onto topographical maps where the average height within each compartment is estimated and the overall TC deduced. The accuracy of the TCs computed by this method are limited by the accuracy and resolution of the available topographic maps, by the use of too few compartments out to a given distance in an area of rugged topography, and the ability of the interpreter to correctly average the height differences in each compartment (Nowell, 1999). The use of Hammer charts to determine TCs is a very labour-intensive process, it is for this reason that the approach has generally been superseded by the fast Fourier transform (FFT) and prism approaches described below.

Zone	Inner Radius	Outer Radius	Number of Compartments
A	0.0	2.0	1
B	2.0	16.6	4
C	16.6	53.3	6
D	53.3	170.1	6
E	170.1	390.1	8
F	390.1	894.9	8
G	894.9	1530	12
H	1530	2615	12
I	2615	4469	12
J	4469	6653	16
K	6653	9903	16
L	9903	14,742	16
M	14,742	21,944	16

Table 4.1 Hammer zones used for computation of TCs (radii in metres)

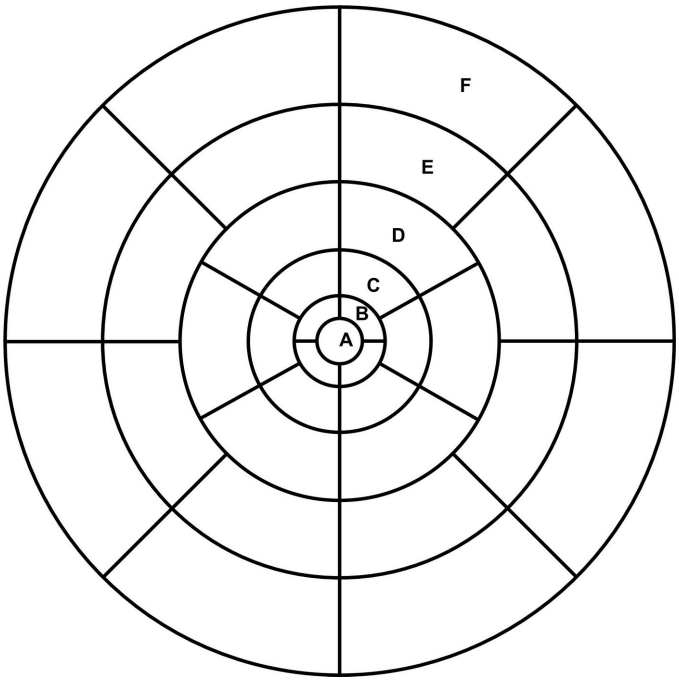

Figure 4.3 Hammer zones and compartments up to zone F

GNS Science (www.gns.cri.nz) provided TCs computed from Hammer charts at the locations of each of the 30,876 land gravity anomalies (described in Sections 3.3 and B.7). These were computed as inner- and outer-zone components (Reilly, 1972;

Woodward, 1982). The inner-zone component was calculated by the observer's field assessment of the topography from zone B (2 metres) out to either zone D (170.1 metres) or zone F (894.9 metres) depending on when the gravity observation was made (Reilly, 1972). The outer-zone components were evaluated from the edge of the inner-zone out to zone M (21.994 kilometres) using the 1:63,360 topographic maps (contoured to 100 feet or ~30 metres) that were available in the 1970s using the procedure described in Woodward and Ferry (1973).

The Hammer TCs are assessed on the surface of the Earth and calculated using the spherical approximation (cf. Section 4.4), giving corrections that are residual to a spherical Bouguer cap of thickness equal to the gravity observation elevation H and a radius of 21.994 km (Hammer zone M). They were computed using a constant mass density of 2,670 kgm^{-3} (Woodward and Ferry, 1973). The sum of the inner and outer zone corrections gives a band-limited TC signal (i.e. from 2 m to 21.994 km). The GNS Hammer TCs are shown in Figure 4.4.

4.7.2 Terrain corrections by two-dimensional Fourier transform

In recent times, it has become possible to efficiently compute TCs using regular grids of elevations available in DEM data. With the use of a computer and some approximations, it is possible to utilise the FFT (e.g. Forsberg, 1985; Sideris, 1985; Schwarz *et al*., 1990; Parker, 1995, 1996; Kirby and Featherstone, 1999, 2002). A major weakness of TCs determined using DEM data is that that the elevation values of a given cell generally relate to the average topographic height within that cell and so do not represent well the actual topographic morphology. Thus, the near-station effects of the topography can be omitted. It is however acknowledged that average values are beneficial for the numerical evaluation of integral functions. The magnitude of the effect due to using averaged heights is a function of the DEM cell size and the roughness of the topography and can reach several tens of mGal in magnitude (e.g., Leaman, 1998; Nowell, 1999). The consequence of using a DEM is that the resulting TC will be band-limited from a distance of half the DEM cell size, up to the maximum distance of the computation (cf. Kirby and Featherstone, 2002).

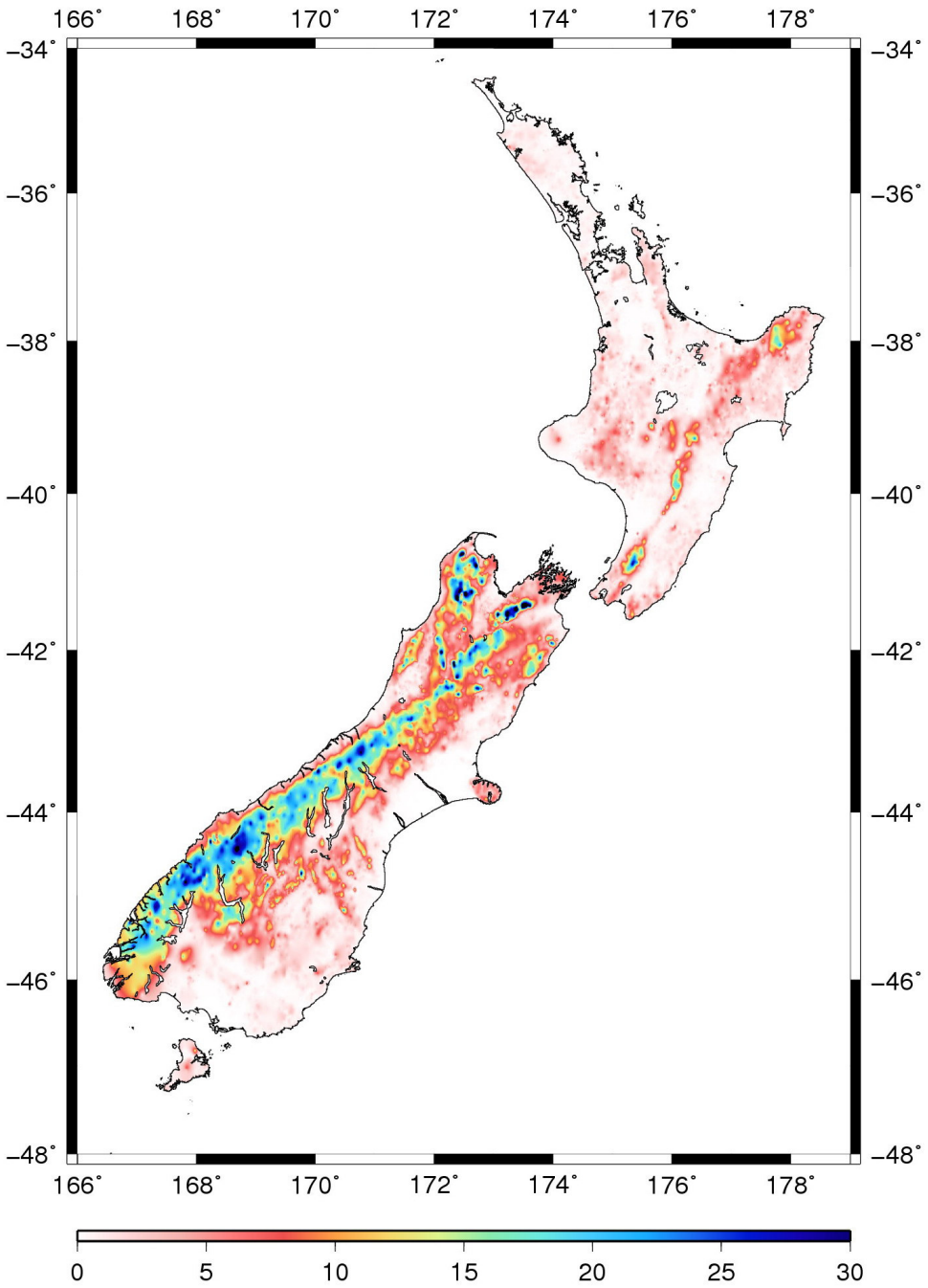

Figure 4.4 A generalised (30") image of the Hammer TCs (mGal, Mercator projection)

When the topography is represented in a regular grid such as a DEM, the height in each cell is represented by a prism with average height and average mass-density of the topography. This is termed the mass-prism topographic model (Li and Sideris, 1994). If the mass of the prism is then mathematically concentrated along its vertical symmetric axis, then the topography within the prism is represented by a line, which gives rise to the mass-line topographic model (Li and Sideris, 1994). When the

DEM grid spacing is small enough (e.g. <100 metres) the difference between the two approaches is likely to be negligible (Tziavos *et al*., 1996).

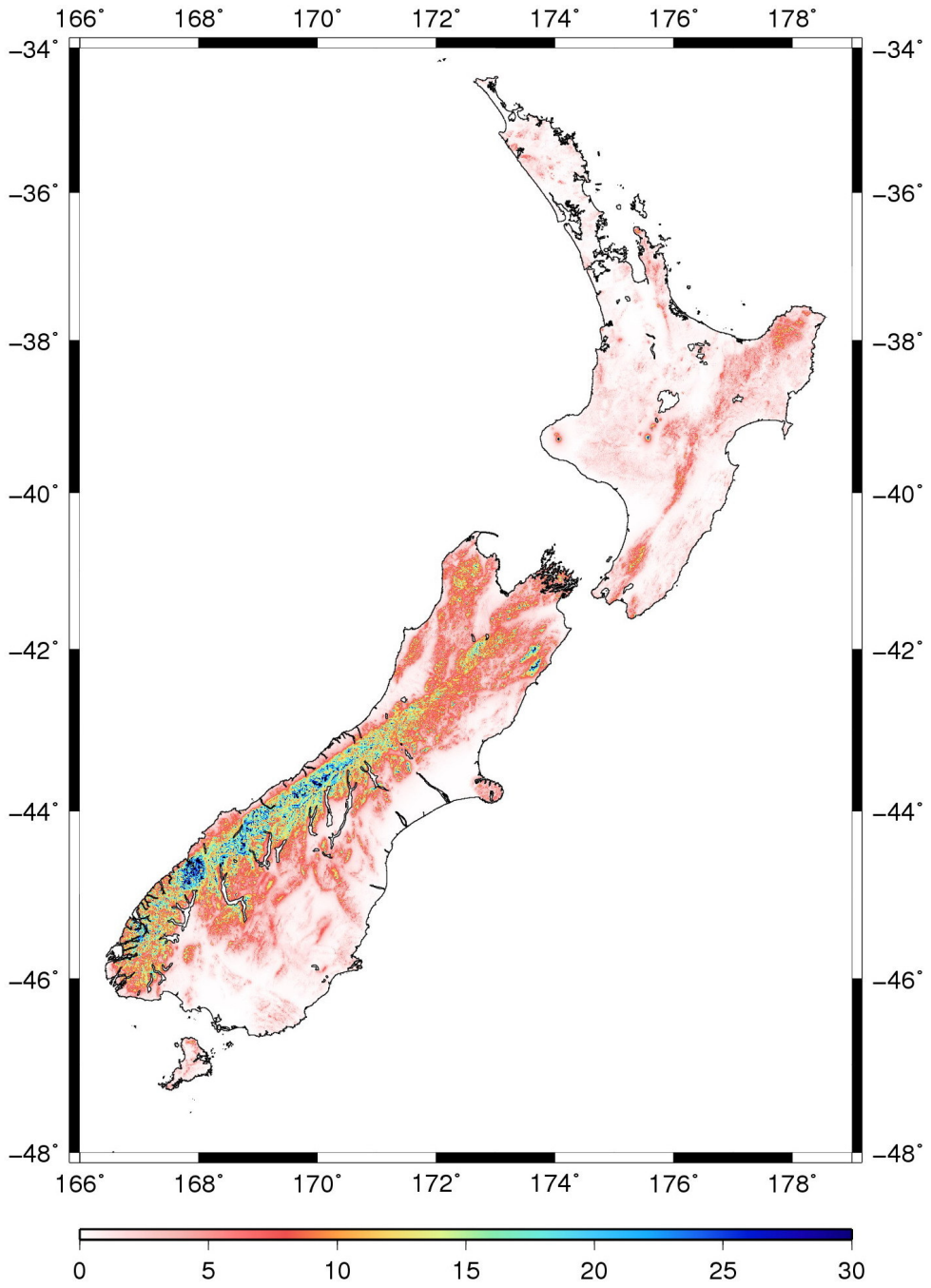

Figure 4.5 A generalised (30") image of the FFT Moritz TCs (mGal, Mercator projection)

A 1.8" (~56 metre) resolution grid of TCs was computed over NZ using the planar 2D-FFT implementation of Moritz's (1968) algorithm (Schwarz *et al*., 1990; Kirby and Featherstone, 1999). The FFT TCs were computed over a cap size of 100 km by

100 km about each computation point using a constant mass-density of 2,670 kg/m^3. This computation cap was chosen because the effect of increasing the residual topographic effect outside this radius under a planar approximation is minimal (Li and Sideris, 1994; Ma and Watts, 1994, Kirby and Featherstone, 1999). The Moritz algorithm for the TC includes an implicit DC; hence the calculation is performed at the geoid as opposed to the Earth's surface in the Hammer method. The computed TCs are shown in Figure 4.5. The image has been generalised to a 30" grid for display purposes.

4.7.3 Terrain corrections by prism integration

The method of prism integration as a means of calculating TCs was proposed by Nagy (1966a, 1966b). This approach simply represents the terrain as a regular grid of prisms that correspond to a DEM of the topography with the base of the prisms at sea level and the tops defined by the elevation in the DEM. The vertical component of the gravitational attraction of each prism is assessed through numerical integration and the sum of these components gives the TC (Forsberg, 1984; Nagy *et al*., 2000). Nagy *et al*. (2000, 2002) showed that the integration of the gravity disturbance over a rectangular prism gives closed formulas for the potential and its derivatives (up to third order).

The prism approach is relatively simple to implement and it does not suffer from the same numerical instabilities that affect the FFT approach, so it is ideal for use in areas of rough topography. However it can take a very long time to perform the calculations since the computation time increases exponentially with an increase in the DEM resolution (see below). In addition, the use of flat-topped prisms (while computationally efficient) does not give a realistic depiction of the actual topography, especially in the zone close to the computation point. An alternative is to use prisms with inclined (or curved) tops (e.g., Blais and Ferland, 1984; Ma and Watts, 1994; Smith, 2000). While this is more realistic, it adds significantly to the computational burden of evaluating the TC so is not an efficient approach over a large area. A different approach is to use the rigor of the prism approach in areas close to the computation point and to use the relatively speedy FFT method further away, thus getting the best from both methods (e.g., Tsoulis, 1998; 2003). This combined approach was not used in NZ; instead (as described below) the prism

method was implemented using DEM information of different resolutions to increase the computational efficiency.

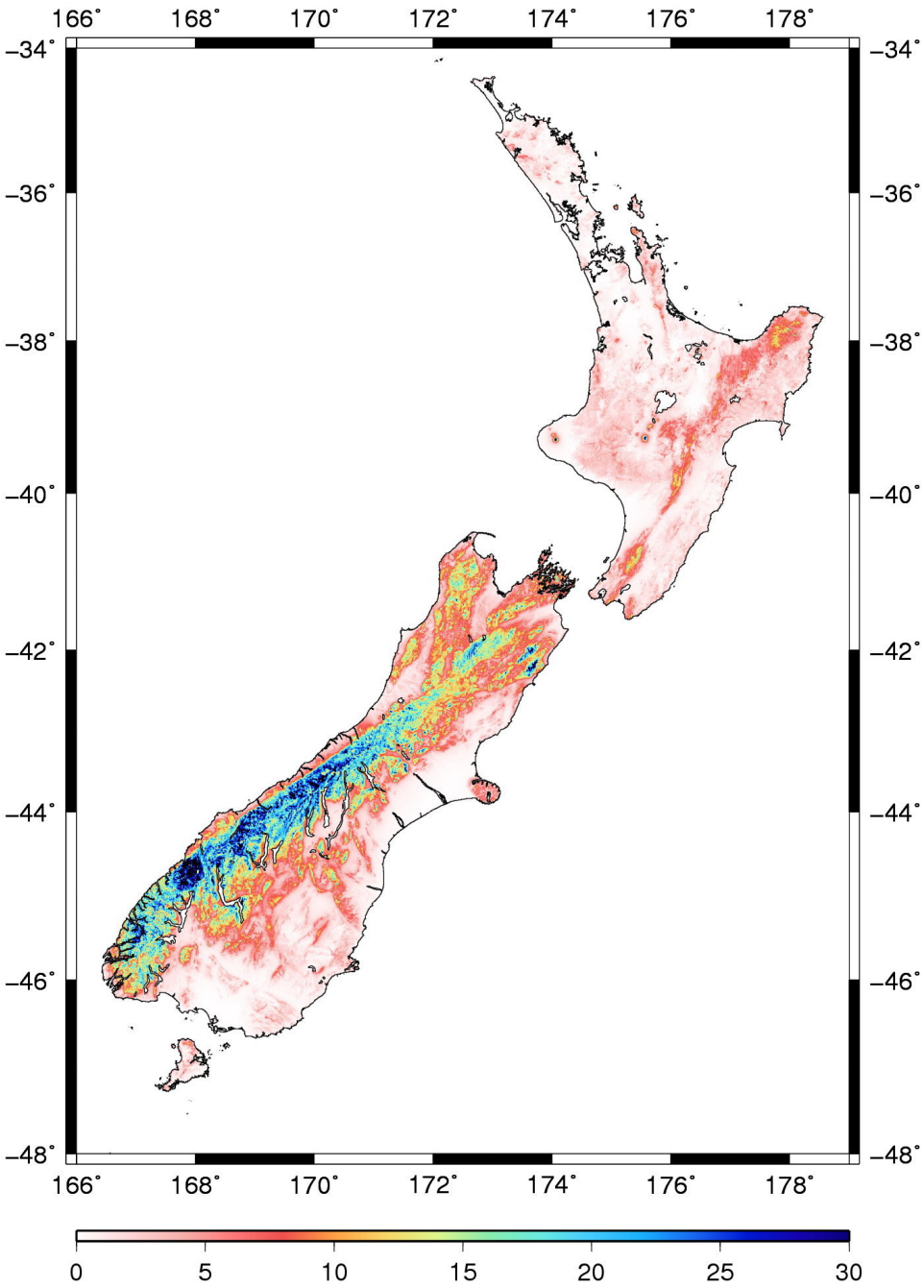

Figure 4.6 A generalised (30") image of the prism TCs (mGal, Mercator projection)

A set of TCs were also computed over NZ using the prism integration approach (Figure 4.6). The corrections were evaluated using the TC routine in GRAVSOFT computer software using a constant mass density of 2,670 kgm^{-3} (Forsberg, 1984). Like the FFT approach described in Section 4.7.2, the prism TCs were evaluated

with respect to a spherical Bouguer plate. The computations were evaluated using the 56 m NZ DEM (cf. Section 3.7) out to a distance of 12 kilometres from the computation point, a coarser 250 metre DEM (obtained by re-sampling the former) was used outside this to the computational limit of 50 kilometres.

The main difficulty in implementing the prism integration approach is that it is computationally intensive. To minimise the computer memory requirements, the TC calculations were split into 1 x 1 degree tiles (a total of 64 over NZ). For each tile a 3 x 3 degree extract from the DEM (centred on the calculation tile) was used to determine the TC at each cell within the tile. In addition to reducing the memory requirements, the tiled approach enabled simultaneous calculations on an eight-processor Sun™ server. Even with this "multi-tasking", the TCs took a total of 2.5 months to calculate.

4.8 Comparisons among TC computational models

To determine the best TC computation approach for use in NZ, the three sets of TCs described above were compared. It is acknowledged that the Hammer TCs use a different conceptual model (spherical approximation) to the FFT Moritz and prism approaches (planar and linear approximation). The TCs have also been computed with different "band-limits": the FFT TCs are from ~28 m to 50 km; the prism TCs are ~28 m to 55 km; and the Hammer TCs are 2 m to 21.994 km. The final major difference between the different approaches relates to where the TC is calculated, the Hammer TC is evaluated at the Earth's surface whereas the FFT and prism approaches are at the geoid (because Moritz's algorithm incorporates implicit DC).

Conceptually, the Hammer TCs are superior to the FFT and prism TCs because they consider a spherical approximation model (cf. Section 4.4) and provide for more of the near-gravimeter effects (as little as 2 m from the observation point). However, this must be balanced against the additional need to perform DC prior to geoid computation (cf. Jekeli and Serpas, 2003), whereas the DC is implicit to the FFT and prism TCs [under some assumptions (e.g., Martinec *et al*., 1993, 1996)]. Also the spatial coverage of the Hammer TCs is relatively sparse (cf. Figure 3.2) so they are not as suited to gridding etc. Nevertheless, it remains instructive to compare the different TCs (Table 4.2).

It can be seen in the top section of Table 4.2 that the different approaches of computing the TCs give quite different results. To enable a valid comparison between the gridded TCs and the point Hammer TCs, the FFT and prism corrections were also interpolated (using a bi-cubic spline) to the locations of the former. This results in both reduced values for the maximum values and also the mean correction values. An explanation for the observed reduction is that the gravity observations are generally made at easily accessible locations where the topography is not so rough and so the corresponding TC will be less. The effect of the unrepresentative gravity observation locations in relation to gridding of the gravity field is examined in Section 4.11.

Quantity	Max	Min	Mean	Std Dev
Hammer TCs (at gravity observation points)	49.12	0.00	2.05	3.66
FFT TCs (all NZ)	174.98	0.00	1.84	3.95
FFT TCs (at gravity observation)	36.20	0.00	1.72	2.89
Prism TCs (all NZ)	131.06	0.00	2.64	5.35
Prism TCs (at gravity observation)	42.39	0.00	2.47	3.79
Hammer – FFT TCs (at gravity observation)	27.95	-10.71	0.33	1.35
Hammer – prism TCs (at gravity observation)	23.79	-15.24	-0.42	1.21
Prism – FFT TCs (at gravity observation)	15.21	-2.27	0.75	1.06
Prism – FFT TCs (all NZ)	128.27	-58.80	-0.80	1.60

Table 4.2 Statistics of and comparisons between TC calculation methods over NZ using the 1.8” DEM and at the 40,440 gravity observation locations (mGal)

The bottom section of Table 4.2 shows the differences between each of the TC solutions (again the gridded TCs have also been evaluated at the gravity observation locations). The differences between the TC solutions are relatively constant at the locations of the gravity observations. This was expected for the same reasons as described in the paragraph above. The differences between the prism and FFT TCs are much larger when evaluated over the entire 1.8” grid. This was suspected to be caused by numerical instabilities in the FFT approach that occur in areas of steep topography (Section 4.9). This suspicion was reinforced by Figure 4.7 which shows that the larger TC differences coincide remarkably well with the mountainous areas of NZ (specifically the Southern Alps/Kā Tiritiri o te Moana).

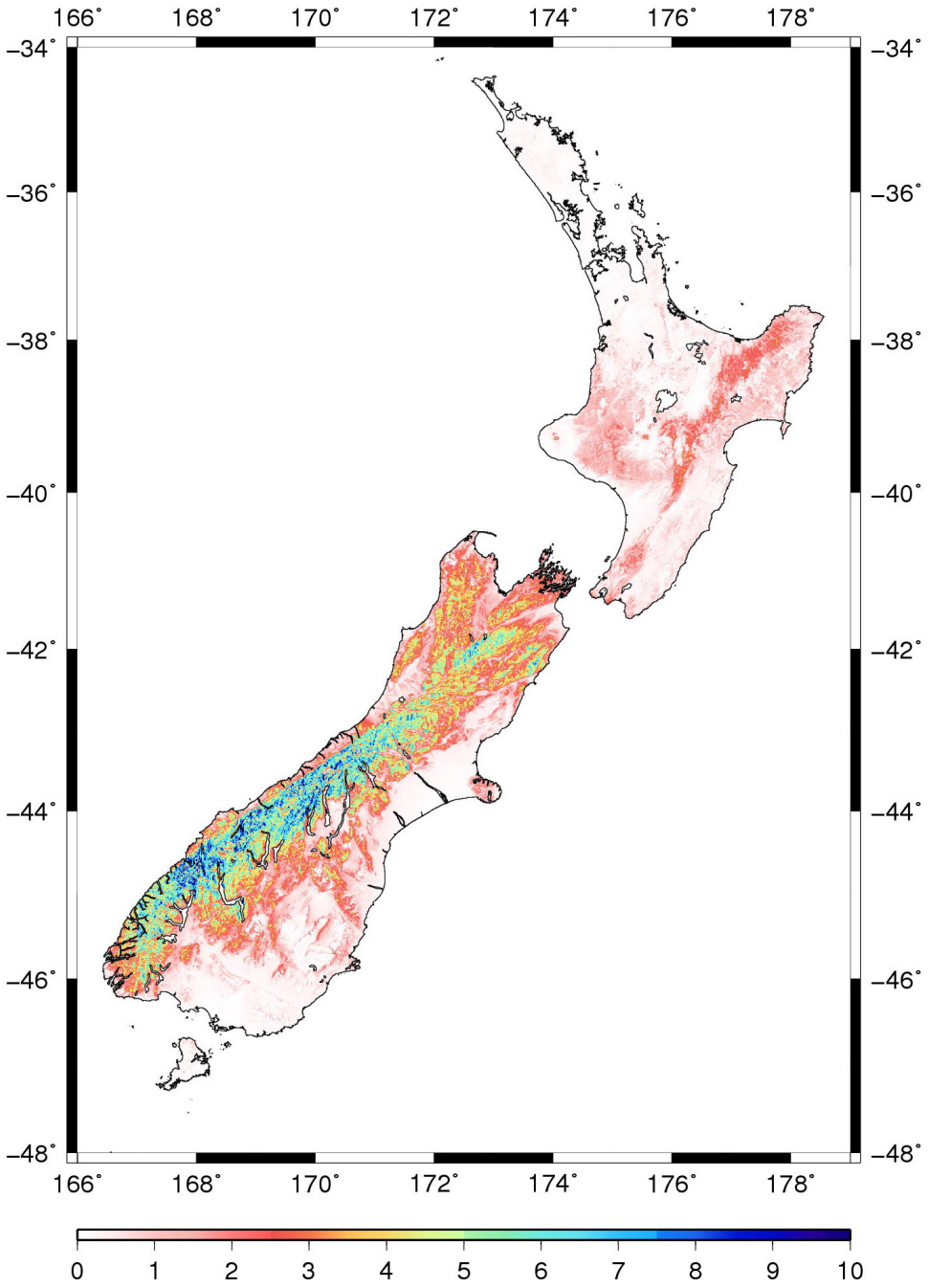

Figure 4.7 Generalised (30") absolute differences between prism and FFT TCs (mGal, Mercator projection)

4.9 Topographic gradients

Numerical instabilities occur in the FFT implementation of Moritz's (1968) algorithm (cf. Section 4.7.2) when the change in height between adjacent DEM cells is larger than the size of the cell (i.e. the condition $(\Delta h / l)^2 > 1$ exists, where Δh is the height difference between adjacent DEM cells and l is the DEM cell size;

Tsoulis, 2001). This corresponds to a requirement that the topography immediately surrounding the computation point does not exceed 45°. This instability is the most significant in areas of rough (i.e., steep) topography when combined with a high-resolution DEM (e.g., Forsberg, 1985; Klose and Ilk, 1993; Martinec *et al*., 1996; Tsoulis 2001). Figure 4.8 shows that the requirement for the topographic gradient to be less that 45° is not achieved in large areas of NZ.

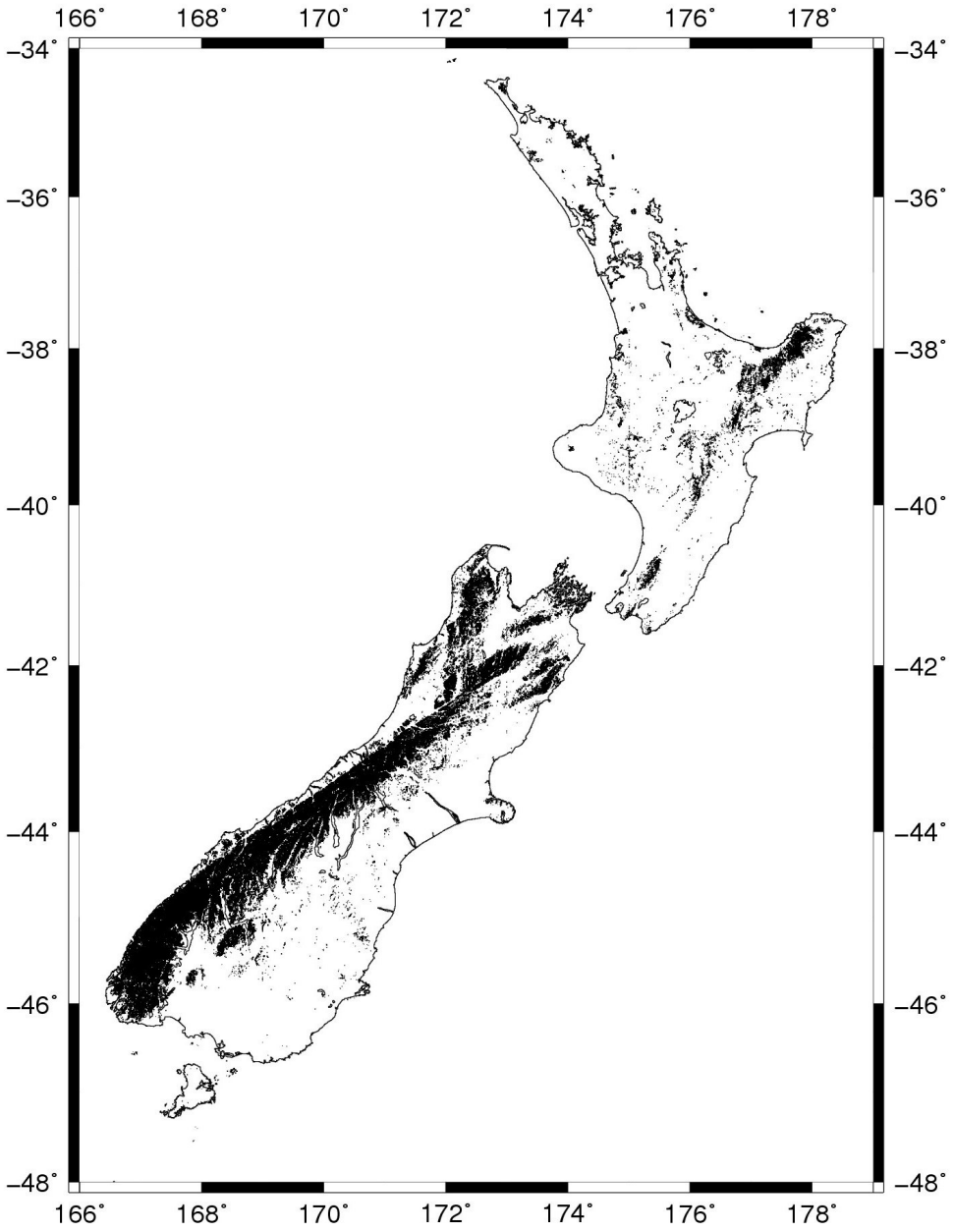

Figure 4.8 NZ topographic gradients over 45° computed from 56 metre DEM (Mercator projection)

The topographical gradients of the NZ DEM (cf. Section 3.7) were computed to ascertain whether this (< 45°) requirement was satisfied in NZ. The gradients were computed using the GMT *grdgradient* function (Wessel and Smith, 1998) in north-south and east-west directions and the statistics of these are given in Table 4.3. The locations of gradients over 45° are shown in Figure 4.8. It is clear from both Table 4.3 and Figure 4.8 that there are significant areas of NZ that are steeper then 45° (e.g. the Southern Alps/ Kā Tiritiri o te Moana). This indicates that the FFT TCs (Section 4.7.2) may be unreliable in these areas.

The TC differences were then classified into the 5° gradient bands for each direction shown in Table 4.4. It can be seen that the mean and standard deviation values increase with the increasing topographic gradient (as implied by Figure 4.7); this suggests a relationship between increasing gradient and TC difference. However, due to the magnitude of the change, it is not conclusive.

DEM Gradient	Max	Min	Average	STD
East-west	86°	0°	4.8°	9.1°
North-south	85°	0°	4.4°	8.5°

Table 4.3 Statistics of the 56m DEM gradients

Gradient	Points	Max	Min	Average	STD
30-35° EW	4191815	70.5	-36.9	-4.2	2.2
30-35° NS	3243492	20.1	-33.4	-4.1	2.2
35-40° EW	2375371	127.0	-32.0	-5.1	2.4
35-40° NS	1935219	113.6	-51.0	-4.8	2.3
40-45° EW	1044504	126.5	-30.6	-6.1	2.6
40-45° NS	811836	20.3	-36.9	-5.8	2.6
45-50° EW	444158	128.0	-51.0	-7.2	2.8
45-50° NS	342837	18.9	-36.9	-6.8	2.8
50-55° EW	192760	17.61	-36.9	-8.2	3.1
50-55° NS	155214	53.8	-33.3	-7.7	3.2
55-60° EW	82614	72.9	-35.7	-9.1	3.4
55-60° NS	67577	92.0	-51.0	-8.5	3.5
60-65° EW	30999	15.0	-50.2	-10.0	3.8
60-65° NS	24899	17.6	-32.6	-9.1	4.1
65+° EW	11570	15.0	-51.0	-11.4	4.7
65+° NS	8100	128.0	-35.4	-9.6	6.2

Table 4.4 Statistics of the difference between FFT and prism derived TCs at different 56-metre resolution DEM gradients (mGal)

To obtain a better insight into the correlation between topographic gradient and the TCs, the observed differences between the FFT and prism approaches were plotted at their full (1.8") resolution (Figure 4.9). The area between 169°E – 170W° and 45°S – 46°S (Lake Wakatipu) was chosen because it contains some of the larger TC differences (cf. Figure 4.7).

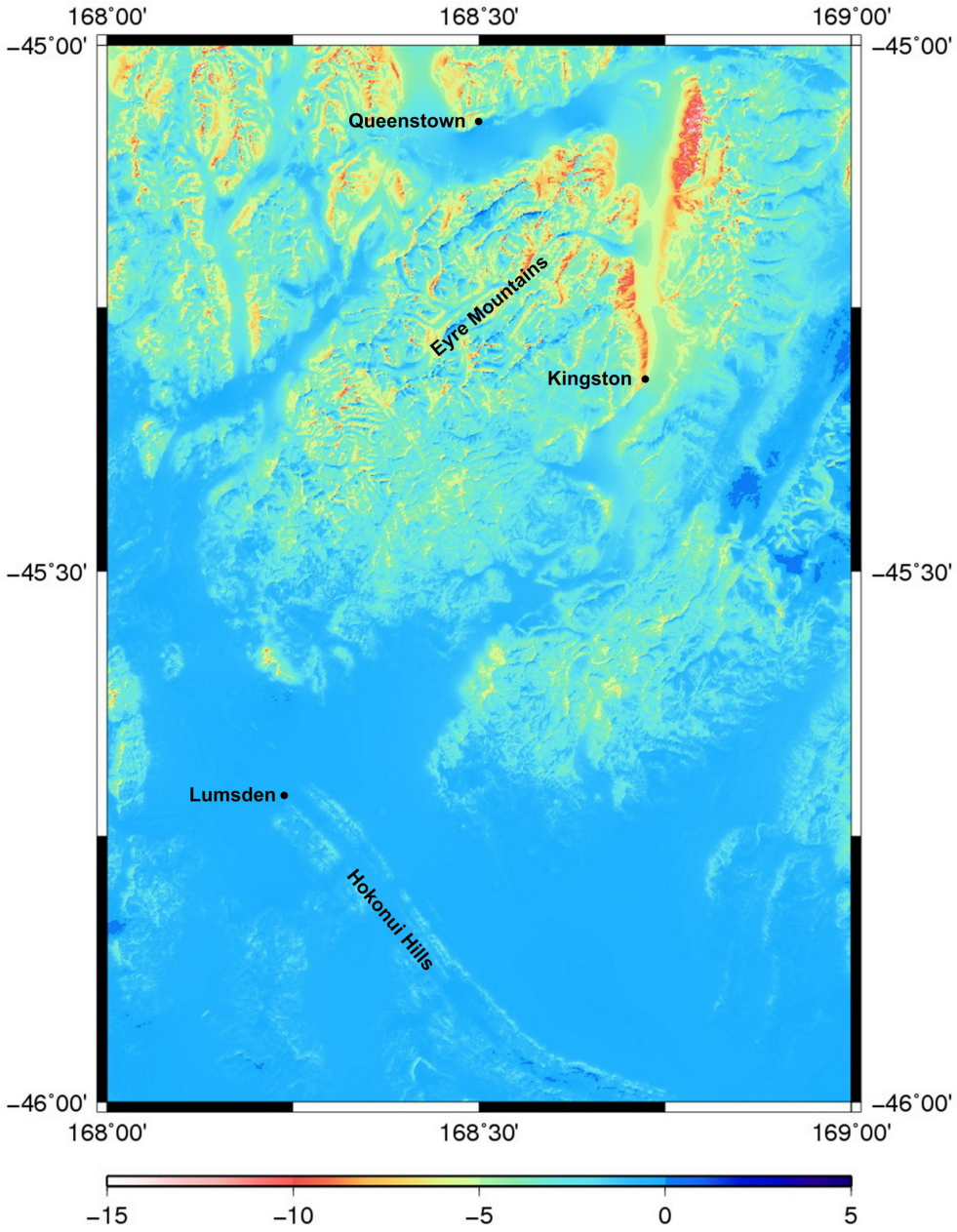

Figure 4.9 Differences between prism and FFT TCs in vicinity of Lake Wakatipu (mGal, Mercator projection)

When compared with the locations of topographic gradients that are over 45° (Figure 4.10), it is apparent that the larger TC differences occur where the gradients are also higher. This does not conclusively prove that the prism TC is better than the FFT TC in NZ. However, the documented problems with the FFT TC in areas of steep topography indicate that it may not be appropriate to use them in the NZ quasigeoid computations.

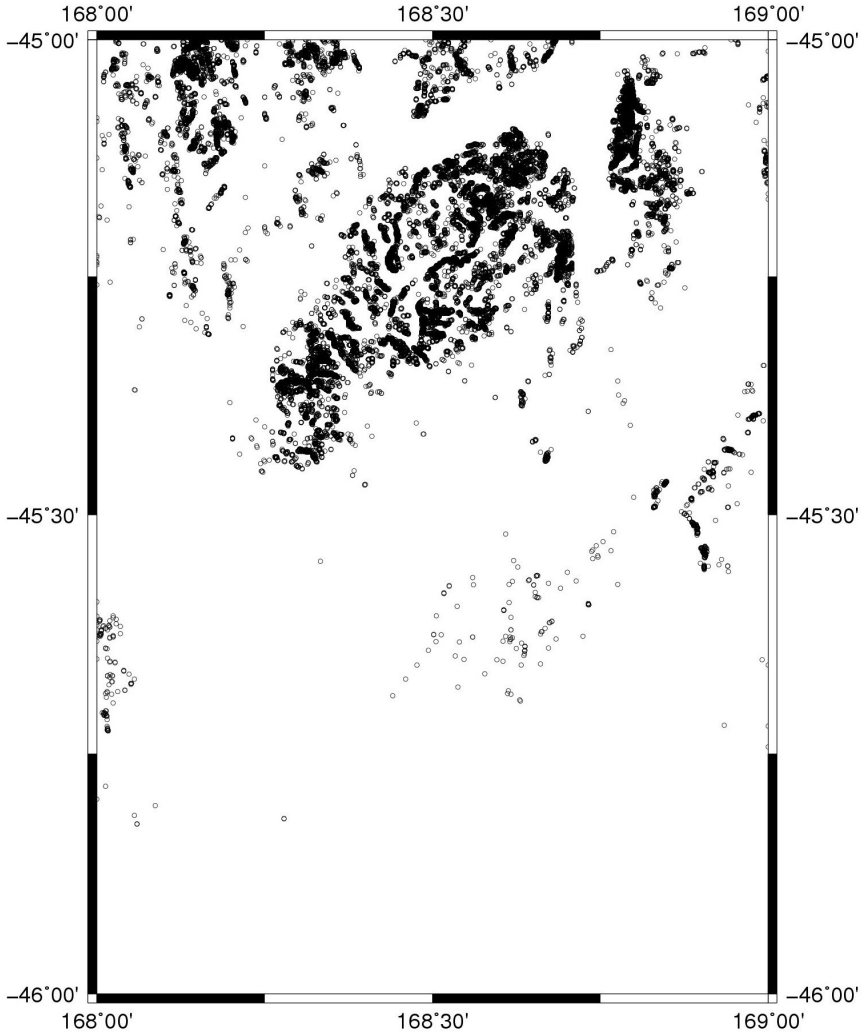

Figure 4.10 Location of topographic gradients larger than 45° TCs in vicinity of Lake Wakatipu (Mercator projection)

4.10 Topographic mass-density modelling in TC computation

An additional aspect that needs to be considered in the computation of TCs is the treatment of the topographical mass-density. When topographic reductions (such as TCs) are determined in practise, it is normally assumed that the density of the

topography is constant (2,670 kg/m^3). Several investigations (e.g. Martinec, 1998; Huang *et al*., 2001; Nahavandchi and Sjöberg, 2001; Kuhn 2003; Sjöberg, 2004a) have been undertaken to determine the effect of using more realistic values of the Earth's density that is known to vary laterally. It has been shown by, for example, Tziavos and Featherstone (2001) that the use of actual density information (if available) improves the quality of the TCs. Novák *et al*. (2001a) found that the omission of (actual) mass-density information will limit the accuracy of the computed TC regardless of the choice of planar or spherical Bouguer model. Likewise for gravity reconstruction (Section 4.11.2) density information should be used if it is available (Goos *et al*., 2003; Bajracharya and Sideris, 2005a)

It was not possible to include variations in topographical density in the NZ calculations because no digital density information is available. It could be possible to infer crustal-density information from the NZ national 1:250,000 geological map series. This map series is currently undergoing extensive revision hence a national coverage is not available. When the series is complete (tentatively 2010) it will provide a digital geological map that could easily be converted to a surface density model. However, it may not be possible to convert the mapping to a three-dimensional model because surface geology is not always representative of the structure through the topography.

4.11 Gravity aliasing and gridding

Both the FFT and prism TC computations described above (and the quasigeoid computations described in Section 6.2) require regular grids of gravity anomalies. When surface gravity observations are made for mapping or exploration purposes, the ideal situation is for them to be located so that they are spatially distributed to adequately sample the gravity field (Figure 4.11b). This means that, in ideal circumstances, there will be a higher density of observations where the gravity field is rapidly changing and a lower density where it changes more smoothly. In reality, the areas where the gravity field is more variable (e.g., mountainous regions) are frequently the areas where gravity observations are more sparsely located (Figure 4.11a) due to difficulties physically accessing the desired locations, terrain roughness and problems with gravimeter drift (e.g., Janák and Vaníček, 2005). To overcome these limitations, Featherstone and Kirby (2000) proposed a gravity "reconstruction"

technique to predict the gravity field using high-frequency topography information from a DEM (Figure 4.11c).

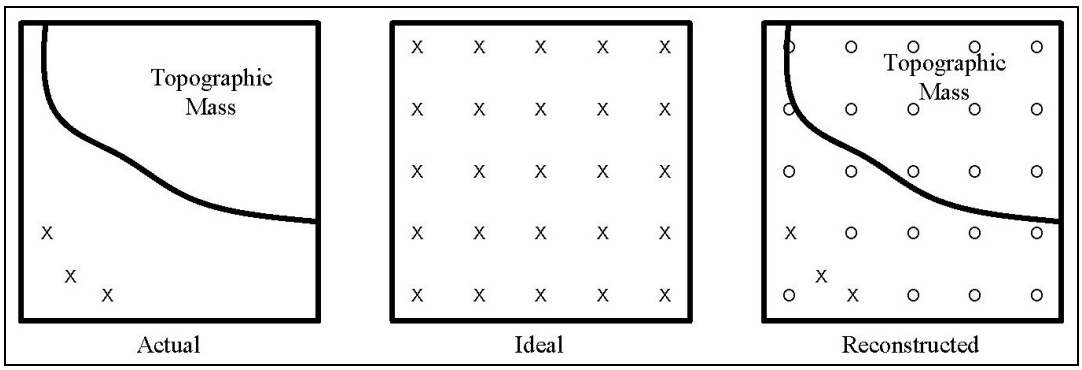

Figure 4.11 The gravity reconstruction concept: (a) typical gravity observation scheme, (b) ideal observation scheme, (c) reconstructed gravity field (X and O are the actual and reconstructed observations respectively)

4.11.1 Gravity pseudo-aliasing

The NZ gravity observations (cf. Figure 3.2) are not regularly spaced. This is demonstrated in Figure 4.12 which shows the gravity observations in the vicinity of Hanmer Springs in the Southern Alps/Kā Tiritiri o te Moana of the South Island. It can be seen that the observations are clustered around the Hanmer Plain (central east of map) and the Canterbury Plains (south-east of map). Most of the remaining observations are systematically located along the valley floors where driving (or more commonly walking in the case of NZ) is easier. Infrequent observations have also been made on ridges where they were accessed by helicopter (cf. Figure 4.12). The irregular spatial distribution of surface gravity observations becomes a problem when they are interpolated because the interpolated surface is not representative of the actual gravity field (e.g., Reilly, 1972).

Featherstone and Kirby (2000) and Goos *et al*. (2003) explain that the effect of irregular sampling (Figure 4.11a) is similar to the phenomenon of aliasing in signal processing. This is because both involve sampling a continuous function at discrete intervals that can not duplicate the desired function. In signal processing, the samples are usually made at regular intervals, where information at frequencies higher than twice the sampling frequency (Nyquist frequency) is incorrectly

represented. According to sampling theory, this high-frequency information becomes aliased into the lower frequencies, thus contaminating the sampled function.

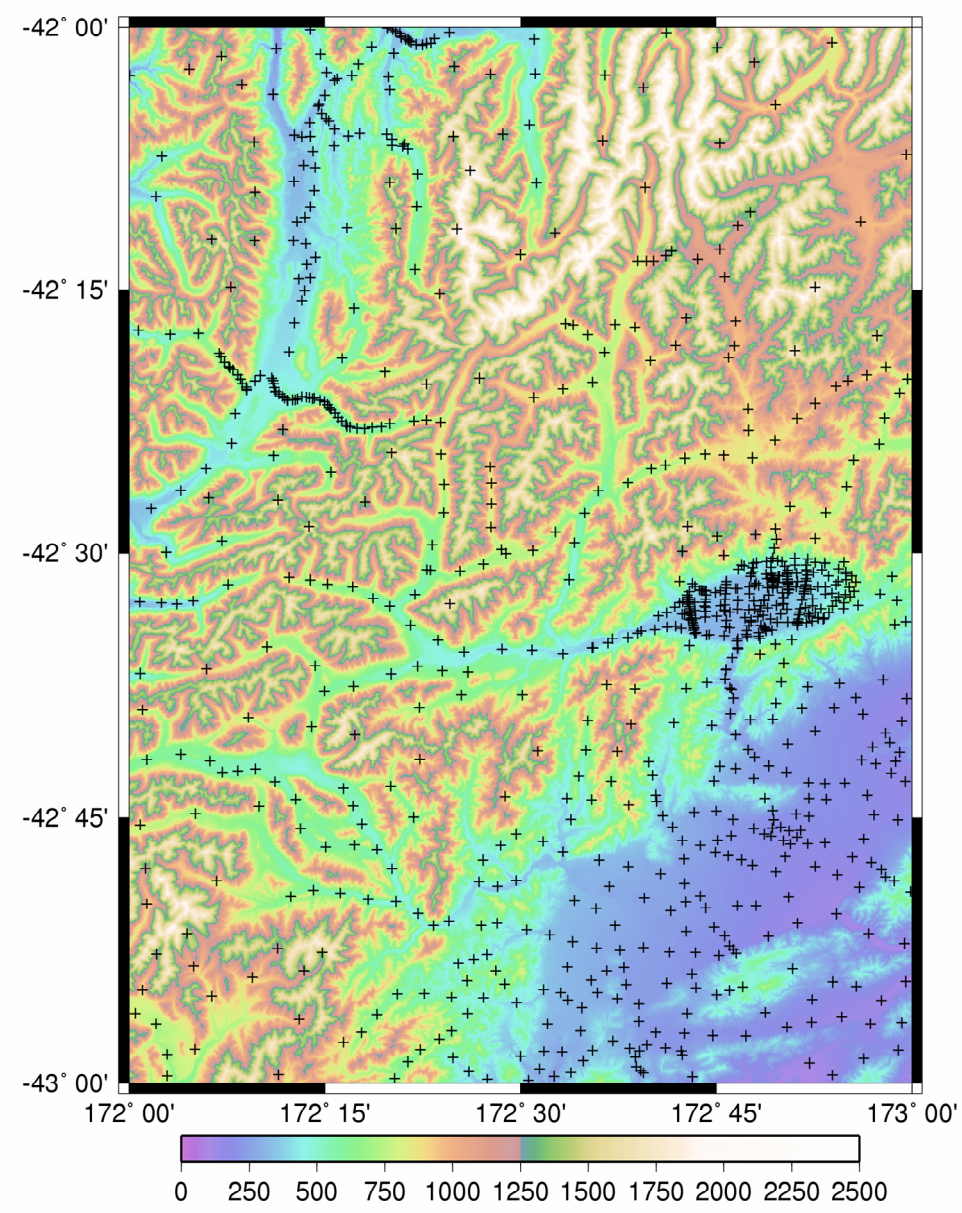

Figure 4.12 Gravity observations in part of the Hanmer Springs region of the Southern Alps/Kā Tiritiri o te Moana, South Island, NZ (heights in metres, Mercator projection)

With gravity data acquisition, the sampling interval is usually irregular but the consequence is similar; the gravity signal is sampled such that higher-frequency information is omitted and may be aliased into the lower frequencies. As stated above (and shown in Figure 4.12), because most of the NZ gravity observations have been made in the valleys between large mountains, it is likely that simple averaging

of the values will result in a non-representative estimation of the mean gravity field. The mean gravity field is required to numerically solve Stokes's integral (Heiskanen and Moritz, 1967; cf. Section 5.2).

4.11.2 Gravity reconstruction

Free-air gravity anomalies are highly correlated with the height of the observation points. This means that the "roughness" of the free-air anomalies is similar to that of the topography, thus in mountainous areas (e.g., Figure 4.12) it is not sensible to directly interpolate and average the anomalies because of aliasing (e.g., Featherstone and Kirby, 2000). To minimise the interpolation error, a common method is to grid Bouguer (or refined Bouguer) anomalies which are by definition "smoother" than their free-air counterparts (e.g., Featherstone and Kirby, 2000; Goos *et al*., 2003; Janák and Vaníček, 2005). Because the same (limited) number of gravity observations is still being used, this approach will still give a surface that is aliased.

Featherstone and Kirby (2000) proposed a method to reduce the effects of both gravity aliasing and the irregularly spaced gravity observations where supplementary terrain information from a DEM is used to compute additional "reconstructed" anomalies at unobserved locations on the topography (Figure 4.13). Termed the "reconstruction" technique, the resulting Faye gravity anomaly grid is a better representation of the true integral mean over the topography than simple averaging of the original Faye anomalies (cf. Figure 4.11). This method has been implemented in a number of other studies, such as Goos *et al*. (2003); Janák and Vaníček (2005); Bajracharya and Sideris (2005a, 2005b).

The reconstruction method (Figure 4.13) initially reduces the individual gravity observations to their planar Bouguer anomaly equivalents using (alternatively the spherical approximation could be used, cf. Section 4.3):

$$\Delta g_B = g_S - \gamma(\phi) + \delta g_F(\phi, H) - \delta g_B(H) \tag{4.6}$$

where g_S is the observed gravity acceleration on the Earth's surface; γ is normal gravity at the reference ellipsoid, computed from the geocentric latitude ϕ of the observation using the Somigliana formula (Moritz, 1980a); $\delta g_F(\phi, H)$ is the

second-order free-air gravity reduction (e.g. Featherstone, 1995) and $\delta g_B(H)$ is the Bouguer plate reduction given by (cf. Equation 4.1) as:

$$\delta g_B(H) = 2\pi G\rho H \tag{4.7}$$

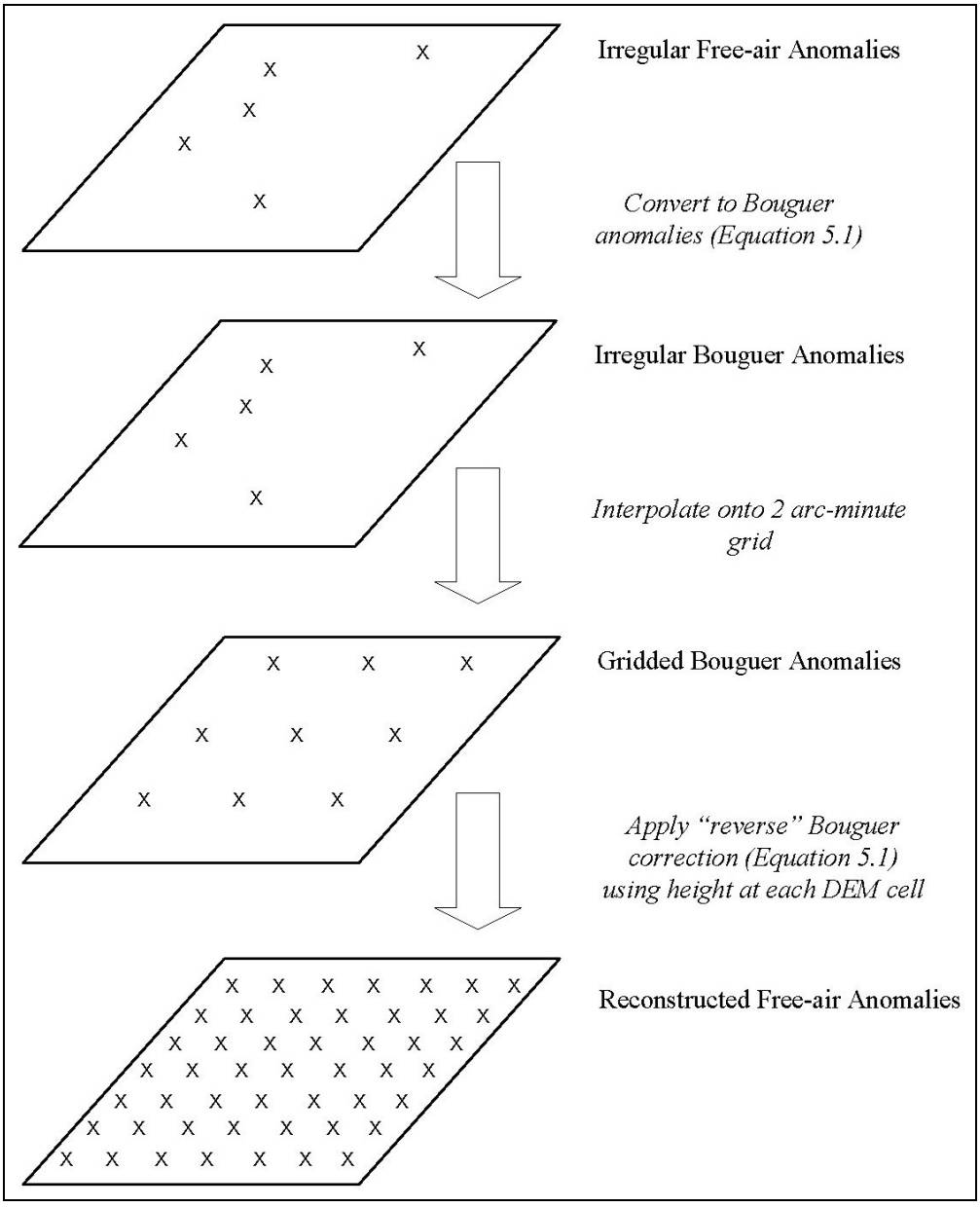

Figure 4.13 The gravity reconstruction process

Therefore, the individual free-air anomalies are reduced to their planar Bouguer equivalents and then interpolated onto a relatively coarse grid (Figure 4.13). A high-resolution DEM is then used to reconstruct free-air anomalies at each higher resolution DEM element by the application of a "reverse" Bouguer correction

(Figure 4.13). Bajracharya and Sideris (2005b) showed that the best results are achieved when a DEM with the highest resolution is utilised. The resulting high-resolution grid of free-air anomalies is then interpolated onto the coarser grid that can be used for geoid computation. The resulting grid of free-air anomalies should theoretically be more representative of the actual gravity field than the grid obtained by simply interpolating the original observations.

The above procedure was used by Goos *et al*. (2003) in Australia, and by Janák and Vaníček (2005) and Bajracharya and Sideris (2005a) in the Canadian Rocky Mountains. The general procedures followed were the same, however they reached different conclusions regarding what was the best type of Bouguer anomaly to use in gravity data interpolation for subsequent geoid computation. Both of the Australian studies (albeit performed by the same team) found that the use of simple Bouguer anomalies gave better results while both Canadian studies favoured the use of refined Bouguer anomalies. This difference was attributed to the more rugged terrain that is found in Canada (and similarly in NZ) versus that in Australia and the corresponding sparse gravity observations. The topography of NZ is probably closer to that of Canada (particularly in the South Island) although the gravity coverage in the areas of rough topography is not as dense (cf. Figure 4.12). This suggests that the direct interpolation of refined Bouguer anomalies in NZ will not produce un-aliased values.

4.11.3 Gridding comparisons

The experiments undertaken by Goos *et al*. (2003), relating to the comparison of gridding simple Bouguer (SB) and refined Bouguer (RB) anomalies, have been replicated for the NZ terrestrial gravity observations with the intent of determining the best gridding method for this data set (cf. Janák and Vaníček, 2005). The gravity gridding process is schematically shown in Figure 4.14. The SB technique involves the following stages (Featherstone and Kirby, 2000):

(i) Compute SB anomalies at the observation points from the observed gravity data;

(ii) Interpolate the point SB anomalies onto a 2’ grid using a tensioned spline (Smith and Wessel, 1990);

(iii) Reconstruct free-air anomalies using the 1.8” NZ DEM with Equation (4.6);

(iv) Add the 1.8” Moritz TCs to the reconstructed free-air anomalies to give Faye (approximate Helmert) gravity anomalies, recalling (from Section 4.5) that the Moritz TC includes an implicit DC;

(v) Interpolate the 1.8” reconstructed Faye anomalies onto a 2’ grid using tensioned splines (Smith and Wessel, 1990).

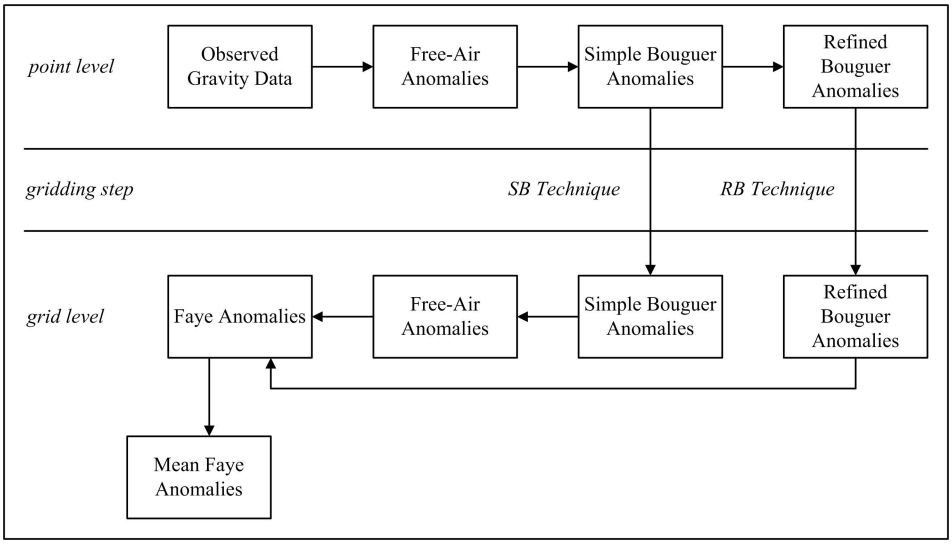

Figure 4.14 Flowchart of the techniques tested to compute grids of mean Faye anomalies (from Goos *et al*., 2003)

The RB technique is largely similar to the SB procedure and can be summarised as follows:

(i) Compute RB anomalies at the observation points using the observed gravity data and the 1.8” Moritz TCs that were bi-cubically interpolated to the observation points;

(ii) Interpolate the point RB anomalies onto regular 2’ grids using tensioned splines (Smith and Wessel, 1990);

(iii) Reconstruct Faye anomalies from the 2’ RB grids using the 1.8” NZ DEM;

(iv) Interpolate the 1.8” reconstructed Faye anomaly grids onto 2’ grids using tensioned splines (Smith and Wessel, 1990).

There are many different gridding operations available (e.g. polynomials, splines, Kriging, collocation) that could be used to achieve the above interpolations (point to 2’ grid and 1.8” grid to 2” grid), however these will not be explicitly tested. Instead, the tensioned spline algorithm of Smith and Wessel (1990) was used firstly for convenience (the operation is incorporated in GMT software, Wessel and Smith 1998) and secondly because it is suited to gridding potential field data (Zhang, 1997; Wessel and Smith 1998; Goos *et al*., 2003).

4.11.4 Comparison of gridding techniques

To compare the three gridding techniques, a quasigeoid model of NZ was computed for each of the three Faye anomaly grids described above. The reconstruction procedures described above only cover the land areas of NZ. It was necessary to incorporate information about the marine gravity field for the subsequent geoid computation so that spurious effects (e.g., the Gibbs phenomenon) did not occur along the coast as a result of the lack of gravity field information in these areas.

The 2’ by 2’ marine gravity field grid derived from the KMS02 satellite altimetry (Andersen *et al*., 2005) and crossover adjusted ship-track anomalies as described in Section 3.6 was used. The two grids were combined using the GMT *grdlandmask* and *grdmath* functions (Wessel and Smith, 1998) to set the grid cells on and off the coast (as appropriate) to zero. The grids were then “added” together to give a 2’ by 2’ grid of Faye anomalies over the geoid computation area (160°E-170°W, 25°S-60°S).

The merged GGM02S/EGM96 GGM (cf. Section 3.2.2) was then used to remove the low-frequency gravity anomalies from the combined Faye anomaly grids. The residual anomaly grids were then subjected to a 1D-FFT gravity-to-geoid transformation (described in Section 5.2.4) with the Featherstone *et al*. (1998) modified Stokes kernel (using a 1.5° integration cap and 40 degree integer removal as described in Section 5.4.5) to evaluate the residual co-quasigeoid. This was then

restored with the GGM02S/EGM96 GGM, and the primary indirect effect (Section 4.5) was applied to give five quasigeoid solutions:

- MSB: from gridded SB anomalies with Moritz FFT TCs (Section 4.7.2) applied after the gridding (cf. Kirby and Featherstone, 2001);
- PSB: from gridded SB anomalies with prism TCs (Section 4.7.3) applied after the gridding;
- HRB: from gridded RB anomalies with GNS Science's Hammer TCs (Section 4.7.1) applied before the gridding;
- MRB: from gridded RB anomalies with Moritz FFT TCs applied before the gridding;
- PRB: from gridded RB anomalies with prism TCs applied before the gridding.

These tests are an extension to those presented in Amos and Featherstone (2004). The main differences are that the current comparisons were additionally evaluated using prism-integration-derived TCs, the geoids were evaluated using optimised computation parameters (kernel modification, cap size and truncation degree, cf. Section 5.4.5); and additional recently observed GPS-levelling points were used. For this comparison the gravity observations were assumed to be on the same vertical datum and so the iterative procedure (Section 6.4) was not used.

4.11.5 Results of gridding comparison

The quasigeoids were compared with a nation-wide set of 1422 GPS-levelling points (refer Section 3.8), the GGM02S/EGM96 GGM was also evaluated for comparative purposes (Appendix D). The results of these comparisons are summarised in Table 4.5. The levelled heights are based on 13 different vertical datums, which will bias the differences computed. When the comparisons in Table 4.5 are repeated on a datum-by-datum basis, the above findings are confirmed, albeit with lower standard deviations (Table 4.6). The full descriptive statistics are given in Tables D.1 to D.6 in Appendix D.

	Max	Min	Average	STD
GGM02S/EGM96	1.421	-1.453	-0.394	0.472
MSB quasigeoid	0.971	-0.664	-0.172	0.354
PSB quasigeoid	-0.005	-0.698	-0.362	0.127
HRB quasigeoid	0.086	-0.679	-0.336	0.135
MRB quasigeoid	0.208	-0.661	-0.304	0.154
PRB quasigeoid	0.016	-0.692	-0.352	0.126

Table 4.5 Statistics of comparisons between quasigeoid solutions and 1422 GPS-levelling points on assumed single vertical datum (metres)

Datum	Points	GGM	MSB	PSB	HRB	MRB	PRB
One Tree Point	51	0.158	0.067	0.067	0.069	0.068	0.068
Auckland	137	0.129	0.069	0.066	0.069	0.070	0.068
Moturiki	258	0.290	0.064	0.060	0.064	0.063	0.060
Gisborne	61	0.110	0.111	0.104	0.100	0.101	0.100
Taranaki	70	0.307	0.072	0.069	0.065	0.070	0.066
Napier	54	0.255	0.075	0.066	0.067	0.076	0.068
Wellington	78	0.205	0.043	0.043	0.042	0.043	0.043
Nelson	111	0.430	0.109	0.070	0.057	0.096	0.062
Lyttelton	251	0.535	0.146	0.097	0.118	0.140	0.097
Dunedin	73	0.256	0.196	0.154	0.163	0.176	0.150
Dunedin-Bluff	181	0.294	0.260	0.074	0.084	0.095	0.074
Bluff	92	0.216	0.175	0.052	0.054	0.055	0.052
Stewart Island	5	0.116	0.094	0.134	0.129	0.130	0.130
All Points	1422	0.472	0.354	0.127	0.135	0.154	0.126

Table 4.6 Standard deviation of comparisons between quasigeoids and GPS-levelling points on respective vertical datums (metres)

Unlike in Amos and Featherstone (2004), where it was found that the RB models were much better than the others, the current tests show that there is not a single definitive method that gives a conclusively better fit to the GPS-levelling points. It appears that the problems associated with the FFT TCs (cf. Section 4.7.2) cause the MSB and MRB solutions to be worse than their prism-derived counterparts. Most of the 1422 GPS-levelling points are located alongside major roads in the topographically flatter areas. This means that the areas where the effect of gravity reconstruction is expected to be greatest (i.e. the mountainous regions) will not be

represented from the GPS-levelling dataset, however a general impression of their effect can be inferred.

4.11.6 Summary of gridding comparison

The insignificant difference between the PSB and PRB solutions is not in agreement with the findings of other studies. Goos *et al*. (2003) found that SB anomalies were the best gridding surface in the relatively flat continent of Australia. This is contrasted by the finding of Janák and Vaníček (2005), who concluded that RB anomalies were preferable in the Rocky Mountains of Canada. This difference can be explained because the topography of NZ lies somewhere between the extremes of Australia and Canada so the SB and RB anomalies should be about the same. It is evident however that the prism-integration derived TCs should be used irrespective of the gridding procedure. The reconstruction using PRB anomalies was selected for use in reconstruction for the NZ quasigeoid computations (Chapters 5 and 6) because it should give a smoother interpolation surface that is more representative of the actual gravity field in areas of sparse observations (i.e. the mountains).

4.12 Summary

This Chapter has described the DTE, DC, PITE and SITE corrections that need to be applied to gravity observations made on or above the surface of the Earth so that they are in accordance with Helmert's second method of condensation so that they can be used in Stokes's method of geoid computation. The M-P approach to DC was selected for use in the gravity reductions because it was implicit in the TC. For the DTE, the planar and spherical conceptual models of the Bouguer plate/shell and the TC were presented. Given these approximations three different methods of computing the TCs were then described (Hammer, FFT and prism). The advantages and disadvantages of each approach were discussed and a set of TCs derived from each was calculated over NZ. The FFT TCs are subject to numerical instabilities in areas of steep topography so an investigation was undertaken to determine if this was a problem in NZ. An analysis of the topographic gradients (derived from the NZ DEM) showed that there were large areas where the topographic gradient was steeper than 45º and hence the FFT TCs were likely to be unreliable.

The use of topographic mass-density data was also considered, however, because this information is not available for NZ it was not implemented. The reconstruction of gravity anomalies was discussed to establish the best method of interpolating the sparse gravity observations onto a regular grid for computing the NZ quasigeoid. It was found that gravity reconstruction using prism TCs with either simple or refined Bouguer anomalies gave results superior to both the Hammer and FFT TCs. The refined Bouguer approach was chosen for gravity reconstruction in the NZ quasigeoid computations because it should give a smoother interpolation surface in areas of sparse gravity observations.

The Hammer TCs were probably the best conceptually however their limited spatial distribution and poor performance in the reconstruction tests makes them unsuitable for NZ quasigeoid computation. There is also no conclusive evidence that the prism TC is significantly better than the FFT TC. However, suspicion over the quality of the FFT TC modelling in the steep NZ topography makes their use undesirable. The superior performance of the prism TCs in both the TC comparisons and the reconstruction tests meant that they will be used consistently for the NZ quasigeoid computations discussed in the remainder of this thesis.

5 GRAVIMETRIC QUASIGEOID COMPUTATION AND STOKES'S INTEGRAL KERNEL MODIFICATION

5.1 Introduction

The gravimetric approach to quasigeoid computation converts observed and reduced gravity anomalies into quasigeoid undulations or height anomalies (ζ). This conversion is often achieved using the widely accepted Stokes formula to enhance a GGM over a region. Because regional quasigeoids only use gravity observations over regional extents, this can introduce a truncation error into the computed quasigeoid undulations. The magnitude of this error can be reduced through the modification of the integration kernel of Stokes formula or GGM (or both). This Chapter presents and then compares five deterministic kernel modifications over NZ. The purpose of this comparison is to determine the best modification and its associated parameters for the computation of a regional NZ quasigeoid that is used in the datum unification described in Chapter 6.

5.2 Quasigeoid computation theory

5.2.1 Stokes integral and kernel

The most widely accepted method of evaluating the quasigeoid from (global) gravity anomalies is through the solution to the geodetic boundary-value problem (GBVP) that was proposed by Stokes (1849). Stokes's formula enables the determination of the geoid from the global coverage of gravity anomalies. When gravity anomalies are reduced using normal-orthometric heights (as opposed to orthometric heights) Stokes's formula yields a quasigeoid rather than a geoid. Heiskanen and Moritz (1967, p. 94) gives this to a spherical approximation as:

$$\zeta = \frac{R}{4\pi\gamma} \iint_{\sigma} S(\cos\psi)\, \Delta g \; d\sigma \tag{5.1}$$

where R is the mean Earth radius, σ is the sphere of integration, Δg the gravity anomalies reduced to the quasigeoid (Section 4.2), $d\sigma$ is an element of surface area on the sphere, and $S(\psi)$ is the spherical Stokes integration kernel given in *ibid.* (p. 94) as:

$$S(\cos\psi) = \csc\left(\frac{\psi}{2}\right) - 6\sin\left(\frac{\psi}{2}\right) + 1 - \cos\psi\left(5 + 3\ln\left[\sin\frac{\psi}{2} + \sin^2\frac{\psi}{2}\right]\right) \quad (5.2)$$

The surface spherical radius (ψ) between two points on the sphere is given by spherical trigonometry as:

$$\cos\psi = \sin\phi\sin\phi' + \cos\phi\cos\phi'\cos(\lambda' - \lambda) \quad (5.3)$$

where ϕ, λ are the geographical coordinates of the computation point and ϕ', λ' are the coordinates of the variable surface element $d\sigma$. $S(\psi)$ can also be expressed as an infinite Fourier series of Legendre polynomials (P_n), this is given by *ibid.* (p. 97) as:

$$S(\cos\psi) = \sum_{n=2}^{\infty} \frac{2n+1}{n-1} P_n(\cos\psi) \quad (5.4)$$

The integration element $d\sigma$ in Equation (5.1) can be transformed into integration elements expressed in terms of surface spherical coordinates ($d\psi$, $d\alpha$) whose origin is at the quasigeoid computation point, and where α is the azimuth. Thus the element of solid angle is given in *ibid.* (p. 95) as

$$d\sigma = \sin\psi\, d\psi\, d\alpha \quad (5.5)$$

and since all points of the sphere are equivalent, the relation in Equation (5.5) holds for an arbitrary point P so that the change of variables is

$$\iint_{\sigma} d\sigma = \int_{\alpha=0}^{2\pi}\int_{\psi=0}^{\pi} \sin\psi\, d\psi\, d\alpha \quad (5.6)$$

for $0 \le \psi \le \pi$ and $0 \le \alpha \le 2\pi$. This is equivalent to using spherical polar coordinates centred on each computation point rather than the North Pole. A singularity occurs in Stokes's function when $\psi \to 0$. When the transformation in Equation (5.6) is applied to Equation (5.1), the following is obtained (*ibid.* p. 95):

$$\zeta = \frac{r}{4\pi\gamma}\int_{\alpha=0}^{2\pi}\int_{\psi=0}^{\pi} S(\cos\psi)\ \Delta g\ \sin\psi\, d\psi\, d\alpha \quad (5.7)$$

Equation (5.7) is simplified by introducing the substitution $\kappa = r / 4\pi\gamma$ and abbreviating the lower integral limits as 0. This gives (in terms of surface spherical coordinates):

$$\zeta = \kappa \int_0^{2\pi} \int_0^{\pi} S(\cos\psi)\, \Delta g\, \sin\psi\, d\psi\, d\alpha \tag{5.8}$$

Equation (5.8) represents a spherical approximation (e.g., Heiskanen and Moritz, 1967, p. 95; Moritz, 1980b, p. 15). It is only correct for a reference ellipsoid that: has the same potential $U_0 = W_0$ as the quasigeoid; encloses a mass that is numerically equal to the Earth's mass; and has its centre coincident with the centre of gravity of the Earth. In addition, T is assumed to be harmonic outside the quasigeoid. This means that the effect of the masses above the quasigeoid must be removed by appropriate gravity reductions before Equation (5.8) can be used (Section 4.2). The condition $U_0 = W_0$ can be difficult to achieve in practise, hence Equation (5.8) can be generalised so that it applies to any arbitrary ellipsoid that is close enough to the quasigeoid that the deviations can be treated as linear (Heiskanen and Moritz, 1967, p. 98). For the purpose of this study, only the explicit form of Equation (5.8) will be considered.

It is also useful to re-iterate the caveat in Moritz (1980b, p. 15) that the spherical approximation does not mean that a sphere is used as the reference surface for the quasigeoid; rather the flattening coefficients are neglected in the ellipsoidal formulae so that a spherical relationship is obtained. The spherical approximation can introduce a relative error in the order of 3×10^{-3} in equations relating the quantities of the anomalous field (e.g., Heiskanen and Moritz, 1967, p. 87). This is normally permissible because, for example, the effect on the quasigeoid is 0.003 ζ, which is approximately 10 cm in NZ. Nevertheless, the so-called "ellipsoidal correction" has been extensively investigated by a number of authors in an attempt to better model its effect in the quest of a one-centimetre quasigeoid (recent studies include Fei and Sideris, 2000, 2001; Sjöberg, 2003b, 2004b; Huang *et al.*, 2003; Heck and Seitz, 2003; Hipkin *et al.*, 2004; Claessens, 2006).

5.2.2 Truncation of Stokes's formula

The principal difficulty with the practical application of Equation (5.8) is the requirement for continuous gravity data covering the entire Earth. This lack of global coverage has led to the natural approximation where the integration is limited to a spherical cap around the point of calculation (Figure 5.1; Jekeli, 1981b). The use of a cap also has the benefit that the smaller amount of data reduces the requirements for computer memory and subsequent processing time.

When gravity data are limited by a spherical cap, this causes a truncation error to occur due to the omission of the gravity field outside the cap (far zone contribution). This was identified by Molodensky *et al*. (1962), where they proposed a modification to Stokes's formula to reduce the effect of the error. This modification was not widely adopted due to the lack of low-frequency quasigeoid information derived from satellite orbit analysis that was available at the time (Featherstone, 1999).

In addition to the reduction of the truncation error, some modifications to Stokes's formula possess some preferential high-pass filtering properties (Vaníček and Featherstone, 1998) that lessen the low-frequency errors in terrestrial gravity databases (cf. Heck, 1990), while others can simultaneously reduce the effect of the truncation error as well as errors in the gravity data and/or the GGM (e.g., Sjöberg, 1984, 1991, 2003c; Sjöberg and Hunegnaw, 2000; Featherstone, 2003c). These benefits are discussed more in Section 5.3.

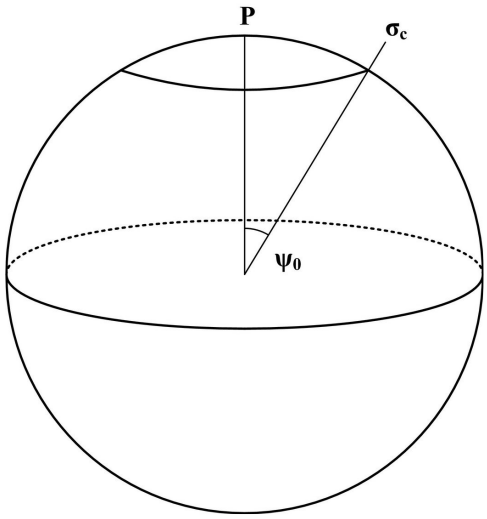

Figure 5.1 The spherical cap σ_c with radius ψ_0

The effect of neglecting the distant zones through the use of a spherical cap in Stokes's integral has been derived by Heiskanen and Moritz (1967, p. 259). The truncation error ($\delta\zeta$) can be incorporated in Equation (5.8) to give:

$$\zeta = \kappa \int_0^{\psi_0} \int_0^{2\pi} S(\cos\psi)\, \Delta g\, \sin\psi\, d\psi\, d\alpha + \delta\zeta \tag{5.9}$$

where the truncation error is given by:

$$\delta\zeta = \kappa \int_{\psi_0}^{\pi} \int_0^{2\pi} K(\cos\psi)\, \Delta g\, \sin\psi\, d\psi\, d\alpha \tag{5.10}$$

using the error kernel function:

$$K(\cos\psi) = \begin{cases} 0 & \text{for } 0 \le \psi < \psi_0 \\ S(\cos\psi) & \text{for } \psi_0 \le \psi \le \pi \end{cases} \tag{5.11}$$

If Equation (5.11) is expanded into a series of Legendre polynomials

$$K(\cos\psi) = \sum_{n=0}^{\infty} \frac{2n+1}{2} Q_n(\cos\psi_0)\, P_n(\cos\psi) \tag{5.12}$$

where $Q_n(\cos\psi_0)$ are the spherical truncation coefficients given by (e.g., Molodensky *et al*., 1962) and computed by Paul (1973) or Hagiwara (1972, 1976):

$$Q_n(\cos\psi_0) = \int_{\psi_0}^{\pi} S(\cos\psi)\, P_n(\cos\psi)\, \sin\psi\, d\psi \tag{5.13}$$

Using the two series, Equations (5.12) and (5.18), in Equation (5.10), and performing the integrations (e.g., Heiskanen and Moritz, 1967, Section 2.5), gives the series expansion of the truncation error in surface spherical harmonics:

$$\delta\zeta = \frac{R}{2\gamma} \sum_{n=2}^{\infty} Q_n(\cos\psi_0)\, \Delta g_n \tag{5.14}$$

The spherical truncation coefficients $Q_n(\cos\psi_0)$ are proportional to the integration kernel (Equation (5.13); Heiskanen and Moritz, 1967, p. 260). This means that the coefficients can be altered to achieve a reduction in $\delta\zeta$. Thus, the modification of the

integration kernel is the basis of the minimisation of the truncation error (e.g., Featherstone, 1992).

5.2.3 Generalised Stokes scheme

Today, the use of GGMs in conjunction with terrestrial gravity data using a truncated form of Stokes's integral is now commonplace (e.g., Vincent and Marsh, 1973; Rapp and Rummel, 1975; Sideris and She, 1995; Huang *et al*., 2000; Featherstone, 2003b; etc.). This combination is often implemented as the so-called remove-compute-restore (RCR) scheme (Vaníček and Merry, 1973; Rapp and Rummel, 1975; Sjöberg, 2005a) where the full degree of a GGM is removed from the terrestrial gravity anomalies, spherical Stokes's function (Equation 5.9) is evaluated with a spherical cap, and the GGM quasigeoid contribution is restored (see Section 5.2.4). Sjöberg (2005a) showed that simply using the high-order GGM without modifying Stokes's function will not necessarily take advantage of the high-quality low-degree signal of the GGM. Hence the RCR technique should be implemented in conjunction with a modified Stokes kernel (as well as proper topographic, atmospheric and other corrections).

A formal description of the combination of GGMs, terrestrial gravity data and spherical caps is given in Vaníček and Sjöberg (1991), where they refer to it as the *generalised Stokes scheme* for quasigeoid computation. The generalised approach parallels the classical Stokes approach when the reference ellipsoid is replaced by a Mth degree spheroid, normal gravity on the reference ellipsoid (γ) is replaced by a model gravity on the spheroid, and the Stokes integration kernel S is replaced by the spheroidal kernel $S^{M}(\psi)$ (this equivalent to the Wong and Gore (1969) modification, cf. Section 5.3.3). Gravity anomalies are reduced by subtracting model gravity to give residual high-frequency gravity anomalies (Vaníček and Sjöberg 1991). Martinec and Vaníček (1996) point out that this approach satisfies a solution to the geodetic boundary-value problem when formulated for a higher than second-degree reference model. The generalised Stokes scheme builds on the common RCR technique (described above) in that it also considers the use of modified integration kernels (see Section 5.3).

In the generalised Stokes scheme, the low-frequency quasigeoid undulations are computed from a global geopotential model (ζ_M) and these are extended into the high frequencies by the global integration of high frequency terrestrial gravity anomalies (Δg^M). This substitution is possible because the effect of the terrestrial anomalies (in regards to the shape of Stokes kernel, Figure 5.2) tapers off rapidly to zero with an increasing radius from the computation point (e.g., Jekeli, 1980), thus the effect of the distant anomalies on the local quasigeoid height is reduced (Vaníček and Sjöberg, 1991). The generalised scheme also reduces the impact of the spherical approximations inherent in Stokes's formula (Heiskanen and Moritz, 1967, p. 97) because the majority of the quasigeoid's power is contained within the low frequencies (Vaníček and Sjöberg, 1991; Vaníček and Featherstone, 1998).

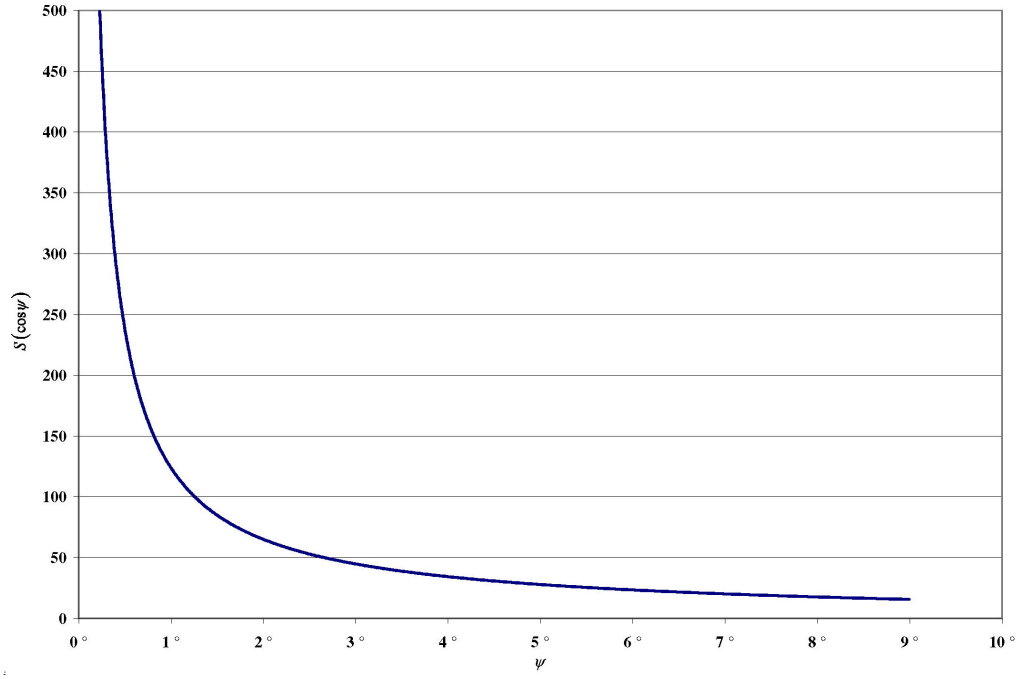

Figure 5.2 Magnitude of Stokes spherical kernel with increasing surface spherical distance from the computation point

The generalised Stokes scheme can be written as a revised form of Equation (5.8)

$$\zeta = \zeta_M + \kappa \int_0^{2\pi} \int_0^{\pi} S^M(\cos\psi)\, \Delta g^M \sin\psi \, d\psi \, d\alpha \tag{5.15}$$

where S^M is the spheroidal form of Stokes kernel that is implicit to the generalised scheme and has the series expansion:

$$
\begin{aligned}
S^M &= \sum_{n=M+1}^{\infty} \frac{2n+1}{n-1} P_n(\cos\psi) \\
&= S(\psi) - \sum_{2}^{M} \frac{2n+1}{n-1} P_n(\psi)
\end{aligned}
\tag{5.16}
$$

The low-frequency component of the quasigeoid undulation (ζ_M) in Equation (5.15) can be computed from spherical harmonic coefficients (cf. Section 3.2) using:

$$
\zeta_M = \frac{GM}{r\gamma} \sum_{n=2}^{M} \left(\frac{a}{r}\right)^n \sum_{m=0}^{n} \left(\delta\overline{C}_{nm} \cos m\lambda + \overline{S}_{nm} \sin m\lambda\right) \overline{P}_{nm}(\cos\theta) \tag{5.17}
$$

where *GM* is the product of the Newtonian gravitational constant and mass of the solid Earth, oceans and atmosphere; *a* is the semi-major axis of the reference ellipsoid; (r, θ, λ) are the geocentric polar coordinates of the computation point; $\delta\overline{C}_{nm}$ and $\delta\overline{S}_{nm}$ are fully normalised geopotential coefficients of degree *n* and order *m*, which have been reduced by the zonal harmonics of the reference ellipsoid; and $\overline{P}_{nm}(\cos\theta)$ are the fully normalised Legendre functions. The first- and second-degree harmonic terms are assumed to be inadmissible because they vanish in any spherical-harmonic expansion of the Earth's potential (e.g., Heiskanen and Moritz, 1967, p. 62).

The high-frequency gravity anomalies (Δg^M) in Equation (5.15) are computed by subtracting the spherical harmonic global geopotential model contribution from the terrestrial anomalies

$$
\Delta g^M = \Delta g - \frac{GM}{r^2} \sum_{n=2}^{M} \left(\frac{a}{r}\right)^n (n-1) \sum_{m=0}^{n} \left(\delta\overline{C}_{nm} \cos m\lambda + \overline{S}_{nm} \sin m\lambda\right) \overline{P}_{nm}(\cos\theta) \tag{5.18}
$$

5.2.4 Remove-compute-restore (RCR) quasigeoid computation

The RCR technique (described in Section 5.2.3) is the most well known method for regional gravimetric quasigeoid determination today. It has been applied extensively; for example: the Nordic region (Forsberg 1990, 2001), Europe (Denker *et al*., 1996), the United States (Smith and Milbert, 1999), Canada (Sideris and She, 1995; Fotopoulos *et al*., 1999), Australia (Featherstone *et al*., 2004), and Africa (Gachari and Olliver, 1998; Merry *et al*., 2005). Typically it has been implemented

using the maximum expansion (M) of the GGM and an (unmodified) spherical Stokes kernel.

An alternative technique, proposed by researchers at the University of New Brunswick (UNB) does not use the full expansion of the GGM for the "remove" and "restore" components (e.g., Vaníček and Kleusberg, 1987; Vaníček and Sjöberg, 1991; i.e., the generalised Stokes approach). Instead, a low degree expansion of a satellite-only GGM (degree ~20), a deterministically modified spheroidal Stokes kernel and an explicit computation of a truncation bias term from a combined GGM is used. There are fewer quasigeoids computed by this technique, however examples of its use include Canada (Vaníček *et al*., 1995) and South East Asia (Kadir *et al*., 1999). Featherstone *et al*. (2004) compared the UNB and RCR approaches in Australia. They concluded that while the UNB technique appeared to give a better agreement to GPS-levelling observations, this may have been as a result of errors cancelling rather than a better numerical model. On balance, a combination of the RCR technique with modified kernels was used for quasigeoid computations in this study (Sections 4.11.4, 5.4 and 6.5).

The RCR technique can be efficiently implemented using the FFT technique (e.g. Schwarz *et al*., 1990; Strang van Hees, 1990) in either one- and two-dimensional (1-D, 2-D) convolutions. Tziavos (1996) noted that the 2-D-FFT introduces an error when computing quasigeoid heights for each parallel. This error is avoided by using the 1-D-FFT (Haagmans *et al*., 1993). The 1-D-FFT is also quicker to compute since it only needs to form 1-D arrays. Featherstone *et al*. (2001) point out that while quadrature-based numerical integration techniques are quicker than the 1-D-FFT, they give the same results and hence they were not trialled for this study.

The RCR quasigeoid computations described here (Sections 4.11.4, 5.4 and 6.5) were undertaken using the following procedure. Firstly the GGM gravity contribution (M = 360) is removed from the gridded gravity anomalies in the computation area (160ºE – 170ºW, 25ºS – 60ºS) to give residual gravity anomalies. The residual anomalies were then subjected to a 1-D-FFT (Haagmans *et al*., 1993) to give residual co-geoid undulations using the 1-D-FFT software with kernel modifications from Curtin University of Technology (Featherstone and Sideris, 1998). This software is a modified version of a software package developed at the

University of Calgary (Sideris, 1994). Following the procedure used by Featherstone and Sideris (1998), the kernel was set to zero outside the integration cap radius (see Section 5.3) before being transformed into the frequency domain. This prevented the whole grid of gravity anomalies being used during the 1-D-FFT quasigeoid computation. The integration kernel used in the FFT is discussed extensively in Section 5.3. The "restore" part of the RCR process involves adding back the GGM quasigeoid contribution to the residual co-geoid, this gives a co-geoid. The PITE (Section 4.6) is then also added to the co-geoid give the final quasigeoid.

5.3 Kernel modification

As stated previously, Stokes's (1849) solution to the GBVP (Section 5.2.1) requires a global integration of gravity anomalies. Because there is an incomplete global coverage of gravity data (or the ready access to it, e.g., due to military restrictions, etc.) and the frequent unavailability of accurate terrestrial data, it is not possible to carry out a precise gravimetric determination using Stokes's formula. The Molodensky *et al*. (1962) approach to reduce the truncation error associated with using limited spatial data applies a modification to the integration kernel of Stokes's formula (e.g., Featherstone, 2003b).

5.3.1 Kernel modification approaches

There are two main groups into which the modifications to the kernel of Stokes's integral can be categorised: deterministic and stochastic. The deterministic approaches reduce the effect of the truncation error caused by the neglected remote-zones. However, no attempt is made to account for the accuracy estimates of the geopotential coefficients and terrestrial data, even though the effect of these propagates into the resulting quasigeoid height (e.g., Ellmann, 2005). Prominent deterministic approaches that have been proposed include: Molodensky *et al*. (1962); de Witte (1967); Wong and Gore (1969); Meissl (1971); Vincent and Marsh (1973); Heck and Grüninger (1987); Vaníček and Kleusberg (1987); Vaníček and Sjöberg (1991); Featherstone *et al*. (1998); and Evans and Featherstone (2000).

The stochastic approach attempts to reduce the GGM, truncation error and gravity data errors through the use of stochastic models in the computation (Ellmann, 2005).

Examples of stochastic methods include: Sjöberg (1980, 1981, 1984, 1991, 2003c, 2005b), Wenzel (1983); Vaníček and Sjöberg (1991); and Sjöberg and Hunegnaw (2000). Following Featherstone (2003c), the stochastic modifications have also not been considered here because reliable estimates of the error variances of the Earth's gravity data are not currently known in NZ.

Kernel modifications have also been suggested to reduce the truncation error for integration areas other than spherical caps (e.g., Neyman *et al.*, 1996; Zelin and Zoufa, 1992). However these do not appear to be as popular as the spherical cap approach (Featherstone and Sideris, 1998). In addition to kernel modifications reducing truncation errors, they also have filtering properties that can reduce the effect of errors in the gravity observations and GGMs on the computed quasigeoid (Vaníček and Featherstone, 1998). These are discussed as appropriate in the following Sections.

5.3.2 Meissl

The $Q_n(\cos\psi_0)$ spherical truncation coefficients (Equation 5.13) govern the rate at which the truncation error associated with the spherical Stokes kernel converges. The rate of decay of the truncation coefficients is determined by the mathematical smoothness properties of the error kernel $K(\cos\psi)$ in Equation (5.11). However, this error kernel is not a continuous function at the integration cap radius. Meissl (1971) found that the function could be made continuous by subtracting the value of the kernel at the cap radius from the kernel itself. This modification, termed the Meissl modification (abbreviated ML), is:

$$S_{ML}(\cos\psi) = \begin{cases} S(\cos\psi) - S(\cos\psi_0) & \text{for } 0 \le \psi \le \psi_0 \\ 0 & \text{for } \psi_0 < \psi \le \pi \end{cases} \tag{5.19}$$

Substituting Equation (5.19) into Equation (5.15) gives the ML-modified version of Stokes's function:

$$\zeta_{ML} = \zeta_M + \kappa \int_0^{2\pi} \int_0^{\psi_0} S_{ML}(\cos\psi)\, \Delta g^M \sin\psi \, d\psi \, d\alpha \tag{5.20}$$

with a truncation error of:

$$\delta\zeta_{ML} = \zeta - \zeta_{ML} = \kappa \int_0^{2\pi} \int_0^{\pi} K_{ML}(\cos\psi)\, \Delta g^M \sin\psi \, d\psi \, d\alpha \tag{5.21}$$

and an associated error kernel of:

$$K_{ML}(\cos\psi) = \begin{cases} S(\cos\psi_0) & \text{for } 0 \le \psi \le \psi_0 \\ S(\cos\psi) & \text{for } \psi_0 < \psi \le \pi \end{cases} \tag{5.22}$$

ML is now a continuous function across the cap radius and takes the constant value of $S(\cos\psi_0)$ within the spherical cap.

The Fourier series expansion for the ML error kernel is:

$$K_{ML}(\cos\psi) = \sum_{n=0}^{\infty} \frac{2n+1}{2} \{Q_{ML}\}_n (\cos\psi_0)\, P_n\, (\cos\psi) \tag{5.23}$$

where the ML truncation coefficients are given by:

$$\{Q_{ML}\}_n (\cos\psi_0) = \int_{\psi_0}^{\pi} S_{ML}(\cos\psi) P_n(\cos\psi) \sin\psi \, d\psi \, d\alpha \tag{5.24}$$

and the spectral representation of the ML truncation error becomes:

$$\{\delta\zeta_{ML}\}_1 = c \sum_{n=M+1}^{\infty} \{Q_{ML}\}_n (\cos\psi_0) \Delta g_n \tag{5.25}$$

where $c = 2\pi\kappa = R/2\gamma$ and Δg_n is the n-th degree surface spherical harmonic of the gravity anomalies given by Equation (3.2):

While Jekeli (1981b) showed that although the Fourier coefficients of a continuous function converge to zero faster than that of a discontinuous function, Smeets (1994) showed that the consequent improved convergence rate did not guarantee a smaller error. Because much of the power of the error occurs in the low degrees, if $n_{\max} < 2$ (i.e. no harmonic terms are used) then the error $\{\delta\zeta_{ML}\}_1$ will be larger than the corresponding error $\delta\zeta$ in Equation (5.14) for $\psi_0 < 40°$ (Jekeli 1980). As the value of $n_{\max}$ increases (e.g., $n_{\max} = 20$ or 36) the low degree harmonics enter primarily into the computation of N and not the truncation error, however it does not necessarily follow that the RMS error is also decreased (Jekeli 1980, 1981b). Featherstone (2003c) points out that the use of a GGM to provide the low-degree gravity field will overcome this problem.

5.3.3 Wong and Gore

The spheroidal Stokes kernel (Section 5.2.3) and the modification of Wong and Gore (1969) (abbreviated to WG) are obtained by removing the low-degree Legendre polynomial terms of degrees $2 \le n \le P$ from the spherical Stokes kernel. This gives the WG modified kernel as (cf. Equation 5.4):

$$\begin{aligned} S_P(\cos\psi) &= S(\cos\psi) - \sum_{n=2}^{P} \frac{2n+1}{n-1} P_n(\cos\psi) \\ &= \sum_{n=P+1}^{\infty} \frac{2n+1}{n-1} P_n(\cos\psi) \quad \text{for } 0 \le \psi \le \pi, \;\; P \le M \end{aligned} \tag{5.26}$$

where P corresponds to the degree of spheroidal kernel modification. Here it is assumed that P is less than or equal to the maximum degree M of the geopotential model. When $P = M$, Equation (5.26) is the spheroidal Stokes kernel that is implicit to the generalised Stokes scheme (Vaníček and Kleusberg, 1987; Vaníček and Sjöberg, 1991, Martinec and Vaníček, 1996) as described in Section 5.2.3. When $P < M$, Equation (5.26) is the WG modification of the spherical Stokes kernel. The case where $P > M$ will not be considered here because it causes additional terms to rise that are not really necessary and thus impractical to compute (Featherstone, 2003c).

When Equation (5.26) is substituted in Equation (5.15) and Stokes's integral is split into the sum integration domains between the spherical cap and the remainder of the sphere:

$$\begin{aligned} \zeta = \zeta_M &+ \kappa \int_0^{2\pi} \int_0^{\psi_0} S_P(\cos\psi)\, \Delta g^M \sin\psi \, d\psi \, d\alpha \\ &+ \kappa \int_0^{2\pi} \int_{\psi_0}^{\pi} S_P(\cos\psi)\, \Delta g^M \sin\psi \, d\psi \, d\alpha \end{aligned} \tag{5.27}$$

In practise, where $P \le M$, the quasigeoid height is approximated by the truncated integral:

$$\zeta_P \simeq \zeta_M + \kappa \int_0^{2\pi} \int_0^{\psi_0} S_P(\cos\psi)\, \Delta g^M \sin\psi \, d\psi \, d\alpha \tag{5.28}$$

This has a corresponding spheroidal (if $P = M$) or WG (if $P < M$) truncation error of:

$$\begin{aligned}\delta\zeta_P &= \zeta - \zeta_P \\ &= \kappa \int_0^{2\pi} \int_0^{\pi} K_P(\cos\psi)\, \Delta g^M \sin\psi \, d\psi \, d\alpha \\ &= c \sum_{n=M+1}^{\infty} \{Q_P\}_n (\cos\psi_0)\, \Delta g_n\end{aligned} \tag{5.29}$$

where $\{Q_P\}_n(\cos\psi_0)$ are the spheroidal/WG truncation coefficients and the spheroidal/WG error kernel is defined as

$$K_P(\cos\psi) = \begin{cases} 0 & \text{for } 0 \le \psi \le \psi_0 \\ S_P(\cos\psi) & \text{for } \psi_0 < \psi \le \pi \end{cases} \tag{5.30}$$

This WG error kernel is a discontinuous function across the spherical cap radius (cf. Equation 5.11). Therefore, the expansion coefficients $\{Q_P\}_n(\cos\psi_0)$ of the spheroidal/WG error kernel decay and the truncation error (Equation (5.29) converges at the rate of $\mathcal{O}(n^{-1})$. Vaníček and Featherstone (1998) showed that the numerical values of the truncation coefficients from spheroidal modifications become unstable in the vicinity of M = 360. This was attributed to the Gibbs phenomenon, where the spheroidal Stokes kernel is made discontinuous by the removal of the Legendre polynomials.

It is shown by Vaníček and Featherstone (1998) (and reiterated by Featherstone, 2003c) that the spheroidal Stokes kernel is a very efficient high-pass filter when using a global integration (i.e., no cap and global gravity data is available), but the power of the filter diminishes when a limited integration domain is used. This means that leakage of low-frequency errors from the terrestrial gravity data will occur, but less so than would occur from using the truncated unmodified spherical Stokes kernel. Because the low-order terms are normally determined from the satellite-only components of a GGM the spheroidal Stokes kernel can be considered superior to the spherical Stokes kernel.

Featherstone (2003c) demonstrated that as the degree of spheroidal modification increases, the oscillation of the spheroidal kernel also increases due to the removal of the low-degree Legendre polynomials. Although increasing the degree of the spheroidal modification increases the amount of high-pass filtering and counteracts the effect of using an integration cap, it needs to be balanced against the increasing

oscillation of the kernel and the resultant non-representative solutions (i.e., it becomes harder to get the average kernel using numerical integration). When the kernel is oscillating it makes it difficult to solve Stokes's integral numerically (Featherstone, 1992). This means that only low degrees of the spheroidal/WG modification should be used.

5.3.4 Vaníček and Kleusberg

The kernel modification presented by Vaníček and Kleusberg (1987) applies the Molodensky *et al*. (1962) modification of the spherical Stokes kernel to the spheroidal kernel (cf. Equation 5.26) in conjunction with a Molodensky-type minimisation to the upper bound of the truncation error. The Vaníček and Kleusberg (VK) modified kernel is also described in Vaníček and Sjöberg (1991) and is given by:

$$S_P^L(\cos\psi) = \begin{cases} S_P(\cos\psi) - \sum_{k=2}^{L} \frac{2k+1}{2}\, t_k(\cos\psi_0)\, P_k(\cos\psi) & \text{for } 0 \le \psi \le \psi_0 \\ 0 & \text{for } \psi_0 < \psi \le \pi \end{cases} \tag{5.31}$$

The superscript L indicates a Molodensky-type modification of degree L. The cases where $L > M$ and $L > P$ are not considered here because they cause additional terms to arise that are not really necessary and are thus impractical to compute (cf. Section 5.3.3). M is the degree of the GGM used in the RCR scheme and P is the degree of spheroidal kernel modification.

The VK modification coefficients $t_k(\cos\psi_0)$ $(2 \le k \le L)$ are determined by minimising the L_2 norm of the error kernel (Equation 5.37), which generates the following set of linear equations (Vaníček and Kleusberg, 1987; Vaníček and Sjöberg, 1991):

$$\begin{aligned} &\sum_{k=2}^{L} \frac{2k+1}{2}\, t_k(\cos\psi_0)\, e_{nk}(\cos\psi_0) \\ &= Q_n(\cos\psi_0) - \sum_{k=2}^{L} \frac{2k+1}{k-1}\, e_{nk}(\cos\psi_0) \quad \text{for } 2 \le n \le L \end{aligned} \tag{5.32}$$

where Q_n are given by Equation (5.13), and:

$$e_{nk}\left(\cos\psi_0\right)=\int_{\psi_0}^{\pi} P_n\left(\cos\psi\right)\,P_k\left(\cos\psi\right)\sin\psi\,d\psi \tag{5.33}$$

Featherstone (2003c) also emphasises that the coefficients $e_{nk}\left(\cos\psi_0\right)$ and hence $t_k\left(\cos\psi_0\right)$ depend on the integration cap radius, which must be selected before the VK modification is made. For $L \le M$ and $L \le P$, the quasigeoid height is approximated by:

$$\zeta_P^L \simeq \zeta_M + \kappa\int_0^{2\pi}\int_0^{\psi_0} S_P^L\left(\cos\psi\right)\,\Delta g^M \sin\psi\,d\psi\,d\alpha \tag{5.34}$$

with a truncation error of:

$$\begin{aligned}\delta\zeta_P^L &= \zeta-\zeta_P^L\\ &= \kappa\int_0^{2\pi}\int_0^{\psi_0} K_P^L\left(\cos\psi\right)\,\Delta g^M\sin\psi\,d\psi\,d\alpha\\ &= c\sum_{n=M+1}^{\infty}\left\{Q_P^L\right\}_n\left(\cos\psi_0\right)\,\Delta g_n\end{aligned} \tag{5.35}$$

and the truncation coefficients given by:

$$\left\{Q_P^L\right\}_n\left(\cos\psi\right)=\sum_{k=2}^{L}\frac{2k+1}{2}\,t_k\left(\cos\psi_0\right)\,e_{nk}\left(\cos\psi_0\right) \tag{5.36}$$

and the associated error kernel:

$$K_P^L\left(\cos\psi\right)=\begin{cases}0 & \text{for}\quad 0<\psi\le\psi_0\\ S_P^L\left(\cos\psi\right) & \text{for}\quad \psi_0<\psi\le\pi\end{cases} \tag{5.37}$$

5.3.5 Heck and Grüninger

The modification proposed by Heck and Grüninger (1987) applies a Meissl (1971) modification to the WG (spheroidal) Stokes kernel. Like the ML modification, to make the function continuous the value of the spheroidal kernel at the integration cap radius is subtracted from the WG kernel inside the cap.

The Heck and Grüninger (HG) modified kernel is:

$$S_{HG}\left(\cos\psi\right)=\begin{cases}S_P\left(\cos\psi\right)-S_P\left(\cos\psi_0\right) & \text{for}\quad 0\le\psi\le\psi_0\\ 0 & \text{for}\quad \psi_0<\psi\le\pi\end{cases} \tag{5.38}$$

The quasigeoid height is approximated by:

$$\zeta_{HG} \simeq \zeta_M + \kappa \int_0^{2\pi} \int_0^{\psi_0} S_{HG}\left(\cos\psi\right) \Delta g^M \sin\psi \, d\psi \, d\alpha \tag{5.39}$$

with a truncation error of:

$$\begin{aligned} \delta\zeta_{HG} &= \zeta - \zeta_{HG} \\ &= \kappa \int_0^{2\pi} \int_0^{\pi} K_{HG}\left(\cos\psi\right) \Delta g^M \sin\psi \, d\psi \, d\alpha \\ &= c \sum_{n=M+1}^{\infty} \left\{Q_{HG}\right\}_n \left(\cos\psi_0\right) \Delta g_n \end{aligned} \tag{5.40}$$

where $\left\{Q_{HG}\right\}_n \left(\cos\psi_0\right)$ are the HG truncation coefficients given by Equation (5.13) and the associated error kernel is:

$$K_{HG}\left(\cos\psi\right) = \begin{cases} S_P\left(\cos\psi_0\right) & \text{for} \quad 0 \le \psi \le \psi_0 \\ S_P\left(\cos\psi\right) & \text{for} \quad \psi_0 < \psi \le \pi \end{cases} \tag{5.41}$$

The truncation coefficients for the expansion series of the HG error kernel satisfy the improved convergence rate of $\mathcal{O}\left(n^{-2}\right)$ (Featherstone, 2003c). The convergence rate for the WG error kernel is $\mathcal{O}\left(n^{-1}\right)$ (see Section 5.3.3). When combined with the RCR scheme for quasigeoid evaluation, the truncation error is reduced further (Featherstone, 2003c).

Heck and Grüninger (1987) also propose an alternative approach to the subtraction in Equation (5.38), where L is chosen such that the spheroidal Stokes kernel is zero at the truncation radius. While this ensures a continuous error kernel and an improved convergence rate for the truncation error, it also limits the combinations of ψ_0 and L that can be used. Because ψ_0 normally depends on data availability, this would imply a high degree of modification which is undesirable due to the high-pass filtering properties (cf. Section 5.3.3).

5.3.6 Featherstone, Evans and Olliver

The modification published by Featherstone *et al*. (1998) applies a Meissl (1971) modification to the Vaníček and Kleusberg (1987) kernel [a Molodensky *et al*. (1962) modified WG (spheroidal) kernel with minimisation of the upper bound

error]. According to Featherstone *et al*. (1998) and Featherstone (2003c), this increases the rate of convergence of the truncation coefficients from $\mathcal{O}\left(n^{-1}\right)$ to $\mathcal{O}\left(n^{-2}\right)$ and thus reduces the truncation error further when implemented with the RCR scheme. This approach is similar to the alternative HG methodology (Section 5.3.5) where the WG modification is chosen for a particular *M* such that the first zero point of the error kernel coincides with the truncation radius.

The Featherstone, Evans and Olliver (FEO) modified kernel is:

$$S_{FEO}\left(\cos\psi\right)=\begin{cases} S_P^L\left(\cos\psi\right)-S_P^L\left(\cos\psi_0\right) & \text{for } \ 0\le\psi\le\psi_0 \\ 0 & \text{for } \ \psi_0<\psi\le\pi \end{cases} \tag{5.42}$$

The coefficients $t_k\left(\cos\psi_0\right)$ are determined in the same way as for the VK modification (Section 5.3.4). In practise for $L \le M$ and $L \le P$, the quasigeoid height is approximated by:

$$\zeta_{FEO} \simeq \zeta_M + \kappa\int_0^{2\pi}\int_0^{\psi_0} S_{FEO}\left(\cos\psi\right)\,\Delta g^M \sin\psi\, d\psi\, d\alpha \tag{5.43}$$

with a truncation error of:

$$\begin{aligned} \delta\zeta_{FEO} &= \zeta - \zeta_{FEO} \\ &= \kappa\int_0^{2\pi}\int_0^{\pi} K_{FEO}\left(\cos\psi\right)\,\Delta g^M \sin\psi\, d\psi\, d\alpha \\ &= c\sum_{n=M+1}^{\infty}\left\{Q_{FEO}\right\}_n\left(\cos\psi_0\right)\,\Delta g_n \end{aligned} \tag{5.44}$$

where $\left\{Q_{FEO}\right\}_n\left(\cos\psi_0\right)$ are the FEO truncation coefficients given by Equation (5.13) and the associated error kernel is the continuous function given by:

$$K_{FEO}\left(\cos\psi\right)=\begin{cases} S_P^L\left(\cos\psi_0\right) & \text{for } \ 0\le\psi\le\psi_0 \\ S_P^L\left(\cos\psi\right) & \text{for } \ \psi_0\le\psi\le\pi \end{cases} \tag{5.45}$$

Featherstone *et al*. (1998) considered this modification to be an advance on the other deterministic modifications described in Sections 5.3.2 to 5.3.5 because it combines the perceived advantages of each into a single modification scheme. As such, it was used for the development of the Australian gravimetric quasigeoid model, AUSGeoid98 (Featherstone *et al*., 2001).

5.4 Evaluation of kernel modifications

5.4.1 Comparison of kernel modifications in the RCR approach

From the literature discussing the above modifications, it is not clear which combination of kernel modification, integration cap size and degree removal (where applicable) provides the best results in a given location. Theoretically, each of the modifications outlined above should be improvements on their predecessors. However, recent evidence has shown that no single combination provides the best result in all situations (e.g., Forsberg and Featherstone, 1998; Featherstone and Sideris, 1998; Higgins *et al*., 1998; Featherstone *et al*., 2004; Ågren, 2004; Ellmann, 2005). In addition, various studies that have investigated the differences between the modifications (e.g., Sjöberg and Hunegnaw, 2000; Omang and Forsberg, 2002; Featherstone, 2003c; Sjöberg, 2003d; Ellmann, 2005) have given inconclusive results in that they can not be generalised. This is likely to be due to the spatially varying error characteristics of the different gravity data sources giving different results in their respective computation/evaluation areas.

To ascertain the best combination of kernel modification and its associated parameters for the NZ quasigeoid, a comparison of different deterministic modifications was undertaken. The five deterministic modifications described in Sections 5.3.2 to 5.3.6 above, as well as the unmodified spherical Stokes kernel, were implemented using the procedure documented in Section 5.2.4. Stochastic kernel modifications were not considered in this study because accurate estimates of the errors in the NZ terrestrial gravity data are not currently available.

All of the modified kernels discussed above (ML, WG, VK, HG and FEO) and the unmodified spherical Stokes kernel (SS) were computed with integration cap radii shown in Table 5.1. The SS kernel was also evaluated with no integration cap (because the terrestrial gravity coverage is only 30° x 35° a 180° cap is the equivalent of not limiting the integration radius). The WG, VK, HG and FEO modifications were also evaluated with each of the kernel modification degree values (L) given in Table 5.1 for each of the integration cap radii (ψ_0). The SS kernel and ML modification do not have degree removal in their definition so these have only been evaluated with the integration cap variations. The computations have utilised ψ_0 ranging from 0.25° (the Nyquist frequency of EGM96, M = 360) to 10° (M = 12).

The values selected for testing (Table 5.1) were chosen to provide a range of solutions that covered the extents of the NZ terrestrial gravity data. The tested degrees of modification (L) were arbitrarily selected so that they broadly corresponded to the (currently available) range of the maximum degrees of complete harmonic expansion ($M_{\max}$) from satellite based GGMs.

Integration cap radii, ψ_0	Degree of modification, L
0.25°	2
0.5°	5
1.0°	10
1.5°	15
2.0°	20
2.5°	25
3°	30
4°	40
5°	50
6°	60
7°	70
8°	80
9°	90
10°	100
180° (SS only)	

Table 5.1 Parameters evaluated in kernel modification comparison

5.4.2 Results of comparison

The quality of the different kernel modification and parameter combinations can be determined by comparing agreement of the resulting quasigeoid with GPS-levelling derived geometric quasigeoid heights (albeit on different LVDs). The "best" combination of modification, ψ_0 and L will occur where the standard deviation of the comparison is at its minimum.

To determine the optimum combination for NZ, the GPS-levelling dataset (Section 3.8) was compared with each combination described in Table 5.1. It is important to note that the NZ precise levelling heights have been observed in relation to different vertical datums that are offset from each other (cf. Section 5.4.4). To ensure that the datum offsets (i.e., Section 2.4.3) do not affect the error estimate for each modification comparison the standard deviation σ_i for the GPS-levelling points on each datum was computed separately. The separate σ_i were then combined using

Equation (5.46) to give a weighted average (σ_{average}) of the complete GPS-levelling dataset (1014 points); where N_i is the number of points on each datum i.

$$\sigma_{\text{average}} = \frac{\sum N_i \sigma_i}{\sum N_i} \tag{5.46}$$

The average standard deviations for each of the tested kernel modifications are shown in Figure 5.3 to Figure 5.7.

The unmodified SS kernel (Figure 5.3) has a ψ_0 minimum of 9.4 cm at 4° (from the range of ψ_0 tested). Another local minimum also occurs at 1°. The distinctive oscillating shape of the SS curve was described by Kearsley (1988) as a "W-curve" and explained as an artefact of the residual gravity data used in the integration kernel. The "W-curve" is not visible in the ML modification results (Figure 5.3; cf. Stewart 1990; Featherstone, 1992). The ML curve has a single 7.6 cm minimum at 1.5° that is almost 2 cm lower than that achieved by the SS kernel.

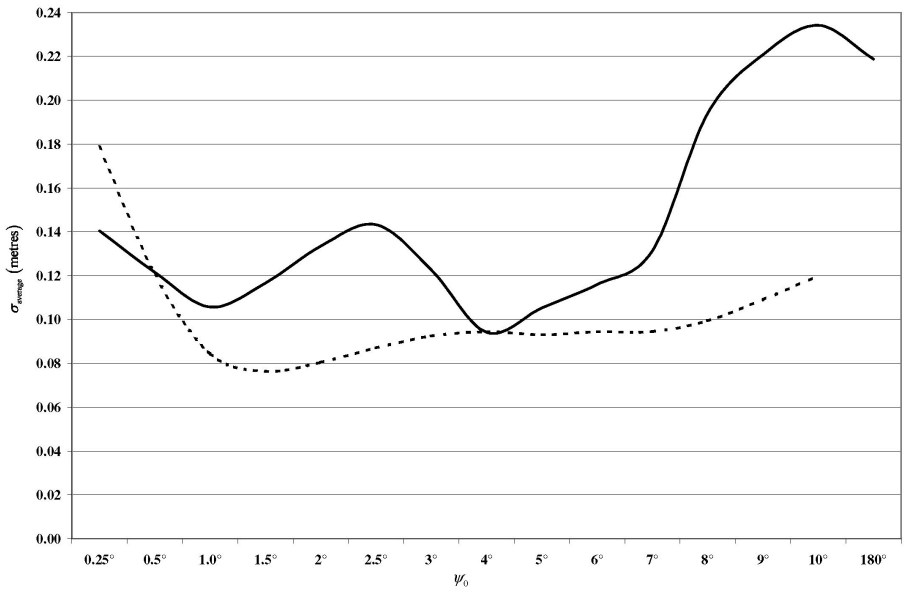

Figure 5.3 Standard deviation of the SS (solid line) and ML (dotted line) kernel quasigeoids when compared with GPS-levelling

The WG kernel (Figure 5.4) is characterised by a range of local minima and maxima and a distinct spike with large integration caps ($\psi_0 < 7°$). The overall minimum of 7.1 cm occurs where $\psi_0 = 2.5°$, $L = 50 - 80$. Because the WG modification should not be used with high values of L because of its high-pass filtering characteristics and the subsequent oscillating kernel (cf. Section 5.3.3; Featherstone, 1992), only low

values of L should be used (i.e., 2 - 30). In this limited range, the minimum of 8.0 cm occurs at $\psi_0 = 1.5°$, $L = 30$. Surface plots (e.g., Figure 5.4) are used (as opposed to line graphs or tables) to compare the different combinations of ψ_0 and L (e.g., Figure 5.4) because they provide a better visual representation of the different combinations and make spurious results easier to detect.

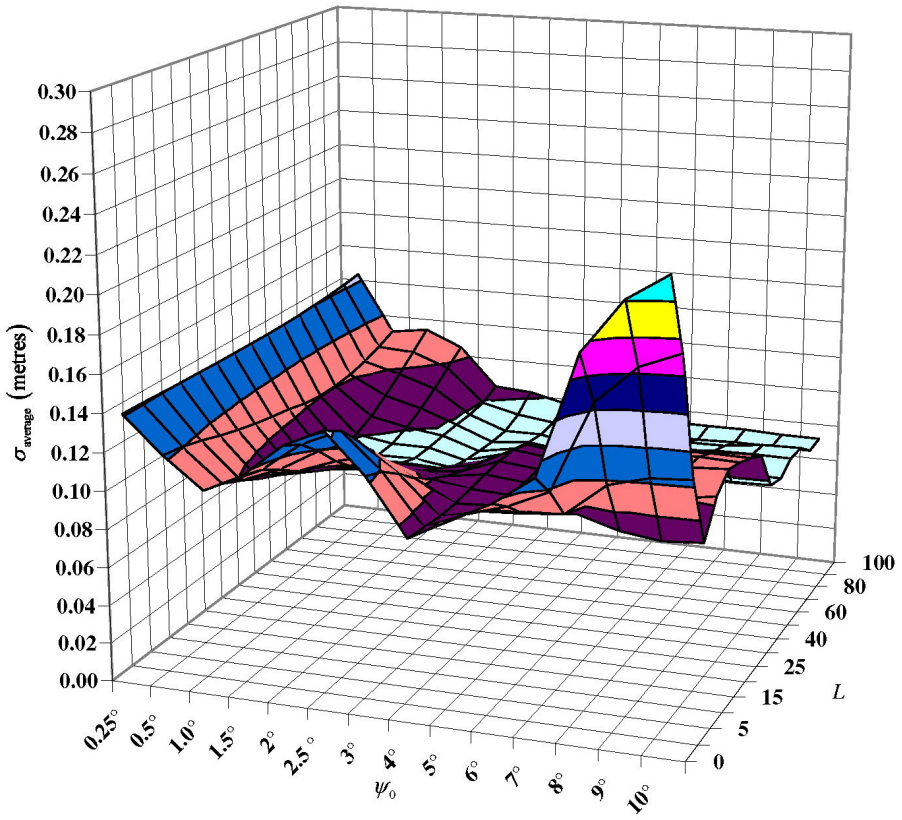

Figure 5.4 Standard deviation of the WG kernel quasigeoid compared with GPS-levelling

The HG kernel (Figure 5.5) produced a smooth surface that is similar to the ML kernel (Figure 5.3). This was expected as the HG modification is based in similar principles in that it applies a ML modification to the WG kernel (cf. Section 5.3.5). Unlike WG (Figure 5.4), the HG comparison results are more stable. The minimum value of 7.6 cm is achieved when $\psi_0 = 1.5°$ and L is between 0 - 30.

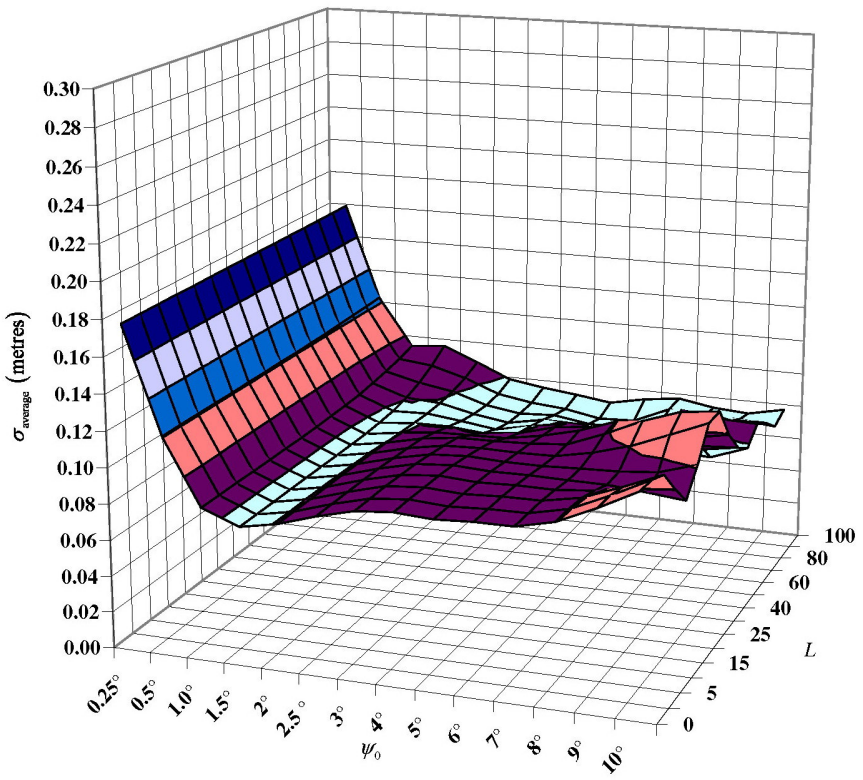

Figure 5.5 Standard deviation of the HG kernel quasigeoid compared with GPS-levelling

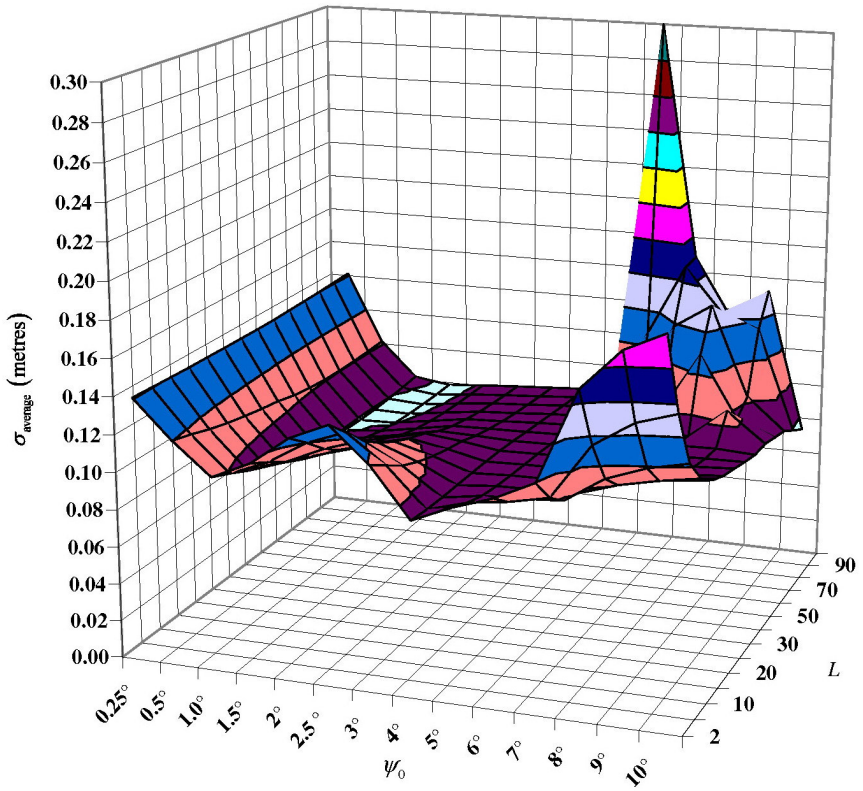

Figure 5.6 Standard deviation of the VK kernel quasigeoid compared with GPS-levelling

The VK kernel (Figure 5.6) is similar to the WG kernel (Figure 5.4) at small integration caps ($\psi_0 < 4°$). The distinctive "bump" around $\psi_0 = 1° - 3°$ and "wing" around $\psi_0 = 7\text{-}10°$ (both at low L values) are present in both comparisons. This similarity is expected because the VK kernel is obtained by applying the Molodensky *et al*. (1962) modification to the spheroidal WG kernel (cf. Section 5.3.3). The significant difference is a large spike that is centred on the $\psi_0 = 6°$, $L = 90$ combination. This spike is investigated further in Section 5.4.3. The minimum of 7.8 cm is achieved at $\psi_0 = 1.5°$, $L = 80 - 90$.

The FEO kernel (Figure 5.7) exhibits the same smooth surface of the HG kernel (Figure 5.5) except for the large spike centred on $\psi_0 = 6°$, $L = 90$ that is caused by the VK kernel (Figure 5.6). These similarities are expected because the FEO kernel is obtained by applying a ML modification to the VK kernel (cf. Section 5.3.6) and the HG kernel is a ML modified WG kernel. This spike is investigated further in Section 5.4.3. The minimum of 7.6 cm is achieved at $\psi_0 = 1.5°$, $L = 2 - 40$.

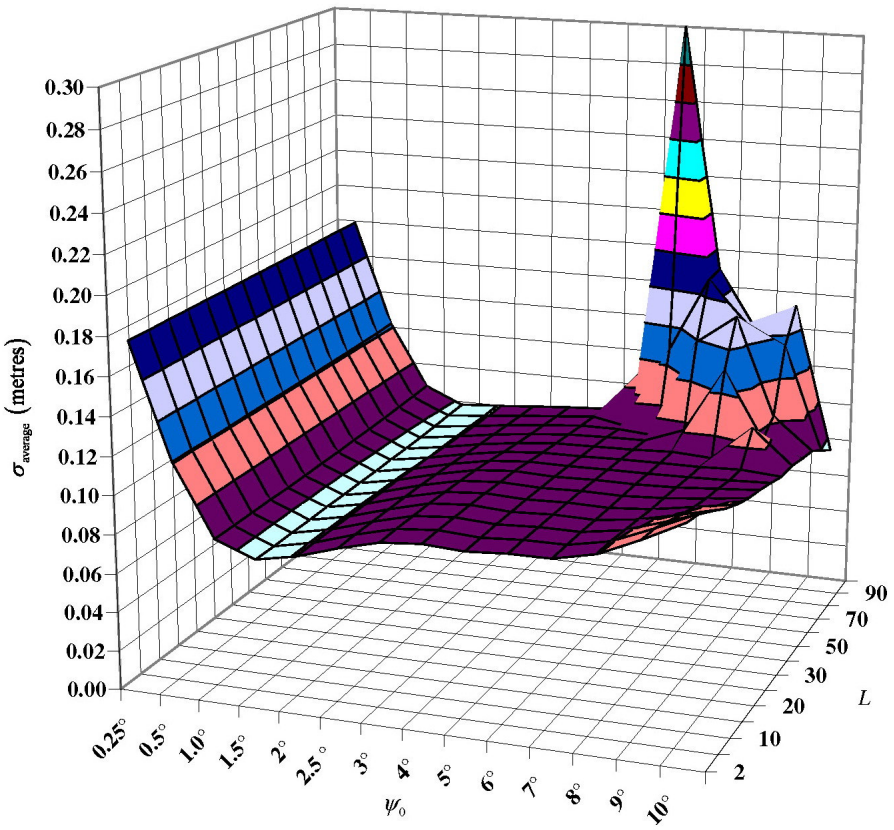

Figure 5.7 Standard deviation of the FEO kernel quasigeoid compared with GPS-levelling

Modification	ψ_0	L	σ_{average} (m)
SS	4°	-	0.094
ML	1.5°	-	0.076
WG	2.5°	50 – 80	0.071
HG	1.5°	0 – 30	0.076
VK	1.5°	80 – 90	0.078
FEO	1.5°	2 – 40	0.076

Table 5.2 Minimum average standard deviation range for each kernel modification compared to GPS-levelling

It can be seen in Figures 5.3 to 5.7 that σ_{average} varies significantly depending on the modification, ψ_0 and L chosen. The overall σ_{average} minimum for each modification are summarised in Table 5.2. In several cases, there is a range of L values given where the standard deviation was the same. The overall minimum occurs using the WG modification for $\psi_0 = 2.5°$, $L = 50$ - 80. Because the WG modification should not be used with high degree modifications, this combination will not be used for the NZ quasigeoid computations. Similarly, the relatively high L for the VK modification (80 - 90) indicates a numerically unstable solution (this is investigated in Section 5.4.3). The remaining modifications (ML, HG and FEO) all have minimum values within 2 mm of each other. Based on σ_{average} alone, no one kernel modification gives a *significantly* better result than another in NZ. Therefore additional comparisons need to be made before a kernel modification can be chosen for the NZ quasigeoid computations.

5.4.3 Numerical instabilities in the VK and FEO kernels

A notable feature that is seen in both the VK and FEO solutions is the large spike that appears at $\psi_0 = 6°$, $L = 90$ (Figures 5.6 and 5.7). Because these spikes only occur with certain combinations of ψ_0 and L, it is likely that it is due to either a numerical instability in the VK/FEO kernels or a problem in the Featherstone (2003c) software. Only the VK kernel has been investigated to identify the cause of the spike. This is because the FEO kernel is a modification of VK (and is computed with the same software code), so the spike can be attributed to it.

To better understand the nature of the spike the VK kernel (Equation (5.31)) was evaluated for different L values using the Featherstone (2003c) software. The VK kernel for $L = 50$ (Figure 5.8) produces the expected smooth asymptotic curves for

each ψ_0 plotted. When the same kernel is plotted with L = 100 (Figure 5.9) the resulting curves are more irregular. They plot as expected up to ψ_0 = 4°, above this the kernel becomes more erratic and large oscillations occur. When ψ_0 = 10° the kernel returns to the expected asymptotic shape. The oscillations appear to achieve maximum values for ψ_0 = 5° – 8°.

Featherstone (2003c) showed that a numerical instability that occurs in the $t_k(\cos\psi_0)$ VK modification coefficients when small ψ_0 are combined with large L. This instability was highlighted by examination of the determinant (cf. condition number) of the matrix that is inverted to compute the $t_k(\cos\psi_0)$ coefficients, which becomes worse as it approaches unity. To ascertain whether a numerical instability the $t_k(\cos\psi_0)$ coefficient matrix was causing the oscillations in the VK kernel, the determinant of the matrix was evaluated for a range of ψ_0, L combinations (Figure 5.10). The smooth S-shaped curves replicate those of Featherstone (2003c) and demonstrate the reported instability when small ψ_0 are combined with large L (i.e. the determinant is close to unity). Because the curves are smooth, regular and generally trend towards zero for all L this does not indicate a numerical instability in the $t_k(\cos\psi_0)$ coefficients causing the oscillations in Figure 5.9.

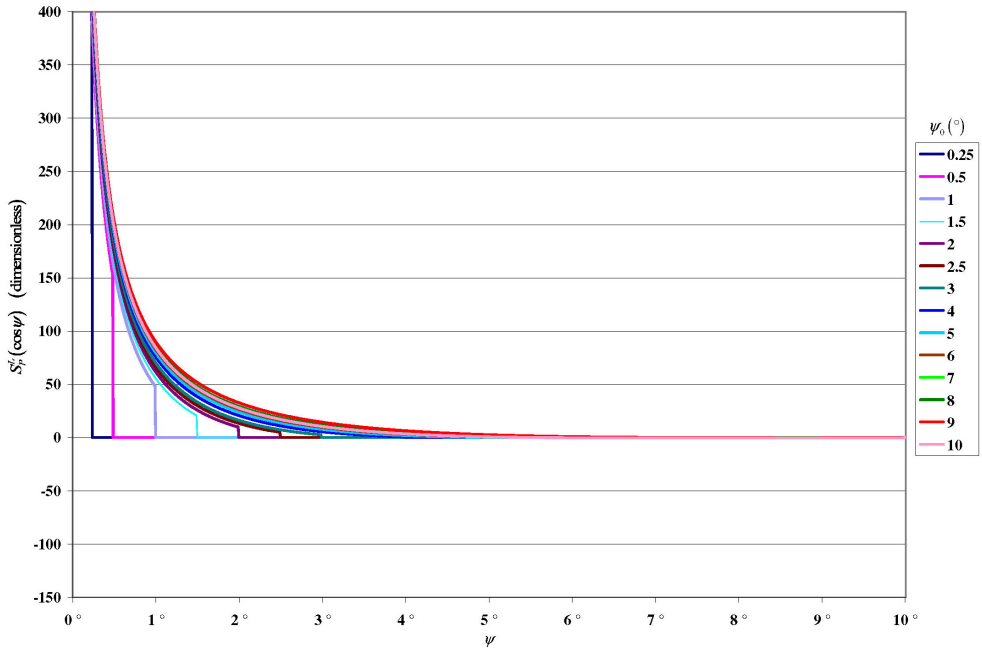

Figure 5.8 VK modified kernel, L = 50

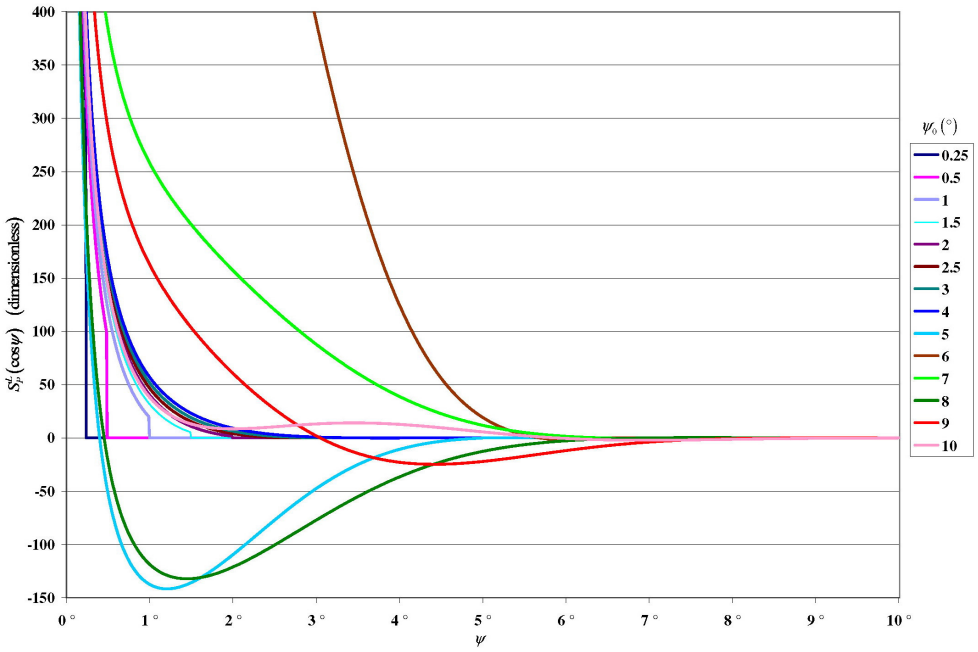

Figure 5.9 VK modified kernel, $L = 100$

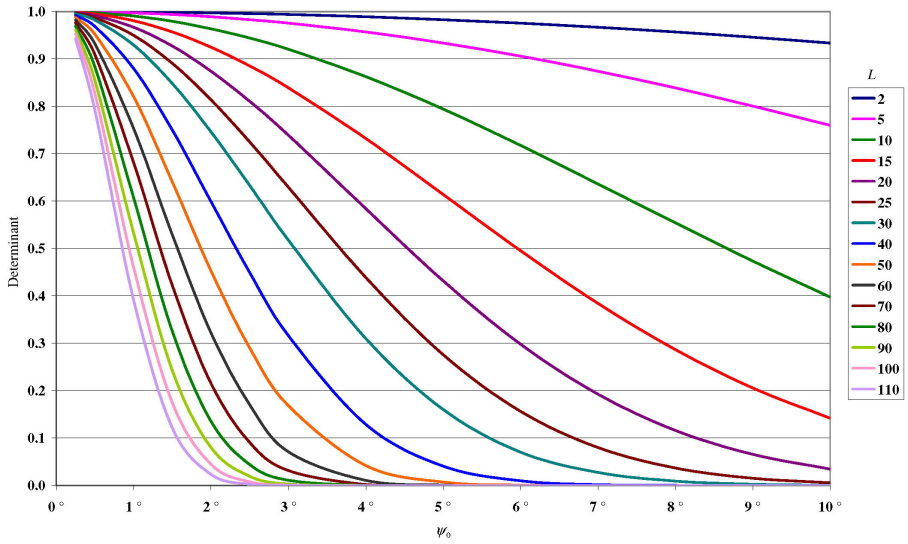

Figure 5.10 Determinant of the VK kernel modification coefficient matrix, $t_k(\cos\psi_0)$

The other potential cause of the VK kernel oscillations is an error the Featherstone (2003c) software. To isolate the location of potential software bugs each term of Equation (5.31) was evaluated separately; these are the SS kernel (Figure 5.2), the "spheroidal" term (Figure 5.11a) and the VK "subtracted" term (Figure 5.11b). The kernel was computed for $L = 100$ and $\psi_0 = 4° - 9°$ because that incorporates the large oscillations seen in Figure 5.9. It can be seen in Figure 5.11 that the kernel oscillations are originating in the VK "subtracted" term. It is well known that the

subtraction of two similar terms can cause numerical instabilities in computer software as a result of arithmetic precision limitations. It is possible that the oscillations in the "subtracted" term are being caused by this instability.

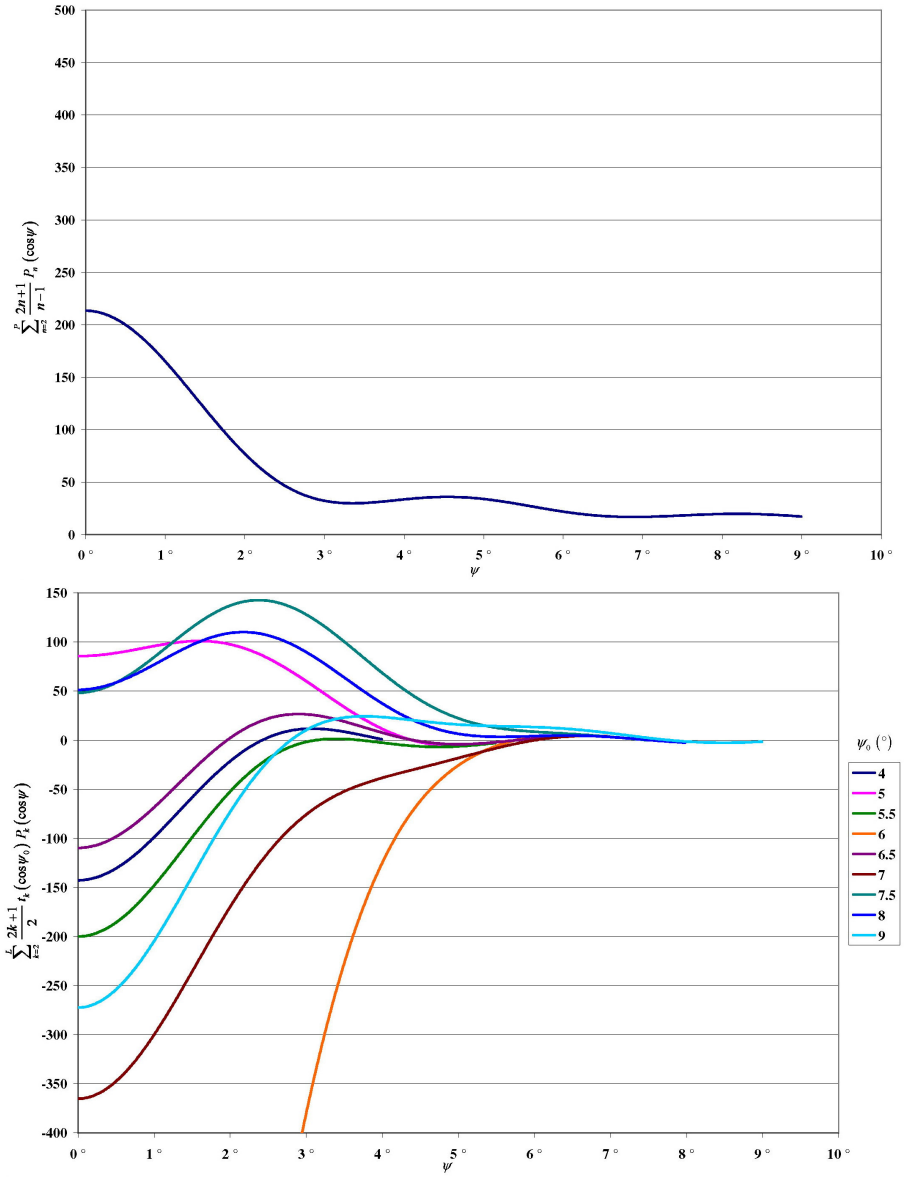

Figure 5.11 VK kernel components, L = 100 (a) "spheroidal" term, (b) VK "subtracted" term

Given the oscillations evident in Figure 5.11b and the smooth determinant for ψ_0 and L (Figure 5.10) it is concluded that the oscillations in Figure 5.9 and the spike in Figure 5.6 are attributed to a spurious numerical instability in the VK kernel. This then propagates into the FEO kernel resulting in the spike in Figure 5.7. Because the spikes only occur with large ψ_0, and the kernels perform best with relatively small ψ_0, they will not impact on the choice of parameters for the NZ quasigeoid

computations. Consequently, the cause of the numerical instability is not investigated further here.

5.4.4 Results of datum offset comparison

Because the standard deviation analysis did not conclusively provide a set of kernel modification parameters that were better than any others, some additional investigation was necessary. This involved performing a datum-by-datum analysis that looked at the average computed LVD offsets (for each ψ_0 and L combination) to determine which values looked reasonable based on the corresponding observed values (Table 5.3).

Vertical Datum	Datum Zero Ellipsoidal Height	GGM quasigeoid Height	Observed Offset	Offset Less Wellington
One Tree Point 1964	37.739	37.834	-0.095	0.295
Auckland 1946	34.202	34.477	-0.275	0.116
Moturiki 1953	30.949	31.197	-0.248	0.143
Gisborne 1926	21.839	22.315	-0.475	-0.085
Napier 1962	18.201	18.518	-0.318	0.073
Taranaki 1970	22.800	22.854	-0.054	0.336
Wellington 1953	12.719	13.110	-0.391	0.000
Nelson 1955	16.158	15.820	0.338	0.729
Lyttelton 1937	11.747	12.265	-0.518	-0.128
Dunedin 1958	5.411	5.882	-0.471	-0.080
Dunedin-Bluff 1958	4.757	5.363	-0.606	-0.216
Bluff 1955	3.647	4.026	-0.379	0.012
		Average	-0.291	0.100

Table 5.3 Observed NZ LVD offsets from GGM02S-EGM96 GGM and differences from Wellington 1953 datum offset (metres)

The LVD offsets were computed from the difference between the ellipsoidal height of the datum zero level and the GGM used in the kernel modification comparisons (GGM02S/EGM96, Section 3.2.2). Relative offsets for each datum were then computed by subtracting the Wellington 1953 offset from the other absolute values. The offsets (relative to the Wellington 1953 datum) were then combined using a weighted average (cf. Equation 5.46). The relative offsets enable a better comparison of the performance of each ψ_0 and L combination because they are all "centred" around a common zero point. The Wellington 1953 datum was arbitrarily chosen as a reference datum because it is geographically central (in NZ). The average offset with respect to the Wellington 1953 datum is +10 cm. No offset has

been calculated for the Stewart Island 1977 datum because it was not possible to determine the ellipsoidal height of the datum zero point. The Balclutha Fundamental (B3ME) was used as the "zero" of the Dunedin-Bluff 1958 datum as this datum does not have a tide gauge origin. The accuracy of the offsets is estimated as 14 cm based on the accuracy of the (typically third order) ellipsoidal height of the LVD zero (cf. Section 3.8).

The SS and ML kernel average offsets are shown in Figure 5.12. The SS offsets (solid line) trends downwards with localised undulations that correspond to the "W-curve" noted in Figure 5.3. The average offsets oscillate around the observed offset (dashed line) up to $\psi_0 = 2.5°$ before diverging. Because the offsets vary so much the choice of ψ_0 is important to ensure a good agreement with the GPS-levelling observations. The ML offsets (dotted line in Figure 5.12) change more smoothly than the SS values and generally agrees with the observed values between $\psi_0 = 1.5°$ and 7°; this broadly correlates with the shape of the standard deviation curve (Figure 5.3).

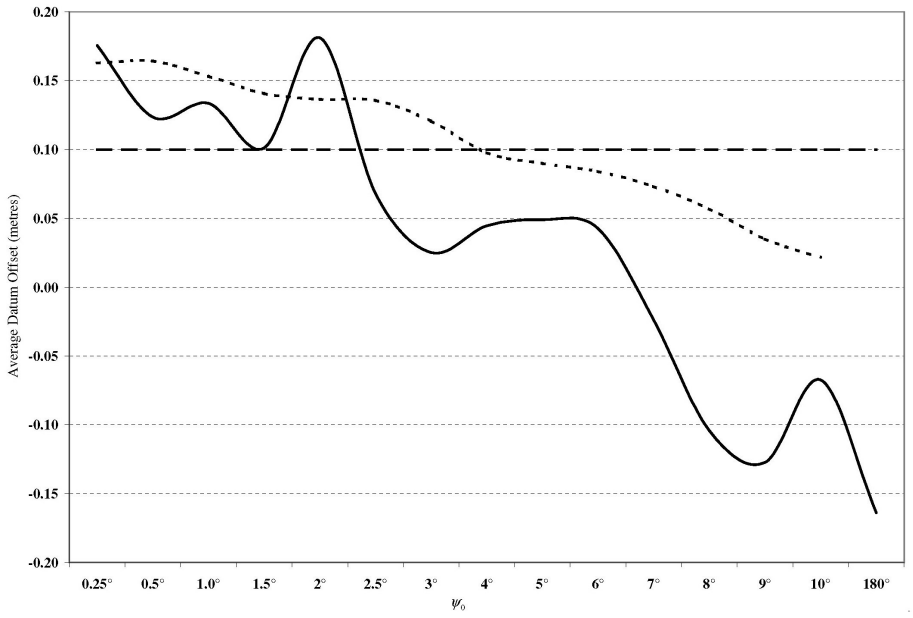

Figure 5.12 Average offsets (relative to Wellington) of SS (solid line) and ML (dotted line) kernel quasigeoids compared with GPS-levelling; and the observed average offset (dashed line)

The WG kernel offsets produce an undulating surface that degrades with increasing ψ_0 (Figure 5.13). A large divergence can be seen when $\psi_0 < 6°$ and $L > 10$. In contrast a positive divergence is seen when the $L < 40$. These features correspond

well to the spikes in the standard deviation comparison (cf. Figure 5.4). The offsets that are closest to the observed offset with $\psi_0 = 1.5°$ and $L = 0 – 5$.

The HG kernel offsets (Figure 5.14) produce a smoother surface than the WG kernel that is similar to that from the standard deviation analysis (Figure 5.5). The closest fit to the observed offset is around $\psi_0 = 5°$ and $L = 15$, because the surface is relatively flat many of the offsets are within 5 cm of the observed value.

The VK kernel offsets (Figure 5.15) show striking similarities to the standard deviation comparison (Figure 5.6). The numerical instability discussed in Section 5.4.3 is clearly visible, although the previous maximum appears as a minima spike of 1.1 m. The small "wing" that occurred with high ψ_0 and low L in the standard deviation comparison also translates to a minima in the offset comparison. Again, there are large areas within 5 cm of the observed offset.

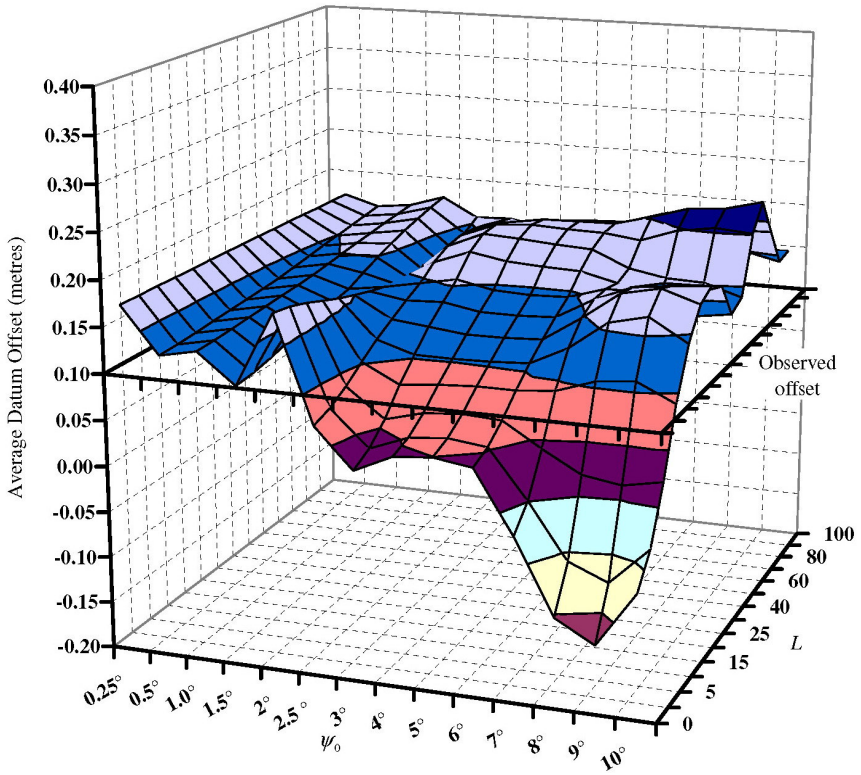

Figure 5.13 Average offset (relative to Wellington) of WG kernel quasigeoid compared with GPS-levelling, observed average offset shown as horizontal plane

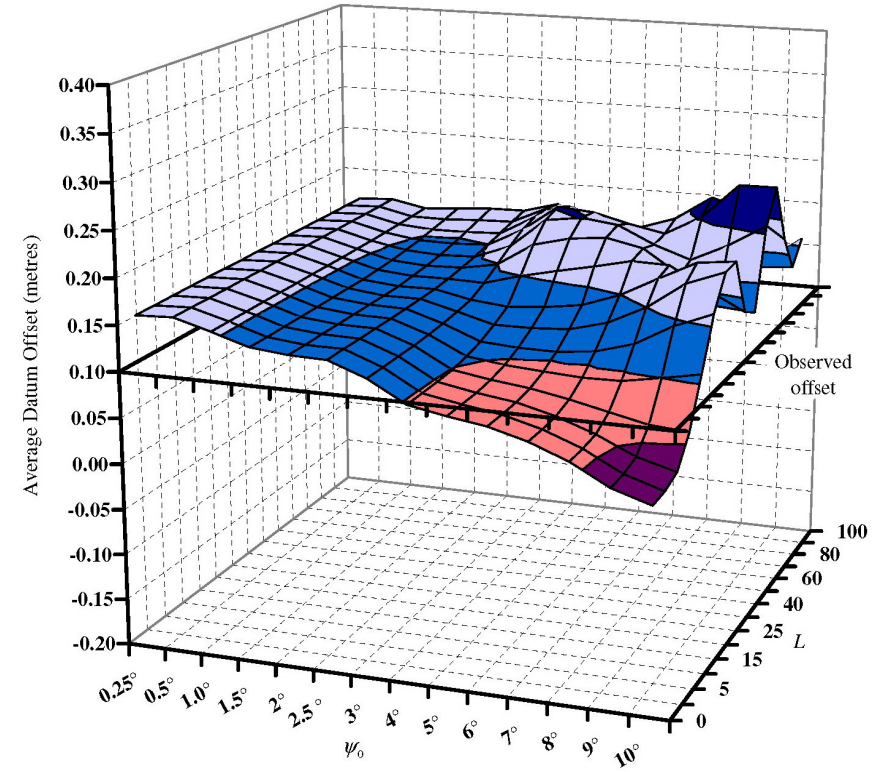

Figure 5.14 Average offset (relative to Wellington) of HG kernel quasigeoid compared with GPS-levelling, observed average offset shown as horizontal plane

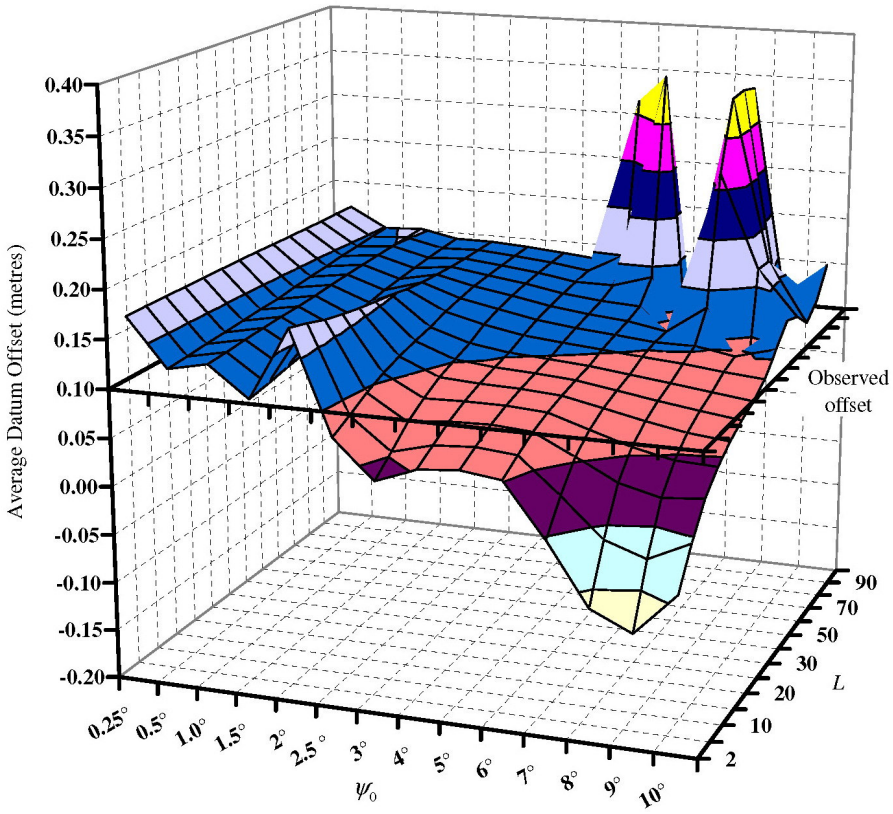

Figure 5.15 Average offset (relative to Wellington) of VK kernel quasigeoid compared with GPS-levelling, observed average offset shown as horizontal plane

The FEO kernel offsets (Figure 5.16) produce the smoothest surface if the spike centred on $\psi_0 = 6°$, $L = 90$ is excluded. Like for the VK kernel, the effect of the numerical instability in the FEO kernel can be seen at this location. The otherwise smooth surface produces a wide range of ψ_0, L combinations that give agreement with the observed offset (within 5 cm).

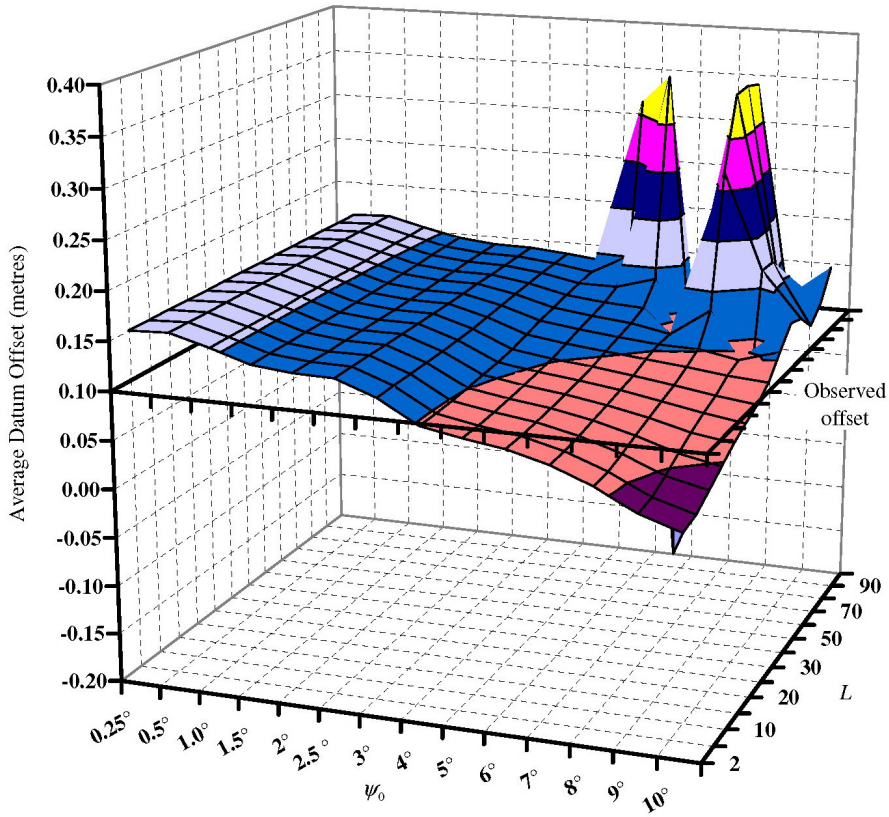

Figure 5.16 Average offset (relative to Wellington) of FEO kernel quasigeoid compared with GPS-levelling, observed average offset shown as horizontal plane

A combined analysis of the standard deviation and the average vertical datum offset (relative to Wellington 1953 datum) still does not give a single ψ_0, L kernel modification combination that is *significantly* better than any other. However, the FEO offset gives the smoothest surface (excluding the spike discussed in Section 5.4.3) that is in agreement with the observed value, implying a more stable solution. The use of the offset analysis on its own is not a strong selection criterion, however, when combined with the standard deviation comparison (Section 5.4.2), it can be used to objectively choose the best parameters (within the 14 cm nominal error of the observed offset).

The standard deviation comparison (Section 5.4.2) concluded that the ML, HG and FEO modifications gave the best solutions. Because the FEO modification also had the smoothest offset surface (i.e., the offset is relatively insensitive to changes in ψ_0 and L) it (with $\psi_0 = 1.5°$ and $L = 40$) was selected for use in the NZ quasigeoid computations.

5.4.5 Summary of kernel modification comparisons

In theory, the FEO modification claims to be the optimum selection because it combines the advantageous features of almost all the previous deterministic kernels (Featherstone *et al.*, 1998). Given its theoretical advantage and effective implementation in AUSGeoid98 (cf. Featherstone *et al.*, 2001), the FEO model has been selected for usage in the quasigeoid computations described in Section 5.2.4. The FEO kernel minimum σ_{average} occurs at $\psi_0 = 1.5°$, $L = 40$ (cf. Section 5.4.2; Figure 5.7). Consequently these parameters will be used in for the NZ quasigeoid computations.

This choice of parameters corresponds well with the $\psi_0 = 1°$, $L = 20$ that was used in the development of AUSGeoid98 (Featherstone *et al.*, 2001). The larger integration cap for NZ ($\psi_0 = 1.5°$) implies that the NZ gravity anomalies are better than in Australia (cf. Vaníček and Featherstone, 1998). The higher value of L selected for the NZ data is attributed to the inclusion of the recent GRACE data in the GGM02S GGM that was not available to Featherstone *et al.* (2001). This data provides a better estimate of the long wavelength quasigeoid signal; hence a higher L than in Australia can be used (cf. Section 3.2).

5.5 Summary

This Chapter has described how gravity observations are converted into a gravimetric quasigeoid using the truncated and deterministically modified Stokes kernel to enhance a GGM. It described five deterministic modifications to Stokes's kernel and evaluated them over a range of ψ_0 and L combinations. Each solution was compared against GPS-levelling observations on the 13 NZ vertical datums and the resulting standard deviations and relative datum offsets used to ascertain the best modification for use in the NZ quasigeoid computations. The standard deviation analysis revealed

a numerical instability in the VK and FEO modifications ($\psi_0 = 6°$ and $L = 90$) that was also reflected in the relative offsets. The cause of this instability was not categorically identified; however, it did not affect the final ψ_0 and L selection. In the end, the FEO deterministic modification was selected with $\psi_0 = 1.5°$ and $L = 40$ for use in the NZ quasigeoid computations. This combination gave the lowest σ_{average} and also exhibited a relative offset that was in agreement with the observed values. Because the FEO σ_{average} was not significantly better than the others, this choice remains somewhat arbitrary.

6 VERTICAL DATUM UNIFICATION

6.1 Introduction

To fix the heights of benchmarks on land requires that the height (or potential) of one (or more) points is fixed (Section 2.3.1). These values are normally selected using long-period sea level observations so that the heights are broadly in agreement with local mean sea level (Section 2.3.2). Sea surface topography (Section 2.3.3) or land movements (Section 2.3.4) lead to differences between different height datum systems (Arabelos and Tscherning, 2001). The concept of vertical datum definition is described in detail in Chapter 2.

It is well known that local vertical datums (LVDs) are often offset from each other. These LVD offsets can be on global [e.g., Colombo, 1980; Laskowski, 1983; Rapp and Balasubramania 1992; Heck, 1990), continental (e.g., Europe (Ihde *et al*., 2002), Africa (Merry, 2003), South America (Hernández *et al*., 2002)], country [e.g., Indonesia (Kasenda and Kearsley 2002), Uruguay (Subiza Piña *et al*., 2002), United Kingdom (Iliffe *et al*., 2003), Australia (Rizos *et al*., 1991; Kearsley *et al*., 1993; Featherstone 2000, 2002a), New Zealand (Hannah 2001), North America (Burša *et al*., 2007)] and local levels. The ideal situation is that they can be unified by relating each datum to a common reference surface (e.g., a precise geoid/quasigeoid model).

This section discusses the problem of LVD unification in NZ. It describes three existing methods of achieving datum unification and highlights the shortcomings in these approaches. Following this, a new iterative technique for unification that accounts for the effect of the offsets between the different datums is presented. The new approach is then implemented over the 13 NZ vertical datums (Section 2.4.3; Figure 6.4) to unify them.

6.2 Vertical datum offsets

6.2.1 Datum reference surfaces

In an ideal world, a geoid coincident with MSL would be able to be used as a global reference surface. MSL would represent a constant equipotential at all locations, it would not change over time and it would be easy to define at coastal sites to establish

reference marks for the origins of local or national datums: this is not the case. Heights could then be transferred from these origin points using techniques such as precise spirit levelling, where precise levelling lines from adjacent datums meet the heights in terms of those datums would theoretically be identical (in the absence of errors in the precise levelling).

The real world is, unfortunately, different from this ideal. Phenomena such as tides (cf. Section 2.3.2), sea surface topography (cf. Section 2.3.3), currents and storm surges (cf. Section 2.4.5) collude to cause MSL to deviate from an equipotential surface. The relationship between observed MSL and the land reference marks is not constant due to changes in sea level and the uplift/subsidence of the land (cf. Sections 2.3.4 and 2.4.6), thus datums defined at different times may refer to different levels. This means that when local MSL is used to define a vertical datum, it is likely to be different to local MSL at a different location, consequently when vertical datums are compared; they are offset from each other.

The above effects are compounded by differences in the choice of height system (cf. Section 2.2); Earth-tide model (cf. Section 2.3.5); datum definition (adjustment) technique (cf. Section 2.3.1); and errors in levelling. From a vertical datum users' perspective, it is useful to have all points within a given region that are at sea level to have a height equal to zero. If a vertical datum is defined by fixing MSL at a single tide gauge point (e.g., NZ [Section 2.4.4]; United States NAVD 88 [Zilkoski *et al*., 1992]) it can result in the "zero height" departing from MSL at other locations in the datum.

A practise that has been adopted in many countries (e.g., Australia AHD [Roelse *et al*., 1975; Section 2.5.1]; Canada CGVD28 [Kingdon *et al*., 2005; Section 2.5.3]) is to constrain multiple tide-gauge MSL values to zero in their respective precise levelling adjustments. This approach gives a vertical datum with a "zero level" that is close to the observed MSL at all locations, but it does not represent an equipotential surface. For example, the Australian AHD adjustment fixes 30 tide-gauges to "absorb" the effect of SSTop that is known to cause MSL to deviate by 70 cm around the Australian coast (Featherstone and Kuhn, 2006). If datums are not defined in relation to equipotential surfaces, it is more difficult to determine their relationship to other vertical datums (cf. Section 6.3).

6.2.2 Effect of vertical datum offsets on gravity observations

When gravity observations are reduced to gravity anomalies, the "height" of the observation is an important quantity. Heights are used for several reductions (cf. Section 3.3) and in the computation of terrain corrections (cf. Section 4.4). Where all heights are in terms of the same datum, the reductions and calculations will be consistent.

Where heights are not in terms of the same vertical datum or the vertical datum used is distorted, for example where adjacent datums abut or where a regional or global unification of vertical datums is being attempted, the different heights will be inconsistent. It follows that the quantities derived from these heights, namely free-air and Bouguer anomalies, will also be inconsistent (e.g., Section 3.3). When inconsistent gravity anomalies are converted into a geoid, a step (smoothed by the filtering in Stokes function) will occur in the geoid surface that is related to the offset between the vertical datums (Figure 6.1). The significance of these steps will be affected by the magnitude of systematic errors in the heights that are used to reduce the gravity anomalies.

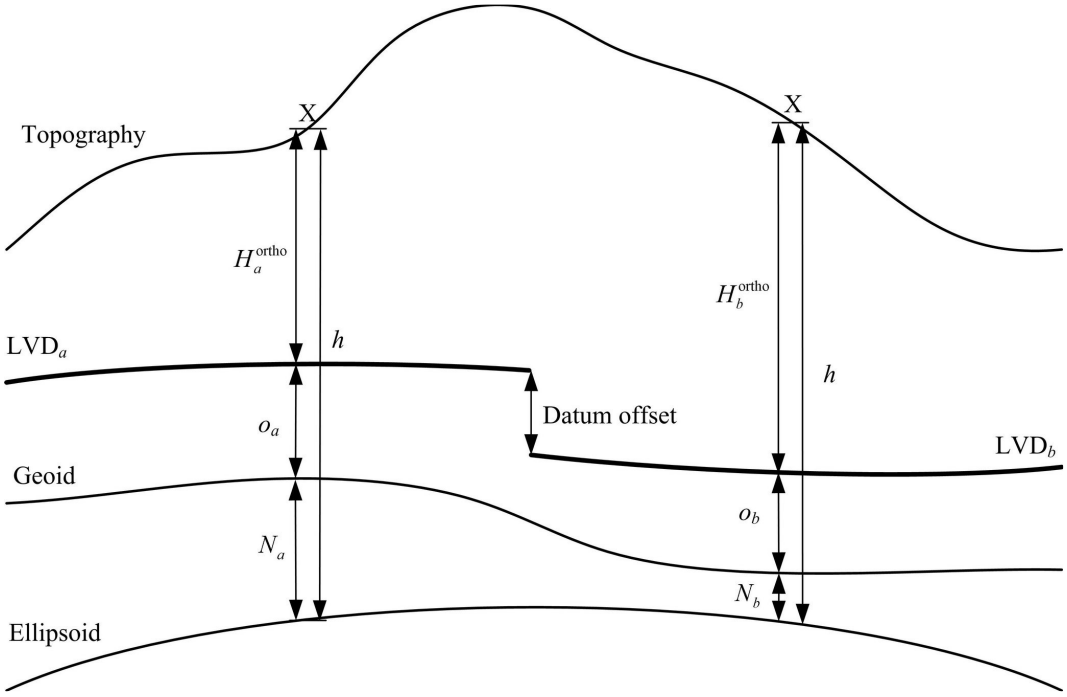

Figure 6.1 Height and datum offset relationships

6.2.3 Height and offset relationships

When two or more vertical datums are not defined in terms of the same equipotential surface, they can not be unified by simply comparing heights in each system (i.e., points in the different systems with the same height "values" will not be located on the same equipotential surface). Where the different datums physically abut, it can be possible to directly observe the datum offset (o) at that point by comparing the heights from the respective systems (i.e. $o = H_a - H_b$). Obviously this approach is not possible where the datums are not physically connected due to the presence of water bodies, for example between the North and South Islands of NZ.

Satellite-based GNSS positioning provides a method to transfer ellipsoidal heights across large distances. When combined with a GGM, ellipsoidal heights can be converted into orthometric heights using the relationship given in Section 2.2.10 (and described further in Section 6.3.2). This approach assumes that the GGM coincides with the "zero" of both vertical datums. When these surface do not coincide an offset (o) exists:

$$H_a^{\text{ortho}} - h - N = o_a \tag{6.1}$$

where H_a is the orthometric height in terms of the local vertical datum, h is the ellipsoidal height and N is the geoid height. Similarly for normal-orthometric heights ($H^{N\text{-O}}$) and the quasigeoid (ζ) the offset is given by:

$$H_a^{N-O} - h - \zeta = o_a \tag{6.2}$$

6.3 Vertical datum unification techniques

If it is not possible to directly connect adjacent vertical datums, for example due to a body of water or large distances between benchmarks, an alternative method is required. The following sections describe the main approaches that have been proposed by other authors for vertical datum unification.

6.3.1 Geopotential numbers

The global geopotential (W_0), as specified by Gauss (1828) and Bessel (1837), represents the mean of the geopotential over the world's oceans. The global potential, W_0, is given in Burša *et al*. (2007) as:

$$W_0 = 62\ 636\ 856.0 \pm 0.5\ \mathrm{m^2 s^{-2}}$$
$$R_0 = \frac{GM}{W_0} = 6363672.56 \pm 0.05\ \mathrm{m} \tag{6.3}$$

As stated in Section 6.2, most LVDs are defined in terms of one or more local tide gauge stations, and by definition local estimates of W_0 (this is the case in NZ). A description of the procedure to unify vertical datums using geopotential numbers is given in Burša *et al*. (1999a; 1999b; 2001; 2007). In simple terms, the actual geopotential, $(W_0)_A$, is computed at the origin (tide-gauge) of each LVD using a GGM and GPS-levelling. These values are then compared with the global geopotential to give geopotential numbers using (cf. Equation 2.1):

$$C_A = W_0 - (W_0)_A \tag{6.4}$$

The offset between the LVDs *A* and *B* is then given by (where γ is normal gravity):

$$o_{AB} = \frac{C_A - C_B}{\gamma} \tag{6.5}$$

This approach has been implemented in several locations, normally between countries, for example Grafarend and Ardalan (1997) in the Baltic region, Burša *et al*. (2007) in North America, and Burša *et al*. (1999a, 1999b; 2001; 2002; 2004) on several countries on a global scale. This technique of datum unification requires GGM and GPS-levelling information at each of the datum origins (tide-gauges) to compute the geopotential for each LVD. The downside of using a single point for each datum is that the assumptions must be made that the datum offsets are constant across the datum and that the datums are not inclined or distorted (e.g., due to multiple tide gauges being fixed in the precise levelling adjustment).

6.3.2 Gravimetric geoid

Different height systems can be related by using a geoid model and GPS-levelling observations to provide a consistent reference surface to which the systems can be related. Given that the computation of precise regional geoids is becoming straight-forward, this technique has been implemented extensively, for example: Arabelos

and Tscherning (2001); Goldan and Seeber (1994); Featherstone (2000); Kumar and Burke (1998); Nahavandchi and Sjöberg (1998b); Rapp (1995); Pan and Sjöberg (1998); Rizos *et al*. (1991); and Rapp and Balasubramania (1992). However, geoids still have errors in them, so this approach does not give exact datum unification.

If the orthometric heights of two points, H_A^{ortho} and H_B^{ortho}, in two different height systems are known, then, given the ellipsoidal heights, h_A and h_B, of those same points, and the geoid height difference

$$N_{AB} = N_A - N_B \tag{6.6}$$

between the points. The offset between the datums can be determined by:

$$o_{AB} = \left(h_A - h_B\right) - N_{AB} - \left(H_A^{\text{ortho}} - H_B^{\text{ortho}}\right) \tag{6.7}$$

As the name of this approach suggests, the application of Equation (6.7) is dependent on the availability of accurate geoid height differences between the datums. The common method of gravimetric geoid computation is the so-called "remove-compute-restore" approach where a global spherical harmonic model is enhanced with additional gravity and topographic information. Any error in the spherical harmonic model, particularly long wavelength errors that are not corrected by the additional gravity and topography data, will be transferred directly to the computed geoid when using the RCR technique (Section 5.2.4; Vaníček and Featherstone, 1998). These errors will then propagate into the calculated vertical offsets. However, when the datums are regional in nature and close together (as is the case in NZ), the long wavelength errors inherent in the spherical harmonic model will have a similar effect on all of the offsets.

Arabelos and Tscherning (2001) have shown that the CHAMP mission, and predicted that the GRACE and GOCE, satellite gravity missions are likely to improve the long-wavelength spherical harmonic models. The use of these more accurate spherical harmonic models, as they become available, will make this approach more accurate.

For this approach to datum unification to be strictly followed, the orthometric heights, gravity data heights and topographic heights used to calculate the

gravimetric geoid need to be in terms of a consistent datum. This is known to not be the case (and is the reason for undertaking datum unification in the first place).

When datums are being unified by this technique, it is often assumed that each datum is constrained at a single fundamental reference point. In this situation, it can normally be assumed that the offset by a constant value. In Australia, for example, the AHD is constrained to 30 tide-gauges around the coast that are affected differently by SSTop (among other factors). This meant that when datum unification was attempted between mainland Australia and Tasmania the computed offset changes depending on the subset of points that was used (Featherstone, 2000).

6.3.3 Sea surface topography

The sea surface topography (SSTop), which causes differences between vertical datums based on coastal MSL observations, is the effect of oceanographic phenomena such as oceanic currents, meteorological effects, spatial variation of temperature and salinity etc. (cf. Section 2.3.3). If these phenomena can be modelled, then the resulting SSTop surface (which approximates the geoid at the metre level; e.g., Hipkin, 2000) can be used to relate different datums (Heck and Rummel, 1990).

The main problems in this approach are the complexity and the lack of resolution of these techniques, especially in the coastal regions where the tide-gauges used to define vertical datums are typically placed (e.g., Lehmann, 2000). This means that the height relationships between datums can not at present be modelled to a high precision. A modification to this procedure is to locate the tide-gauges offshore (where the SSTop models are better), however then a precise geoid is required to relate the tide-gauge to the vertical datum that it is being used to define (Ihde, 2007).

6.3.4 Limitations of geopotential and geoid approaches

The information used by the geopotential (Section 6.3.1), gravimetric geoid (Section 6.3.2) and the SSTop (Section 6.3.3) approaches to vertical datum unification typically includes GGMs, gravity observations/anomalies, orthometric or normal heights etc., and GPS (ellipsoidal) heights This information is frequently reduced to, or is in terms of, the local datums that relate to different equipotential surfaces or to

surfaces that are not even equipotential (e.g., due to over-constrained levelling network adjustments). Because these datums are offset from each other, the data that is being used to achieve the datum unification is not in terms of a common reference system. This means the unification achieved using this data will be biased by any offset between the different vertical datums.

Laskowski (1983) simulated datum offsets on a continental scale ranging from -55 cm to +30 cm (approximating the effect of SSTop) and found that the cumulative error up to degree 180 in the geoid was 44.67 cm, which is almost the magnitude of the SSTop variation. He then showed that 90 percent of that effect was attributed to the low order (up to degree 10) geopotential coefficients. This simulation confirmed that the effect of the offset vertical datums is likely to be seen in the low-frequency part of the gravity spectrum, which is known to have a large effect on the geopotential and the geoid (e.g., Vaníček and Featherstone, 1998). Where the datums are physically close together (as in NZ), the effect from the low-frequency part of the gravity spectrum on the geoid will be similar for each datum and the resulting datum offsets (cf. Section 6.3.2).

In a strict sense, each data set should be reduced to a common reference surface before unification is attempted, thus accounting for the fact that the surface being used for the datum unification is itself distorted. The challenge is that this problem is somewhat circular, namely to get the data on a common reference surface it needs to be unified, however the problem is that the datums are not unified.

The GBVP and iterative geoid approaches, described next in Sections 6.3.5 and 6.4 respectively, differ from the above two approaches in that they attempt to account for the datum offsets that are known to exist in the source data.

6.3.5 Geodetic boundary-value problem approach

Two vertical datums can be connected indirectly by means of a combination of precise geocentric positions of two points, their potential (or height) value in each respective datum and their geoid height difference. Rummel and Teunissen (1988) presented a method of determining the geoid height difference based on an extended formulation of the GBVP which made the realistic assumption that the observable

potential (or height) and gravity values used in its solution refer to a variety of height datums with unknown height differences between them.

The general solution to the GBVP approach is (Rummel and Teunissen, 1988):

$$T(P) = \frac{GM - GM'}{R} + \frac{R}{4\pi}\int_{\sigma} S(\psi_{PQ})\left\{\Delta g^{j} + \frac{2}{R}C_{Q_j 0}\right\} d\sigma_j \tag{6.8}$$

where G is the gravitational constant, M' and M are the approximate and actual masses of the Earth respectively. It is reasonable to make the assumption that $GM - GM' = 0$ because GM' can be accurately determined (Xu and Rummel, 1991). R is the radius of the Earth, $S(\psi_{PQ})$ is Stokes integral function, Δg^{j} the gravity anomaly, and $C_{Q_j 0}$ the potential difference to datum j.

A detailed description of the method is provided in both Rummel and Teunissen (1988) and Heck and Rummel (1990). There are, however, three basic requirements for the method, these are (1) geodetic (ϕ, λ, h) coordinates for at least one station in each datum, (2) precise orthometric (or normal) heights or potential differences are available for all stations, and (3) gravity anomalies referring to the (I + 1) vertical datums are known globally (Xu, 1992).

An example of the linear adjustment model that can be formed for each of the K space stations P_k (Rummel and Teunissen 1988, Xu and Rummel 1991) is:

$$y_k = -\frac{\Delta W_0}{\gamma} + \left[1 + 2S_{PQ_i}\right]\frac{C_{Q_i 0}}{\gamma} + 2\sum_{j=1\,(j\neq 1)}^{n} S_{P_k Q_j}\frac{C_{Q_j 0}}{\gamma} \tag{6.9}$$

where S_{PQ_i} and $S_{P_k Q_j}$ are the Stokes's integrals evaluated over the respective datum zones i and j at station P_k and γ is normal gravity. With $K \geq I + 1$ and at least one station in each datum zone, the unknown $C_{Q_i 0}$ and ΔW_0 are estimable from Equation (6.9).

Biases introduced by inconsistencies in gravity, vertical and horizontal datums; error due to use of a simplified free-air gravity reduction; and the combination of different height systems, are all detrimental to the precision of the computed terrestrial gravity

anomalies. Other effects such as periodic and secular variations in the Earth's gravity field, plate tectonics, glacial isostatic adjustment and atmospheric variations also impact the gravity field (cf. Section 2.3). The GBVP approach relies on the vertical datum effect to be the only major systematic error source in the gravity anomaly data, consequently the data needs to be reduced for the other effects before correct offsets can be evaluated (Heck, 1990).

Pan and Sjöberg (1998) used Equation (6.9) to determine the datum offset between the Swedish and Finnish height systems as part of a wider Fennoscandia datum unification study. They found a "surprisingly good agreement" with the results of the precise levelling derived offsets, 19.3 cm versus the 16.2 cm and 19.2 cm from different levelling sources. It was not possible to locate any other practical implementations of this technique. However, it has been implemented theoretically by Xu and Rummel (1991) and Xu (1992) who performed implementations using simulated data. In addition van Olsen and van Gelderen (1998) computed an error propagation solution to prove the viability of the technique.

6.4 Iterative quasigeoid unification scheme

6.4.1 Overview and principles

The objective of vertical datum unification is to determine a relationship between each of the vertical datums so that the heights of points on each datum can be expressed in terms of a single common system. Traditionally, local datums are based on MSL observed at tide gauges in the area of interest. Because the mean sea surface in the open ocean is known to deviate from a constant surface by more than one metre (e.g., Section 2.3.3; Pugh, 2004) the (normally) equipotential surfaces that form local datums will not be coincident and will be offset from each other by an unknown amount.

When observations are reduced using heights in terms of a LVD (e.g., gravity reductions) are combined with observations reduced using heights from an adjacent datum, their combination will be biased because the heights have not been reduced in terms of a consistent reference surface. This effect was noted and quantified in relation to datum unification problems by Laskowski (1983). He proposed a datum

offset correction ($\delta\Delta g$) to correct gravity observations for the effect of the offset vertical datums and thus convert them to a consistent reference system prior to quasigeoid computation. $\delta\Delta g$ has the form of the (first-order) free-air gravity correction (cf. Section 3.3.2) and units of mgal.

$$\delta\Delta g = \Delta g^* - \Delta g = \frac{\partial g}{\partial h} o \cong 0.3086\, o \tag{6.10}$$

where:

$$\Delta g^* = g_{obs} - \frac{\partial g}{\partial h}\left(h_D + o\right) - \gamma$$

$$\Delta g = g_{obs} - \frac{\partial g}{\partial h} h_D - \gamma$$

o = vertical datum offset (metres)

g_{obs} = observed value of gravity

$\frac{\partial g}{\partial h}$ = vertical gradient of normal gravity

h_D = height difference between surface point of measurement and corresponding point on the geoid (implied by vertical datum D)

γ = normal gravity on the reference ellipsoid

It is not necessary to use the second-order free air correction (Equation 3.7) in Equation (6.10) because of the small height differences involved ($o \leq 2$ m).

Laskowski (1983) showed, in relation to spherical harmonic analysis, that the zero height implied by different vertical datums is not unique and varies from datum to datum by 1-2 metres (approximately the magnitude of SSTop, cf. Section 2.3.3). It was concluded that mean gravity anomaly data, $\Delta\overline{g}$, should be further reduced to the modelled quasigeoid by the height difference between the zero-height implied by each vertical datum and the zero-height implied by the modelled quasigeoid (in much the same way that the indirect effect is used to correct for the change of mass under Helmert's condensation, cf. Section 4.6).

A limitation of Laskowski's (1983) approach is its requirement that the magnitude of the vertical datum offsets is known *before* the correction can be applied and the quasigeoid computed. In many situations, the offset will not be known beforehand; for example, where it is not possible to directly measure between adjacent datums.

The iterative quasigeoid unification scheme proposed and used here utilises the gravimetric quasigeoid technique (Section 6.3.2) to initially estimate the offsets between vertical datums and then uses Laskowski's (1983) height correction function to correct the gravity anomaly values for the effect of the offset vertical datums.

The iterative scheme described above could be used as the basis for datum unification using the other techniques described in Section 6.3 (geopotential numbers, SSTop, GBVP). The evaluation of these alternatives is beyond the scope of this research because: gravity observations are not available in NZ to compute geopotential numbers; SSTop models are not sufficiently accurate to relate the NZ LVDs; and the GBVP technique has not been practically implemented.

6.4.2 Gravimetric quasigeoid computation

The general process followed in the iterative unification procedure is shown in Figure 6.2. The first step is to compute a preliminary gravimetric quasigeoid using gravity anomalies reduced to their respective local vertical datums. The procedure used to compute the gravimetric quasigeoid has been documented in Section 5.2.4. Essentially, the quasigeoid should be determined using rigorously reduced data sets (cf. Chapter 3) best corrections (cf. Chapter 4) and optimised computation procedures (cf. Chapter 5) for the area concerned. Studies by Featherstone (2003d) and Novák *et al*. (2001b) have shown that it is possible to determine the high-frequency quasigeoid to an accuracy of approximately 1-cm using synthetic data (i.e., if the error in the GGM is ignored). Using the recent GRACE-derived GGMs (cf. Appendix A.2.1) and correctly processed (real) data, it is probably possible to resolve a quasigeoid to ~10 cm or so on land.

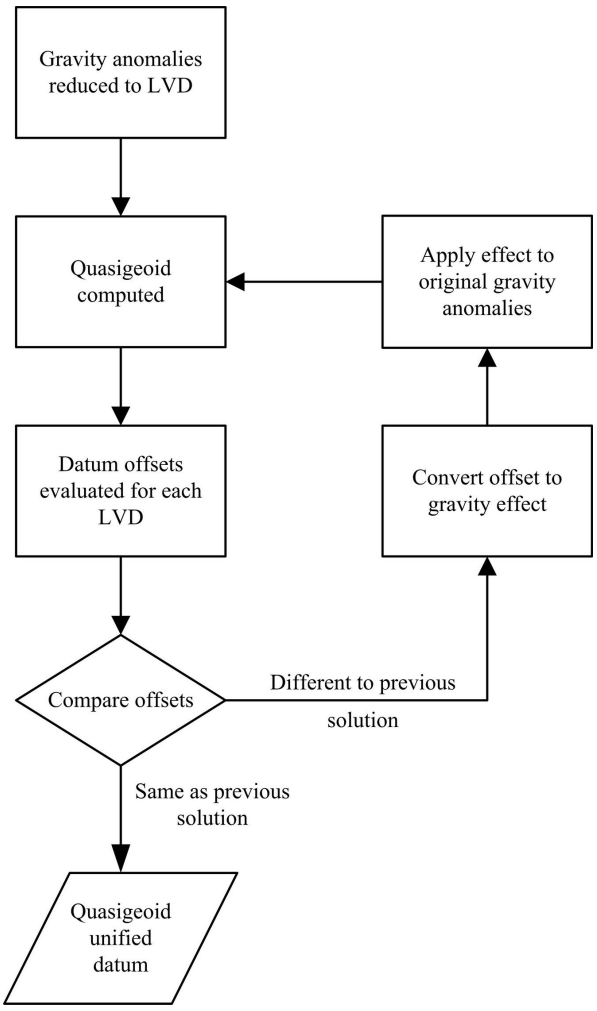

Figure 6.2 Iterative quasigeoid unification procedure

6.4.3 Vertical datum offset computation

GPS-levelling observations are then used to estimate the datum offsets for each vertical datum. It has been shown in Section 2.2.10 that the normal-orthometric (H^{N-O}), quasigeoid (ζ) and ellipsoidal (h) heights of a point are related by $h = \zeta + H^{N-O}$. In an ideal, errorless situation, where the origin of the vertical datum coincides with the quasigeoid, the datum offset (o) will equal zero:

$$o = H^{N-O} + \zeta - h = 0 \tag{6.11}$$

In the real world, the origin of the local vertical datum will not coincide with the quasigeoid and errors exist in all of the above three heights used to determine e. This causes the computed vertical datum offsets to contain both noise and a bias. When GPS-levelling observations are used to estimate the datum offsets for each vertical

datum they will show an offset (average difference between quasigeoid and GPS-levelling) and an error (standard deviation of the difference).

6.4.4 Datum offset correction

The computed offsets are then used with Equation (6.10) to determine $\delta\Delta g$ for each vertical datum. The original gravity anomalies are then "corrected" by adding the applicable $\delta\Delta g$ for the datum to which they belong. The effect of using $\delta\Delta g$ to unify two datums with the iterative geoid datum unification scheme is shown in Figure 6.3. The gravity anomalies are initially reduced to the respective LVD which are offset from each other, in this case, *a* or *b*. This information is then used to compute a preliminary geoid (indicated by the dotted line in Figure 6.3). It can be seen that where the two LVD meet a step (smoothed by the filtering in Stokes function) occurs in the computed geoid as a result of the offset.

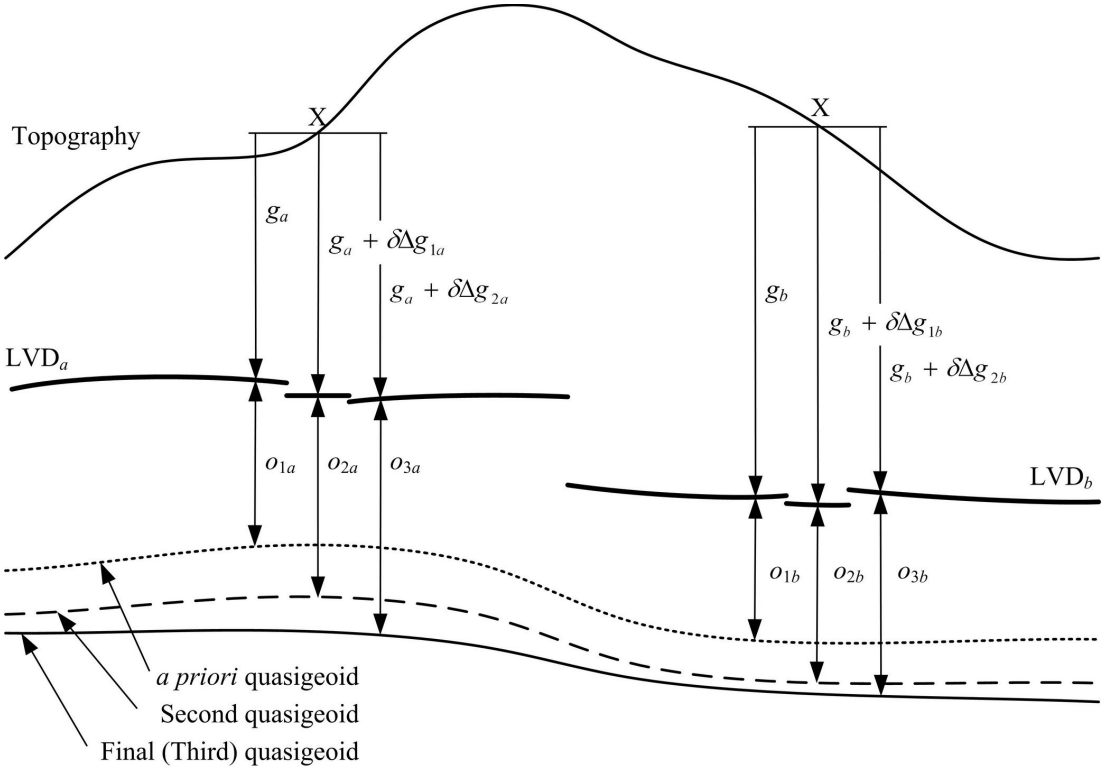

Figure 6.3 Iterative quasigeoid datum unification scheme

The initial offsets for each datum, o_{1a} and o_{1b}, are evaluated from GPS-levelling information, an *a priori* gravimetric quasigeoid (ζ_1) using:

$$o_{1a} = \zeta_1 + (H_a^{N-O} - h) \tag{6.12}$$

Equation (6.10) is then used to determine the effect of the offset on the gravity anomalies, $\delta\Delta g_{1a}$ and $\delta\Delta g_{1b}$, on their respective datums. The original anomalies (g_a, g_b) are then corrected by the addition of the offset effect:

$$g_{1a} = g_a + \delta\Delta g_{1a} \tag{6.13}$$

It is pertinent to note that this assumes that the heights used to reduce the gravity anomalies were in fact in terms of the datums, and therefore subject to the datum bias.

6.4.5 Re-compute gravimetric quasigeoid

The "corrected" gravity anomalies are then used to evaluate a second quasigeoid (ζ_2) (shown as a dashed line in Figure 6.2). The step in the geoid at the datum boundary has been smoothed in comparison to the preliminary quasigeoid. This is because the offset bias is being better modelled by the offset correction applied above. The original GPS-levelling data is then used again with the second quasigeoid to re-evaluate the datum offsets, o_{2a} and o_{2b}:

$$o_{2a} = \zeta_2 + (H_a^{N-O} - h) \tag{6.14}$$

The offsets are then converted to the gravity effects, $\delta\Delta g_{2a}$ and $\delta\Delta g_{2b}$ (Equation 6.10). These are then applied to the original gravity anomalies to give:

$$g_{2a} = g_a + \delta\Delta g_{2a} \tag{6.15}$$

The corrected anomalies (g_{2a}, g_{2b}) are then used to compute a third quasigeoid (ζ_3), shown as a solid line in Figure 6.2. This geoid is even smoother than the second geoid across the datum boundary. Again the original GPS-levelling data is used to evaluate the datum offsets, o_{3a} and o_{3b}. This process is repeated until the offsets computed in successive iterations are constant.

6.5 Implementation of the iterative quasigeoid computation scheme in NZ

To determine the feasibility and practicality of the iterative quasigeoid computation approach to vertical datum unification, it has been implemented over NZ. The NZ normal-orthometric heights (Section 2.4.3) are divided between thirteen vertical datums that are based on local determinations of sea level, in locations where these datums abut or overlap it has been shown that offsets exist between them (Section 2.4.4).

6.5.1 Gravity data division

The gravity observations (Section 3.3) used for the computation of the quasigeoid are assumed to be reduced to the vertical datums in which they are located. Because the spatial extents of the 13 LVDs are not explicitly defined and the datum used to reduce the gravity observations has not been recorded, it is not possible to categorically ascertain whether the reduction to the LVDs has occurred or not. However it is strongly suspected, and with the lack of evidence to the contrary, it is necessary to make this assumption.

Before the iterative unification technique can be implemented, it is necessary to separate the gravity anomalies according to the LVD that they are situated in. Because the applicable LVDs are not recorded with the gravity observations it was necessary to deduce the likely LVD for each observation point. A visual inspection of topographic maps that showed the locations of all geodetic marks with normal-orthometric heights on each LVD (this includes low-accuracy heights) allowed lines to be drawn to approximate the LVD boundaries (Figure 6.4). Where actual datum boundary points were known to exist these were used (cf. Table 2.3, Figures 2.4 and 2.5). However the majority of the boundaries were plotted by hand on 1:500,000 topographic maps. It is acknowledged that this method is approximate and that it ignores the situation where adjacent datums overlap. Because the boundaries of the LVDs are not well-defined, this will affect the quality of the offsets computed from GPS-levelling points near to them. The majority of levelling points that are in the vicinity of the more arbitrary boundary positions are of lower accuracy and without ellipsoidal heights, therefore this demarcation procedure is considered acceptable.

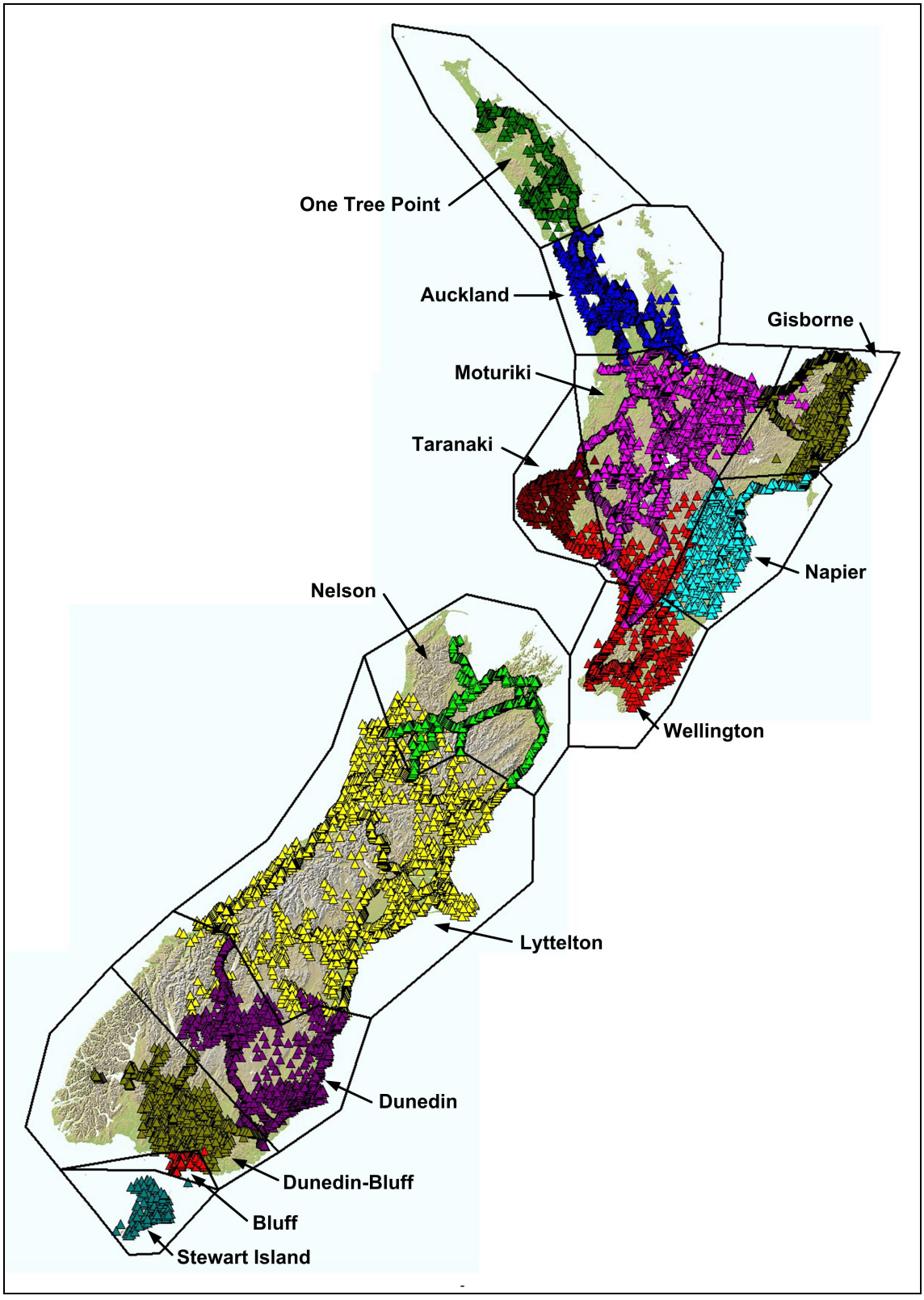

Figure 6.4 New Zealand vertical datum extents, triangles show the location of geodetic marks with normal-orthometric heights (all orders)

The LVD boundaries shown in Figure 6.4 were then captured as regions in the *MapInfo* version 6.5 geographic information system software (www.mapinfo.com). These boundaries were used to allocate each terrestrial gravity observation into its respective vertical datum. This resulted in separate gravity data file for each of the 14 vertical datums (the 13 LVDs in Figure 6.4 and also the Chatham Islands).

6.5.2 *A priori* geoid solution

A gravimetric quasigeoid was computed over NZ using the datasets and following the procedure described in Section 5.2.4. In summary, the gravity observations consisted of cross-over adjusted marine observations merged with satellite altimetry data in marine areas and terrestrial anomalies that had been terrain-corrected and densified using the 56-metre DEM. The GGM02S-EGM96 merged GGM was used as a reference model in the modified RCR geoid computation procedure. The Featherstone *et al*. (1998) deterministic modification with $\psi_0 = 1.5°$ and $L = 40$ was applied to Stokes's integral before it was evaluated via a 1D-FFT.

The average datum offsets were evaluated from the 1422 GPS-levelling points (cf. Section 3.8) that were divided into their respective LVDs using Equation (6.11). These points are not evenly distributed either spatially between the 13 LVDs or geographically because the precise levelling routes (the source of the normal-orthometric heights) are located along the state highway network (cf. Figure 3.7).

It was not possible to evaluate offsets in the Chatham Islands because there is currently no ellipsoidal height information at the small number levelling points on the island. As such, the offset for the Chatham Island vertical datum has been assumed to be coincident with the quasigeoid in all computations (i.e., the offset was assumed to be zero). The average offset and associated statistics for each datum are shown in Table 6.1. The last two rows in Table 6.1 give respectively, the statistics of all 1422 points on a single datum (i.e. if the datum offsets are ignored), and the statistics when the average offset for each datum has been removed from the offset at each point (hence the zero average). The standard deviation (STD) of last row is a useful estimate of the quality of the quasigeoid as the influence of the datum offsets has been reduced.

Datum	Points	Max	Min	Average	STD
One Tree Point 1964	51	-0.148	-0.414	-0.245	0.063
Auckland 1946	137	-0.317	-0.658	-0.497	0.068
Moturiki 1953	258	-0.169	-0.524	-0.316	0.061
Gisborne 1926	61	-0.432	-0.698	-0.585	0.087
Taranaki 1970	70	-0.326	-0.595	-0.457	0.066
Napier 1962	54	-0.115	-0.467	-0.304	0.070
Wellington 1953	78	-0.422	-0.616	-0.509	0.040
Nelson 1955	111	-0.026	-0.434	-0.257	0.081
Lyttelton 1937	251	+0.011	-0.614	-0.350	0.097
Dunedin 1958	73	-0.152	-0.727	-0.491	0.162
Dunedin – Bluff 1960	181	-0.025	-0.577	-0.261	0.076
Bluff 1955	92	-0.207	-0.466	-0.380	0.051
Stewart Island 1977	5	-0.238	-0.592	-0.398	0.116
All Data	1422	+0.011	-0.727	-0.367	0.127
All Data, Zero Datum Average	1422	+0.361	-0.315	0.000	0.081

Table 6.1 Descriptive statistics of the comparison of the *a priori* quasigeoid with GPS-levelling points on the 13 LVDs (metres)

A relatively large STD was observed on the Dunedin 1958 LVD (±0.162 m). This was investigated and it was noted that the size of the quasigeoid and GPS-levelling residuals got systematically larger as the precise levelling lines moved north-west from the Dunedin tide-gauge (cf. Figures 2.5 and 3.7). It is possible that this could be due to a tilt in the datum offset rather than the constant offset that has been assumed in this study. The limited number and geographical extent of GPS-levelling points (cf. Figure 2.5) has meant that it was not possible to verify the cause of this anomaly. Future studies (with additional GPS-levelling data) that investigate the use of inclined planes or even polynomial offset surfaces would help to isolate the cause of this discrepancy.

Statistical tests were carried out to establish whether or not the observed datum offsets given in Table 6.1 are significant. These tests (described in Appendix E.4) showed that all 13 offsets were significantly different to zero (Table E.1) and hence it can be concluded that the datums are in fact offset from the quasigeoid model. It was also found that of the 16 abutments, the offsets at 14 were significantly different and only the Napier-Moturiki and Bluff-Stewart Island were not (the full analysis is provided in Table E.2). These findings may be optimistic given that the analysis

does not address the potential presence of systematic errors in the heights used to reduce the gravity anomalies (cf. Section B.3). Because the errors could not be reliably quantified they were not included them in the above analysis.

An additional validation of the computed offsets can be obtained by comparing them with the observed differences at the junction points of the precise levelling lines (cf. Table 2.3, Figures 2.4 and 2.5). The results of this comparison are summarised in Table 6.2 (the full analysis is in Table E.3). It was found that ten of the 13 observed offsets agreed with the computed values (a combined standard deviation of ±0.071 m was conservatively estimated for the levelling heights). The three observed offsets that did not agree with the computed offsets were Gisborne-Moturiki, Lyttelton-Dunedin and Dunedin-Dunedin-Bluff. The Lyttelton-Dunedin and Dunedin-Dunedin-Bluff differences are likely to be caused by the high STD of the Dunedin 1958 offset (Table 6.1) resulting from the potential tilt in the vertical datum. The Gisborne-Moturiki difference might be caused by the poor spatial coverage of the GPS-levelling points used to evaluate the quasigeoid offset (cf. Figure 3.7). The majority of the Gisborne 1926 datum, notably the large loop around East Cape (37° 41'S, 178° 32'E) and the levelling line between AD2J and ABX2 (Figure 2.4), has no GPS-levelling observations on it.

From	To	*a priori* quasigeoid		Precise levelling		Offsets Agree?
		Offset	95% CI	Offset	95% CI	
Auckland	One Tree Point	-0.252	± 0.021	-0.206	± 0.139	Yes
Auckland	Moturiki	-0.181	± 0.014	-0.070	± 0.139	Yes
Gisborne	Moturiki	-0.269	± 0.023	-0.075	± 0.139	No
Gisborne	Napier	-0.281	± 0.029	-0.166	± 0.139	Yes
Moturiki	Napier	-0.012	± 0.020	-0.099	± 0.139	Yes
Taranaki	Napier	-0.153	± 0.025	-0.046	± 0.139	Yes
Taranaki	Wellington	0.052	± 0.018	0.147	± 0.139	Yes
Taranaki	Moturiki	-0.141	± 0.017	-0.162	± 0.139	Yes
Napier	Wellington	0.205	± 0.021	0.237	± 0.139	Yes
Nelson	Lyttelton	0.093	± 0.019	-0.027	± 0.139	Yes
Lyttelton	Dunedin	0.141	± 0.040	-0.071	± 0.139	No
Dunedin - Bluff	Dunedin	0.230	± 0.039	-0.019	± 0.139	No
Dunedin - Bluff	Bluff	0.119	± 0.015	-0.001	± 0.139	Yes

Table 6.2 Summary of comparison between *a priori* quasigeoid and observed precise levelling offsets, full analysis is in Table E.3 (95% CI, Student t distribution, metres)

6.5.3 Second quasigeoid solution

An offset correction $\delta\Delta g$ was then computed for each LVD using the average offsets (Table 6.1) and Equation (6.11) and then added to the original terrestrial gravity anomalies. A second gravimetric quasigeoid was then computed using the "corrected" gravity anomalies using exactly the same process as above (including gravity densification with the DEM). The datum offsets were then re-evaluated using the same GPS-levelling data as above with the second gravimetric quasigeoid (Table 6.3). The differences between the *a priori* and second quasigeoid computed offsets (Tables 6.2 and 6.3) are very small and statistically insignificant (Table E.4).

Datum	Points	Max	Min	Average	STD
One Tree Point 1964	51	-0.145	-0.410	-0.242	0.063
Auckland 1946	137	-0.309	-0.651	-0.491	0.068
Moturiki 1953	258	-0.161	-0.517	-0.309	0.062
Gisborne 1926	61	-0.424	-0.690	-0.578	0.087
Taranaki 1970	70	-0.318	-0.590	-0.450	0.067
Napier 1962	54	-0.108	-0.461	-0.298	0.070
Wellington 1953	78	-0.415	-0.608	-0.503	0.039
Nelson 1955	111	-0.020	-0.430	-0.252	0.082
Lyttelton 1937	251	+0.019	-0.609	-0.343	0.097
Dunedin 1958	73	-0.142	-0.721	-0.484	0.164
Dunedin – Bluff 1960	181	-0.008	-0.572	-0.255	0.077
Bluff 1955	92	-0.200	-0.463	-0.375	0.051
Stewart Island 1977	5	-0.236	-0.589	-0.395	0.116
All Data	1422	+0.019	-0.721	-0.361	0.127
All Data, Zero Datum Average	1422	+0.362	-0.317	0.000	0.081

Table 6.3 Descriptive statistics of the comparison of the second geoid with GPS-levelling points on the 13 vertical datums (metres)

6.5.4 Third geoid and unified vertical datum

To confirm that the iterative solution had converged, the procedure was repeated for a third time. Again the effect of the total datum offset was computed using Equation (6.11) and this total correction was then added to the *original* gravity anomalies. The same quasigeoid computation procedure was again repeated to give a third quasigeoid. Like before, this was then compared with the GPS-levelling observations to estimate the datum offsets given in Table 6.4. The differences

between the second and third quasigeoid computed offsets (Tables 6.3 and 6.4) are very small and statistically insignificant (Table E.5).

Datum	Points	Max	Min	Average	STD
One Tree Point 1964	51	-0.145	-0.411	-0.242	0.063
Auckland 1946	137	-0.309	-0.651	-0.491	0.068
Moturiki 1953	258	-0.161	-0.517	-0.309	0.062
Gisborne 1926	61	-0.424	-0.690	-0.578	0.087
Taranaki 1970	70	-0.318	-0.590	-0.450	0.067
Napier 1962	54	-0.109	-0.461	-0.298	0.070
Wellington 1953	78	-0.415	-0.608	-0.503	0.039
Nelson 1955	111	-0.020	-0.430	-0.252	0.082
Lyttelton 1937	251	+0.019	-0.610	-0.343	0.097
Dunedin 1958	73	-0.141	-0.721	-0.484	0.164
Dunedin – Bluff 1960	181	-0.009	-0.572	-0.255	0.077
Bluff 1955	92	-0.200	-0.463	-0.376	0.051
Stewart Island 1977	5	-0.236	-0.589	-0.395	0.116
All Data	1422	+0.019	-0.721	-0.361	0.127
All Data, Zero Datum Average	1422	+0.362	-0.317	0.000	0.081

Table 6.4 Descriptive statistics of the comparison of the third quasigeoid with GPS-levelling points on the 13 LVDs (metres)

From	To	Third quasigeoid		Precise levelling		Offsets Agree?
		Offset	95% CI	Offset	95% CI	
Auckland	One Tree Point	-0.249	± 0.021	-0.206	± 0.139	Yes
Auckland	Moturiki	-0.182	± 0.014	-0.070	± 0.139	Yes
Gisborne	Moturiki	-0.269	± 0.023	-0.075	± 0.139	No
Gisborne	Napier	-0.280	± 0.029	-0.166	± 0.139	Yes
Moturiki	Napier	-0.011	± 0.020	-0.099	± 0.139	Yes
Taranaki	Napier	-0.152	± 0.025	-0.046	± 0.139	Yes
Taranaki	Wellington	0.053	± 0.018	0.147	± 0.139	Yes
Taranaki	Moturiki	-0.141	± 0.018	-0.162	± 0.139	Yes
Napier	Wellington	0.205	± 0.021	0.237	± 0.139	Yes
Nelson	Lyttelton	0.091	± 0.019	-0.027	± 0.139	Yes
Lyttelton	Dunedin	0.141	± 0.040	-0.071	± 0.139	No
Dunedin - Bluff	Dunedin	0.229	± 0.040	-0.019	± 0.139	No
Dunedin - Bluff	Bluff	0.121	± 0.015	-0.001	± 0.139	Yes

Table 6.5 Summary of comparison between third quasigeoid and observed precise levelling offsets, full analysis is in Table E.6 (95% CI, Student t distribution, metres)

The computed offsets were then compared with the observed differences at the junction points of the precise levelling lines (cf. Table 2.3, Figures 2.4 and 2.5). The results of this comparison are summarised in Table 6.5 (the full analysis is in Table E.5). In concurrence with the *a priori* geoid, it was found that ten of the 13 observed offsets agreed with the computed values.

Table 6.6 is included for comparative purposes. It shows the offsets computed from the three successive quasigeoid models. It shows conclusively that the computed offsets have converged.

Vertical Datum	***a priori***	**Second**	**Third**
One Tree Point 1964	-0.245	-0.242	-0.242
Auckland 1946	-0.497	-0.491	-0.491
Moturiki 1953	-0.316	-0.309	-0.309
Gisborne 1926	-0.585	-0.578	-0.578
Taranaki 1970	-0.457	-0.450	-0.450
Napier 1962	-0.304	-0.298	-0.298
Wellington 1953	-0.509	-0.503	-0.503
Nelson 1955	-0.257	-0.252	-0.252
Lyttelton 1937	-0.350	-0.343	-0.343
Dunedin 1958	-0.491	-0.484	-0.484
Dunedin – Bluff 1960	-0.261	-0.255	-0.255
Bluff 1955	-0.380	-0.375	-0.376
Stewart Island 1977	-0.398	-0.395	-0.395

Table 6.6 Datum offsets computed from successive quasigeoid models (metres)

The converged gravimetric quasigeoid solution (Table 6.4) represents a surface that has been corrected for the biases introduced as a result of the input data (i.e., gravity anomalies) being reduced in terms of offset vertical datums. For this reason, the converged quasigeoid solution can be used as a transformation surface from the reference ellipsoid (in this case GRS80) to each of the local vertical datums when combined with the respective datum offset (Table 6.7). For example, an ellipsoidal height can be transformed to its normal-orthometric equivalent in terms of LVD "*a*" using:

$$H_a^{N-O} = h + \zeta + o_a \tag{6.16}$$

Datum	Offset (o)	STD
One Tree Point 1964	-0.24	0.06
Auckland 1946	-0.49	0.07
Moturiki 1953	-0.31	0.06
Gisborne 1926	-0.58	0.09
Taranaki 1970	-0.45	0.07
Napier 1962	-0.30	0.07
Wellington 1953	-0.50	0.04
Nelson 1955	-0.25	0.08
Lyttelton 1937	-0.34	0.10
Dunedin 1958	-0.48	0.16
Dunedin – Bluff 1960	-0.26	0.08
Bluff 1955	-0.38	0.05
Stewart Island 1977	-0.40	0.12

Table 6.7 Final LVD offsets from NZ quasigeoid and standard deviations (metres)

In this sense, it can be said that the NZ vertical datums have been unified.

6.6 Summary

This Chapter has discussed the practicalities of, and issues related to, the unification of vertical datums in NZ. It was shown that combining gravity anomalies that have been reduced to different vertical datums introduces a bias when they are used to compute a gravimetric quasigeoid. Similarly, the unification of vertical datums using ellipsoidal heights can be inhibited if the normal-orthometric heights are in terms of different datums. Two existing techniques of datum unification were presented that used geopotential numbers and a gravimetric geoid respectively. Although both approaches have been implemented, it was noted that they do not allow for the different vertical datums being offset for each other. The GBVP approach was then described. This method solves for the biases that occur between vertical datums, it relies on the datum offset being the only systematic error source and that all the other biases have been corrected for. This approach has not been used to practically unify datums before. The new iterative quasigeoid computation scheme was then described. It uses a datum offset correction function to iteratively modify the input gravity anomalies used in the gravimetric geoid approach to datum unification. The iterative approach was then successfully implemented over NZ to produce a gravimetric quasigeoid that can be used to unify the 13 disparate LVDs.

7 CONCLUSIONS AND RECOMMENDATIONS

7.1 A new vertical datum for NZ

The limitations of the current height NZ height systems and vertical datums were described in Chapter 2. It has been the aim of this study to unify these 13 disparate vertical datums and to propose a modernised vertical reference system for NZ based on the iterative quasigeoid model computed in Section 6.5.

7.1.1 Height system

NZ currently uses the normal-orthometric height as its authoritative height system (Section 2.4.2). Because gravity observations have not been made at many precise levelling benchmarks (and none is likely to be observed in the foreseeable future) the retention of the normal-orthometric height system is recommended. It is not possible to implement Heck's (2003a) rigorous normal-orthometric correction (NOC) (Equation 2.16) because the azimuth and position of the intermediate precise levelling setups are not known. The approximate NZ NOC formula (Equation 2.19) could be updated from the GRS67 reference field to GRS80, however the difference between the two formulae is very small and can be considered to be only a technical change (as opposed to a change of practical significance) to reflect the use of GRS80 in NZGD2000 (cf. Section 2.4.7).

The official geocentric geodetic datum for NZ, NZGD2000, is defined in terms of the GRS80 reference ellipsoid (ITRF96, epoch 1 January 2000, Section 2.4.7). Hence ellipsoidal heights (in terms of GRS80) are implicitly defined as the authoritative 'geometric" height system. Since these heights are "compatible" with existing GNSS technology (and there is no other practical alternative), the continued use of GRS80 ellipsoidal heights (for geometric heighting) is recommended.

NZ did not have a national quasigeoid available to transform heights between the 13 normal-orthometric levelling datums and NZGD2000. There is a pressing need for such a quasigeoid to be published so that GNSS technology (and NZGD2000) can be effectively used in NZ with the 13 LVDs (Section 2.6). The work in this thesis has now rectified this deficiency.

7.1.2 Vertical datum

A national NZ vertical datum can be defined using the gravimetric quasigeoid computed in Section 6.5 as its reference surface. The calculated datum offsets (Table 6.4) can then be used with the quasigeoid to convert the LVD normal-orthometric heights to NZGD2000 (GRS80) ellipsoidal heights (and vice versa).

This approach retains the existing LVDs for "conventional" heighting applications and also enables the use of GNSS technology to derive gravity-related heights in NZ (Section 2.6). It is also very similar to the method that is being implemented in Canada (Section 2.5.3).

The use of a quasigeoid to define the national vertical datum is different to the "conventional" method which fixes the height/potential at one or more points and then uses a least-squares adjustment to combine precisely-levelled height differences (cf. Section 2.3.1). The precise-levelling adjustment approach to datum definition was not used for the new NZ vertical datum because it would not give a national coverage, is not compatible with GNSS/NZGD2000 heights, and is expensive to maintain (cf. Section 2.4.7).

7.1.3 Implementation of the new vertical datum

The new NZ vertical datum can be practically implemented by LINZ with relative ease. The LINZ geodetic database (www.linz.govt.nz/gdb) currently publishes ellipsoidal heights (in terms of NZGD2000) of all points where they are available. Similarly, for marks where normal-orthometric heights have been observed, these heights are also published in terms of one (or more) LVD. To implement the new datum it is only necessary to embed the gravimetric quasigeoid (and offset) to provide the conversion between the different LVDs and the NZGD2000 (1 January 2000) ellipsoidal heights.

7.1.4 Longevity of the new vertical datum

The geoid model computed in Section 6.5 is the best available at the end of 2006. It is likely that with the imminent release of the new EGM07/8 model (in mid 2008) and the new GGMs that will result from the GRACE, upcoming GOCE gradiometry

satellite missions (Section A.3.3) that a better regional quasigeoid (and hence vertical datum) will be possible in the future. The timing for a new quasigeoid can not be specified here because it depends on the availability of new global models, however, given that GOCE is scheduled for launch in 2008, it could be expected that results will be available from 2008/9.

Another motivating factor for revising the vertical datum in the future relates to the IAG Inter-Commission Project (ICP) 1.2 on vertical reference frames. If the recommendations of the ICP are adopted by the IAG in 2007 and they recommend a different W_0 to that which is used in the GGM02S GGM (this GGM was used as the basis for the NZ geoid) then it may be necessary to update the vertical datum to reflect this change.

When the decision is made (by LINZ) to update the NZ vertical datum, this should only be done if it results in a "significant" improvement to the users of the datum. Nevertheless the proposed vertical datum is a significant improvement on the existing situation in NZ and should be a suitable until the improved GGMs described above are available. If a datum (vertical or otherwise) is updated too frequently there is a risk that users will become confused between the different systems or subjected to additional data migration costs. Similarly, if datums are updated for no perceivable benefit to its users, it is likely that the change to a new datum will be resisted (cf. Section 2.5.5; Cross *et al*., 1987).

The NZGD2000 is a semi-dynamic datum in that its observations are "corrected" for the effects of horizontal deformation using a deformation model from the time of observation to a reference epoch (cf. Section 2.4.8). At present, no vertical deformation model exists for NZ, however with the increased promulgation of continuous GNSS receivers throughout NZ [e.g., PositioNZ (www.linz.govt.nz/positionz); GeoNet (www.geonet.org.nz); Section 2.4.6] it is possible that such a model could be developed in the future. If a model does become available, then the practicality of a time-varying vertical datum that accounts for the effects of deformation should be investigated as a method of extending the longevity of NZ vertical datums.

7.2 Summary of research

This objective of this study was to unify the 13 disparate LVDs that are currently used in NZ and to propose a modernised national vertical reference system in NZ. Before defining a new national vertical datum, it was important to assess and compare the different height systems and vertical datums that are currently used in NZ and those that could be used in the future. Chapter 2 presented the different height systems (which depend on the way that the Earth's gravity field is treated). It also discussed the different ways that vertical datums can be defined and identified the ways that they can be distorted.

Importantly, to provide an international context, the height systems and vertical datums of five different jurisdictions were also evaluated with respect to NZ. The Chapter concluded with a proposal for a NZ vertical datum that retained the existing normal-orthometric LVDs and uses a gravimetric quasigeoid to model the difference between them and the NZGD2000 ellipsoidal heights. Therefore, the thesis was mainly concerned with the development of the gravimetric quasigeoid, the effect of the offset LVDs on its constituent data sets and their use in the iterative quasigeoid method of vertical datum unification.

The different data sets and their preparation for use in the quasigeoid computations were described in Chapter 3. A number of GGMs were evaluated (including some merged models created specifically for this study) against GPS-levelling, terrestrial gravity and vertical deflection datasets. These comparisons concluded that the GGM02S/EGM96 merged GGM was the "best" global geopotential model for the NZ region. The terrestrial gravity anomalies from GNS Science were re-reduced to ensure that they were in terms of a consistent gravity datum. A significant aspect of the data preparation involved the crossover adjustment of the marine ship-track gravity observations. This was completed under contract by *Intrepid Geophysics* and then combined with a grid of satellite altimetry derived gravity anomalies using LSC. The 56-metre DEM and the 1422 GPS-levelling observations were also presented.

Chapter 4 discussed the different topographic reductions that are applied to gravity observations before geoid computation by Stokes's formula. Three techniques of computing TCs were compared, these were: planar TCs by FFT and prism integration, and spherical TCs using Hammer charts. It was concluded that while the

Hammer TCs were theoretically better, their low spatial density meant that they were inappropriate for use in a national quasigeoid. The FFT TCs were unstable in areas of steep terrain, while the prism TCs (which took much longer to compute) appeared to give better results.

Because the gravity observations are spaced irregularly, it was necessary to "reconstruct" mean gravity anomalies using a DEM for the evaluation of Stokes's formula by FFT. A number of different gravity anomaly and TC combinations were compared to determine the best fit to the NZ GPS-levelling observations. It was concluded that gridding refined Bouguer anomalies (that had been reduced with the prism TCs at the DEM resolution) gave the optimum interpolation solution. This agreed with similar experiments performed in Canada (Janák and Vaníček, 2005). Based on the results of the TC and gridding comparisons the prism integration computed TCs were selected for use in the NZ quasigeoid computations.

The physical computation of gravimetric quasigeoids using Stokes function was discussed in Chapter 5. This involved the comparison of five deterministic modifications to Stokes's integration kernel that all aim at reducing the truncation error associated with using a limited integration radius and that have different filtering properties. These comparisons involved evaluating each modification with a range of integration caps and modification degrees and then evaluating them against the standard deviation and offset fit to the GPS-levelling observations (after accounting for the offsets). This analysis showed a numerical instability in the VK kernel, but the FEO modification was optimum for NZ when combined with a cap of $\psi_0 = 1.5°$ and a modification degree of $L = 40$.

The unification of vertical datums was addressed in Chapter 6. Three existing techniques of achieving datum unification were presented (these were geopotential numbers, gravimetric geoids and solving the GBVP). These methods did not adequately deal with the effect caused by datum offsets in the quasigeoid computation datasets in NZ. To remedy this limitation, a new process that modifies the gravimetric quasigeoid approach was proposed. This process accounts for datum offsets by using an initial quasigeoid solution to estimate the offsets and then corrects the source observations for its effect. The quasigeoid is then subsequently recomputed iteratively to produce a model that is not biased by the offset datums.

This new approach was then successfully implemented over NZ to give a quasigeoid that can be used to unify the 13 LVDs. Most importantly, these results agreed with the offsets computed at the junction points of the precise levelling LVDs.

A new vertical datum for NZ was then proposed in Section 7.1. This new datum will enable the unification of the 13 LVDs through the gravimetric quasigeoid model and an additional offset per LVD. This will allow users of the NZ vertical datum to convert heights between the official geometric and normal-orthometric height systems as needed. The production of this unified vertical datum provides NZ with a modern height system.

7.3 Recommendations for future work

The computed gravimetric quasigeoid and the new national vertical datum proposed for NZ in Section 7.1 are likely to meet the needs of a majority of users at the current time (cf. Pearse, 2001). A number of issues were raised during this study that warrant further investigation if a better quasigeoid and vertical datum are desired for the future, these are described below (in addition to the points raised in Section 7.1.4).

The proposed vertical datum only uses a constant offset between the geoid and each LVD. It is possible that due to the way that the LVDs are defined (i.e. MSL at a single tide-gauge) that the use of an offset is not the best approach. Future investigations should evaluate the use of inclined planes or even polynomial surfaces to optimise the transformation between gravimetric and geometric height systems. An inclined plane could be of benefit for the Dunedin LVD where the standard deviation of the GPS-levelling fit was much larger than that seen for the other datums (Table 6.3). Caution needs to be taken with polynomial surfaces because they effectively model and absorb the difference between the LVD and quasigeoid and so, inherently produce very good fits (cf. Featherstone, 2006).

Additional GPS-levelling observations should be acquired where possible (cf. Section 3.8). If more observations are available to evaluate the datum offsets and the quasigeoid fit then a better overall vertical datum will be possible. The most beneficial locations for additional GPS-levelling points are in mountainous areas (where the quasigeoid is harder to model) and in regions/LVDs where few points

currently exist (e.g., the East Cape of the North Island and the West Coast of the South Island, Figure 3.7).

The computation of the TCs is an area that could be re-visited for the evaluation of a future gravimetric quasigeoid. The use of a higher-resolution DEM in the computations would provide more topographic information in the immediate vicinity of the gravity observation, as well as a better representation of the topography further away. The topography near to the gravimeter has the biggest effect on the TC (and also DC, Section 4.5), so if a DEM with a 20 metre resolution was used (instead of the current 56 m) this may improve the quality of the TC (and DC) when combined with the gravity reconstruction process (Section 4.11.2). The use of spherical (or global) TCs (Section 4.4) should be trialled as they are conceptually more realistic than the planar approximation.

The effect of marine bathymetry on the reduction of the ship-track gravity observations should be investigated since it is known that in parts of the NZ coast it is very steep (e.g. Fiordland, Kaikoura coast).

REFERENCES

Ádám, J., Augath, W., Brouwer, F., Engelhardt, G., Harsson, B.G., Ihde, J., Ineichen, D., Lang, H., Luthardt, J., Sacher, M., Schlüter, W., Springer, T. and Wöppelmann, G. (2000) Status and development of the European height systems, in: Schwarz, K.-P. (Ed.) *Geodesy Beyond 2000 – The Challenges of the First Decade*, Springer, Berlin, Germany, pp. 55-60.

Ågren, J. (2004) The analytical continuation bias in geoid determination using potential coefficients and terrestrial gravity data, *Journal of Geodesy*, Vol. 78, No. 4-5, pp. 314-332, doi: 10.1007/s00190-004-0395-0.

Akima, H. (1978) A method of bivariate interpolation and smooth surface fitting for irregularly distributed data points, *ACM Transactions on Mathematical Software*, Vol. 4, No. 2, pp. 148-159.

Allister, N.A. and Featherstone, W.E. (2001) Estimation of Helmert orthometric heights using digital barcode levelling, observed gravity and topographic mass-density data over part of the Darling Scarp, Western Australia, *Geomatics Research Australasia*, No. 75, pp. 25-52.

Amos, M.J. (2006) A new vertical datum for New Zealand, *Survey Quarterly*, No. 46, pp. 18-20.

Amos, M.J. and Featherstone, W.E. (2003a) Preparations for a new gravimetric geoid model of New Zealand, and some preliminary results, *New Zealand Surveyor*, No. 293, pp. 3-14.

Amos, M.J. and Featherstone, W.E. (2003b) Comparisons of recent global geopotential models with terrestrial gravity field observations over New Zealand and Australia, *Geomatics Research Australasia*, No. 79, pp. 1-20.

Amos, M.J. and Featherstone, W.E. (2003c) Progress towards a gravimetric geoid for New Zealand and a single national vertical datum, in Tziavos, I.N. (Ed.) *Gravity and Geoid 2002*, Ziti Editions, Thessaloniki, Greece, pp. 395-400.

Amos, M.J. and Featherstone, W.E. (2004) *A comparison of gridding techniques for terrestrial gravity observations in New Zealand*, poster presented to the Gravity, Geoid and Space Missions Symposium 2004, Oporto, Portugal, 30 August – 1 September, URL: http://www.fc.up.pt/ggsm2004/index.html.

Amos, M.J., Featherstone, W.E. and Brett, J. (2005) Crossover adjustment of New Zealand marine gravity data, and comparisons with satellite altimetry and global geopotential models, in: Jekeli, C., Bastos, L. and Fernandes, J. (Eds.) *Gravity, Geoid and Space Missions*, Springer, Berlin, Germany, pp. 266-271.

Andersen, O.B. and Knudsen, P. (1998) Global marine gravity field from the ERS-1 and GEOSAT geodetic mission altimetry, *Journal of Geophysical Research*, Vol. 103, No. C4, pp. 8129-8137, doi: 10.1029/97JC02198.

Andersen, O.B. and Knudsen, P. (2000) The role of satellite altimetry in gravity field modelling in coastal areas, *Physics and Chemistry of the Earth*, Vol. 25, No. 1, pp. 17-24, doi: 10.1016/S1464-1895(00)00004-1.

Andersen, O.B., Knudsen, P. and Trimmer, R. (2005) Improved high resolution altimetric gravity field mapping (KMS2002 global marine gravity field), in: Sansò, F. (Ed.) *A Window on the Future of Geodesy*, Springer, Berlin, Germany, pp. 326-331.

Anderson, H. and Webb, T. (1994) New Zealand seismicity: patterns revealed by the upgraded national seismograph network, *New Zealand Journal of Geology and Geophysics*, Vol. 37, No. 4, pp. 477-493.

Arabelos, D. and Tscherning, C.C. (2001) Improvements in height datum transfer expected from the GOCE mission, *Journal of Geodesy*, Vol. 75, No. 5-6, pp. 308-312, doi: 10.1007/s001900100187.

Bajracharya, S. (2003) Terrain effects on geoid determination, *UCGE Reports 20181*, Department of Geomatics Engineering, University of Calgary, Alberta, Canada, 114 pp.

Bajracharya, S. and Sideris, M.G. (2005a) Density and gravity interpolation effects on Helmert geoid determination, *Geodezja I Kartografia, Geodesy and Cartography*, Vol. 54, No. 2, pp. 51-68.

Bajracharya, S. and Sideris, M.G. (2005b) Terrain-aliasing effects on gravimetric geoid determination, *Geodezja I Kartografia, Geodesy and Cartography*, Vol. 54, No. 1, pp. 3-16.

Balmino, G., Perosanz, F., Rummel, R., Sneeuw, N. and Sünkel, H. (1999) CHAMP, GRACE and GOCE: mission concepts and simulations, *Bolletino di Geofisica Teorica e Applicata*, Vol. 40, No. 3-4, pp. 555-563.

Beanland, S., Blick, G.H. and Darby, D.J. (1990) Normal faulting in a back-arc basin: geological and geodetic characteristics of the 1987 Edgecumbe earthquake, New Zealand, *Journal of Geophysical Research*, Vol. 95, No. B4, pp. 4693-4707.

Beavan, R.J. (1998) Revised horizontal velocity model for the New Zealand geodetic datum, *Client Report 43865B*, Institute of Geological and Nuclear Sciences, Lower Hutt, New Zealand 46 pp.

Beavan, R.J. and Haines, A.J. (1997) Velocity map of New Zealand for provisional 1997/98 dynamic datum, *Client Report 42793D.10*, Institute of Geological and Nuclear Sciences, Lower Hutt, Wellington, 45 pp.

Beavan, R.J., Matheson, D.W., Denys, P., Denham, M., Herring, T., Hager, B. and Molnar, P. (2004) A vertical deformation profile across the Southern Alps, New Zealand, from 3.5 years of continuous GPS data, in: van Dam, T. and Francis, O. (Eds.) *Proceedings of the Cahiers du Centre Européen de Géodynamique et de Séismologie workshop: The State of GPS Vertical Positioning Precision: Separation of Earth Processes by Space Geodesy*, Luxembourg, No. 23, pp. 111-123.

Begg, J.G. and McSaveney M.J. (2005) Wairarapa fault rupture – vertical deformation in 1855 and a history of similar events from Turakirae Head, in Langridge R., Townend, J. and Jones, A. (Eds.), *The 1855 Wairarapa Earthquake Symposium Proceedings*, Greater Wellington Regional Council, Wellington, New Zealand, pp. 21-30.

Bell, R.G., Goring, D.G. and de Lange, W.P. (2000) Sea-level change and storm surges in the context of climate change, *IPENZ Transactions*, Vol. 27, No. 1, pp. 1-10.

Berryman, K. (1984) Late quaternary tectonics in New Zealand, in Walcot, R.I. (Ed.), *An Introduction to the Recent Crustal Movements of New Zealand*, Royal Society Miscellaneous Series 7, Royal Society of New Zealand, Wellington, New Zealand, pp. 91-107.

Berryman, K., Marden, M., Eden, D., Mazengarb, C., Ota, Y. and Moriya, I. (2000) Tectonic and paleoclimatic significance of Quarterny river terraces of the Waipaoa River, east coast, North Island, New Zealand, *New Zealand Journal of Geology and Geophysics*, Vol. 43, No. 2, pp. 229-245.

Bessel, F.W. (1837) Über den einfluss der unregelmaessigkeiten der figure der erdw auf geodätische arbeiten und ihre vergleichung mit den astronomischen bestimmungen, *Astronomische Nachrichten*, Vol. 14, pp. 329-331.

Beutler, G., Rothacher, M., Schaer, S., Springer, T.A., Kouba, J. and Neilan, R. (1999) An interdisciplinary service in support of Earth sciences, *Advances in Space Research*, Vol. 23, No. 4, pp. 631-635.

Bevin, A.J., Otway, P.M. and Wood, P.R. (1984) Geodetic monitoring of crustal deformation in New Zealand, in Walcott, R.I. (Ed.), *An Introduction to the Recent Crustal Movements of New Zealand*, Royal Society Miscellaneous Series 7, Royal Society of New Zealand, Wellington, New Zealand, pp. 13-60.

Bevis, M., Scherer, W. and Merrifield, M. (2002) Technical issues and recommendations related to the installation of continuous GPS stations at tide gauges, *Marine Geodesy*, Vol. 25, No. 1-2, pp. 87-99, doi: 10.1080/014904102753516750.

Biancale, R., Balmino, G., Lemoine, J.M., Marty, J.C., Moynot, B., Barlier, F., Exertier, P., Laurain, O., Gegout, P., Schwintzer, P., Reigber, Ch., Bode, A., König, R., Massmann, F.H., Raimondo, J.C., Schmidt, R. and Zhu, S.Y. (2000) A new global Earth's gravity field model from satellite orbit perturbations: GRIM5-S1, *Geophysical Research Letters,* Vol. 27, No. 22, pp. 3611-3615, doi: 10.1029/2000GL011721, [coefficients available from www.gfz-potsdam.de/pb1/pg3/grim/grim5_e.html].

Bjerhammar, A. (1987) Discrete physical geodesy, *Report 380*, Department of Geodetic Science and Surveying, Ohio State University, Columbus, USA, 109 pp.

Blais, J.A.R. and Ferland, R. (1984) Optimization in gravimetric terrain corrections, *Canadian Journal of Earth Sciences*, Vol. 21, No. 5, pp. 505-515.

Blick, G.H. (2003) Implementation and development of NZGD2000, *New Zealand Surveyor*, No. 293, pp. 15-19.

Blick, G.H., Amos, M.J. and Grant, D.B. (2001) Preferred option for development of a national vertical reference system, *OSG Technical Report 16*, Land Information New Zealand, Wellington, New Zealand, 10 pp., available from: www.linz.govt.nz/surveypublications.

Blick, G.H., Mole, D., Pearse, M.B. and Wallen, B. (1997) Land Information New Zealand role in and needs for sea level data, *Immediate Report 97/17*, Land Information New Zealand, Wellington, New Zealand, 26 pp., available from: www.linz.govt.nz/surveypublications.

Bomford, G. (1980) *Geodesy*, Fourth Edition, Oxford University Press, Oxford, United Kingdom, 855 pp.

Boucher, C., Altamimi, Z. and Sillard, P. (1998) Results and analysis of the ITRF96, *IERS Technical Note 24*, Observatoire de Paris, Paris, France, 166 pp.

Brett, J. (2004) Marine gravity crossover adjustment for New Zealand, *Report to Land Information New Zealand*, Intrepid Geophysics, Melbourne, Australia, 24 pp.

Burša, M. (1995) Primary and derived parameters of common relevance of astronomy, geodesy and geodynamics, *Earth, Moon and Planets*, Vol. 69, No. 1, pp. 51-63, doi: 10.1007/BF00627769.

Burša, M., Kouba, J., Raděj, K., Vatrt, V., Vojtíšková, M. and True, S. (1999a) Determination of the geopotential at the tide gauge defining the North American Vertical Datum 1988 (NAVD88), *Geomatica*, Vol. 53, No. 3, pp. 291-296.

Burša, M,. Kouba, J., Kumar, M., Müller, A., Raděj, K., True, S.A., Vatrt, V. and Vojtíšková, M. (1999b) Geoidal geopotential and world height system, *Studia Geophysica et Geodaetica*, Vol. 43, No. 4, pp. 327-337, doi: 10.1023/a:1023273416512.

Burša, M., Kouba, J., Müller, A., Raděj, K., True, S.A., Vatrt, V. and Vojtíšková, M. (2001) Determination of geopotential differences between local vertical datums and realization of a world height system, *Studia Geophysica et Geodaetica*, Vol. 45, No. 2, pp. 127-132, doi: 10.1023/A:1021860126850.

Burša, M., Kenyon, S., Kouba, J., Raděj, K., Vatrt, V., Vojtíšková, M., Šimek, J. (2002) World height system specified by geopotential at tide gauge stations, in: Drewes, H., Dodson, A., Fortes, L.P.S., Sánchez, L. and Sandoval, P. (Eds.), *Vertical Reference Systems*, Springer, Berlin, Germany, pp. 291-296.

Burša, M., Kenyon, S., Kouba, J., Šíma, Z., Vatrt, V. and Vojtíšková, M. (2004) A global vertical reference frame based on four regional vertical datums, *Studia Geophysica et Geodaetica*, Vol. 48, No. 3, pp. 493-502, doi: 10.1023/b:sgeg.0000037468.48585.e6.

Burša, M., Kenyon, S., Kouba, J., Šíma, Z., Vatrt, V., Vítek, V. and Vojtíšková, M. (2007) The geopotential value W_0 for specifying the relativistic atomic time scale and a global vertical reference system, *Journal of Geodesy*, Vol. 81, No. 2, pp. 103-110, doi: 10.1007/s00190-006-0091-3.

Cartwright, D.E. and Crease, J. (1963) A comparison of the geodetic reference levels of England and France by means of the sea surface, *Proceedings of the Royal Society of London, Series A Mathematical and physical Sciences*, Vol. 272, No. 1355, pp. 558-580.

CGRSC (2004) *Report to the Council on Geomatics (CGOG) on the modernization of the Canadian height reference system*, prepared by Canadian Geodetic Reference System Committee, Ottawa, Canada, 25 pp., available from: http://www.geod.nrcan.gc.ca/hm/pdf/modern_e.pdf.

Church, J.A. and White, N.J. (2006) A 20th century acceleration in global sea-level rise, *Geophysical Research Letters*, Vol. 33, L01602, doi: 10.1029/2005GL024826.

Claessens, S.J. (2006) Solutions to ellipsoidal boundary value problems for gravity field modelling, *PhD thesis*, Curtin University of Technology, Perth, Australia, 220 pp.

Cole, J.W. (1990) Structural control and origin of volcanism in the Taupo volcanic zone, New Zealand, *Bulletin of Vulcanology*, Vol. 53, No. 6, pp. 445-459.

Colombo, O.L. (1980) Transoceanic vertical datum connections, in *Proceedings of the 2nd International Symposium on Problems Related to the Redefinition of North American Vertical Geodetic Networks*, The Canadian Institute of Surveying, Ottawa.

Cooper, A.F. and Norris, R.J. (1995) Displacement on the alpine fault at Haast River, South Westland, New Zealand, *New Zealand Journal of Geology and Geophysics*, Vol. 38, No. 4, pp. 509-514.

Crook, C. and Pearse, M.B. (2001) Development of transformation parameters from NZGD49 to NZGD2000, *OSG Technical Report 13*, Land Information New Zealand, Wellington, New Zealand, 22 pp., available from: www.linz.govt.nz/surveypublications.

Cross, P.A., Hannah, J., Hradilek, L., Kelm, R., Mäkinen, J. Merry, C.L., Sjöberg, L.E., Steeves, R.R., Vaníček, P. and Zolkoski, D.B. (1987) Four-dimensional geodetic positioning, *manuscripta geodaetica*, Vol. 12, No. 3, pp. 147-222.

Deng, X.L. and Featherstone, W.E. (2006) A coastal retracking system for satellite radar altimeter waveforms: application to ERS-2 around Australia, *Journal of Geophysical Research*, Vol. 111, C06012, doi: 10.1029/2005JC003039.

Deng, X.L., Featherstone, W.E., Hwang, C. and Berry, P.A.M. (2002) Estimation of contamination of ERS-2 and Poseidon satellite radar altimetry close to the coasts of Australia, *Marine Geodesy*, Vol. 25, No. 4, pp. 249-271, doi: 10.1080/01490410214990.

Denker, H., Behrand, D. and Torge, W. (1996) The European gravimetric quasigeoid EGG95, in: Sansò, F. (Ed.) *New geoids of the world*, International Geoid Service Bulletin, 4, Milano, Italy, pp. 3-12.

Dennis, M.L. and Featherstone, W.E. (2003) Evaluation of orthometric and related height systems using a simulated mountain gravity field, in Tziavos I.N. (Ed.) *Gravity and Geoid 2002*, Ziti Editions, Thessaloniki, Greece, pp. 389-394.

de Mets, C., Gordon, G., Argus, D.F. and Stein, S. (1994) Effect of recent revisions to the geomagnetic reversal time scale on estimates of current plate motions, *Geophysical Research Letters*, Vol. 21, pp. 2191-2194.

de Witte, L. (1967) Truncation errors in the Stokes and Vening-Meinesz formulae for different order spherical harmonic gravity terms, *Geophysical Journal of the Royal Astronomical Society*, Vol. 12, pp. 449-464.

DoSLI (1989) *Geodetic Survey Branch Manual of Instruction*, Department of Survey and Land Information, Wellington, New Zealand, 117 pp.

Douglas, B.C. (1991) Global sea level rise, *Journal of Geophysical Research*, Vol. 96, No. C4, pp. 6981-6992.

Drinkwater, M.R., Floberghagen, R., Haagmans, R., Muzi, D. and Popescu, A. (2003) GOCE: ESA's first Earth explorer core mission, in: Beutler, G.B., Drinkwater, M.R., Rummel, R. and von Steiger, R. (Eds.), *Earth Gravity Field from Space – from Sensors to Earth Sciences*, Space Sciences Series of ISSI, Vol. 18, pp. 419-432.

Ekman, M. (1989) Impacts of geodynamic phenomena on systems for heights and gravity, *Bulletin Géodésique*, Vol. 63, No. 3, pp. 281-296, doi: 1007/BF02520477.

Ekman, M. (1995) What is the geoid? in Vermeer, M. (Ed.) *Coordinate Systems, GPS and the Geoid*, Reports of the Finnish Geodetic Institute, Vol. 95, No. 4, Helsinki, Finland, pp. 49-51.

Ekman, M. (1996) A consistent map of the postglacial uplift of Fennoscandia, *Terra Nova*, Vol. 8, No. 2, pp. 158-165.

Ellmann, A. (2005) Two deterministic and three stochastic modifications of Stokes's formula: a case study for the Baltic countries, *Journal of Geodesy*, Vol. 79, No. 1, pp. 11-23, doi: 10.1007/s00190-005-0438-1.

Engels, J., Grafarend, E., Keller, W., Martinec, Z., Sansò, F. and Vaníček, P. (1993) The geoid as an inverse problem to be regularized, in: *Inverse Problems: Principles and Applications in Geophysics, Technology and Medicine*, Anger, G., Gorenflo, R., Jochmann, H., Moritz, H. and Webers, W. (Eds.), Akademie Verlag, Berlin, Germany, pp. 122-167.

ESA (2006) ESA's gravity mission GOCE, *Publication BR-209*, June 2006 Revision, European Space Agency, Noodwijk, The Netherlands, 18 pp., available at: http://esamultimedia.esa.int/docs/BR209web.pdf.

EUREF (2006) European Vertical Reference System, EUREF website, URL: www.euref-iag.net, last accessed 6/12/2006.

Evans, J.D. and Featherstone, W.E. (2000) Improved convergence rates for the truncation error in gravimetric geoid determination, *Journal of Geodesy*, Vol. 74, No. 2, pp. 239-248, doi: 10.1007/s001900050282.

Featherstone, W.E. (1992) A GPS controlled gravimetric determination of the geoid of the British Isles, *D. Phil thesis*, Oxford University, Oxford, United Kingdom, 272 pp.

Featherstone, W.E. (1995) On the use of Australian geodetic datums in gravity field determination, *Geomatics Research Australasia*, No. 62, pp. 17-37.

Featherstone, W.E. (1998) Do we need a gravimetric geoid or a model of the base of the Australian Height Datum to transform GPS heights?, *The Australian Surveyor*, Vol. 43, No. 4, pp. 273-280.

Featherstone, W.E. (1999) Tests of two forms of Stokes's integral using a synthetic gravity field based on spherical harmonics, in: *Quo Vadis Geodesia*, Krumm, F. and Schwarze, V. (Eds.), Institute of Geodesy, University of Stuttgart, Stuttgart, Germany, pp. 101-112.

Featherstone, W.E. (2000) Towards the unification of the Australian height datum between mainland and Tasmania using GPS and AUSGeoid98, *Geomatics Research Australasia*, No. 73, pp. 33-54.

Featherstone, W.E. (2001) Absolute and relative testing of gravimetric geoid models using global positioning system and orthometric height data, *Computers and Geosciences*, Vol. 27, No. 7, pp. 807-814, doi: 10.1016/s0098-30040000169-2.

Featherstone, W.E. (2002a) Attempts to unify the Australian height datum between the mainland and Tasmania, in: Drewes, H., Dodson, A., Fortes, L.P.S., Sánchez, L. and Sandoval, P. (Eds.), *Vertical Reference Systems*, Springer, Berlin, Germany, pp. 328-333.

Featherstone, W.E. (2002b) Expected contributions of dedicated satellite gravity field missions to regional geoid computations, *Journal of Geospatial Engineering*, Vol. 4, No. 1, pp. 2-19.

Featherstone, W.E. (2003a) Comparison of different satellite altimeter-derived gravity anomaly grids with ship-borne gravity data around Australia, in: Tziavos, I.N. (Ed.) *Gravity and Geoid 2002*, Ziti Editions, Thessaloniki, Greece, pp. 326-331.

Featherstone, W.E. (2003b) Band-limited kernel modifications for regional geoid determination based on dedicated satellite gravity field missions, in: *Gravity and Geoid 2002*, Tziavos, I.N. (Ed.), Ziti Editions, Thessaloniki, Greece, pp. 341-346.

Featherstone, W.E. (2003c) Software for computing five existing types of deterministically modified integration kernel for gravimetric geoid determination, *Computers and Geosciences*, Vol. 29, No. 2, pp. 183-193, doi: 10.1016/s0098-3004(02)00074-2.

Featherstone, W.E. (2003d) Improvement to long-wavelength Australian gravity anomalies expected from the CHAMP, GRACE and GOCE dedicated satellite gravimetry missions, *Exploration Geophysics*, Vol. 34, No. 1-2, pp. 69-76.

Featherstone, W.E. (2004) Evidence of a north-south trend between AUSGeoid98 and AHD in southwest Australia, *Survey Review*, Vol. 37, No. 291, pp. 334-343.

Featherstone, W.E. (2006) Yet more evidence for a north-south slope in the Australian height datum, *Journal of Spatial Science*, Vol. 52, No. 2, pp. 1-6.

Featherstone, W.E. and Dentith, M.C. (1997) A geodetic approach to gravity reduction for geophysics, *Computers and Geosciences*, Vol. 23, No. 10, pp. 1063-1070, doi: 10.1016/s0098-3004(97)00092-7.

Featherstone, W.E. and Kirby, J.F. (1998) Estimates of the separation between the geoid and the quasigeoid over Australia, *Geomatics Research Australasia*, No. 68, pp. 79-90.

Featherstone, W.E. and Kirby, J.F. (2000) The reduction of aliasing in gravity anomalies and geoid heights using digital terrain data, *Geophysical Journal International*, Vol. 141, No. 1, pp. 204-212, doi: 10.1046/j.1365-246x.2000.00082.x.

Featherstone, W.E. and Kuhn, M. (2006) Height systems and vertical datums: a review in the Australian context, *Journal of Spatial Science*, Vol. 51, No. 1, pp. 21-41.

Featherstone, W.E. and Olliver, J.G. (1994) A new gravimetric determination of the geoid of the British Isles, *Survey Review*, Vol. 32, No. 254, pp. 487-492.

Featherstone, W.E. and Rüeger, J.M. (2000) The importance of using deviations of the vertical in the reduction of terrestrial survey data to a geocentric datum, *Trans-Tasman Surveyor*, Vol. 1, No. 3, pp. 46-61.

Featherstone, W.E. and Sideris, M.G. (1998) Modified kernels in spectral geoid determination: first results from Western Australia, in: Forsberg, R., Feissl, M. and Dietrich, R. (Eds.), *Geodesy on the Move*, Springer, Berlin, pp. 188-193.

Featherstone, W.E. and Sproule, D.M. (2006) Fitting the AUSGeoid98 to the Australian height datum using GPS-levelling and least squares collocation: application of a cross-validation technique, *Survey Review*, Vol. 38, No. 301, pp. 573-582.

Featherstone, W.E., Evans, J.D. and Olliver, J.G. (1998) A Meissl-modified Vaníček and Kleusberg kernel to reduce the truncation error in gravimetric geoid computations, *Journal of Geodesy*, Vol. 72, No. 3, pp. 154-160, doi: 10.1007/s001900050157.

Featherstone, W.E., Kirby, J.F., Kearsley, A.H.W., Gilliland, J.R., Johnston, G.M., Steed, J., Forsberg, R. and Sideris M.G. (2001) The AUSGeoid98 geoid model of Australia: data treatment, computations and comparisons with GPS-levelling data, *Journal of Geodesy*, Vol. 75, No. 5-6, pp. 313-330, doi: 10.1007/s001900100177.

Featherstone, W.E., Holmes, S.A., Kirby, J.F. and Kuhn, M. (2004) Comparison of remove-compute-restore and University of New Brunswick techniques to geoid determination over Australia, and inclusion of Wiener-type filters in reference field contribution, *Journal of Surveying Engineering*, Vol. 130, No. 1, pp. 40-47, doi: 10.1061/(ACSE)0733-9453(2004)130:1(40).

Fei, Z.L. and Sideris, M.G. (2000) A new method for computing the ellipsoidal correction for Stokes's formula, *Journal of Geodesy*, Vol. 74, No. 2, pp. 223-231, doi: 10.1007/s001900050280.

Fei, Z.L. and Sideris, M.G. (2001) Corrections to "A new method for computing the ellipsoidal correction for Stokes's formula", *Journal of Geodesy*, Vol. 74, No. 9, p. 671, doi: 10.1007/s001900000131.

Fjeldskaar, W., Lindholm, C., Dehls, J.F. and Fjeldskaar, I. (2000) Postglacial uplift, neotectonics and seismicity in Fennoscandia, *Quaternary Science Reviews*, Vol. 19, No. 14, pp. 1413-1422, doi: 10.1016/s0277-3791(00)00070-6.

Forsberg, R. (1984) A study of terrain reductions, density anomalies and geophysical inversion methods in gravity field modelling, *Report 355*, Department of

Geodetic Science and Surveying, Ohio State University, Columbus, USA, 129 pp.

Forsberg, R. (1985) Gravity field terrain effect computations by FFT, *Bulletin Géodésique*, Vol. 59, No. 4, pp. 342-360, doi: 10.1007/BF02521068.

Forsberg, R. (1990) A new high-resolution geoid of the Nordic area, in: Rapp, R.H. and Sansò, F. (Eds.) *Determination of the geoid*, Springer, Berlin, Germany, pp. 241-250.

Forsberg, R. (2001) Development of a Nordic cm-geoid – with basics of geoid determination, in: Harsson B.G. (Ed.) *Lecture notes for autumn school organised by the Nordic Geodetic Commission*, Fevik, 28 August – 2 September 2000, Statens kartverk, Hønefoss, Norway.

Forsberg, R. and Featherstone, W.E. (1998) Geoids and cap sizes, in: *Geodesy on the Move*, Forsberg, R., Feissel M. and Dietrich, R. (Eds.), Springer, Berlin, Germany, pp. 194-200.

Forsberg, R. and Tscherning, C.C. (1981) The use of height data in gravity field approximation by collocation, *Journal of Geophysical Research*, Vol. 86, No. B9, pp. 7843-7854.

Förste, C., Flechtner, F., Schmidt, R., Meyer, U., Stubenvoll, R., Barthelmes, F., Bruinsma, S., Lemoine, J.M. and Raimondo, J.C. (2005) A new resolution global gravity field model derived from combination of GRACE and CHAMP mission and altimetry/gravimetry surface gravity data, *Poster presented at EGU General Assembly 2005*, Vienna, Austria [coefficients available from: http://www.gfz-potsdam.de/pb1/op/grace/results].

Förste, C., Flechtner, F., Schmidt, R., König, R., Meyer, U., Stubenvoll, R., Rothacher, M., Barthelmes, F., Neumayer, K.H., Biancale, R., Bruinsma, S. and Lemoine, J.M. (2006) A mean global gravity field model from the combination of satellite mission and altimetry/gravimetry surface gravity data, *Poster presented at EGU General Assembly 2006*, Vienna, Austria [coefficients available from: http://www.gfz-potsdam.de/pb1/op/grace/results].

Fotopoulos, G., Kotsakis, C. and Sideris, M.G. (1999) A new Canadian geoid model in support of leveling by GPS, *Geomatica*, Vol. 53, No. 1, pp. 53-62.

Gachari, M.K. and Olliver, J.G. (1998) A high-resolution gravimetric geoid of East Africa, *Survey Review*, Vol. 34, No. 269, pp. 421-436.

Gauss, C.F. (1828) Bestimmung des breitenunterschiedes zwischen den sternwarten von goettingen und altona durch beobachtungen am ramsdenschen zenithsector, Vanderschoeck und Ruprecht, Goettingen, pp. 48-50.

Gilliland, J.R. (1987) A review of the levelling networks of New Zealand, *New Zealand Surveyor*, No. 271, pp. 7-15.

Gilliland, J.R. (1989) A gravimetric geoid of Australia, *The Australian Surveyor*, Vol. 34, No. 7, pp. 699-706.

Gilliland, J.R. (1990) A gravimetric geoid for the New Zealand region, *The New Zealand Surveyor*, Vol. 32, No. 271, pp. 7-15.

Goldan, H.-J. and Seeber, G. (1994) Precise tide gauge connection to the island of Helgoland, *Marine Geodesy*, Vol. 17, No. 2, pp. 147-152.

Goos, J.M., Featherstone, W.E., Kirby, J.F. and Holmes, S.A. (2003) Experiments with two different approaches to gridding terrestrial gravity anomalies and their effect on regional geoid computation, *Survey Review*, Vol. 37, No. 288, pp. 91-105.

Grafarend, E.W. and Ardalan, A.A. (1997) W_0: an estimate of the Finnish Height Datum N60, epoch 1993.4 from twenty-five GPS points of the Baltic sea level

project, *Journal of Geodesy*, Vol. 71, No. 11, pp. 673-679, doi: 10.1007/s001900050134.

Grafarend, E.W. and Krumm, F. (1998) The Abel-Poisson kernel and the Abel-Poisson integral in a moving tangent space, *Journal of Geodesy*, Vol. 72, No. 7-8, pp. 404-410, doi: 10.1007/s001900050179.

Grossman, W. and Peschel, H. (1964) Bestimmung der schweredifferenz zwischen Potsdam und Bad Harzberg mit askania-gravimetern, *Bulletin Géodésique*, Vol. 38, No. 4, pp. 335-340, doi: 10.1007/BF02526828.

Gruber, T., Anzenhofer, M., Rentcsh, M. and Schwintzer, P. (1997) Improvements in high-resolution gravity field modelling at GFZ, in: Segawa, J., Fujimoto, H. and Okubo, S., (Eds.) *Gravity, Geoid and Marine Geodesy*, Springer, Berlin, Germany, pp. 445-452 [coefficients not online].

Gruber, T., Bode, A., Reigber, C., Schwintzer, P., Balmino, G., Biancale, R. and Lemoine, J.M. (2000) GRIM5-C1: combination solution of the global gravity field to degree and order 120, *Geophysical Research Letters*, Vol. 27, No. 24, pp. 4005-4009, doi: 10.1029/2000GL011589, [coefficients available from http://www.gfz-potsdam.de/pb1/pg3/grim/grim5_e.html].

Haagmans, R., De Min, E. Van Gelderen, M. (1993) Fast evaluation of convolution integrals on the sphere using 1D FFT, and a comparison with existing methods for Stokes' integral, *manuscripta geodaetica*, Vol. 18, No. 5, pp. 227-241.

Hackney, R.I. and Featherstone, W.E. (2003) Geodetic versus geophysical perspectives of the 'gravity anomaly', *Geophysical Journal International*, Vol. 154, No. 1, pp. 35-43, doi: 10.1046/j.1365-246x.2003.01941.x (errata published in (2003) Vol. 154, No. 2, p. 596; (2006) Vol. 167, No. 2, p. 585).

Hagiwara, Y. (1972) Truncation error formulas for the geoidal height and the deflection of the vertical, *Bulletin Géodésique*, Vol. 46, No. 4, pp. 453-466, doi: 10.1007/BF02522052.

Hagiwara, Y. (1976) A new formula for evaluating the truncation error coefficient, *Bulletin Géodésique*, Vol. 50, No. 2, pp. 131-135, doi: 10.1007/BF02522312.

Hammer, S. (1939) Terrain corrections for gravimeter stations, *Geophysics*, Vol. 4, No. 3, pp. 184-194, doi: 10.1190/1.1440495.

Hannah, J. (1988) Analysis of mean sea level trends in New Zealand from historical tidal data, *Report Number 2*, Department of Survey and Land Information, Wellington, New Zealand, 41 pp.

Hannah, J. (1990) Analysis of mean sea level data from New Zealand for the period 1899 – 1988, *Journal of Geophysical Research*, Vol. 95, No. B8, pp. 12399-12405.

Hannah, J. (2001) An assessment of New Zealand's height systems and options for a future height datum, *Report prepared for Land Information New Zealand*, University of Otago, Dunedin, New Zealand, 38 pp.

Hannah, J. (2004) An updated analysis of long term sea level change in New Zealand, *Geophysical Research Letters*, Vol. 31, L03307, doi: 10.1029/2003GL019166.

Haxby, W.F., Karner, G.D., LaBrecque, J.L. and Weissel, J.K. (1983) Digital images of combined oceanic and continental data sets and their use in tectonic studies, *EOS: Transactions of the American Geophysical Union*, Vol. 64, pp. 995-1004.

Hayford, J.F. (1909) *The figure of the Earth and isostasy from measurements in the United States*, US Coast and Geodetic Survey, Washington DC, USA.

Heck, B. (1990) An evaluation of some systematic error sources affecting terrestrial gravity anomalies, *Bulletin Géodésique*, Vol. 64, No. 1, pp. 88-108, doi: 10.1007/BF02530617.

Heck, B. (1993) A revision of Helmert's second method of condensation in geoid and quasigeoid determination, in: *Geodesy and Physics of the Earth*, Montang, H. and Reigber, C. (Eds.), Springer, Berlin, Germany, pp. 246-251.

Heck, B. (2003a) *Rechenverfahren und Auswertemodelle der Landesvermessung*, 3rd Edition, Wichman, Karlsruhe, Germany, 473 pp.

Heck, B. (2003b) On Helmert's methods of condensation, *Journal of Geodesy*, Vol. 77, No. 3-4, pp. 155-170, doi: 10.1007/s00190-003-0318-5.

Heck, B. (2005) Comments and reply regarding Heck (2003) "On Helmert's methods of condensation", *Journal of Geodesy*, Vol. 78, No. 7-8, pp. 457-461, doi: 10.1007/s00190-004-0412-3.

Heck, B. and Grüninger, W. (1987) *Modification of Stokes's integral formula by combining two classical approaches*, Proceedings of the XIX General Assembly of the International Union of Geodesy and Geophysics, Vol. 2, Vancouver, Canada, pp. 309-337.

Heck, B. and Rummel, R. (1990) Strategies for solving the vertical datum problem using terrestrial and satellite geodetic data, in: Sünkel, H. and Baker, T. (Eds.) *Sea-surface topography and the geoid*, Springer, Berlin, Germany, pp. 116-128.

Heck, B. and Seitz, K. (2003) Solutions of the linearized geodetic boundary value problem for an ellipsoidal boundary to order e^3, *Journal of Geodesy*, Vol. 77, No. 3-4, pp. 182-192, doi: 10.1007/s00190-002-0309-y.

Heiskanen, W.A. and Moritz, H. (1967) *Physical Geodesy*, W.H. Freeman and Company, San Francisco, USA, 364 pp.

Helmert, F.R. (1884) *Die mathematischen und physikalischen Theorieen der höheren Geodäsie*, Vol. 2, BG Teubner, Leipzig, Germany.

Helmert, F.R. (1890) *Die Schwerkraft im Hochgebirge insbesondere in den Tyroler Alpen in geodätischer und geologischer Beziehung*, Veröffentlichung Königliche Preussiche Geodätischen Institutes und Centralbureaus der Internationalen Erdmessung., No. 1, Berlin, Germany, 52 pp.

Henderson, J. (1933) The geological aspects of the Hawkes Bay earthquakes, *New Zealand Journal of Science and Technology*, Vol. 15, No. 1, pp. 38-75.

Hernández, J.N., Blitzkow, D., Luz, R., Sánchez, L., Sandoval, P. and Drewes, H. (2002) Connection of the vertical control networks of Venezuela, Brazil and Colombia, in: Drewes, H., Dodson, A., Fortes, L.P.S., Sánchez, L. and Sandoval, P. (Eds.), *Vertical Reference Systems*, Springer, Berlin, Germany, pp. 324-327.

Higgins, M.B., Forsberg, R. and Kearsley, A.H.W. (1998) The effects of varying cap sizes on geoid computations: experiences with FFT and ring integration, in: *Geodesy on the Move*, Forsberg, R., Feissel M. and Dietrich, R. (Eds.), Springer, Berlin, Germany, pp. 201-206.

Hipkin, R.G. (2000) Modelling the geoid and sea surface topography in coastal areas, *Physics and Chemistry of the Earth*, Vol. 25, No. 1, pp. 9-16, doi: 10.1016/S1464-1895(00)00003-X.

Hipkin, R., Haines, K., Beggan, C., Bingley, R., Hernandez, F., Holt, J. and Baker, T. (2004) The geoid EDIN2000 and mean sea surface topography around the British Isles, *Geophysical Journal International*, Vol. 157, No. 2, pp. 565-577, doi: 10.1111/j.1365-246x.2004.01989.x.

Holgate, S.J. and Woodworth, P.L. (2004) Evidence for enhanced coastal sea level rise during the 1990s, *Geophysical Research Letters*, Vol. 31, L07305, doi: 10.1029/2004GL019626.

Holloway, R.D. (1988) The integration of GPS heights into the Australian Height Datum, *UNISURV S-33*, School of Surveying, University of New South Wales, Sydney, Australia, 151 pp.

Howe, E. and Tscherning, C.C. (2005) Gravity field model UCPH2004 from one year of CHAMP data using energy conservation, *Newton's Bulletin*, No. 2, Bureau Gravimétrique International and International Geoid Service Joint Bulletin, pp. 1-4, available from www.iges.polimi.it, [coefficients available from: www.gfy.ku.dk/~eva/sagrada/UCPH2004_en.php].

Howe, E., Stenseng, L. and Tscherning, C.C. (2002) CHAMP gravity field model UCPH2002_02, poster available from: www.gfy.ku.dk/~stenseng/sagrada/poster.pdf [coefficients available from: www.gfy.ku.dk/~stenseng/sagrada.php].

Huang, J. and Véronneau, M. (2005) Applications of downward-continuation in gravimetric geoid modelling: case studies in Western Canada, *Journal of Geodesy*, Vol. 79, No. 1-3, pp. 135-145, doi: 10.1007/s00190-005-0452-3.

Huang, J.P. Vaníček, P. and Novák, P. (2000) An alternative algorithm to FFT for the numerical evaluation of Stokes's integral, *Studia Geophysica et Geodaetica*, Vol. 44, No. 3, pp. 374-380, doi: 10.1023/a:1022160504156.

Huang, J., Vaníček, P., Pagiatakis, S.D. and Brink, W. (2001) Effect of topographical density on geoid in the Canadian Rocky Mountains, *Journal of Geodesy*, Vol. 74, No. 11-12, pp. 805-815, doi: 10.1007/s001900000145.

Huang, J., Sideris, M.G., Vaníček, P. and Tziavos, I.N. (2003) Numerical investigation of downward continuation for gravity anomalies, *Bolletino Di Geodesia e Scienze Affini*, Vol. 62, No. 1, pp. 33-48.

Humphries, T. (1908) *Circular 847*, Surveyor-General, Department of Lands and Survey, Wellington, New Zealand.

Hunt, T.M. and Ferry, L.M. (1975) Gravity measurements at principal New Zealand stations, *New Zealand Journal of Geology and Geophysics*, Vol. 18, No. 3, pp. 713-720.

Hwang, C., Kao, E.C. and Parsons, B.E. (1998) Global derivation of marine gravity anomalies, *Geophysical Journal International*, Vol. 134, No. 2, pp. 449-459.

Hwang, C., Hsu, H.-Y. and Jang, R.-J. (2002) Global mean sea surface and marine gravity anomaly from multi-satellite altimetry: applications of deflection-geoid and inverse Vening Meinesz formulae, *Journal of Geodesy*, Vol. 76, No. 8, pp. 407-418, doi: 10.1007/s00190-002-0265-6.

IAG (1984) IAG Resolution 16, Geodesists Handbook, *Bulletin Géodésique*, Vol. 58, No. 3, p. 321, doi: 10.1007/BF02519005.

ICSM (2002) *Standards and Practices for Control Surveys*, Version 1.5, Inter-Governmental Committee on Surveying and Mapping, Canberra, Australia, available at: http://www.icsm.gov.au/icsm/publications/sp1/sp1.htm.

Ihde, J. (2007) *Conventional Vertical Reference System (CVRS) Conventions*, International Association of Geodesy Inter-Commission Project 1.2: Vertical Reference Frames.

Ihde, J., Gurtner, W., Ádám, J., Harsson, B.G., Schlüter, W. and Wöppelmann, G. (2000) The height solution of the European Vertical Reference Network (EUVN), presented to EUREF Symposium 2000, 22-24 June 2000, Tromsø, Norway, available from http://crs.bkg.bund.de/evrs/Papers.html.

Ihde, J., Augath, W. and Sacher, M. (2002) The vertical reference system for Europe, in: Drewes, H., Dodson, A., Fortes, L.P.S., Sánchez, L. and Sandoval, P. (Eds.), *Vertical Reference Systems*, Springer, Berlin, Germany, pp. 345-350.

Iliffe, J.C., Ziebart, M., Cross, P.A., Forsberg, R., Strykowski, G. and Tscherning, C.C. (2003) OSGM02: A new model for converting GPS-derived heights to local height datums in Great Britain and Ireland, *Survey Review*, Vol. 37, No. 290, pp. 276-293.

Janák, J. and Vaníček, P. (2005) Mean free-air gravity anomalies in the mountains, *Studia Geophysia et Geodaetica*, Vol. 49, No. 1, pp. 31-42, doi: 10.1007/s11200-005-1624-6.

Jekeli, C. (1980) Reducing the error of geoid undulation computations by modifying Stokes' function, *Report 301*, Department of Geodetic Science, Ohio State University, Columbus, USA, 50 pp.

Jekeli, C. (1981a) The downward continuation to the Earth's surface of truncated spherical and ellipsoidal harmonic series of the gravity and height anomalies, *Report 323*, Department of Geodetic Science and Surveying, Ohio State University, Columbus, USA, 140 pp.

Jekeli, C. (1981b) Modifying Stokes' function to reduce the error of geoid undulation computations, *Journal of Geophysical Research*, Vol. 86, No. B8, pp. 6985-6990.

Jekeli, C. (1999) An analysis of vertical deflections derived from high-degree spherical harmonic models, *Journal of Geodesy*, Vol. 73, No. 1, pp. 10-22, doi: 10.1007/s001900050213.

Jekeli, C. (2000) Heights, the Geopotential, and Vertical Datums, *Report 459*, Department of Civil and Environmental Engineering and Geodetic Science, Ohio State University, Columbus, Ohio, USA, 34 pp.

Jekeli, C. and Serpas, J.G. (2003) Review and numerical assessment of the direct topographical reduction in geoid determination, *Journal of Geodesy*, Vol. 77, No. 3-4, pp. 226-239, doi: 10.1007/s00190-003-0320-y.

Kadir, M.A., Fashir, H.H. and Omar, K. (1999) A regional gravimetric co-geoid over South East Asia, *Geomatics Research Australasia*, No. 71, pp. 37-56.

Kasenda, A. and Kearsley, A.H.W. (2002) Towards the establishment of an Indonesian unified vertical datum, in: Drewes, H., Dodson, A., Fortes, L.P.S., Sánchez, L. and Sandoval, P. (Eds.), *Vertical Reference Systems*, Springer, Berlin, Germany, pp. 334-338.

Kearsley, A.H.W. (1988) Tests on the recovery of precise geoid height differences from gravimetry, *Journal of Geophysical Research*, Vol. 93, No. B6, pp. 6559-6570.

Kearsley, A.H.W. and Forsberg, R. (1990) Tailored geopotential models – applications and shortcomings, *manuscripta geodaetica*, Vol. 15, No. 1, pp. 151-158.

Kearsley, A.H.W. and Govind, R. (1991) Geoid evaluation in Australia a status report, *The Australian Surveyor*, Vol. 36, No. 1, pp. 30-40.

Kearsley, A.H.W., Ahmad, Z. and Chan, A. (1993) National height datums, levelling GPS heights and geoids, *Australian Journal of Photogrammetry and Surveying*, No. 59, pp. 53-88.

Kenyon, S., Factor, J., Pavlis, N. and Holmes, S. (2006) Towards the next EGM: Progress in gravity data preparation, *Presentation at First International Gravity Field Service Symposium*, 28 August – 1 September 2006, İstanbul, Turkey.

Kingdon, R., Vaníček, P., Santos, M., Ellmann, A. and Tenzer, R. (2005) Toward an improved height system for Canada, *Geomatica*, Vol. 59, No. 3, pp. 241-249.

Kirby, J.F. and Featherstone, W.E. (1997) A study of zero- and first-degree terms in geopotential models over Australia, *Geomatics Research Australasia*, No. 66, pp. 93-108.

Kirby, J.F. and Featherstone, W.E. (1999) Terrain correcting the Australian gravity database using the national digital elevation model and the fast Fourier transform, *Australian Journal of Earth Sciences*, Vol. 46, No. 4, pp. 555–562, doi: 10.1046/j.1440-0952.1999.00731.x.

Kirby, J.F. and Featherstone, W.E. (2001) Anomalously large gradients in the "GEODATA 9 Second" digital elevation model of Australia, and their effects on gravimetric terrain corrections, *Cartography*, Vol. 30, No. 1, pp. 1-10.

Kirby, J.F. and Featherstone, W.E. (2002) High resolution grids of gravimetric terrain corrections and complete Bouguer gravity reductions over Australia, *Exploration Geophysics*, Vol. 33, No. 3-4, pp. 161-165.

Kirby, J.F. and Forsberg, R. (1988) A comparison of techniques for the integration of satellite altimeter and surface gravity data for geoid determination, in: Forsberg, R., Feissel, M. and Dietrich, R. (Eds.) *Geodesy on the Move*, Springer, Berlin, Germany, pp. 207-212.

Klose, U. and Ilk, K.H. (1993) A solution to the singularity problem occurring in the terrain correction formula, *manuscripta geodaetica*, Vol. 18, No. 5, pp. 263-279.

Koch, K.R. (2005) Determining the maximum degree of harmonic coefficients in geopotential models by Monte Carlo methods, *Studia Geophysica et Geodaetica*, Vol. 49, No. 3, pp. 259-275, doi: 10.1007/s11200-005-009-1.

Krakiwsky, E.J. (1965) Heights, *Master of Science Thesis*, Department of Geodetic Science and Surveying, Ohio State University, Columbus, USA, 157 pp.

Kuhn, M. (2003) Geoid determination with density hypotheses from isostatic models and geological information, *Journal of Geodesy*, Vol. 77, No. 1-2, pp. 50-65, doi: 10.1007/s00190-002-0297-y.

Kuhn, M. (2006) Spherical and ellipsoidal terrain corrections, poster presented at *gravity field of the Earth, 1st International Symposium of the International Gravity Field Service*, Istanbul, Turkey, 28 August – 1 September 2006.

Kumar, M. and Burke, K.J. (1998) Realizing a global vertical datum with the use of the geoid, in: Vermeer, M. and Ádám, J. (Eds.), *Report 98:4, Second Continental Worksop on the Geoid*, Finnish Geodetic Institute, Masala, Finland, pp. 87-94.

Lambeck, K., Smither, C. and Ekman, M. (1998) Tests of glacial rebound models for Fennoscandinavia based on instrumented sea- and lake-level records, *Geophysical Journal International*, Vol. 135, No. 2, pp. 375-387, doi: 10.1046/j.1365-246x.1998.00643.x.

Laskowski, P. (1983) The effect of vertical datum inconsistencies on the determination of gravity related quantities, *Report 349*, Department of Geodetic Science and Surveying, Ohio State University, Columbus, Ohio, USA, 87 pp.

Leaman, D.E. (1998) The gravity terrain correction – practical considerations, *Exploration Geophysics*, Vol. 29, No. 3-4, pp. 476–471.

Lee, L.P. (1978) First-order geodetic triangulation of New Zealand 1909-49 1973-74, *Technical Series No. 1*, Department of Lands and Survey, Wellington, New Zealand, 97 pp.

Lehmann, R. (2000) Altimetry-gravimetry problems with free vertical datum, *Journal of Geodesy*, Vol. 74, No. 3-4, pp. 327-334, doi: 10.1007/s001900050290.

Lemoine, F.G., Kenyon, S.C., Factor, R.G., Trimmer, R.G., Pavlis, N.K., Chinn, D.S., Cox, C.M., Klosko, S.M., Luthcke, S.B., Torrence, M.H., Wang, Y.M., Williamson, R.G., Pavlis, E.C., Rapp, R.H. and Olson, T.R. (1998) The development of the joint NASA GSFC and the National Imagery and Mapping Agency (NIMA) geopotential model EGM96, *NASA/TP-1998-206861*, Goddard Space Flight Center, Greenbelt, USA, 575 pp.

Lensen, G.J. and Otway, P.M. (1971) Earthshift and post earthshift deformation associated with the May 1968 Inangahua earthquake, New Zealand, *Royal Society of New Zealand Bulletin*, Vol. 9, No. 1, pp. 107-167.

Li, Y.C. (1993) Optimized spectral geoid determination, *UCSE Report 20050*, Department of Geomatics Engineering, University of Calgary, Calgary, Canada.

Li, Y.C. and Sideris, M.G. (1994) Improved gravimetric terrain corrections, *Geophysical Journal International*, Vol. 119, No. 3, pp. 740-752.

Li, Y.C. and Sideris, M.G. (1997) Marine gravity and geoid determination by optimal combination of satellite altimetry and shipborne gravimetry data, *Journal of Geodesy*, Vol. 71, No. 4, pp. 209-216, doi: 10.1007/s001900050088.

Lidberg, M., Johansson, J.M., Scherneck, H.-G. and Davis, J.L. (2007) An improved and extended GPS-derived 3D velocity field of the glacial isostatic adjustment (GIA) in Fennoscandia, *Journal of Geodesy*, Vol. 81, No. 3, pp. 213-230, doi: 10.1007/s00190-006-0102-4.

Ma, X.Q. and Watts, D.R. (1994) Terrain correction program for regional gravity surveys, *Computers and Geosciences*, Vol. 20, No. 6, pp. 961-972, doi: 10.1016/0098-3004(94)90037-X.

Mackie, J.B. (1982) The relationship between the WGS72 Doppler satellite datum and the New Zealand Geodetic Datum 1949, *Report No. 178*, Geophysics Division, Department of Scientific and Industrial Research, Wellington, New Zealand.

Mader, K. (1954) Die orthometrische Schwerekorrektion des Präzisions-Nivellements in den Hohen Tauren (The orthometric weight correction of precision levelling in high terrain), *Österreichische Zeitschrift für Vermessungswesen*, Sonderheft 15, Vienna.

Mainville, A. and Craymer, M.R. (2005) Present-day tilting of the Great Lakes region based on water level gauges, *The Geological Society of America Bulletin*, Vol. 117, No. 7-8, pp. 1070-1080, doi: 10.1130/b25392.1.

Marti, U. (2003) Modelling of differences of height systems in Switzerland, in Tziavos, I.N., (Ed.) *Gravity and Geoid 2002*, Ziti Editions, Thessaloniki, Greece, pp. 379-383.

Martinec, Z. (1996) Stability investigations of a discrete downward continuation problem for geoid determination in the Canadian Rocky Mountains, *Journal of Geodesy*, Vol. 70, No. 11, pp. 805-828, doi: 10.1007/BF00867158.

Martinec, Z. (1998) *Boundary Value Problems for Gravimetric Determination of a Precise Geoid*, Lecture Notes in Earth Sciences, No. 73, Springer, Berlin, Germany, 223 pp.

Martinec, Z. and Vaníček, P. (1994a) Direct topographical effect of Helmert's condensation for a spherical approximation of the geoid, *manuscripta geodaetica*, Vol. 19, No. 5, pp. 257-268.

Martinec, Z. and Vaníček, P. (1994b) The indirect effect of topography in the Stokes-Helmert technique for a spherical approximation of the geoid, *manuscripta geodaetica*, Vol. 19, No. 4, pp. 213-219.

Martinec, Z. and Vaníček, P. (1996) Formulation of the boundary-value problem for geoid determination with a higher-degree reference field, *Geophysical Journal International*, Vol. 126, No. 1, pp. 219-228.

Martinec, Z., Matyska, C., Grafarend, E.W. and Vaníček, P. (1993) On Helmert's second condensation reduction, *manuscripta geodaetica*, Vol. 18, No. 6, pp. 417-421.

Martinec, Z., Vaníček, P., Mainville, A. and Véronneau, M. (1996) Evaluation of topographical effects in precise geoid computation from densely sampled heights, *Journal of Geodesy*, Vol. 70, No. 11, pp. 746-754, doi: 10.1007/BF00867153.

Mayer-Gürr, T., Ilk, K.H., Eicker, A. and Feuchtinger, M. (2005) ITG-CHAMP01: A CHAMP gravity field model from short kinematical arcs of a one-year observation period, *Journal of Geodesy*, Vol. 78, No. 7-8, pp. 462-480, doi: 10.1077/s00190-004-0413-2.

Meissl, P. (1971) Preparations for the numerical evaluation of second-order Molodensky-type formulas, *Report 163*, Department of Geodetic Science and Surveying, Ohio State University, Columbus, USA, 72 pp.

Melchior, P. (1981) *The Tides of the Planet Earth*, Pergamon Press, Oxford, England, 655 pp.

Merry, C.L. (2003) The African geoid project and its relevance to the unification of African vertical reference frames, *Proceedings of the 2nd FIG Regional Conference*, Marrakech, Morocco, 2-5 December 2003, available at: www.fig.net/pub/morocco/proceedings/TS9/TS9_3_merry.pdf.

Merry, C. and Vaníček, P. (1983) Investigation of local variations of sea surface topography, *Marine Geodesy*, Vol. 7, No. 2, pp. 101-126.

Merry, C.L., Blitzkow, D., Abd-Elmotaal, H., Fashir, H.H., John, S., Podmore, F. and Fairhead, J.D. (2005) A preliminary geoid for Africa, in: Sansò, F. (Ed.) *A Window on the Future of Geodesy*, Springer, Berlin, pp. 374-379.

Meyer, T.H., Roman, D.R. and Zilkoski, D.B. (2004) What does height really mean? Part I: Introduction, *Surveying and Land Information Science*, Vol. 64, No. 4, pp. 223-233.

Meyer, T.H., Roman, D.R. and Zilkoski, D.B. (2005) What does height really mean? Part II: Physics and gravity, *Surveying and Land Information Science*, Vol. 65, No. 1, pp. 5-15.

Meyer, T.H., Roman, D.R. and Zilkoski, D.B. (2006a) What does height really mean? Part III: Height systems, *Surveying and Land Information Science*, Vol. 66, No. 2, pp. 149-160.

Meyer, T.H., Roman, D.R. and Zilkoski, D.B. (2006b) What does height really mean? Part IV: GPS heighting, *Surveying and Land Information Science*, Vol. 66, No. 3, pp. 165-183.

Milbert, D.G. (1991) Computing GPS-derived orthometric heights with the GEOID90 geoid height model, in: *Technical Papers of the 1991 ICSM-ASPRS Fall Convention*, Atlanta, Georgia, USA, pp. A46-55.

Mohr, P.J. and Taylor, B.N. (2007) The fundamental physical constants, *Physics Today*, URL: http://www.physicstoday.org/guide/fundconst.pdf, last accessed 13/02/2007.

Molodensky, M.S., Eremeev, V.F. and Yurkina, M.I. (1962) *Methods for the study of the external gravitational field and figure of the Earth*, Israeli Programme for the Translation of Scientific Publications, Jerusalem, Israel, 248 pp.

Morelli, C., Gantar, C., Honkaslo, T., McConnell, R.K., Tanner, T.G., Szabo, B., Uotila, U. and Whalen, C.T. (1974) The International Gravity Standardisation Network 1971 (IGSN71), *Special Publication 4 of Bulletin Géodésique*, International Association of Geodesy, Paris, France.

Moritz, H. (1968) On the use of the terrain correction in solving Molodensky's problem, *Report 108*, Department of Geodetic Science, Ohio State University, Columbus, USA, 46 pp.

Moritz H (1980a) Geodetic Reference System 1980, *Bulletin Géodésique*, Vol. 54, No. 3, pp. 395-405, doi:10.1007/BF02521480.

Moritz, H. (1980b) *Advanced Physical Geodesy*, Abacus Press, Tunbridge Wells, United Kingdom, 500 pp.

Nagy, D. (1966a) The prism method for terrain corrections using digital computers, *Pure and Applied Geophysics*, Vol. 63, No. 1, pp. 31-39, doi: 10.1007/BF00875156.

Nagy, D. (1966b) The gravitational attraction of a right angular prism, *Geophysics*, Vol. 31, No. 2, pp. 362-371, doi: 10.1190/1.1439779.

Nagy, D., Papp, G. and Benedek, G. (2000) The gravitational potential and its derivatives for the prism, *Journal of Geodesy*, Vol. 74, No. 7-8, pp. 552-560, doi: 10.1007/s001900000116.

Nagy, D., Papp, G. and Benedek, G. (2002) Corrections to "The gravitational potential and its derivatives for the prism", *Journal of Geodesy*, Vol. 76, No. 8, p. 475, doi: 10.1007/s00190-002-0264-7.

Nahavandchi, H. (2000) The direct topographical correction in gravimetric geoid determination by the Stokes-Helmert method, *Journal of Geodesy*, Vol. 74, No. 6, pp. 488-496, doi: 10.1007/s001900000110.

Nahavandchi, H. and Sjöberg, L.E. (1998a) Terrain correction to power H^3 in gravimetric geoid determination, *Journal of Geodesy*, Vol. 72, No. 3, pp. 124-135, doi: 10.1007/s001900050154.

Nahavandchi, H. and Sjöberg, L.E. (1998b) Unification of vertical datums by GPS and gravimetric geoid models using modified Stokes formula, *Marine Geodesy*, Vol. 21, No. 4, pp. 261-273.

Nahavandchi, H. and Sjöberg, L.E. (2001) Precise geoid determined over Sweden using the Stokes-Helmert method and improved topographic corrections, *Journal of Geodesy*, Vol. 75, No. 2-3, pp. 74-88, doi: 10.1007/s001900000154.

Nerem, R.S., Jekeli, C. and Kaula, W.M. (1995) Gravity field determination and characteristics: retrospective and prospective, *Journal of Geophysical Research*, Vol. 100, No. B8, pp. 15053-15074.

Neyman, Y.M., Li, J. and Liu, Q. (1996) Modification of Stokes and Vening-Meinesz formulas for the inner zone of arbitrary shape by minimisation of upper bound truncation errors, *Journal of Geodesy*, Vol. 70, No. 7, pp. 410-418, doi: 10.1007/bf01090816.

Niethammer, T. (1932) Nivellement und Schwere als Mittel zur Berechnung wahrer Meereshöhen (Levelling and weight as means for the computation of true sea level heights), *Schweizersche Geodätische Kommission*, Berne, 76 pp.

Novák, P. and Heck, B. (2002) Downward continuation and geoid determination based on band-limited airborne gravity data, *Journal of Geodesy*, Vol. 76, No. 5, pp. 269-278, doi: 10.1007/s00190-002-0252-y.

Novák, P., Vaníček, P., Martinec, Z. and Véronneau, M. (2001a) Effects of the spherical terrain on gravity and the geoid, *Journal of Geodesy*, Vol. 75, No. 9-10, pp. 491-504, doi: 10.1007/s001900100201.

Novák, P., Vaníček, P., Veronneau, M., Holmes, S.A. and Featherstone, W.E. (2001b) On the accuracy of modified Stokes formula, *Journal of Geodesy*, Vol. 74, No. 9, pp. 644-654, doi: 10.1007/s001900000126.

Novák, P., Kern, M., Schwarz, K.-P., Sideris, M.G., Heck, B., Ferguson, S., Hammada, Y. and Wei, M. (2003) On geoid determination from airborne gravity, *Journal of Geodesy*, Vol. 76, No. 9-10, pp. 510-522, doi: 10.1007/s00190-002-0284-3.

Nowell, D.A.G. (1999) Gravity terrain corrections – an overview, *Journal of Applied Geophysics*, Vol. 42, No. 2, pp. 117-134, doi: 10.1016/S0926-9851(99)00028-2.

NTHA (2006) Technical specification for the maintenance of NZ Topo data, *TH Specification 106, Version 1.8*, National Topographic/Hydrographic Authority, Land Information New Zealand, Wellington, New Zealand, 82 pp., available from www.linz.govt.nz.

NZNCGG (1991) New Zealand geodetic operations 1987-1990, *Report for the General Assembly of the International Union of Geodesy and Geophysics, Vienna, Austria*, New Zealand National Committee for Geodesy and Geophysics, Wellington, New Zealand, 20 pp.

Olgiati, A., Balmino, G., Sarrailh, M. and Green, C.M. (1995) Gravity anomalies from satellite altimetry: comparison between computation via geoid heights and via deflections of the vertical, *Bulletin Géodésique*, Vol. 69, No. 4, pp. 252-260, doi: 10.1007/BF00806737.

Omang, O.C.D. and Forsberg, R. (2000) How to handle topography in practical geoid determination: three examples, *Journal of Geodesy*, Vol. 74, No. 6, pp. 458-466, doi: 10.1007/s001900000107.

Omang, O.C.D. and Forsberg, R. (2002) The northern European geoid: a case study on long-wavelength geoid errors, *Journal of Geodesy*, Vol. 76, No. 6-7, pp. 369-380, doi: 10.1007/s00190-002-0261-x.

OSG (2003) Accuracy standards for geodetic surveys, *SG Standard 1*, Office of the Surveyor-General, Land Information New Zealand, Wellington, New Zealand, 26 pp., available from www.linz.govt.nz/surveypublications.

Ota, Y., Hull, A.G., Iso, N., Ikeda, Y., Moriya, I. and Yoshikawa, T. (1992) Holocene marine terraces on the northeast coast of North Island, New Zealand, and their tectonic significance, *New Zealand Journal of Geology and Geophysics*, Vol. 35, No. 3, pp. 273-288.

Otway, P.M., Blick, G.H. and Scott, B.J. (2002) Vertical deformation at Lake Taupo, New Zealand, from lake levelling surveys, *New Zealand Journal of Geology and Geophysics*, Vol. 45, No. 1, pp. 121-132.

Pan, M. and Sjöberg, L. (1998) Unification of vertical datums by GPS and gravimetric geoid models with application to Fennoscandia, *Journal of Geodesy*, Vol. 72, No. 2, pp. 64-70, doi: 10.1007/s001900050149.

Papp, G. and Benedek, J. (2000) Numerical modelling of gravitational field lines – the effect of mass attraction on horizontal coordinates, *Journal of Geodesy*, Vol. 73, No. 12, pp. 648-659, doi: 10.1007/s001900050003.

Parker, R.L. (1995) Improved Fourier terrain corrections: Part I, *Geophysics*, Vol. 60, No. 4, pp. 1007-1017, doi: 10.1190/1.1443829.

Parker, R.L. (1996) Improved Fourier terrain corrections: Part II, *Geophysics*, Vol. 61, No. 2, pp. 365-372, doi: 10.1190/1.1443965.

Paul (1973) A method of evaluating the truncation error coefficients for geoidal height, *Bulletin Géodésique*, Vol. 47, No. 4, pp. 413-425, doi: 10.1007/BF02521951.

Pavlis, N.K. (1998) Observed inconsistencies between satellite-only and surface gravity-only geopotential models, in: Forsberg, R., Feissel, M. and Dietrich, R. (Eds.) *Geodesy on the Move*, Springer, Berlin, pp. 144-149.

Pavlis, N.K., Chinn, D.S., Cox, C.M. and Lemoine, F.G. (2000) Geopotential model improvement using POCM4_B dynamic ocean topography information: PGM2000A, *paper presented at TOPEX/JASON Science Working Team Meeting*, Miami, Florida, USA, [coefficients available from http://bowie.gsfc.nasa.gov/926/PGM2000A/index.html].

Pearse, M.B. (1998) A modern geodetic reference system for New Zealand, *UNISURV S-52*, School of Geomatic Engineering, University of New South Wales, Australia, 324 pp.

Pearse, M.B. (2001) A proposal for vertical datum development in New Zealand, *OSG Technical Report 10*, Land Information New Zealand, Wellington New Zealand, 38 pp., available from: www.linz.govt.nz/surveypublications.

Pearse, M.B. and Crook, C. (1997) Recommended transformation parameters from WGS84 to NZGD49, *Geodetic System Technical Report GS 1997/11*, Land Information New Zealand, Wellington, New Zealand, 15 pp., available from: www.linz.govt.nz/surveypublications.

Pellinen, L.P. (1962) Accounting for topography in the calculation of quasigeoidal heights and plumb-line deflections from gravity anomalies, *Bulletin Géodésique*, Vol. 36, No. 1, pp. 57-65, doi: 10.1007/BF02528175.

Peltier, W.R. (2000) Global glacial isostatic adjustment and modern instrumental records of relative sea level history, in Douglas, BC, Kearney, M.S. and Leatherman, S.P. (Eds.) *Sea Level Rise History and Consequences*, Elsevier, San Diego, 232 pp.

Poutanen, M., Vermeer, M. and Mäkinen, J. (1996) The permanent tide in GPS positioning, *Journal of Geodesy*, Vol. 70, No. 8, pp. 499-504, doi: 10.1007/s001900050038.

Pugh, D. (1987) *Tides, Surges and Mean Sea-level: A Handbook for Engineers and Scientists*, John Wiley and Sons, Chichester, United Kingdom, 486pp.

Pugh, D. (2004) *Changing Sea Levels: Effects of Tides, Weather and Climate*, Cambridge University Press, Cambridge, United Kingdom, 265 pp.

Rapp, R.H. (1961) The orthometric height, *Master of Science Thesis*, Department of Geodetic Science, Ohio State University, Columbus, USA, 117 pp.

Rapp, R.H. (1981) The Earth's gravity field to degree and order 180 using SEASAT altimeter data, terrestrial gravity data and other data: OSU81, *Report No. 322*, Department of Geodetic Science and Surveying, Ohio State University, Columbus, Ohio, USA, 52 pp.

Rapp, R.H. (1982) A FORTRAN program for the computation of gravimetric quantities from high-degree spherical harmonic expansions, *Report 334*, Department of Geodetic Science and Surveying, Ohio State University, Columbus, Ohio, USA, 23 pp.

Rapp, R.H. (1983) The need and prospects for a world vertical datum, *Proceedings of the International Association of Geodesy Symposia, Vol. 2, International*

Union of Geodesy and Geophysics XVIII General Assembly, Hamburg, Germany, pp. 432-445.

Rapp, R.H. (1989) The treatment of permanent tidal effects in the analysis of satellite altimeter data for sea surface topography, *manuscripta geodaetica*, Vol. 14, No. 6, pp. 368-372.

Rapp, R.H. (1994) Separation between reference surfaces of selected vertical datums, *Bulletin Géodésique*, Vol. 69, No. 1, pp. 26-31, doi: 10.1007/BF00807989.

Rapp, R.H. (1995) A world vertical datum proposal, *Allgemeine Vermessungs-Nachrichten*, Vol. 102, No. 8-9, pp. 297-304.

Rapp, R.H. (1997a) Use of potential coefficient models for geoid undulation determinations using a spherical harmonic representation of the height anomaly/geoid undulation difference, *Journal of Geodesy*, Vol. 71, No. 5, pp. 282-289, doi: 10.1007/s001900050096.

Rapp, R.H. (1997b) Past and future developments in geopotential modelling, in: Forsberg, R., Feissl, M. and Dietrich, R. (Eds.) *Geodesy on the Move*, Springer, Berlin, Germany, pp. 58-78.

Rapp, R.H. and Balasubramania, N. (1992) A conceptual formulation of a world height system, *Report 421*, Department of Geodetic Science and Surveying, Ohio State University, Columbus, Ohio, USA, 55 pp.

Rapp, R.H. and Rummel, R. (1975) Methods for the computation of detailed geoids and their accuracy, *Report 233*, Department of Geodetic Science, Ohio State University, Columbus, USA, 36 pp.

Rapp, R.H., Wang, Y.M. and Pavlis, N.K. (1991a) The Ohio State 1991 geopotential and sea surface topography harmonic coefficient model, *Report 410*, Department of Geodetic Science and Surveying, Ohio State University, Columbus, Ohio, USA, 94 pp.

Rapp, R.H., Nerem, R.S., Shum, C.K., Klosko, S.M. and Williamson, R.G. (1991b) Consideration of permanent tidal deformation in the orbit deformation and data analysis for the TOPEX/Poseidon mission, *NASA Technical Memo 100775*, Goddard Space Flight Center, Greenbelt, USA, 11 pp.

Reigber, Ch., Balmino, G., Schwintzer, P., Biancale, R., Bode, A., Lemoine, J.M., König, R., Loyer, S., Neumayer, H., Marty, J.C., Barthelmes, F., Perosanz, F. and Zhu, S.Y. (2002) A high-quality global gravity field model from CHAMP GPS tracking data and accelerometry, *Geophysical Research Letters*, Vol. 29, No. 14, doi: 10.1029/2002GL015064, [coefficients available from http://op.gfz-potsdam.de/champ/results/grav/004_eigen-1s.html].

Reigber, Ch., Schwintzer, P., Neumayer, K.H., Barthelmes, F., König, R., Förste, C., Balmino, G., Biancale, R., Lemoine, J.M., Loyer, S., Bruinsma, S., Perosanz, F. and Fayard, T. (2003) The CHAMP-only EIGEN-2 Earth gravity field model, *Advances in Space Research*, Vol. 31, No. 8, pp. 1883-1888, [coefficients available from http://op.gfz-potsdam.de/champ/results/grav/007_eigen-2.html]

Reigber, Ch., Jochmann, H., Wünsch, J., Petrovich, S., Schwintzer, P., Barthelmes, F., Neumayer, K.-H., König, R., Förste, Ch., Balimo, G., Biancale, R., Lemoine, J.M., Loyer, S. and Perosanz, F. (2005a) Earth gravity field and seasonal variability from CHAMP, in: Reigber, Ch., Lühr, H., Schwintzer, P. and Wickert, J. (Eds.) *Earth Observation with CHAMP – results from three years in orbit*, Springer, Berlin, Germany, pp. 25-30, [coefficients available from: www.gfz-potsdam.de/champ/results/grav/010_eigen-champ03s.html].

Reigber, Ch., Schmidt, R., Flechtner, F., König, R., Meyer, U., Neumayer, K.-H., Schwintzer, P. and Zhu, S.Y. (2005b) An Earth gravity field model complete to degree and order 150 from GRACE: EIGEN-GRACE02S, *Journal of Geodynamics*, Vol. 39, No. 1, pp. 1-10, doi:10.1016/j.jog.2004.07.001, [coefficients available from: http://www.gfz-potsdam.de/pb1/op/grace/results].

Reilly, W.I. (1970) Topographic-isostatic gravity corrections, *Geophysical Memoir 7*, Geophysics Division, Department of Scientific and Industrial Research, Wellington, New Zealand, 13 pp.

Reilly, W.I. (1972) New Zealand gravity map series, *New Zealand Journal of Geology and Geophysics*, Vol. 15, No. 1, pp. 3-15.

Reilly, W.I. (1990) The geoid and the needs of the GPS user, *New Zealand Surveyor*, Vol. 33, No. 277, pp. 35-41.

Reilly, W.I. and Woodward, D.J. (1971) Adjustment of observations in barometric levelling, *New Zealand Journal of Geology and Geophysics*, Vol. 14, No. 2, pp. 293-298.

Rio, M.-H. and Hernandez, F. (2004) A mean dynamic topography computed over the world ocean from altimetry, in situ measurements and a geoid model, *Journal of Geophysical Research*, Vol. 109, C12032, doi: 10.1029/2003JC002226.

Rizos, C., Coleman, R. and Ananga, N. (1991) The Bass Strait GPS survey: preliminary results of an experiment to connect Australian height datums, *Australian Journal of Photogrammetry and Surveying*, No. 55, pp. 1-25.

Robertson, E.I. and Reilly, W.I. (1960) The New Zealand primary gravity network, *New Zealand Journal of Geology and Geophysics*, Vol. 3, No. 1, pp. 41-68.

Roelse, A., Granger, H.W. and Graham, J.W. (1975) The adjustment of the Australian levelling survey 1970-71, *Report 12*, Division of National Mapping, Canberra, Australia, second edition, 98 pp.

Roman, D.R., Wang, Y.M., Henning, W. and Hamilton, J. (2004) Assessment of the new national geoid height model – GEOID03, *Surveying and Land Information Science*, Vol. 64, No. 3, pp. 153-162.

Rowe, G. (1989) First order geodetic astronomy observations in New Zealand 1980-1986, *Report of the Department of Survey and Land Information Number 1*, Wellington, New Zealand, 58 pp.

Rummel, R. and Teunissen, P.J.G. (1988) Height datum definition, height datum correction and the role of the geodetic boundary value problem, *Bulletin Géodésique*, Vol. 62, No. 4, pp. 477-498, doi: 10.1007/BF02520239.

Rummel, R., Balmino, G., Johnhannessen, J., Visser, P. and Woodworth, P. (2002) Dedicated gravity field missions – principles and aims, *Journal of Geodynamics*, Vol. 33, No. 1-2, pp. 3-20, doi: 10.1016/s0264-3707(01)00050-3.

Sandwell, D.T. and Smith, W.H.F. (1997) Marine gravity anomaly from GEOSAT and ERS 1 satellite altimetry, *Journal of Geophysical Research*, Vol. 102, No. B5, pp. 10039-10054.

Sandwell, D.T. and Smith, W.H.F. (2005) Retracking ERS-1 altimeter waveforms for optimal gravity field recovery, *Geophysical Journal International*, Vol. 163, No. 1, pp. 79-89, doi: 10.1111/j.1365-246X.2005.02724.x.

Sansò, F. and Vaníček, P. (2006) The orthometric height and the holonomity problem, *Journal of Geodesy*, Vol. 80, No. 5, pp. 225-232, doi: 10.1007/s00190-005-0015-7.

Santos, M.C., Vaníček, P., Featherstone, W.E., Kingdon, R., Ellmann, A., Martin, B.-A., Kuhn, M. and Tenzer, R. (2006) The relation between rigorous and Helmert's definitions of orthometric heights, *Journal of Geodesy*, Vol. 80, No. 12, pp. 691-704, doi: 10.1007/s00190-006-0086-0.

Schwarz, K.P. (1978) Geodetic improperly posed problems and their regularization, *Lecture Notes of the 2nd International School of Advanced Geodesy*, Erice, Italy.

Schwarz, K.-P., Sideris, M.G. and Forsberg, R. (1990) The use of FFT techniques in physical geodesy, *Geophysical Journal International*, Vol. 100, No. 3, pp. 485-514.

Schwintzer, P., Kang, Z. and Perosanz, F. (2000) Accelerometry aboard CHAMP, in: Drewes, H., Bosch, W. and Hornik, H. (Eds.), *Towards an Integrated Global Geodetic Observing System*, Springer, Berlin, pp. 197-200.

Sideris, M.G. (1985) A fast Fourier transformation method of computing terrain corrections, *manuscripta geodaetica*, Vol. 10, No. 1, pp. 66-73.

Sideris, M.G. (1987) Spectral methods for the numerical solution of Molodensky's problem, *UCSE Reports*, Department of Surveying Engineering, University of Calgary, Calgary, Canada, 107 pp.

Sideris, M.G. (1990) Rigorous gravimetric terrain modelling using Molodensky's operator, *manuscripta geodaetica*, Vol. 15, No. 2, pp. 97-106.

Sideris, M.G. (1994) Geoid determination by FFT techniques, in *Lecture Notes, International School for the Determination and Use of the Geoid*, Politecnico di Milano, Milano, Italy, pp. 213-277.

Sideris, M.G. and She, B.B. (1995) A new, high-resolution geoid for Canada and part of the US by the 1D-FFT method, *Bulletin Géodésique*, Vol. 69, No. 2, pp. 92-108, doi: 10.1007/BF00819555.

Sjöberg, L.E. (1980) Least squares combination of satellite harmonics and integral formulas in physical geodesy, *Geophysical Journal International*, Vol. 100, No. 5, pp. 485-514.

Sjöberg, L.E. (1981) Least squares combination of satellite and terrestrial data in physical geodesy, *Annals of Geophysics*, Vol. 37, No. 1, pp. 25-30.

Sjöberg, L.E. (1984) Least squares modification of Stokes and Vening-Meinesz formulas by accounting for errors of truncation, potential coefficients and gravity data, *manuscripta geodaetica*, Vol. 9, pp. 209-229.

Sjöberg, L.E. (1991) Refined least-squares modification of Stokes formula, *manuscripta geodaetica*, Vol. 16, pp. 367-375.

Sjöberg, L.E. (1995) On the quasigeoid to geoid separation, *manuscripta geodaetica*, Vol. 20, No. 3, pp. 182-192.

Sjöberg, L.E. (1996) On the error of analytical continuation in physical geodesy, *Journal of Geodesy*, Vol. 70, No. 11, pp. 724-730, doi: 10.1007/s001900050061.

Sjöberg, L.E. (1998) The exterior Airy/Heiskanen topographic-isostatic gravity potential anomaly and the effect of analytical continuation in Stokes's formula, *Journal of Geodesy*, Vol. 72, No. 11, pp. 654-662, doi: 10.1007/s001900050205.

Sjöberg, L.E. (2001) Topographic and atmospheric corrections of gravimetric geoid determination with special emphasis on the effects of harmonics of degrees zero and one, *Journal of Geodesy*, Vol. 75, No. 5-6, pp. 283-290, doi: 10.1007/s00100174.

Sjöberg, L.E. (2003a) A solution to the downward continuation effect on the geoid determined by Stokes's formula, *Journal of Geodesy*, Vol. 77, No. 1-2, pp. 94-100, doi: 10.1007/s00190-002-0306-1.

Sjöberg, L.E. (2003b) Ellipsoidal corrections to order e^2 of geopotential coefficients and Stokes' formula, *Journal of Geodesy*, Vol. 77, No. 3-4, pp. 139-147, doi: 10.1007/s00190-003-0321-x.

Sjöberg, L.E. (2003c) A general model of modifying Stokes' formula and its least-squares solution, *Journal of Geodesy*, Vol. 77, No. 7-8, pp. 459-464, doi: 10.1007/s00190-003-0346-1.

Sjöberg, L.E. (2003d) Comparison of four deterministic modifications of Stokes's formula, *Geomatics Research Australasia*, Vol. 78, pp. 85-106.

Sjöberg, L.E. (2004a) The effect on the geoid of lateral topographic density variations, *Journal of Geodesy*, Vol. 78, No. 1-2, pp. 34-39, doi: 10.1007/s00190-003-0363-0.

Sjöberg, L.E. (2004b) A spherical harmonic representation of the ellipsoidal correction to the modified Stokes formula, *Journal of Geodesy*, Vol. 78, No. 3, pp. 180-186, doi: 10.1007/s00190-004-0378-1.

Sjöberg, L.E. (2005a) A discussion on the approximations made in the practical implementation of the remove-compute-restore technique in regional geoid modelling, *Journal of Geodesy*, Vol. 78, No. 11-12, pp. 645-653, doi: 10.1007/s00190-004-0430-1.

Sjöberg, L.E. (2005b) A local least-squares modification of Stokes' formula, *Studia Geophysica et Geodetica*, Vol. 49, No. 1, pp. 23-30, doi: 10.1007/s11200-005-1623-7.

Sjöberg, L.E. and Hunegnaw, A. (2000) Some modifications of Stokes formula that account for truncation and potential coefficient errors, *Journal of Geodesy*, Vol. 74, No. 2, pp. 232-238, doi: 10.1007/s001900050281.

Sjöberg, L.E. and Nahavandchi, H. (1999) On the indirect effect in the Stokes-Helmert method of geoid determination, *Journal of Geodesy*, Vol. 73, No. 2, pp. 87-93, doi: 10.1007/s001900050222.

Smeets, I. (1994) An error analysis of the height anomaly determined by a combination of mean terrestrial gravity anomalies and a geopotential model, *Bolletino de Geodesia e Scienze Affini*, Vol. 53, No. 1, pp. 57-96.

Smith, D.A. (2000) The gravitational attraction of any polygonally shaped vertical prism with inclined top and bottom faces, *Journal of Geodesy*, Vol. 74, No. 5, pp. 414-420, doi: 10.1007/s001900000102.

Smith, D.A. and Milbert, D.G. (1999) The GEOID96 high-resolution geoid height model for the United States, *Journal of Geodesy*, Vol. 73, No. 5, pp. 219-236, doi: 10.1007/s001900050239.

Smith, D.A. and Roman, D.R. (2001) GEOID99 and G99SSS: 1-arc-minute geoid models for the United States, *Journal of Geodesy*, Vol. 75, No. 9-10, pp. 469-490, doi: 10.1007/s001900100200.

Smith, W.H.F. and Wessel, P. (1990) Gridding with continuous curvature splines in tension, *Geophysics*, Vol. 55, No. 3, pp. 293-305, doi: 10.1190/1.1442837.

Steed, J. and Holtznagel, S. (1994) AHD heights from GPS using AUSGEOID93, *The Australian Surveyor*, Vol. 39, No. 1, pp. 21-27.

Stewart, M.P. (1990) Computation of a gravimetric geoid for the British Isles: an assessment of Fourier and classical techniques, *PhD Thesis*, University of Edinburgh, Edinburgh, United Kingdom, 167 pp.

Stirling, M.W. (1992) Late Holocene beach ridges displaced by the Wellington fault in the Lower Hutt area, New Zealand, *New Zealand Journal of Geology and Geophysics*, Vol. 35, No. 4, pp. 447-453.

Stokes, G.G. (1849) On the variation of gravity at the surface of the Earth, *Transactions of the Cambridge Philosophical Society*, Vol. 8, pp. 672-695.

Strang van Hees, G. (1990) Stokes formula using fast Fourier techniques, *manuscripta geodaetica*, Vol. 15, No. 4, pp. 235-239.

Strange, W.E. (1982) An evaluation of orthometric heights accuracy using borehole gravimetry, *Bulletin Géodésique*, Vol. 56, No. 4, pp. 300-311, doi: 10.1007/BF02525730.

Strykowski, G. and Forsberg, R. (1998) Operational merging of satellite airborne and surface gravity data by draping techniques, in: Forsberg, R., Feissl, M. and Dietrich, R. (Eds.) *Geodesy on the Move*, Springer, Berlin, Germany, pp. 207-212.

Subiza Piña W.H., Rovera Di Landro, H. and Turban, L. (2002) The vertical datum and local geoid models in Uruguay, in: Drewes, H., Dodson, A., Fortes, L.P.S., Sánchez, L. and Sandoval, P. (Eds.), *Vertical Reference Systems*, Springer, Berlin, Germany, pp. 169-175.

Sun, W. and Vaníček, P. (1998) On some problems of the downward continuation of the 5' x 5' mean Helmert gravity disturbance, *Journal of Geodesy*, Vol. 72, No. 7-8, pp. 411-420, doi: 10.1007/s001900050180.

Sünkel, H. (1986) Digital height and density model and its use for the orthometric height and gravity field determination for Austria, *Proceedings of the International Symposium on the Definition of the Geoid*, Florence, Italy, pp. 599-604.

Tapley, B.D., Watkins, M.M., Ries, J.C., Davis, G.W., Eanes, R.J., Poole, S.R., Rim, H.J., Schutz, B.E., Shum, C.K., Nerem, R.S., Lerch, F.J., Marshall, J.A., Klosko, S.M., Pavlis, N.K. and Williamson, R.G. (1996) The joint gravity model 3, *Journal of Geophysical Research*, Vol. 101, No. B12, pp. 28029-28049, doi: 10.1029/96JB01645, [coefficients available from http://icgem.gfz-potsdam.de/ICGEM/shms/jgm3.gfc].

Tapley, B.D., Chambers, D.P., Cheng, M.K., Kim, M.C., Poole, S.R. and Ries, J.C. (2000) The TEG-4 Earth gravity field model, *Paper presented at the XXV General Assembly of the European Geophysical Society*, Nice, France, [coefficients available from: http://icgem.gfz-potsdam.de/ICGEM/shms/teg4.gfc].

Tapley, B.D., Bettadpur, S., Watkins, M. and Reigber, C. (2004) The gravity recovery and climate experiment: mission overview and early results, *Geophysical Research Letters*, Vol. 31, No. 9, L09607, doi: 10.1029/2004GL019920 [coefficients available from: http://www.csr.utexas.edu/grace/gravity/ggm01].

Tapley, B.D., Ries, J., Bettadpur, S., Chambers, D., Cheng, M., Condi, F., Gunter, B., Kang, Z., Nagel, P., Pastor, R., Poole, S. and Wang, F. (2005) GGM02 – an improved Earth gravity field model from GRACE, *Journal of Geodesy*, Vol. 79, No. 8, pp. 467-478, doi: 10.1007/s00190-005-0480-z [coefficients available from: http://www.csr.utexas.edu/grace/gravity].

Teferle, N. (2000) Continuous GPS measurements at UK tide gauge sites, 1997 – 2000, in: *Proceedings of the 13th International Technical Meeting of the Satellite Division of the Institute of Navigation ION GPS-2000*, 19-22 September, Salt Lake City, Utah, USA.

Teferle, F.N., Bingley, R.M., Waugh, A.I., Dodson, A.H., Williams, S.D.P. and Baker, T.F. (2007) Sea level in the British Isles: combining absolute gravimetru and continuous GPS to infer vertical land movements at tide gauges, in: Tregoning, P. and Rizos, C. (Eds.) *Dynamic Planet*, Springer, Berlin, pp. 23-30.

Tenzer, R., Vaníček, P., Santos, M., Featherstone, W.E. and Kuhn, M. (2005) The rigorous determination of orthometric heights, *Journal of Geodesy*, Vol. 78, No. 1-3, pp. 82-92, doi: 10.1007/s00190-005-0445-2.

Tenzer, R., Novák, P., Moore, P., Kuhn, M. And Vaníček, P. (2006) Explicit formula for the geoid-quasigeoid separation, *Studia Geophysica et Geodaetica*, Vol. 50, No. 4, pp. 607-618, doi: 10.1007/s11200-006-0038-4.

Torge, W. (2001) *Geodesy*, 3rd Edition, Walter de Gruyter, Berlin, Germany, 416 pp.

Torge, W. (1989) *Gravimetry*, Walter de Gruyter, Berlin, Germany, 477 pp.

Tscherning, C.C. (2005) Comments and reply regarding Heck (2003) "On Helmert's methods of condensation", *Journal of Geodesy*, Vol. 78, No. 7-8, pp. 457-461, doi: 10.1007/s00190-004-0412-3.

Tscherning, C.C., Forsberg, R. and Knudsen, P. (1992) The GRAVSOFT package for geoid determination, in: Holota, P. and Vermeer, M. (Eds.) *Proceedings of the 1st Continental Workshop on the Geoid in Europe*, May 11-14, Prague, Czech Republic, pp. 327-334.

Tsoulis, D.V. (1998) A combination method for computing terrain corrections, *Physics and Chemistry of the Earth*, Vol. 23, No. 1, pp. 53-58, doi: 10.1016/S0079-1946(97)00241-3.

Tsoulis, D. (2001) Terrain correction computations for a densely sampled DTM in the Bavarian Alps, *Journal of Geodesy*, Vol. 75, No. 5-6, pp. 291-307, doi: 10.1007/s001900100176.

Tsoulis, D. (2003) Terrain modelling in forward gravimetric problems: a case study on local terrain effects, *Journal of Applied Geophysics*, Vol. 54, No. 1-2, pp. 145-160, doi: 10.1016/j.jappgeo.2003.09.001.

Tziavos, I.N. (1996) Comparisons of spectral techniques for regional geoid computations over large regions, *Journal of Geodesy*, Vol. 70, No. 6, pp. 357-373, doi: 10.1007/BF00868188.

Tziavos, I.N. and Featherstone, W.E. (2001) First results of using digital density data in gravimetric geoid computation in Australia, in: Gravity, *Geoid and Geodynamics 2000*, Sideris, M.G. (Ed.), Springer, Berlin, Germany, pp. 335-340.

Tziavos, I.N., Sideris, M.G., Forsberg, R. and Schwarz, K.P. (1988) The effect of the terrain on airborne gravity and gradiometry, *Journal of Geophysical Research*, Vol. 93, No. B8, pp. 9173-9186.

Tziavos, I.N., Sideris, M.G. and Sünkel, H. (1996) The effect of surface density variation on terrain modelling – a case study in Austria, in: *Techniques for Local Geoid Determination, Proceedings Session G7, European Geophysical Society XXI General Assembly*, Tziavos, I.N. and Vermeer, M. (Eds.), Finnish Geodetic Institute, Masala, Finland, pp. 99-110.

van Olsen, K. and van Gelderen, M. (1988) Quality investigation of vertical height datum connection, *Physics and Chemistry of the Earth*, Vol. 23, No. 9-10, pp. 1103-1108.

Vaníček, P. and Featherstone, W.E. (1998) Performance of three types of Stokes's kernel in the combined solution of the geoid, *Journal of Geodesy*, Vol. 72, No. 12, pp. 684-697, doi: 10.1007/s001900050209.

Vaníček, P. and Kleusberg, A. (1987) The Canadian geoid – Stokesian approach, *manuscripta geodaetica*, Vol. 12, No. 2, pp. 86-98.

Vaníček, P. and Krakiwsky, E. (1986) *Geodesy, the Concepts*, second edition, North Holland, Amsterdam, The Netherlands, 697 pp.

Vaníček, P. and Martinec, Z. (1994) Stokes-Helmert scheme for the evaluation of a precise geoid, *manuscripta geodaetica*, Vol. 19, No. 2, pp. 119-128.

Vaníček, P. and Merry, C.L. (1973) Determination of the geoid from deflections of the vertical using a least-squares fitting technique, *Bulletin Géodésique*, Vol. 47, No. 3, pp. 261-279, doi: 10.1007/BF02525574.

Vaníček, P. and Sjöberg, L.E. (1991) Reformulation of Stokes's theory for higher than second-degree reference field and modification of integration kernels, *Journal of Geophysical Research*, Vol. 96, No. B4, pp. 6529-6539.

Vaníček, P., Castle, R.O. and Balazs, E.I. (1980) Geodetic levelling and its applications, *Reviews of Geophysics and Space Physics*, Vol. 18, No. 2, pp. 505-524.

Vaníček, P., Kleusberg, A., Martinec, Z., Sun, W., Ong, P., Najafi, M., Vadja, P., Harrie, L., Tomasek, P. and ter Horst, B. (1995) *Compilation of a precise regional geoid*, Report for Geodetic Survey Division, Geomatics Sector, Natural Resources Canada, Ottawa, Canada.

Vaníček, P., Sun, W., Ong, P., Martinec, Z., Najafi, M., Vadja, P. and Ter Host, B. (1996) Downward continuation of Helmert's gravity anomaly, *Journal of Geodesy*, Vol. 71, No. 1, pp. 21-34, doi: 10.1007/s001900050072.

Vaníček, P., Huang, J., Novák, P., Pagiatakis, M., Véronneau, M., Martinec, Z. and Featherstone, W.E. (1999) Determination of the boundary values for the Stokes-Helmert problem, *Journal of Geodesy*, Vol. 73, No. 4, pp. 180-192, doi: 10.1007/s001900050235.

Vaníček, P., Novák, P. and Martinec, Z. (2001) Geoid, topography, and the Bouguer plate or shell, *Journal of Geodesy*, Vol. 75, No. 4, pp. 210-215, doi: 10.1007/s001900100165.

Vaníček, P., Tenzer, R., Sjöberg, L.E., Martinec, Z. and Featherstone, W.E. (2004) New views of the spherical Bouguer gravity anomaly, *Geophysical Journal International*, Vol. 159, No. 2, pp. 460-472, doi: 10.1111/j.1365-246X.2004.02435.x.

Vergos, G.S., Tziavos, I.N. and Sideris, M.G. (2006) On the validation of CHAMP- and GRACE-type GGMs and the construction of a combined model, *Geodezja I Kartografia, Geodesy and Cartography*, Vol. 55, No. 3, pp. 115-131.

Véronneau, M. (2002) *The Canadian gravimetric geoid model of 2000 (CGG2000)*, Geodetic Survey Division, Natural Resources Canada, Ottawa, Canada, 17 pp., available from: www.geod.nrcan.gc.ca/publications/papers/cgg2000a.pdf.

Véronneau, M., Duval, R. and Huang, J. (2006) A gravimetric geoid model as a vertical datum in Canada, *Geomatica*, Vol. 60, No. 1, pp. 165-172.

Vestøl, O. (2006) Determination of postglacial land uplift in Fennoscandia from levelling, tide-gauges and continuous GPS stations using least squares collocation, *Journal of Geodesy*, Vol. 80, No. 5, pp. 248-258, doi: 10.1007/s00190-006-0063-7.

Vincent, S. and Marsh, J.G. (1973) Global detailed gravimetric geoid, in: *Proceedings of the International Symposium on the use of Artificial Satellites for Geodesy and Geodynamics*, in: Veis, G. (Ed.), Athens, Greece, pp. 825-855.

Walcott, R.I. (1984) The kinematics of the Plate Boundary Zone through New Zealand: a comparison of short- and long-term deformations, *Geophysical Journal of the Royal Astronomical Society*, Vol. 79, No. 2, pp. 613-633.

Wang, Y.M. (1988) Downward continuation of the free-air gravity anomalies to the ellipsoid using the gradient solution, Poisson's integral and terrain correction-numerical comparison and the computations, *Report 393*, Department of Geodetic Science, Ohio State University, Columbus, USA, 37 pp.

Wang, Y.M. (2001) GSFC00 mean sea surface, gravity anomaly, and vertical gravity gradient from satellite altimeter data, *Journal of Geophysical Research*, Vol. 106, No. 12, pp. 31167-31174.

Wang, Y.M. and Rapp, R.H. (1990) Terrain effects on geoid undulation computations, *manuscripta geodaetica*, Vol. 15, No. 1, pp. 23-29.

Wellman, H.W. (1979) An uplift map for the South Island of New Zealand, and a model for uplift of the Southern Alps, in Walcott R.I. and Cresswell, M.M. (Eds.), *The Origin of the Southern Alps*, Bulletin 18, Royal Society of New Zealand, Wellington, New Zealand, pp. 13-20.

Wenzel, H.-G. (1983) Geoid computation by least-squares spectral combination using integral kernels, *Proceedings of the International Association of Geodesy General Meeting*, Tokyo, Japan, pp. 825-855.

Wenzel, H.-G. (1998) Ultra-high degree geopotential models GPM98A, B and C to degree 1800 tailored to Europe, in: Vermeer, M. and Ádám, J. (Eds.), *Report 98:4, Second Continental Worksop on the Geoid*, Finnish Geodetic Institute, Masala, Finland, pp. 71-80.

Wessel, P. and Smith W.H.F. (1998) New, improved version of the Generic Mapping Tools released, *EOS Transactions American Geophysical Union*, Vol. 79, No. 47, p. 579.

Wessel, P. and Watts, A.B. (1988) On the accuracy of marine gravity measurements, *Journal of Geophysical Research*, Vol. 94, No. B4, pp. 7685-7729.

Wichiencharoen, C. (1982) The indirect effects on the computation of geoid undulations, *Report 336*, Department of Geodetic Science and Surveying, Ohio State University, Columbus, USA, 96 pp.

Wong, J.C.F. (2002) On Picard criterion and the well-posed nature of harmonic downward continuation, *GGE Technical Report 213*, Department of Geodesy and Geomatics Engineering, University of New Brunswick, Fredericton, Canada, 85 pp.

Wong, L. and Gore, R. (1969) Accuracy of geoid heights from modified Stokes kernels, *Geophysical Journal of the Royal Astronomical Society*, Vol. 18, pp. 81-91.

Woodward, D.J. (1982) Reduction of gravity observations on the VAX11/780 computer, *Technical Note 83*, Geophysics Division, Department of Scientific and Industrial Research, Wellington, New Zealand, 12 pp.

Woodward, D.J. and Ferry, L.M. (1973) Gravity terrain correction tables, *Technical Note 66*, Geophysics Division, Department of Scientific and Industrial Research, Wellington, New Zealand, 27 pp.

Woodworth, P.L., Tsimplis, M.N., Flather, R.A. and Shennan, I. (1999) A review of the trends observed in British Isles mean sea level data measured by tide gauges, *Geophsical Journal International*, Vol.136, No. 3, pp. 651-670, doi: 10.1046/j.1365-246.x.1999.00751.x.

Wu, P., Johnston, P. and Lambeck, K. (1999) Postglacial rebound and fault instability in Fennoscandia, *Geophysical Journal International*, Vol. 139, No. 3, pp. 657-670, doi: 10.1046/j.1365-246x.1999.00963.x.

Xu, P. (1992) A quality investigation of global vertical datum connection, *Geophysical Journal International*, Vol. 110, No. 2, pp. 361-370.

Xu, P. and Rummel, R. (1991) A quality investigation of global vertical datum connection, *New Series No 34*, Netherlands Geodetic Commission, Delft, The Netherlands, 51 pp.

Zelin, G. and Zuofa, L. (1992) Modified Stokes's integral formulas using FFT, *manuscripta geodaetica*, Vol. 17, No. 4, pp. 227-232.

Zhang, K.F. (1997) An evaluation of FFT geoid determination techniques and their application to Australian GPS heighting, *Ph.D. thesis*, School of Surveying and Land Information, Curtin University of Technology, Perth, Australia

Zilkoski, D.B., Richards, J.H. and Young, G.M. (1992) Results of the general adjustment of the North American Vertical Datum of 1988, *Surveying and Land Information Systems*, Vol. 52, No. 3, pp. 133-149.

APPENDIX A - GLOBAL GEOPOTENTIAL MODELS

A.1 Introduction

This Appendix describes the three main types of GGM that are available for use in regional geoid computations. It also provides a brief description of the current satellite gravimetry missions that are providing information on the Earth's gravity field. It concludes with a series of graphs showing the merged GGMs compared in Section A.4.

A.2 Types of GGM

GGMs can be classified according to the data and method of their computation, namely: satellite only, combined, and tailored (e.g., Rapp, 1997b; Balmino *et al*., 1999; Featherstone, 2002b; Rummel *et al*., 2002).

A.2.1 Satellite-only GGMs

Satellite-only GGMs are derived from the analysis of satellite-based gravity observations. The accuracy and precision of satellite-only GGMs was historically limited by factors such as (from Featherstone, 2002b): the power-decay of the gravitational field with increasing altitude; the requirement to track complete satellite orbits using ground-based stations; imprecise modelling of non-Earth gravity field induced satellite motions such as atmospheric drag and third-body influences; and the incomplete sampling of the global gravity field due to limitations in the coverage of the satellite ground-tracks.

This means that although some satellite-only GGMs are available above degree 70 (cf. Table 3.1), the higher degree coefficients, say greater than 20 (e.g., Vaníček and Sjöberg, 1991) or 30 (e.g., Rummel *et al*., 2002), are heavily contaminated by noise (cf. Koch, 2005). However, several of the above limitations have now been redressed by the use of the dedicated satellite gravimetry missions, whose concepts are summarised in, for example, Tapley *et al*. (2004), Rummel *et al*. (2002) and Featherstone (2002b). It can be seen by comparing UCPH2002_02 (Figure A.4) and the more recent GGMs, based on additional satellite mission data, such as GGM02S (Figure A.8) and EIGEN-GRACE02S (Figure A.10) that the error degradation in

degrees 20 to 100 is significantly reduced. Koch (2005) found that for a CHAMP derived GGMs that the use of coefficients above degree 62 added no extra information to the geopotential model. Reigber *et al*. (2005b) and Mayer-Gürr *et al*. (2005) found similar results (maximum GGM power at degree 60-65) with GRACE data.

A.2.2 Combined GGMs

Combined GGMs are derived from the combination of satellite-based data, land and marine terrestrial gravity observations, airborne gravity data and also marine anomalies derived from satellite radar altimetry (cf. Section 3.5; e.g., Nerem *et al*., 1995; Rapp, 1997b). This combined solution generally enables the maximum degree of harmonic expansion of the GGM to be increased due to the higher resolution of the terrestrial data.

It is important to note that the quality of combined models is limited by the quality of their input data. Namely, the same problems of the (older) satellite GGMs described in Section A.2.1 and also by the spatial distribution and quality of the terrestrial data. An example of this is the distortions in and offsets among the different vertical datums used to reduce terrestrial gravity anomalies can cause long-wavelength errors (Heck, 1990) can generate low-frequency errors in the GGMs if not properly removed by high-pass filtering (cf. Vaníček and Featherstone, 1998).

A.2.3 Tailored GGMs

Tailored GGMs build on an existing satellite-only or combined GGM using additional gravity data to extend the solution to higher degrees. This is normally achieved through the application of integral formulae to apply "corrections" to the existing geopotential coefficients and to add new ones. The main drawback with (regionally) tailored GGMs is that they are only applicable to the area that they have been tailored over because spurious effects occur outside the computation area (e.g., Li, 1993; Kearsley and Forsberg, 1990; Featherstone, 2002b).

A.3 Satellite Gravity Missions

The estimated quality of the satellite-derived component of the GGMs will be improved by the inclusion of data from the different dedicated satellite gravity missions. The CHAllenging Mini-satellite Payload (CHAMP) and Gravity Recovery and Climate Experiment (GRACE) missions have been launched and Gravity field and steady state Ocean Circulation Explorer (GOCE) is currently planned for late 2007. Each mission is described in the following Sections.

A.3.1 CHAMP

The German CHAllenging Mini-satellite Payload (CHAMP) mission consists of a dedicated gravimetry satellite (launched 15 July 2000) in a near-circular orbit at an initial altitude of 454 km and an inclination of 87.3º (Reigber *et al*., 2002). The satellite uses the high-low satellite-to-satellite tracking (hl-SST) system where high-Earth orbiting satellites (notably GPS) are used to determine its position (Figure A.1).

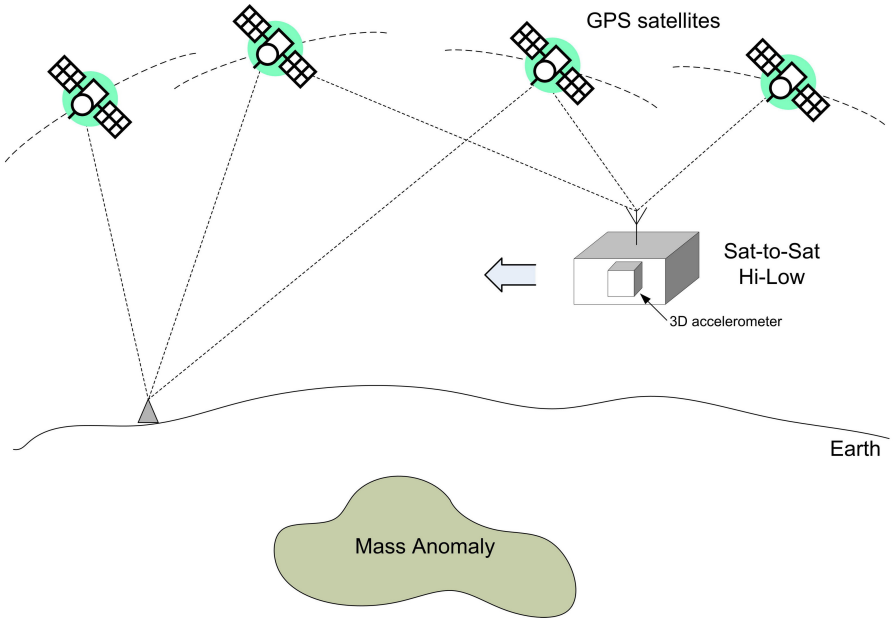

Figure A.1 The CHAMP concept of satellite-to-satellite tracking in the high-low mode (adapted from Rummel *et al*., 2002)

This allows a near-global coverage of gravity field data that was previously unavailable with ground tracked satellites at limited inclinations. The CHAMP satellite also houses a three-axis accelerometer to help reduce the effect of non-

gravitational perturbations (Schwintzer *et al.*, 2000). The CHAMP satellite has produced global gravity models that identify features with a size of a few thousand kilometres (ESA, 2006).

A.3.2 GRACE

The Gravity Recovery and Climate Experiment (GRACE) is a joint German-United States dedicated satellite mission (launched 17 March 2002) whose objective is to map the global gravity field with a spatial resolution of 400 km to 40,000 km every 30 days (Tapley *et al.*, 2004). The mission consists of two identical satellites equipped with micro-accelerometers in near-circular orbits of 450 km altitude and separated by approximately 240 km along track (Figure A.2). The twin GRACE satellites use the low-low satellite-to-satellite tracking configuration to measure the distance between them (e.g., Featherstone, 2003d).

Like CHAMP, the GRACE satellites are also tracked by high-Earth orbiting (GNSS) satellites (hl-SST) giving a near-global coverage (Rummel *et al.*, 2002). The GRACE mission aims to map the temporal changes in the Earth's gravity field by producing monthly solutions for features with a size as small as 600 km to 1,000 km (ESA, 2006).

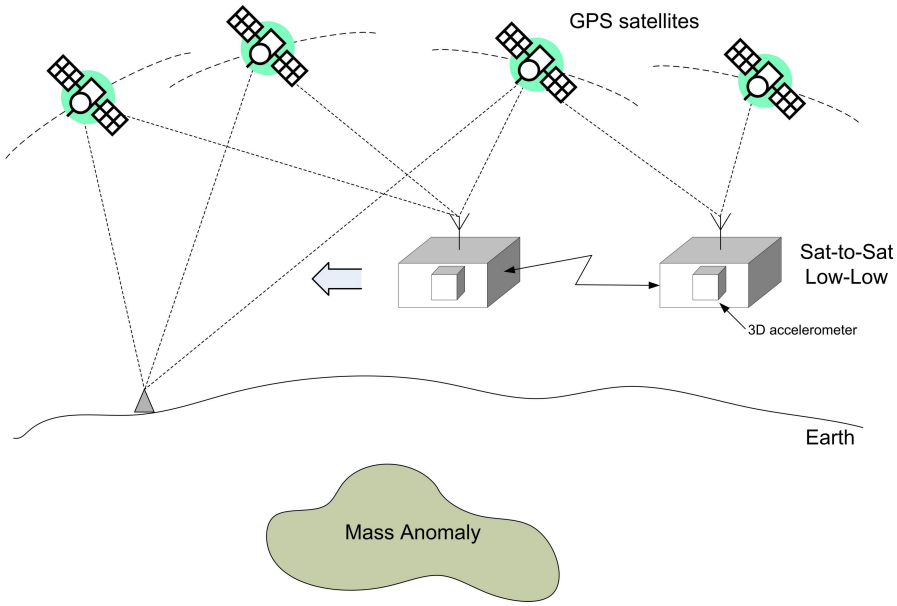

Figure A.2 The GRACE concept of satellite-to-satellite tracking in the low-low mode combined with satellite-to-satellite tracking in the high-low mode (adapted from Rummel *et al.*, 2002)

A.3.3 GOCE

The Gravity field and steady state Ocean Circulation Explorer (GOCE) satellite is being developed by the European Space Agency (ESA) with a scheduled launch date in 2007. It has the mission to measure the Earth's gravity field and model the geoid with extremely high accuracy and resolution (Drinkwater *et al*., 2003). GOCE will use the hl-SST configuration with GPS and GLONASS (Globalnaya Navigaysionnaya Sputnikovaya Sistema) GNSS satellites. It differs from CHAMP and GRACE in that it uses a 3-D gravity gradiometer (consisting of three pairs of accelerometers) to measure the Earth's gravity field in three-dimensions without a preferred direction (Figure A.3).

GOCE is expected to generate a global geoid with a resolution better than 100 km and an accuracy of 1-2 cm (ESA, 2006). It will complement the GRACE mission (which concentrates more on temporal gravity changes) by focussing on attaining the maximum spatial resolution (Rummel *et al*., 2002). The data from the GOCE mission has the potential to significantly improve the quality of high-resolution regional geoids that are currently available (Featherstone, 2003d).

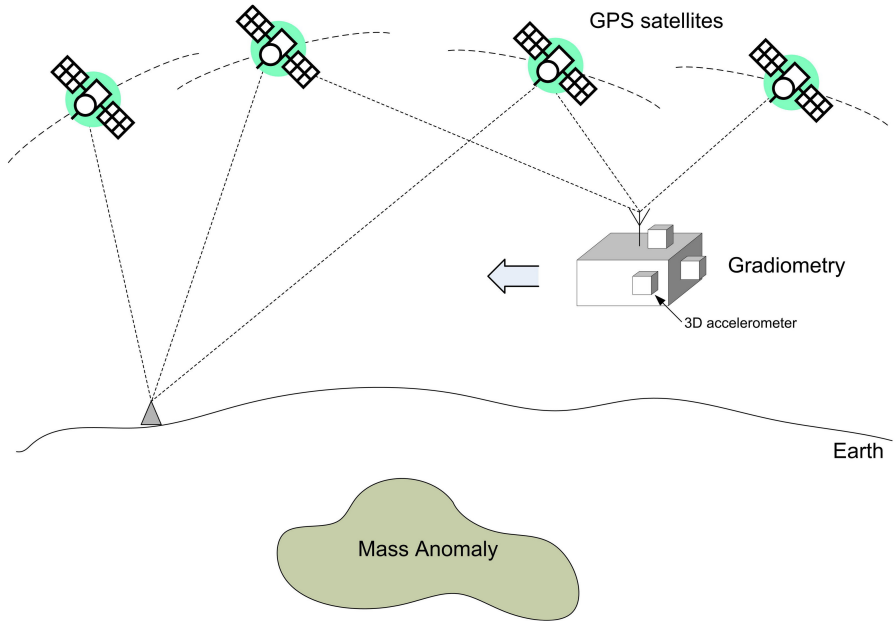

Figure A.3 The GOCE concept of satellite gradiometry combined with satellite-to-satellite tracking in the high-low mode (adapted from Rummel *et al*., 2002)

A.4 Merged GGMs

Merged GGMs are formed by combining two existing GGMs to exploit the advantages of both (cf. Vergos *et al.*, 2006). A detailed description is provided in Section 3.2.2. This Section provides graphs showing the different merged GGMs that have been used in this study.

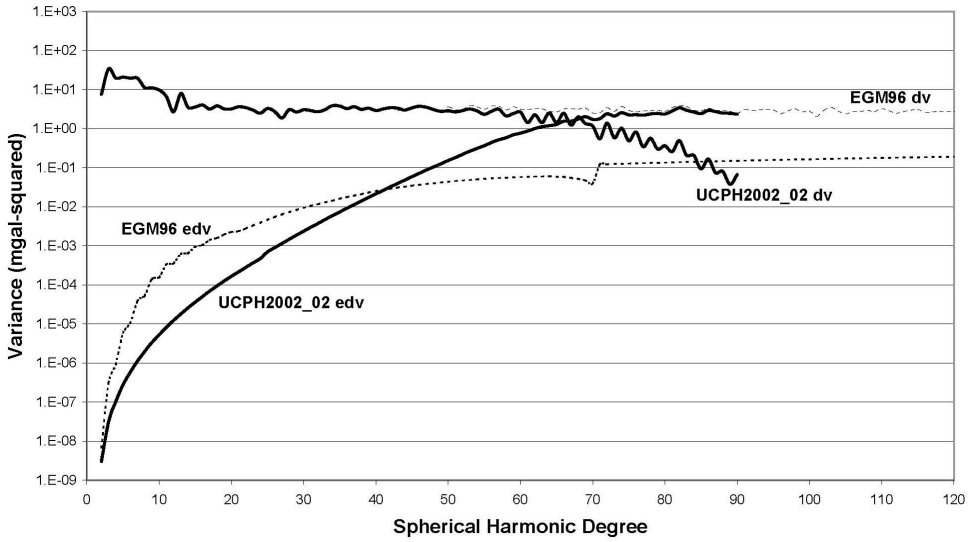

Figure A.4 Error-degree (edv) and degree (dv) variance of UCPH2002_02 and EGM96 global geopotential models

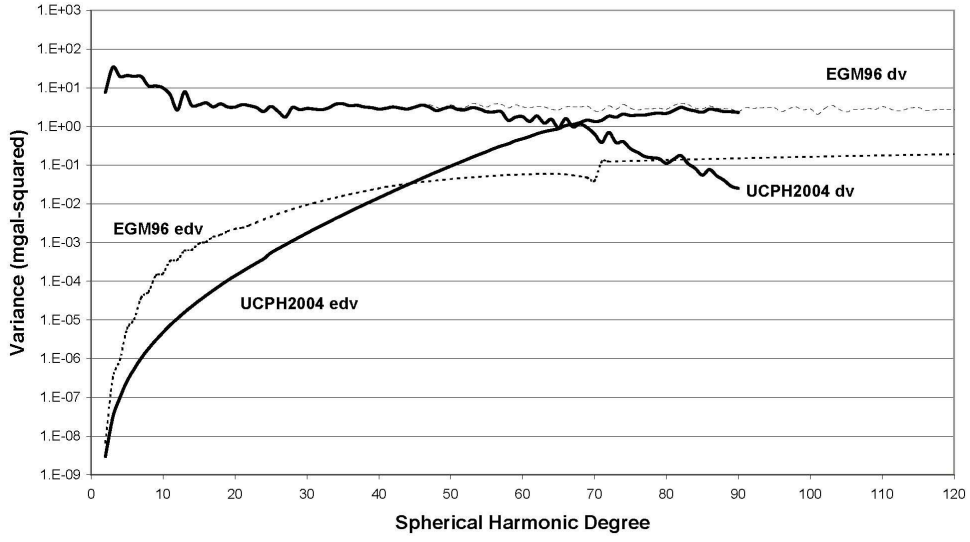

Figure A.5 Error-degree (edv) and degree (dv) variance of UCPH2004 and EGM96 global geopotential models

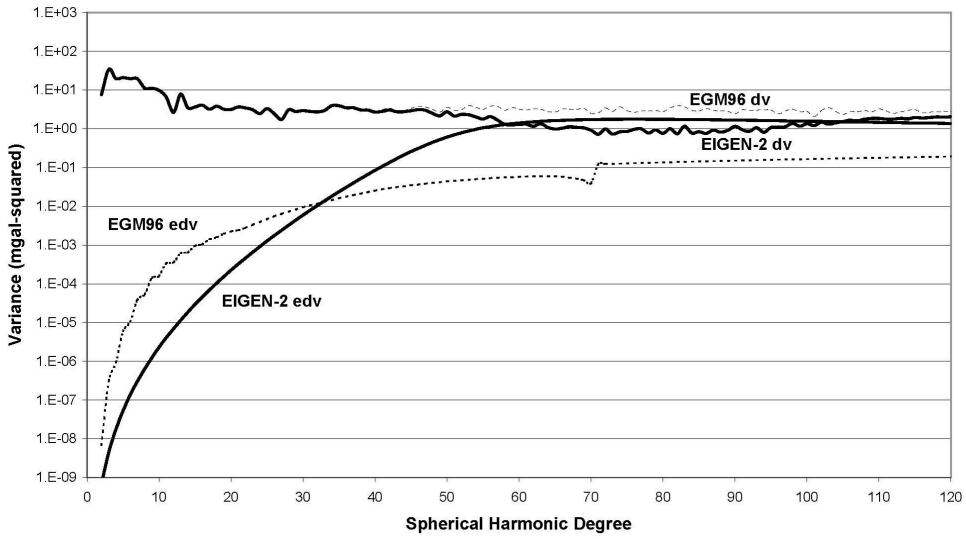

Figure A.6 Error-degree (edv) and degree (dv) variance of EIGEN-2 and EGM96 global geopotential models

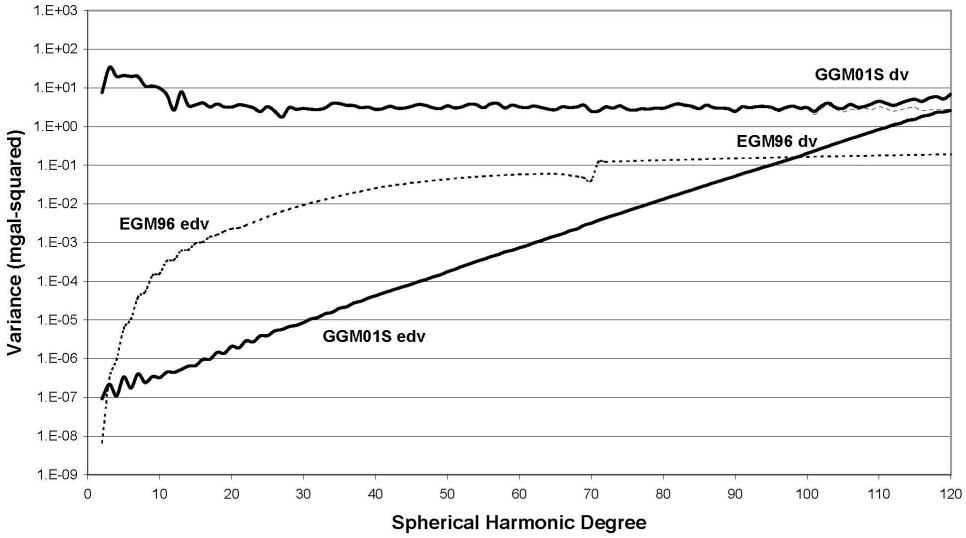

Figure A.7 Error-degree (edv) and degree (dv) variance of GGM01S and EGM96 global geopotential models

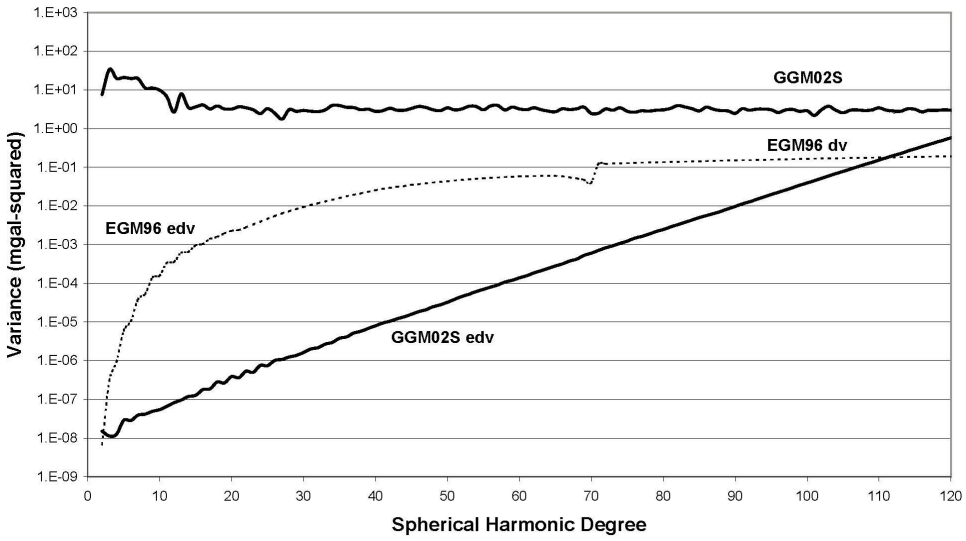

Figure A.8 Error-degree (edv) and degree (dv) variance of GGM02S and EGM96 global geopotential models

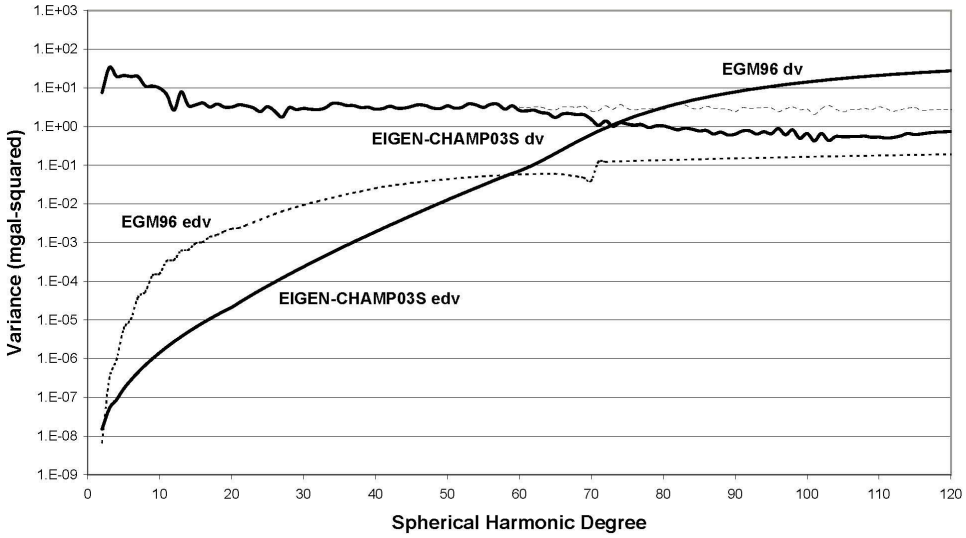

Figure A.9 Error-degree (edv) and degree (dv) variance of EIGEN-CHAMP03S and EGM96 global geopotential models

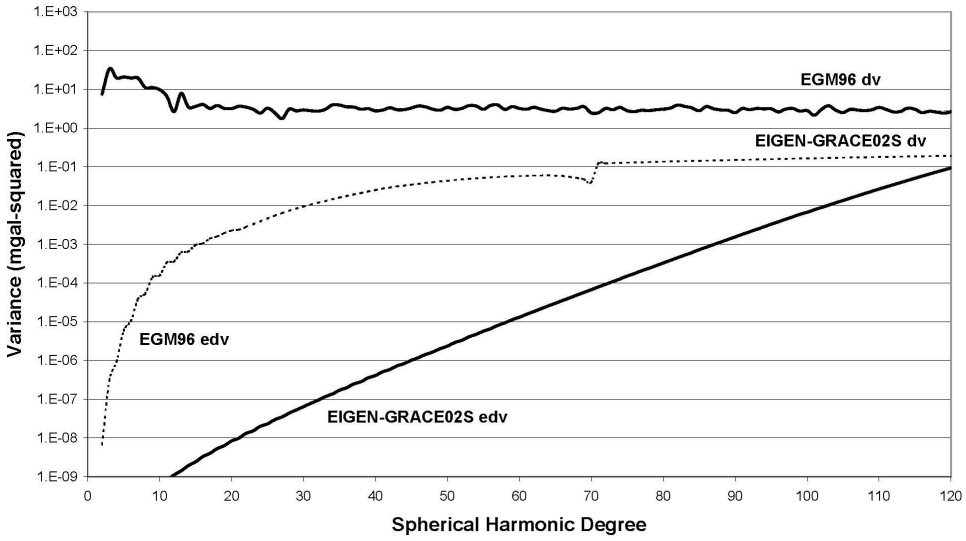

Figure A.10 Error-degree (edv) and degree (dv) variance of EIGEN-GRACE02S and EGM96 global geopotential models

APPENDIX B - LAND GRAVITY DATA AND PROCESSING

B.1 Introduction

The gravity database supplied by GNS Science (www.gns.cri.nz) comprises 40,737 gravity observations acquired for mapping purposes that cover the main islands in the New Zealand (North, South and Stewart/Rakiura) and Chatham (Chatham and Pitt) Island groups (Figure 3.2), a number of smaller offshore islands and 176 sea-floor observations in the Tasman and Golden Bays in the north of the South Island (Figure B.1). The database includes gravity observations, corrections, and other auxiliary information (cf. Table B.1).

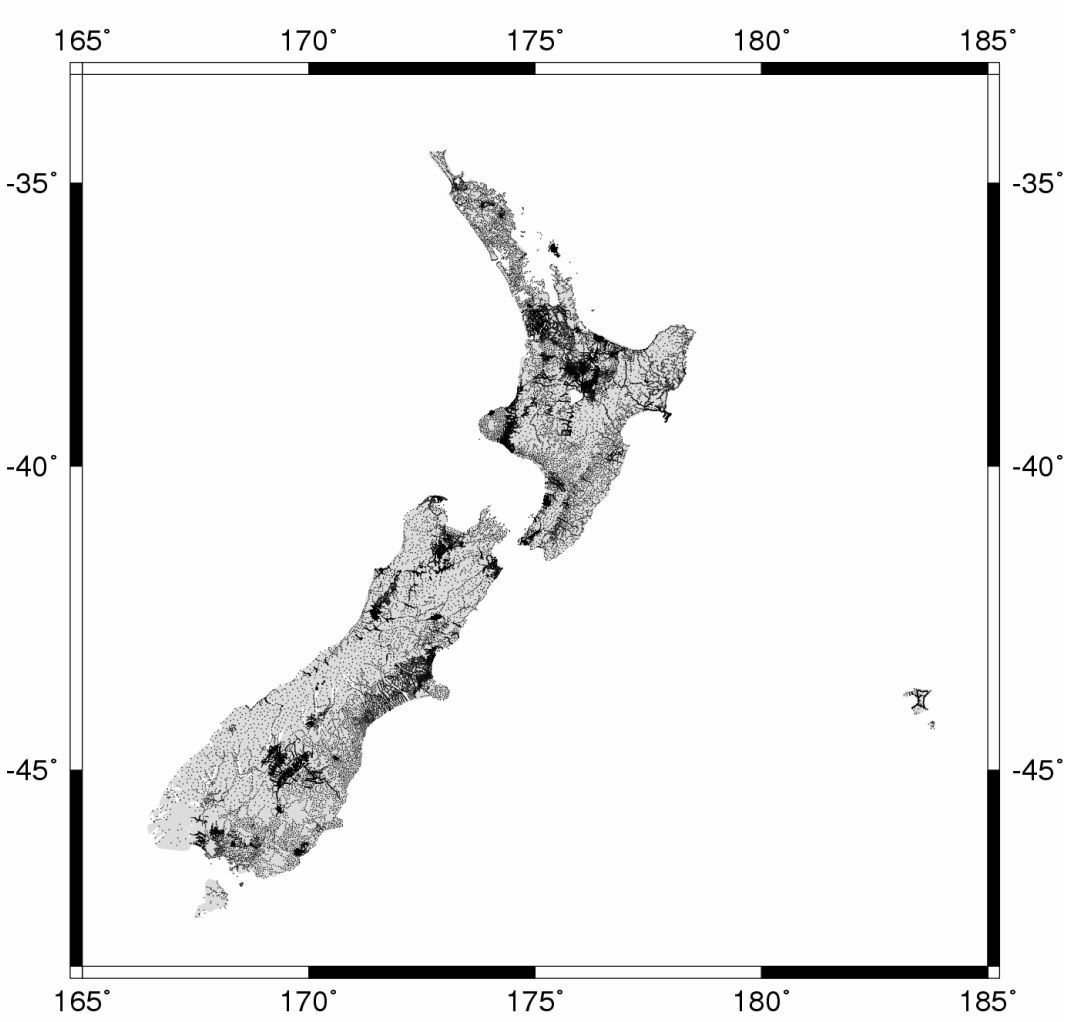

Figure B.1 New Zealand and Chatham Islands land gravity coverage (Mercator projection)

The approximate average spatial density of these data is one observation per 7.5 km-squared, but this is higher in areas of scientific or commercial interest and lower in areas where it is impractical or difficult to collect ground gravity data (notably in mountainous areas). Because the observations were originally reduced for geophysical mapping purposes at the time (Reilly, 1972), it was necessary to re-compute the gravity anomalies to more stringent geodetic requirements to enable their use in gravimetric geoid computations (e.g., Featherstone and Dentith, 1997). While the differences between the reduction schemes are small, they are systematic, so it is essential for them to be re-computed (Featherstone, 1995).

B.2 Horizontal datum transformation

The observations are numbered sequentially according to the 1:250,000 geological mapping sheets in which they fall. The observation coordinates are in terms of three different transverse Mercator projections shown in Table B.2. The datum used depends on the map sheet that the observation is located. The North and South Island projections in Table B.2 are in terms of the NZ Geodetic Datum 1949 (NZGD49) datum (Lee, 1978) and the Chatham Island projection is in terms of the Chatham Islands datum 1971. Both datums use the International 1924 reference spheroid/ellipsoid (a = 6,378.388 km, f = 1/297, Hayford, 1909).

The horizontal coordinates of each station were estimated from the most detailed topographic maps available at the time of observation. Where NZ Map Service Series 1 (NZMS 1) National Yard Grid maps were available (1:63,360) the coordinates are estimated to be accurate to around 100 yards (~100 metres). Where it was necessary to use NZMS 10 (1:253,440) or the later NZMS 18 (1:250,000) the accuracy may be at worst 1 km to 2 km (Reilly, 1972). As well as causing incorrect mapping, erroneous positions can also cause an error in the computation of the gravity anomaly, e.g. 100 m position variation ≅ 0.1 mGal in normal gravity (cf. Equation 3.5).

Record	Description
Sheet Number	Refers to 1:250,000 Geological Map Series (sheets 1-12 North Island; 13-27 South Island; and 523 Chatham Island
Station Number	Sequential number for each sheet
Easting	Yards, based on a different NZGD49 transverse Mercator projection for North, South and Chatham Islands.
Northing	Yards, based on a different NZGD49 transverse Mercator projection for North, South and Chatham Islands.
Height (metres)	Metres
Height Type	0 = Benchmark, 1 = spot height, 2 = barometric height
Gravity	μN/kg in New Zealand Potsdam System (Robertson and Reilly, 1960) less 9,750,000 (1 μN/kg = 0.1 mGal)
Gravimeter Code	Identifier of gravimeter (cf. Table 4 in Woodward, 1982)
Date of Observation	In yymmdd format (all years in 1900s)
Inner Terrain Correction	Calculated from Hammer charts, outer radius depends on terrain code
Outer Terrain Correction	Calculated from Hammer charts to 22.4 kilometres
Terrain Code	Method of terrain calculation (cf. Table 1 in Woodward, 1982)
Topographic Correction	Correction for topography from 22.4 to 166 kilometres
Free-Air Anomaly	Calculated according to Reilly (1972) using the International gravity Formula 1930
Bouguer Anomaly	Calculated according to Reilly (1972) using a Bouguer plate and constant density, and also accounting for the indirect effect and the above terrain corrections
Isostatic Anomaly	Calculated according to Reilly (1972) using the Airy-Heiskanen model
Observer Code	Identifier of observer (cf. Table 2 in Woodward, 1982)
Authority Code	Identifier of observing agency (cf. Table 3 in Woodward, 1982)

Table B.1 Data fields in GNS Science terrestrial gravity database (from Woodward, 1982)

Datum	Longitude Origin	Latitude Origin	False Easting (Yards)	False Northing (Yards)
North Island Yard Grid	175° 30’ E	39° 06’ S	300,000.0	400,000.0
South Island Yard Grid	171° 30’ E	44° 06’ S	500,000.0	500,000.0
Chatham Island TM 1979	176° 30’ W	44° 00’ S	400,000.0	800,000.0

Table B.2 Transverse Mercator projections used for the GNS Science gravity database

Before the observations can be reprocessed, it is necessary to transform the horizontal coordinates to a geocentric datum. For convenience and consistency with the other New Zealand datasets, NZ Geodetic Datum 2000 (NZGD2000, cf. Section 2.4.7) was used. The transformation was carried out using the LINZ *CONCORD* coordinate conversion software (www.linz.govt.nz/downloadsoftware). This software first converts the projection coordinates to NZDG49 geodetic coordinates and then implements the LINZ transformation grid (Pearse and Crook, 1997) to convert coordinates between the NZGD49 and NZGD2000/World Geodetic System 1984 (WGS84) datums (Crook and Pearse, 2001). The transformation grid is the official method of converting between the two systems (seven and three parameter options are also available) and gives a transformation accuracy of better than 10 cm. Given the accuracy of the horizontal coordinates (100 m to 2 km) this method is more than adequate.

B.3 Observation heights

The heights of the observations are given in metres. However, the source, calculation method and consequently the accuracy of the heights is varied. The types of height are indicated in Table B.1. Benchmark heights are generally determined by precise levelling and have an accuracy of 10 cm – 15 cm (cf. Section 2.4.2). Observations located at spot heights on topographic maps (located from map in the field) have a nominal accuracy of 5 m (NTHA, 2006). The majority of the gravity observations have heights obtained from barometric levelling (cf. Woodward, 1982; Reilly and Woodward, 1971). Reilly (1972) indicates that under ideal circumstances the accuracy of this technique is probably in the range of 2 m to 5 m. However, under windy conditions in mountainous areas (which is not uncommon in NZ) the accuracy could fall to 10 m to 20 m. It is not clear which vertical datum the heights are in terms of. Therefore, it is assumed that they are in relation to the nearest local datum (cf. Sections 2.4 and 6.5.1).

B.4 Gravity datum shift

The gravity values, and hence the pre-computed gravity anomalies, in the GNS Science land gravity database are referred to the Potsdam (New Zealand) gravity datum 1959 (Robertson and Reilly, 1960). It has been known for a long time that the

Potsdam datum contains an error (e.g., Torge, 1989). Therefore, a constant value of 15.27 mGal (e.g., Hunt and Ferry, 1975; Torge, 1989) was subtracted from all gravity values in the database to convert them from Potsdam (New Zealand) to the International Gravity Standardisation Network 1971 (IGSN71) global gravity datum (Morelli *et al*., 1974).

B.5 Free-air anomalies

Free-air anomalies were then computed from the IGSN71-corrected gravity observations by subtracting the normal gravity at the geocentric observation latitude and adding an atmospheric correction (Equation 3.5) and second-order free-air-correction (Equation 3.6) for the observation elevation (above local MSL).

B.6 Bouguer anomalies

Simple planar Bouguer gravity anomalies were also recomputed from the above free-air anomalies using (Equation 3.7). The simple anomalies use an infinite lateral plate of thickness equal to the ground height to model the gravitational attraction of topography (cf. Section 3.3). Spherical Bouguer anomalies were not computed (cf. Section 4.4).

B.7 Terrain corrections

The database also includes gravimetric terrain corrections (Table B.1), which have been computed from topographic maps using Hammer (1939) charts out to zones L-M (Reilly, 1972), which equates to a distance for 22.4 km. The terrain corrections for the inner zones (Hammer zone F or 590 m) were calculated from the field estimations of topography (Hammer, 1939; Woodward and Ferry, 1972). The corrections for the outer zones to Hammer zone M (21.94 km) were estimated from the mean elevation on each 1,000 yard grid square on the national yard grid maps (Woodward, 1982).

The corrections were either computed by interpolation from the correction tables in Woodward and Ferry (1972) or by the software described in Woodward (1982). The extent and method of computing both the inner and outer corrections is indicated by the terrain correction code in Table B.1 from Woodward (1982). The terrain

corrections are analysed in detail in Chapter 4, where they are also compared with alternative computation techniques.

The topographic correction field in Table B.1 allows for the topographic effect from zone M (22.6 km) to zone O (166 km). Unlike the inner and outer terrain corrections, the topographic correction is computed from the departure of the land/seabed surface from sea level (not the station height). A consequence of this is that the correction can be either positive or negative (Reilly, 1970).

B.8 Summary

The gravity observations and derived anomalies supplied in the GNS Science database were in terms of the Potsdam (New Zealand) gravity datum. They were also reduced using less rigorous methods than is required for geodetic applications. To enable the observations to be used for gravimetric geoid computations the gravity observations were first converted to the IGNS71 gravity datum and the requisite anomalies were recomputed with rigorous formulae. The resulting free-air anomalies, Bouguer anomalies and terrain corrections are evaluated in Chapter 5.

APPENDIX C - MARINE GRAVITY DATA AND CROSSOVER ADJUSTMENT

C.1 Introduction

The NZ marine ship-track gravity data has been collected over the past 50 years. The data are of varying quality for a variety of reasons (e.g., purpose of cruises, type of gravimeter and positioning system, equipment calibration). Woodward (pers. comm., 2002) estimates the gravity observations to be within 1.0 mGal and notes that the errors in the early positions can be quite large. In general, the later the data, the more accurate both the gravity and position will be. Until now the data has been stored in a variety of formats, and in terms of several different datums. To enable it to be effectively used in gravimetric geoid computations for the NZ region, it was essential to first combine all of the information into a single consistent dataset. This Section describes the processes used to correct the ship-track data into a single reference system and then to cross-over adjust the same data into a consistent dataset (cf. Brett, 2004; Amos *et al*., 2005).

C.2 Ship-track data

The crossover adjustment of the ship-track gravity observations surrounding New Zealand (Figure C.1) was carried out by *Intrepid Geophysics* (www.intrepid-geophysics.com) under contract to Land Information New Zealand (Brett, 2004).

A total of 3,119,289 ship-track gravity observations were collated from recent surveys conducted for New Zealand's UNCLOS (United Nations Convention on the Law of the Sea) continental shelf claim, GNS Science (GNS), the US National Oceanographic and Atmospheric Administration (NOAA) Geophysical Data System (GEODAS) and Geoscience Australia (GA). The area was restricted to 160°E – 170°W and 25°S – 60°S (2,401,932 points) since this is the region of the NZ continental shelf and the area over NZ which the gravimetric quasi-geoid model is to be computed.

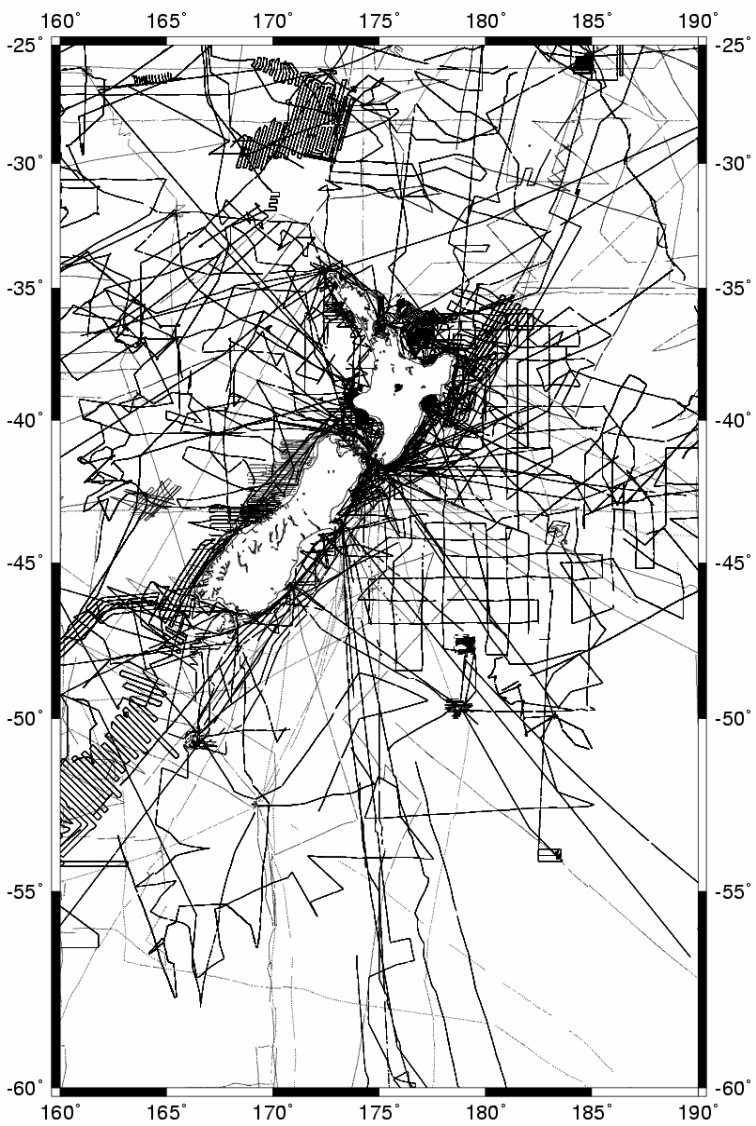

Figure C.1 Coverage of 2,409,932 ship-track gravity observations around New Zealand (Mercator projection)

Where necessary, the gravity datum was transformed from the 1959 New Zealand (Potsdam) datum to IGSN71 by subtracting 15.21 mGal (Section B.4). All horizontal positions were assumed to be on a geocentric horizontal geodetic datum because the survey methods had not been stored in the respective databases (except the UNCLOS data, which is on WGS84 from GPS navigation). Also where necessary, the free-air gravity anomalies were converted from to GRS80 (Moritz 1980a). This was achieved by transforming the GRS67 free-air anomalies to "observed" gravity and then reducing them to free-air anomalies in the GRS80 system.

The marine anomalies were provided in terms of the mean Earth-tide system (see Section 2.3.5). To comply with the International Association of Geodesy resolution on Earth-tide models (IAG, 1984) the anomalies were converted to the zero-tide system using Equation 2.18.

C.3 The *Intrepid Geophysics* marine gravity crossover adjustment

The ship-track data were checked (by *Intrepid Geophysics*) for spikes using a fourth-difference examination of each profile. In addition, statistical reporting (min, max, mean, and standard deviation) was also performed on all data. Any outlier values (e.g., obvious spikes, anomalously high gravity values, high misclosures) were then examined more closely with an interactive data viewer and editor, and a human judgement was made as to whether the spike or feature should be removed or retained.

When initially imported, the data for each ship cruise were stored as a single, long 'line' of data. A necessary step prior to crossover adjustment was to split the cruise data into shorter, approximately straight-line-segments. The advantage of this is that two straight lines either do not cross, or if they do cross, then there is a single crossover. Given this pre-condition, the *INTREPID* computer software (www.intrepid-geophysics.com) uses an efficient algorithm to locate all crossovers without discarding any data. The only outcome was that all points were grouped into line-segments for the purpose of identifying crossovers. The estimated crossover correction was applied to the cruise as a whole, taking no account of the breakdown into 'lines'.

The *INTREPID* computer software also allows for the horizontal positions of the gravity observations to be adjusted. However, their experiments indicated that this made little difference to the results (i.e., crossover statistics), so the horizontal positions were left unchanged.

The datasets were ranked (by *Intrepid*) according to their perceived reliability. This ranking determined the preferred processing order. Starting with the UNCLOS datasets, internal and external crossovers were computed. On the basis of this and the area of coverage the 'res00-11' cruise was ranked highest. Systematic offsets (i.e., biases) were applied to each of the other UNCLOS datasets to reduce the

misclosure statistics for the UNCLOS cruises as a whole. The next ranked dataset was the GNS data, followed by the NOAA data, and then the GA data. This order was determined by *Intrepid* on the basis of internal crossover statistics, data coverage and visual inspection of the raw data.

After applying the offsets to the individual UNCLOS datasets, they were concatenated into a single dataset. This was then adjusted using *Intrepid's* process called "loop closure levelling". This procedure is a single process that consists of several steps. Firstly, the crossovers of a dataset are identified (as described above). Each crossover was then quantified (bias only), where two crossovers were within ~1 km only one bias was evaluated. The misclosure errors around closed loops were then distributed using a least-squares solution of bias and tilt for the network adjustment to produce a correction function. The final levelling adjustment, at every observation point, was then interpolated from the correction function using an Akima spline (Akima, 1978).

The loop closure levelling was then applied to the GNS dataset. The levelled GNS data was gridded and the *Intrepid GridMerge* process used to determine an offset of 4.35 mGal to align it with the UNCLOS data. The GNS data was then appended to the UNCLOS data at the loop closure levelling repeated. The same process was followed to progressively include the NOAA (5.94 mGal offset) and GA (8.16 mGal offset) datasets.

C.4 Adjustment results

Comparing the absolute misclosures at the crossover points in Table C.1 and Table C.2 shows a 714% improvement in the standard deviation (STD) of the crossovers, as well as a significant reduction in the mean differences. Table C.3 gives the statistics of the ship-track gravity anomalies before and after the crossover adjustment.

Data	Crossovers	Max	Min	Mean	STD
UNCLOS	345	79.7	0.0	7.6	12.9
GNS	57512	271.3	0.0	2.5	7.6
NOAA	971988	236.1	0.0	0.7	0.7
GA	36271	52.6	0.0	1.6	2.7
All data	1069289	271.3	0.0	0.8	2.0

Table C.1 Absolute misclosure statistics for the original ship-track observations (mGal)

Data	Crossovers	Max	Min	Mean	STD
UNCLOS	345	12.1	0.0	0.45	1.39
GNS	57512	68.9	0.0	0.19	1.50
NOAA	971988	1.9	0.0	0.09	0.08
GA	36271	14.9	0.0	0.04	0.11
All data	1069244	93.4	0.0	0.05	0.28

Table C.2 Absolute misclosure statistics for the adjusted ship-track observations (mGal)

Adjustment	Max	Min	Mean	STD
Original	477.0	-813.6	4.1	43.2
Adjusted	455.6	-807.7	6.9	42.6

Table C.3 Statistics of the original and adjusted ship-track observations (mGal)

C.5 Summary

This appendix has summarised the crossover adjustment of approximately 90,000-line-km of 2,409,932 ship-track gravity observations around NZ undertaken by *Intrepid Geophysics*. The standard deviation of the ~106 crossovers was reduced from ~2.0 mGal to ~0.3 mGal.

APPENDIX D - DESCRIPTIVE STATISTICS OF GRAVITY GRIDDING QUASIGEOID / GPS-LEVELLING COMPARISONS

The following tables provide the descriptive statistics of the comparisons between the different gravity gridding quasigeoid solutions and the 1422 GPS-levelling points described in Section 4.11.5.

Datum	Points	Max	Min	Average	STD
One Tree Point	51	0.426	-0.202	0.086	0.158
Auckland	137	-0.002	-0.579	-0.234	0.129
Moturiki	258	0.459	-0.989	-0.252	0.290
Gisborne	61	-0.117	-0.650	-0.407	0.110
Taranaki	70	0.2003	-1.014	-0.288	0.307
Napier	54	0.502	-0.479	-0.153	0.255
Wellington	78	-0.028	-1.051	-0.562	0.205
Nelson	111	1.132	-0.669	0.283	0.430
Lyttelton	251	1.421	-1.046	-0.454	0.535
Dunedin	73	-0.272	-1.266	-0.713	0.256
Dunedin-Bluff	181	0.102	-1.453	-1.033	0.294
Bluff	92	-0.248	-1.318	-0.507	0.216
Stewart Island	5	-0.358	-0.675	-0.533	0.116
All Points	1422	1.421	-1.453	-0.394	0.472

Table D.1 Statistics of comparisons between the GGM02S/EGM96 GGM and GPS-levelling points on respective vertical datums (metres)

Datum	Points	Max	Min	Average	STD
One Tree Point	51	-0.139	-0.423	-0.238	0.067
Auckland	137	-0.323	-0.642	-0.496	0.069
Moturiki	258	-0.107	-0.508	-0.273	0.064
Gisborne	61	-0.346	-0.664	-0.527	0.111
Taranaki	70	-0.277	-0.562	-0.415	0.072
Napier	54	-0.080	-0.420	-0.283	0.075
Wellington	78	-0.347	-0.555	-0.452	0.043
Nelson	111	0.238	-0.258	-0.067	0.109
Lyttelton	251	0.147	-0.585	-0.245	0.146
Dunedin	73	0.019	-0.656	-0.391	0.196
Dunedin-Bluff	181	0.952	-0.343	0.280	0.260
Bluff	92	0.971	0.217	0.710	0.175
Stewart Island	5	0.124	-0.141	-0.026	0.094
All Points	1422	0.971	-0.664	-0.172	0.354

Table D.2 Statistics of comparisons between the MSB (Moritz FFT TC, simple Bouguer) quasigeoid and GPS-levelling points on respective vertical datums (metres)

Datum	Points	Max	Min	Average	STD
One Tree Point	51	-0.144	-0.427	-0.242	0.067
Auckland	137	-0.335	-0.651	-0.502	0.066
Moturiki	258	-0.171	-0.517	-0.307	0.060
Gisborne	61	-0.397	-0.698	-0.570	0.104
Taranaki	70	-0.312	-0.606	-0444	0.069
Napier	54	-0.151	-0457	-0.329	0.066
Wellington	78	-0.381	-0.588	-0.484	0.043
Nelson	111	-0.008	-0.354	-0.201	0.070
Lyttelton	251	-0.005	-0.636	-0.362	0.097
Dunedin	73	-0.148	-0.691	-0.464	0.154
Dunedin-Bluff	181	-0.020	-0.580	-0.270	0.074
Bluff	92	-0.210	-0.468	-0.383	0.052
Stewart Island	5	-0.211	-0.599	-0.382	0.134
All Points	1422	-0.005	-0.698	-0.362	0.127

Table D.3 Statistics of comparisons between the PSB (Prism integration TC, simple Bouguer) quasigeoid and GPS-levelling points on respective vertical datums (metres)

Datum	**Points**	**Max**	**Min**	**Average**	**STD**
One Tree Point	51	-0.130	-0.4158	-0.232	0.069
Auckland	137	-0.325	-0.640	-0.496	0.069
Moturiki	258	-0.118	-0.504	-0.289	0.064
Gisborne	61	-0.382	-0.679	-0.553	0.100
Taranaki	70	-0.310	-0.583	-0.438	0.065
Napier	54	-0.118	-0.434	-0.308	0.067
Wellington	78	-0.399	-0.592	-0.482	0.042
Nelson	111	-0.036	-0.313	-0.203	0.057
Lyttelton	251	0.086	-0.593	-0.289	0.118
Dunedin	73	-0.087	-0.673	-0.441	0.163
Dunedin-Bluff	181	0.084	-0.559	-0.235	0.084
Bluff	92	-0.181	-0.457	-0.369	0.054
Stewart Island	5	-0.208	-0.592	-0.372	0.129
All Points	1422	0.086	-0.679	-0.336	0.135

Table D.4 Statistics of comparisons between the HRB (Hammer Chart TC, refined Bouguer) quasigeoid and GPS-levelling points on respective vertical datums (metres)

Datum	Points	Max	Min	Average	STD
One Tree Point	51	-0.129	-0.415	-0.231	0.068
Auckland	137	-0.316	-0632	-0.488	0.070
Moturiki	258	-0.112	-0.496	-0.268	0.063
Gisborne	61	-0.346	-0.661	-0.526	0.101
Taranaki	70	-0.278	-0.556	-0.411	0.070
Napier	54	-0.072	-0.417	-0.279	0.076
Wellington	78	-0.357	-0.560	-0.452	0.043
Nelson	111	0.208	-0.259	-0.087	0.096
Lyttelton	251	0.116	-0.573	-0.242	0.140
Dunedin	73	-0.020	-0.658	-0.417	0.176
Dunedin-Bluff	181	0.157	-0.544	-0.207	0.095
Bluff	92	-0.162	-0.447	-0.359	0.055
Stewart Island	5	-0.199	-0.586	-0.362	0.130
All Points	1422	0.208	-0.661	-0.304	0.154

Table D.5 Statistics of comparisons between the MRB (Moritz FFT TC, refined Bouguer) quasigeoid and GPS-levelling points on respective vertical datums (metres)

Datum	Points	Max	Min	Average	STD
One Tree Point	51	-0.134	-0.418	-0.234	0.068
Auckland	137	-0.326	-0.640	-0.494	0.068
Moturiki	258	-0.170	-0.506	-0.300	0.060
Gisborne	61	-0.398	-0.691	-0.567	0.100
Taranaki	70	-0..311	-0.591	-0.438	0.066
Napier	54	-0.129	-0.449	-0.318	0.068
Wellington	78	-0.392	-0.592	-0.482	0.043
Nelson	111	-0.009	-0.337	-0.206	0.062
Lyttelton	251	0.156	-0.612	-0.340	0.097
Dunedin	73	-0.149	-0.680	-0.456	0.150
Dunedin-Bluff	181	-0.024	-0.569	-0.257	0.074
Bluff	92	-0.201	-0.460	-0.375	0.052
Stewart Island	5	-0.205	-0.593	-0.370	0.130
All Points	1422	0.156	-0.692	-0.352	0.126

Table D.6 Statistics of comparisons between the PRB (Prism integration TC, refined Bouguer) quasigeoid and GPS-levelling points on respective vertical datums (metres)

APPENDIX E - SIGNIFICANCE TESTS FOR VERTICAL DATUM OFFSETS

This Appendix describes the statistical tests that were performed to determine the significance of the computed and observed vertical datum offsets. In all cases, the 95% confidence level (95% significance) has been evaluated.

E.1 Significance of computed offsets

To ascertain if the computed offsets were significant (i.e., non-zero) the 95% Students t confidence interval (CI) was determined using:

$$x - \frac{\sigma_S}{\sqrt{n}} t_{(0.025,n-1)} \le \mu \le x + \frac{\sigma_S}{\sqrt{n}} t_{(0.025,n-1)} \tag{F.1}$$

where x is the average offset, σ_s is the sample standard deviation, n is the number of observations and t is the Students t critical value. The null hypothesis was H_0: $\mu = 0$ and the alternate H_1: $\mu \neq 0$. If the null hypothesis is false then the computed offset is statistically significant.

E.2 Significance of adjacent computed offsets

To determine if two computed datum offsets were significantly different to each other the pooled two-sample Students t CI was determined. For this test the null hypothesis was $H_0 : \mu_1 - \mu_2 = 0$ and the alternate $H_1 : \mu_1 - \mu_2 \neq 0$, where the subscripts indicate the two offsets being considered. The degrees of freedom are given by:

$$\mathrm{Df} = \frac{\left(\frac{\sigma_1^2}{n_1} + \frac{\sigma_2^2}{n_2} \right)^2}{\frac{1}{n_1 - 1}\left(\frac{\sigma_1^2}{n_1} \right)^2 + \frac{1}{n_2 - 1}\left(\frac{\sigma_2^2}{n_2} \right)^2} \tag{F.2}$$

and the CI by:

$$95\% = P\left[\left(x_1 - x_2 \right) - t_{(0.025,\mathrm{df})} \sqrt{\frac{\sigma_1^2}{n_1} + \frac{\sigma_2^2}{n_2}} \le \mu_1 - \mu_2 \le \left(x_1 - x_2 \right) + t_{(0.025,\mathrm{df})} \sqrt{\frac{\sigma_1^2}{n_1} + \frac{\sigma_2^2}{n_2}} \right] \tag{F.3}$$

If the null hypothesis is false, then the computed datum offsets are significantly different.

E.3 Significance of computed and observed offsets

The computed vertical datum offsets can be validated by comparing them with offsets "observed" where the precise levelling lines in the vertical datums abut (cf. Table 2.3). The pooled two-sample Students t CI for the computed offsets was evaluated using Equation (F.3).

The Students t CI for the precise levelling offsets was computed using:

$$95\% = P\left[x_{\text{lev}} - t_{(0.025,z)} \frac{\sigma_{\text{lev}}}{\sqrt{n}_{\text{lev}}} \leq \mu \leq x_{\text{lev}} + t_{(0.025,z)} \frac{\sigma_{\text{lev}}}{\sqrt{n_{\text{lev}}}} \right] \quad \text{(F.4)}$$

If the two CI overlap, then the computed and precise levelling offsets agree.

E.4 *a priori* quasigeoid statistical tests

To ascertain whether the *a priori* quasigeoid computed datum offsets are significant (i.e. non-zero) the 95% Student t CI was established using Equation (F.1) to assess the null hypothesis H_0: $\mu = 0$ (cf. Section 6.5.2). The CI are summarised in Table E.1.

Datum	n	x	σ_s	95% CI			H_0	Significant offset?
One Tree Point	51	-0.245	0.063	-0.262	$\leq \mu \leq$	-0.228	FALSE	**Yes**
Auckland	137	-0.497	0.068	-0.508	$\leq \mu \leq$	-0.486	FALSE	**Yes**
Moturiki	258	-0.316	0.061	-0.323	$\leq \mu \leq$	-0.309	FALSE	**Yes**
Gisborne	61	-0.585	0.087	-0.607	$\leq \mu \leq$	-0.563	FALSE	**Yes**
Taranaki	70	-0.457	0.066	-0.472	$\leq \mu \leq$	-0.442	FALSE	**Yes**
Napier	54	-0.304	0.070	-0.323	$\leq \mu \leq$	-0.285	FALSE	**Yes**
Wellington	78	-0.509	0.040	-0.518	$\leq \mu \leq$	-0.500	FALSE	**Yes**
Nelson	111	-0.257	0.081	-0.272	$\leq \mu \leq$	-0.242	FALSE	**Yes**
Lyttelton	251	-0.350	0.097	-0.362	$\leq \mu \leq$	-0.338	FALSE	**Yes**
Dunedin	73	-0.491	0.162	-0.528	$\leq \mu \leq$	-0.454	FALSE	**Yes**
Dunedin-Bluff	181	-0.261	0.076	-0.272	$\leq \mu \leq$	-0.250	FALSE	**Yes**
Bluff	92	-0.380	0.051	-0.390	$\leq \mu \leq$	-0.370	FALSE	**Yes**
Stewart Island	5	-0.398	0.116	-0.500	$\leq \mu \leq$	-0.296	FALSE	**Yes**

Table E.1 Significance of *a priori* quasigeoid vertical datum offsets (95% CI Student t distribution, metres)

To ascertain whether the adjacent *a priori* quasigeoid computed datum offsets are different the 95% Student t CI was established using Equation (F.3) to assess the null hypothesis H_0: $\mu_1 - \mu_2 = 0$ (cf. Section 6.5.2). The results are summarised in Table E.2.

To ascertain whether the *a priori* quasigeoid computed datum offsets are the same as the observed (by precise-levelling) offsets the 95% Student t CI was established using Equations (F.3) and (F.4) respectively (cf. Section 6.5.2). If the two CI overlap the computed and observed offsets agree. The comparisons are summarised in Table 6.2.

E.5 Second quasigeoid statistical tests

To ascertain whether the datum offsets computed from the *a priori* and second quasigeoids are different the 95% Student t CI was established using Equation (F.3) to assess the null hypothesis H_0: $\mu_1 - \mu_2 = 0$ (cf. Section 6.5.3). The results are summarised in Table E.4.

E.6 Third quasigeoid statistical tests

To ascertain whether the datum offsets computed from the second and third quasigeoids are different the 95% Student t CI was established using Equation (F.3) to assess the null hypothesis H_0: $\mu_1 - \mu_2 = 0$ (cf. Section 6.5.4). The results are summarised in Table E.5.

To ascertain whether the third quasigeoid computed datum offsets are the same as the observed (by precise-levelling) offsets the 95% Student t CI was established using Equations (F.3) and (F.4) respectively (cf. Section 6.5.4). If the two CI overlap the computed and observed offsets agree. The comparisons are summarised in Table E.5.

From	To	n_1	x_1	σ_1	n_2	x_2	σ_2	$x_1 - x_2$	Df	$t_{(0.025,df)}$	95% CI		H_0	Offsets Different?
Auckland	One Tree Point	137	-0.497	0.068	51	-0.245	0.063	-0.252	96	1.984	-0.273	$\leq \mu_1 - \mu_2 \leq$	-0.231	FALSE	Yes
Auckland	Moturiki	137	-0.497	0.068	258	-0.316	0.061	-0.181	253	1.962	-0.195	$\leq \mu_1 - \mu_2 \leq$	-0.167	FALSE	Yes
Gisborne	Moturiki	61	-0.585	0.087	258	-0.316	0.061	-0.269	75	1.990	-0.292	$\leq \mu_1 - \mu_2 \leq$	-0.246	FALSE	Yes
Gisborne	Napier	61	-0.585	0.087	54	-0.304	0.070	-0.281	112	1.962	-0.310	$\leq \mu_1 - \mu_2 \leq$	-0.252	FALSE	Yes
Moturiki	Napier	258	-0.316	0.061	54	-0.304	0.070	-0.012	71	1.990	-0.032	$\leq \mu_1 - \mu_2 \leq$	0.008	TRUE	No
Moturiki	Taranaki	258	-0.316	0.061	70	-0.457	0.066	0.141	103	1.962	0.124	$\leq \mu_1 - \mu_2 \leq$	0.158	FALSE	Yes
Moturiki	Wellington	258	-0.316	0.061	78	-0.509	0.040	0.193	195	1.962	0.181	$\leq \mu_1 - \mu_2 \leq$	0.205	FALSE	Yes
Taranaki	Wellington	70	-0.457	0.066	78	-0.509	0.040	0.052	111	1.962	0.034	$\leq \mu_1 - \mu_2 \leq$	0.070	FALSE	Yes
Napier	Wellington	54	-0.304	0.070	78	-0.509	0.040	0.205	77	1.990	0.184	$\leq \mu_1 - \mu_2 \leq$	0.226	FALSE	Yes
Nelson	Wellington	111	-0.257	0.081	78	-0.509	0.040	0.252	170	1.962	0.234	$\leq \mu_1 - \mu_2 \leq$	0.270	FALSE	Yes
Nelson	Lyttelton	111	-0.257	0.081	251	-0.350	0.097	0.093	250	1.962	0.074	$\leq \mu_1 - \mu_2 \leq$	0.112	FALSE	Yes
Dunedin	Lyttelton	73	-0.491	0.162	251	-0.350	0.097	-0.141	88	1.984	-0.181	$\leq \mu_1 - \mu_2 \leq$	-0.101	FALSE	Yes
Dunedin	Dunedin - Bluff	73	-0.491	0.162	181	-0.261	0.076	-0.230	85	1.984	-0.269	$\leq \mu_1 - \mu_2 \leq$	-0.191	FALSE	Yes
Bluff	Dunedin - Bluff	92	-0.380	0.051	181	-0.261	0.076	-0.119	251	1.962	-0.134	$\leq \mu_1 - \mu_2 \leq$	-0.104	FALSE	Yes
Bluff	Dunedin	92	-0.380	0.051	73	-0.491	0.162	0.111	83	1.984	0.072	$\leq \mu_1 - \mu_2 \leq$	0.150	FALSE	Yes
Bluff	Stewart Island	92	-0.380	0.051	5	-0.398	0.116	0.018	4	2.776	-0.127	$\leq \mu_1 - \mu_2 \leq$	0.163	TRUE	No

Table E.2 Comparison of adjacent *a priori* quasigeoid vertical datum offsets (95% CI Student t distribution, metres)

Vertical Datum		*a priori* quasigeoid computed offset										Precise levelling observed offset					Offsets Agree?
From	To	n_1	x_1	σ_1	n_2	x_2	σ_2	$x_1 - x_2$	Df	$t_{(0.025,df)}$	95% CI	n_{lev}	μ_{lev}	σ_{lev}	$t_{(0.025,z)}$	95 % CI	
Auckland	One Tree Point	137	-0.497	0.068	51	-0.245	0.063	-0.252	96	1.984	$-0.273 \leq \mu_1 - \mu_2 \leq -0.231$	1	-0.206	0.071	1.960	$-0.345 \leq \mu \leq -0.067$	Yes
Auckland	Moturiki	137	-0.497	0.068	258	-0.316	0.061	-0.181	253	1.962	$-0.195 \leq \mu_1 - \mu_2 \leq -0.167$	1	-0.070	0.071	1.960	$-0.209 \leq \mu \leq 0.069$	Yes
Gisborne	Moturiki	61	-0.585	0.087	258	-0.316	0.061	-0.269	75	1.990	$-0.292 \leq \mu_1 - \mu_2 \leq -0.246$	1	-0.075	0.071	1.960	$-0.214 \leq \mu \leq 0.064$	No
Gisborne	Napier	61	-0.585	0.087	54	-0.304	0.070	-0.281	112	1.984	$-0.310 \leq \mu_1 - \mu_2 \leq -0.252$	1	-0.166	0.071	1.960	$-0.305 \leq \mu \leq -0.027$	Yes
Moturiki	Napier	258	-0.316	0.061	54	-0.304	0.070	-0.012	71	1.990	$-0.032 \leq \mu_1 - \mu_2 \leq 0.008$	1	-0.099	0.071	1.960	$-0.238 \leq \mu \leq 0.040$	Yes
Taranaki	Napier	70	-0.457	0.066	54	-0.304	0.070	-0.153	111	1.984	$-0.178 \leq \mu_1 - \mu_2 \leq -0.128$	1	-0.046	0.071	1.960	$-0.185 \leq \mu \leq 0.093$	Yes
Taranaki	Wellington	70	-0.457	0.066	78	-0.509	0.040	0.052	111	1.984	$0.034 \leq \mu_1 - \mu_2 \leq 0.070$	1	0.147	0.071	1.960	$0.008 \leq \mu \leq 0.286$	Yes
Taranaki	Moturiki	70	-0.457	0.066	258	-0.316	0.061	-0.141	103	1.984	$-0.158 \leq \mu_1 - \mu_2 \leq -0.124$	1	-0.162	0.071	1.960	$-0.301 \leq \mu \leq -0.023$	Yes
Napier	Wellington	54	-0.304	0.070	78	-0.509	0.040	0.205	77	1.990	$0.184 \leq \mu_1 - \mu_2 \leq 0.226$	1	0.237	0.071	1.960	$0.098 \leq \mu \leq 0.376$	Yes
Nelson	Lyttelton	111	-0.257	0.081	251	-0.350	0.097	0.093	250	1.962	$0.074 \leq \mu_1 - \mu_2 \leq 0.112$	1	-0.027	0.071	1.960	$-0.166 \leq \mu \leq 0.112$	Yes
Lyttelton	Dunedin	251	-0.350	0.097	73	-0.491	0.162	0.141	88	1.984	$0.101 \leq \mu_1 - \mu_2 \leq 0.181$	1	-0.071	0.071	1.960	$-0.210 \leq \mu \leq 0.068$	No
Dunedin - Bluff	Dunedin	181	-0.261	0.076	73	-0.491	0.162	0.230	85	1.984	$0.191 \leq \mu_1 - \mu_2 \leq 0.269$	1	-0.019	0.071	1.960	$-0.158 \leq \mu \leq 0.120$	No
Dunedin - Bluff	Bluff	181	-0.261	0.076	92	-0.380	0.051	0.119	251	1.962	$0.104 \leq \mu_1 - \mu_2 \leq 0.134$	1	-0.001	0.071	1.960	$-0.140 \leq \mu \leq 0.138$	Yes

Table E.3 Comparison of *a priori* quasigeoid and precise levelling derived vertical datum offsets (95% CI Students t distribution, metres)

Datum	n_1	x_1	σ_1	n_2	x_2	σ_2	$x_1 - x_2$	Df	$t_{(0.025,df)}$	95% CI		H_0	Offsets Different?
One Tree Point	51	-0.245	0.063	51	-0.242	0.063	-0.003	100	1.962	-0.027	$\leq \mu_1 - \mu_2 \leq$ 0.021	TRUE	No
Auckland	137	-0.497	0.068	137	-0.491	0.068	-0.006	272	1.962	-0.022	$\leq \mu_1 - \mu_2 \leq$ 0.010	TRUE	No
Moturiki	258	-0.316	0.061	258	-0.309	0.062	-0.007	514	1.962	-0.018	$\leq \mu_1 - \mu_2 \leq$ 0.004	TRUE	No
Gisborne	61	-0.585	0.087	61	-0.578	0.087	-0.007	120	1.962	-0.038	$\leq \mu_1 - \mu_2 \leq$ 0.024	TRUE	No
Taranaki	70	-0.457	0.066	70	-0.450	0.067	-0.007	138	1.962	-0.029	$\leq \mu_1 - \mu_2 \leq$ 0.015	TRUE	No
Napier	54	-0.304	0.070	54	-0.298	0.070	-0.006	106	1.962	-0.032	$\leq \mu_1 - \mu_2 \leq$ 0.020	TRUE	No
Wellington	78	-0.509	0.040	78	-0.503	0.039	-0.006	154	1.962	-0.018	$\leq \mu_1 - \mu_2 \leq$ 0.006	TRUE	No
Nelson	111	-0.257	0.081	111	-0.252	0.082	-0.005	220	1.962	-0.026	$\leq \mu_1 - \mu_2 \leq$ 0.016	TRUE	No
Lyttelton	251	-0.350	0.097	251	-0.343	0.097	-0.007	500	1.962	-0.024	$\leq \mu_1 - \mu_2 \leq$ 0.010	TRUE	No
Dunedin	73	-0.491	0.162	73	-0.484	0.164	-0.007	144	1.962	-0.060	$\leq \mu_1 - \mu_2 \leq$ 0.046	TRUE	No
Dunedin-Bluff	181	-0.261	0.076	181	-0.255	0.077	-0.006	360	1.962	-0.022	$\leq \mu_1 - \mu_2 \leq$ 0.010	TRUE	No
Bluff	92	-0.380	0.051	92	-0.375	0.051	-0.005	182	1.962	-0.020	$\leq \mu_1 - \mu_2 \leq$ 0.010	TRUE	No
Stewart Island	5	-0.398	0.116	5	-0.395	0.116	-0.003	8	2.306	-0.172	$\leq \mu_1 - \mu_2 \leq$ 0.166	TRUE	No

Table E.4 Comparison of *a priori* and second quasigeoid vertical datum offsets (95% CI Students t distribution, metres)

Datum	n_1	x_1	σ_1	n_2	x_2	σ_2	$x_1 - x_2$	Df	$t_{(0.025,df)}$	95% CI		H_0	Offsets Different?
One Tree Point	51	-0.242	0.063	51	-0.242	0.063	0.000	100	1.962	-0.024	$\leq \mu_1 - \mu_2 \leq$ 0.024	TRUE	No
Auckland	137	-0.491	0.068	137	-0.491	0.068	0.000	272	1.962	-0.016	$\leq \mu_1 - \mu_2 \leq$ 0.016	TRUE	No
Moturiki	258	-0.309	0.062	258	-0.309	0.062	0.000	514	1.962	-0.011	$\leq \mu_1 - \mu_2 \leq$ 0.011	TRUE	No
Gisborne	61	-0.578	0.087	61	-0.578	0.087	0.000	120	1.962	-0.031	$\leq \mu_1 - \mu_2 \leq$ 0.031	TRUE	No
Taranaki	70	-0.450	0.067	70	-0.450	0.067	0.000	138	1.962	-0.022	$\leq \mu_1 - \mu_2 \leq$ 0.022	TRUE	No
Napier	54	-0.298	0.070	54	-0.298	0.070	0.000	106	1.962	-0.026	$\leq \mu_1 - \mu_2 \leq$ 0.026	TRUE	No
Wellington	78	-0.503	0.039	78	-0.503	0.039	0.000	154	1.962	-0.012	$\leq \mu_1 - \mu_2 \leq$ 0.012	TRUE	No
Nelson	111	-0.252	0.082	111	-0.252	0.082	0.000	220	1.962	-0.022	$\leq \mu_1 - \mu_2 \leq$ 0.022	TRUE	No
Lyttelton	251	-0.343	0.097	251	-0.343	0.097	0.000	500	1.962	-0.017	$\leq \mu_1 - \mu_2 \leq$ 0.017	TRUE	No
Dunedin	73	-0.484	0.164	73	-0.484	0.164	0.000	144	1.962	-0.053	$\leq \mu_1 - \mu_2 \leq$ 0.053	TRUE	No
Dunedin-Bluff	181	-0.255	0.077	181	-0.255	0.077	0.000	360	1.962	-0.016	$\leq \mu_1 - \mu_2 \leq$ 0.016	TRUE	No
Bluff	92	-0.375	0.051	92	-0.375	0.051	0.000	182	1.962	-0.015	$\leq \mu_1 - \mu_2 \leq$ 0.015	TRUE	No
Stewart Island	5	-0.395	0.116	5	-0.395	0.116	0.000	8	2.306	-0.169	$\leq \mu_1 - \mu_2 \leq$ 0.169	TRUE	No

Table E.5 Comparison of second and third quasigeoid vertical datum offsets (95% CI Students t distribution, metres)

Vertical datums		Third quasigeoid computed offset										Precise levelling observed offset					Offsets Agree?
From	To	n_1	x_1	σ_1	n_2	x_2	σ_2	$x_1 - x_2$	Df	$t_{(0.025,df)}$	95% CI	n_{lev}	μ_{lev}	σ_{lev}	$t_{(0.025,z)}$	95% CI	
Auckland	One Tree Point	137	-0.491	0.068	51	-0.242	0.063	-0.249	96	1.984	$-0.270 \leq \mu_1 - \mu_2 \leq -0.228$	1	-0.206	0.071	1.960	$-0.345 \leq \mu \leq -0.067$	Yes
Auckland	Moturiki	137	-0.491	0.068	258	-0.309	0.062	-0.182	256	1.962	$-0.196 \leq \mu_1 - \mu_2 \leq -0.168$	1	-0.070	0.071	1.960	$-0.209 \leq \mu \leq 0.069$	Yes
Gisborne	Moturiki	61	-0.578	0.087	258	-0.309	0.062	-0.269	75	1.990	$-0.292 \leq \mu_1 - \mu_2 \leq -0.246$	1	-0.075	0.071	1.960	$-0.214 \leq \mu \leq 0.064$	No
Gisborne	Napier	61	-0.578	0.087	54	-0.298	0.070	-0.280	112	1.984	$-0.309 \leq \mu_1 - \mu_2 \leq -0.251$	1	-0.166	0.071	1.960	$-0.305 \leq \mu \leq -0.027$	Yes
Moturiki	Napier	258	-0.309	0.062	54	-0.298	0.070	-0.011	71	1.990	$-0.031 \leq \mu_1 - \mu_2 \leq 0.009$	1	-0.099	0.071	1.960	$-0.238 \leq \mu \leq 0.040$	Yes
Taranaki	Napier	70	-0.450	0.067	54	-0.298	0.070	-0.152	112	1.984	$-0.177 \leq \mu_1 - \mu_2 \leq -0.127$	1	-0.046	0.071	1.960	$-0.185 \leq \mu \leq 0.093$	Yes
Taranaki	Wellington	70	-0.450	0.067	78	-0.503	0.039	0.053	108	1.984	$0.035 \leq \mu_1 - \mu_2 \leq 0.071$	1	0.147	0.071	1.960	$0.008 \leq \mu \leq 0.286$	Yes
Taranaki	Moturiki	70	-0.450	0.067	258	-0.309	0.062	-0.141	103	1.984	$-0.159 \leq \mu_1 - \mu_2 \leq -0.123$	1	-0.162	0.071	1.960	$-0.301 \leq \mu \leq -0.023$	Yes
Napier	Wellington	54	-0.298	0.070	78	-0.503	0.039	0.205	76	1.990	$0.184 \leq \mu_1 - \mu_2 \leq 0.226$	1	0.237	0.071	1.960	$0.098 \leq \mu \leq 0.376$	Yes
Nelson	Lyttelton	111	-0.252	0.082	251	-0.343	0.097	0.091	247	1.962	$0.072 \leq \mu_1 - \mu_2 \leq 0.110$	1	-0.027	0.071	1.960	$-0.166 \leq \mu \leq 0.112$	Yes
Lyttelton	Dunedin	251	-0.343	0.097	73	-0.484	0.164	0.141	87	1.984	$0.101 \leq \mu_1 - \mu_2 \leq 0.181$	1	-0.071	0.071	1.960	$-0.210 \leq \mu \leq 0.068$	No
Dunedin - Bluff	Dunedin	181	-0.255	0.077	73	-0.484	0.164	0.229	85	1.984	$0.189 \leq \mu_1 - \mu_2 \leq 0.269$	1	-0.019	0.071	1.960	$-0.158 \leq \mu \leq 0.120$	No
Dunedin - Bluff	Bluff	181	-0.255	0.077	92	-0.376	0.051	0.121	253	1.962	$0.106 \leq \mu_1 - \mu_2 \leq 0.136$	1	-0.001	0.071	1.960	$-0.140 \leq \mu \leq 0.138$	Yes

Table E.6 Comparison of third quasigeoid and precise levelling derived vertical datum offsets (95% CI Students t distribution, metres)